

## INFORMATION TO USERS

This manuscript has been reproduced from the microfilm master. UMI films the text directly from the original or copy submitted. Thus, some thesis and dissertation copies are in typewriter face, while others may be from any type of computer printer.

**The quality of this reproduction is dependent upon the quality of the copy submitted.** Broken or indistinct print, colored or poor quality illustrations and photographs, print bleedthrough, substandard margins, and improper alignment can adversely affect reproduction.

In the unlikely event that the author did not send UMI a complete manuscript and there are missing pages, these will be noted. Also, if unauthorized copyright material had to be removed, a note will indicate the deletion.

Oversize materials (e.g., maps, drawings, charts) are reproduced by sectioning the original, beginning at the upper left-hand corner and continuing from left to right in equal sections with small overlaps.

Photographs included in the original manuscript have been reproduced xerographically in this copy. Higher quality 6" x 9" black and white photographic prints are available for any photographs or illustrations appearing in this copy for an additional charge. Contact UMI directly to order.

ProQuest Information and Learning  
300 North Zeeb Road, Ann Arbor, MI 48106-1346 USA  
800-521-0600

UMI<sup>®</sup>



CHARACTERIZATION OF HOMOSERINE DEHYDROGENASE  
FROM SACCHAROMYCES CEREVISIAE:  
AN ANTIFUNGAL TARGET

By  
SUZANNE LYNE JACQUES, B.Sc., M.A.Sc.

A thesis  
Submitted to the School of Graduate Studies  
in Partial Fulfilment of the Requirements  
for the Degree  
Doctor of Philosophy

McMaster University  
© Copyright by Suzanne Lyne Jacques, September 1999

## CHARACTERIZATION OF YEAST HOMOSERINE DEHYDROGENASE

DOCTOR OF PHILOSOPHY (1999)  
(Biochemistry)

McMaster University  
Hamilton, Ontario

TITLE: Characterization of homoserine dehydrogenase from *Saccharomyces cerevisiae*: An antifungal target

AUTHOR: Suzanne Lyne Jacques, B.Sc. (McGill University)  
M.A.Sc. (University of Waterloo)

SUPERVISOR: Professor Gerard D. Wright

NUMBER OF PAGES: xvii, 285

## ABSTRACT

Homoserine dehydrogenase (HSD), the third enzyme in the aspartate biosynthetic pathway producing isoleucine, methionine and threonine, is an important new antifungal target. Previously, (*S*)-2-amino-4-oxo-5-hydroxypentanoic acid (RI-331), an antifungal compound, demonstrated inhibitory activity against HSD from *Saccharomyces cerevisiae*. This pathway is an excellent target for the development of new non-toxic antifungal drugs, as it is absent in mammals. In order to design effective inhibitors of fungal HSD, a full kinetic and mechanistic characterization of this enzyme was required. Consequently, HSD from a model fungus, *S. cerevisiae*, was examined. Surprisingly, yeast HSD was able to bind either cofactor, NADPH or NADH, with high affinity. Product inhibition studies suggested that yeast HSD preferentially binds the nicotinamide cofactor before the amino acid substrate and releases the cofactor last. The inhibition pattern of the newly discovered HSD inhibitor, H-(1,2,4-triazol-3-yl)-*D,L*-alanine, was consistent with the proposed substrate binding order. In addition, viscosity and kinetic isotope experiments provided evidence for a fast catalytic step and a rate-limiting NAD(P)<sup>+</sup> release during HSD catalysis. The stereochemistry of hydride transfer was determined to be from the *pro-S* C-4 nicotinamide hydrogen by kinetic isotope effects. Chemical modification experiments and site-directed mutagenesis of HSD

determined that histidine 309 is an important residue in HSD catalysis. However, the recently solved HSD X-ray structure revealed that His309 may, in fact, be solely important in HSD dimerization. On the other hand, pH studies demonstrated that basic residues are involved primarily in substrate binding, in agreement with lysine residues discovered in the active site of the HSD structure. Lastly, RI-331 demonstrated many properties of a mechanism-based inactivator. This compound appears to form an adduct with NAD(P)<sup>+</sup> in an HSD-dependent manner, thereby producing a tight-binding transition-state analog of yeast HSD. These studies will provide the necessary foundation for the development of a new class of antifungal drugs targeting amino acid biosynthesis.

## ACKNOWLEDGEMENTS

I would like to express my sincere gratitude to several people who contributed in many ways to the completion of this thesis. First of all, I would like to thank my outstanding supervisor, Dr. Gerard Wright, for his guidance, enthusiasm and motivation. I appreciate all the time and effort he dedicated to teaching me how to do good science and all his help and patience during the preparation of this thesis. I am very grateful to the members of my supervisory committee, Dr. Gerhard Gerber and Dr. Herb Schellhorn, who were very helpful over the years with suggestions and advice. I would like to thank Dr. John Honek for the compounds he furnished, for his advice and discussions on RI-331, and also for the help during our frequent visits to the University of Waterloo Biological Mass Spectrometry Laboratory. I also thank the Government of Ontario and the Chemical Institute of Canada for their funding in the form of an Ontario Graduate Scholarship and a Pestcon Graduate Scholarship. I am thankful to the members of the Wright lab and Byron DeLaBarre for their help, valuable discussions and friendships.

I would also like to thank my family and friends for their constant support and advice. Especially my mother for teaching me that there is no time like the present and my parents-in-law for helping me understand the power of positive thinking. In addition, I am grateful for the generous hospitality shown to me by Mary Malvar and Harold Rees, who made me feel at home during my trips back to Ontario.

Of course, this would not have been possible without the constant support of my husband, Rónán O'Hagan, who encouraged me every step of the way.



For Rónán,

## TABLE OF CONTENTS

<b>Abstract</b>	iii
<b>Acknowledgements</b>	v
<b>Table of Contents</b>	vii
<b>List of Tables</b>	x
<b>List of Figures</b>	xi
<b>List of Schemes</b>	xiv
<b>List of Abbreviations</b>	xv
<b>Chapter 1. Introduction</b>	1
1.1. Literature review	2
1.1.1. Fungal disease	2
1.1.2. Antifungal drugs in current use	6
1.1.3. Antifungal drug resistance	15
1.1.4. Search for new antifungal targets	18
1.1.5. Discovery of ( <i>S</i> )-2-amino-4-oxo-5-hydroxypentanoic acid	28
1.1.6. Aspartate pathway of amino acid biosynthesis	31
1.1.6.1. <i>Escherichia coli</i> enzymes of the aspartate pathway	33
1.1.6.2. <i>Saccharomyces cerevisiae</i> enzymes of the aspartate pathway	37
1.1.7. Biosynthesis of edeines in <i>Bacillus brevis</i>	40
1.2. Purpose	46
<b>Chapter 2. Characterization of yeast homoserine dehydrogenase, an antifungal target</b>	48
2.1. Preface	49
2.2 Paper	51

<b>Chapter 3.</b>	<b>Homoserine Dehydrogenase from <i>Saccharomyces cerevisiae</i>: Kinetic Mechanism and Stereochemistry</b>	99
	3.1. Preface	100
	3.2. Paper	101
	Appendix A	149
<b>Chapter 4.</b>	<b>(<i>S</i>) 2-amino-4-oxo-5-hydroxypentanoic acid (RI-311), an Antifungal Compound, is a Mechanism-Based Inactivator of <i>Saccharomyces cerevisiae</i> Homoserine Dehydrogenase</b>	153
	4.1. Preface	154
	4.2. Paper	155
<b>Chapter 5.</b>	<b>Purification of Edeines and the Biosynthetic Enzymes, Tyrosine <math>\alpha,\beta</math>-Amino Mutase and Edeine Synthetase, from <i>Bacillus brevis</i> Vm4</b>	203
	5.1. Preface	204
	5.2. Introduction	205
	5.3. Materials and methods	211
	5.3.1. Materials	211
	5.3.2. Methods	212
	5.4. Results	224
	5.4.1. Production of edeines from <i>Bacillus brevis</i>	224
	5.4.2. Purification and characterization of edeines A and B	227
	5.4.3. Purification of tyrosine $\alpha,\beta$ -amino mutase from <i>Bacillus brevis</i>	245
	5.5. Discussion	256
	5.6. References	265

<b>Chapter 6.</b>	<b>Discussion and Conclusions</b>	<b>267</b>
	6.1 Discussion and conclusions	268
	6.2 Future directions	275
<b>Chapter 7.</b>	<b>References</b>	<b>277</b>

## LIST OF TABLES

2-1.	Purification of <i>S. cerevisiae</i> HSD from <i>E.coli</i> BL21(DE3)/pCP13.	69
2-2.	Steady state kinetic parameters for purified yeast HSD.	73
2-3.	Chemical modification of purified <i>S. cerevisiae</i> HSD.	80
3-1.	Kinetic constants for product inhibition of purified yeast HSD.	114
3-2.	Inhibition of purified yeast HSD.	123
3-3.	Kinetic isotope effects using stereospecifically deuterated NADPH.	129
3-4.	Kinetic constants of yeast HSD as a function of relative viscosity ( $\eta_{rel}$ ).	133
3-5.	“Stickiness” parameters of yeast HSD substrates.	134
3-6.	Summary of pK values for yeast HSD.	139
3-A.	List of compounds surveyed for HSD inhibition.	149
4-1.	Observed inactivation rates ( $k_{obs}$ ) of yeast HSD.	176
5-1.	Minimal media requirements for production of edeines.	224
5-2.	Electrospray mass spectrometry analysis of purified edeines.	234
5-3.	R <sub>F</sub> for 2D thin layer chromatography of component amino acids and hydrolysed edeines.	242

## LIST OF FIGURES

1-1.	The polyene class of antifungal agents.	7
1-2.	The azole class of antifungal agents.	10
1-3.	The morpholine, allylamine and thiocarbamate classes of antifungal agents.	12
1-4.	Other classes of antifungal agents.	14
1-5.	Antifungal agents targeting cell wall biosynthesis	20
1-6.	The biosynthesis of squalene.	22
1-7.	The biosynthesis of ergosterol in fungi.	23
1-8.	The biosynthesis of sphingolipids.	24
1-9.	Structure of ( <i>S</i> )-2-amino-4-oxo-5-hydroxypentanoic acid (RI-331).	28
1-10.	The biosynthesis of the aspartate group of amino acids.	30
1-11.	The biosynthesis of methionine.	32
1-12.	Structure of edeines produced from <i>Bacillus brevis</i> Vm4.	41
2-1.	Purification of <i>S. cerevisiae</i> HSD from <i>E. coli</i> /pCP13.	70
2-2.	Effect of KCl on progress curves of HSD activity at high NADH concentration.	75
2-3.	Effect of KCl on kinetic parameters of yeast HSD.	77
2-4.	Difference spectra for the modification of <i>S. cerevisiae</i> HSD by DEPC.	81
2-5.	Phylogenetic tree of bacterial, fungal and plant HSD/AKHSD.	84
2-6.	Amino acid sequence alignment of <i>S. cerevisiae</i> HSD with the HSD domains of <i>E. coli</i> and plant enzymes.	86
3-1.	Product inhibition of HSD by NADP <sup>+</sup> .	115

3-2.	Product inhibition of HSD by <i>L</i> -Hse.	118
3-3.	Product inhibition of HSD by <i>L</i> -Hse with respect to NADPH at saturating concentrations of ASA.	120
3-4.	Structures of yeast inhibitors, <i>L</i> -aspartate $\beta$ -hydroxamate and H-(1,2,4-triazol-3-yl)- <i>D,L</i> -alanine.	124
3-5.	Inhibition of HSD by H-(1,2,4-triazol-3-yl)- <i>D,L</i> -alanine.	126
3-6.	Effect of relative viscosity on $k_{cat}$ and $k_{cat}/K_m$ for HSD.	130
3-7.	Effect of pH on steady state parameters ( $V_{max}$ and $V_{max}/K_m$ ) of HSD.	136
4-1.	Structures of ( <i>S</i> )-2-amino-4-oxo-5-hydroxypentanoic acid (RI-331), <i>L</i> -aspartate $\beta$ -hydroxamate and 4-oxo- <i>L</i> -norvaline.	160
4-2.	The aspartate pathway of amino acid biosynthesis.	162
4-3.	Time-dependent inactivation of yeast HSD by RI-331.	171
4-4.	Saturation of RI-331 inactivation of yeast HSD.	173
4-5.	Substrate protection from RI-331 inactivation of yeast HSD.	177
4-6.	Gel filtration analysis of yeast HSD inactivated with RI-331 and [ <sup>14</sup> C]-NAD <sup>+</sup> .	181
4-7.	Incorporation of [ <sup>14</sup> C]-NAD <sup>+</sup> during inactivation of yeast HSD by RI-331.	183
4-8.	Positive ion mass spectrometry of A) RI-331-inactivated HSD, low <i>m/z</i> ; B) RI-331-inactivated HSD, high <i>m/z</i> ; and C) phenyl glyoxal-inactivated HSD.	186
4-9.	Purification of NAD-RI-331 adduct by size exclusion chromatography.	191
5-1.	Structure of edeines.	207
5-2.	Growth curve for <i>Bacillus brevis</i> and production of edeines.	225

5-3.	Purification of edeines from spent media by Sephadex G25 size exclusion chromatography.	228
5-4.	Purification of edeines by Mono S cation exchange chromatography.	230
5-5.	Purification of edeines A and B by reverse-phase HPLC.	232
5-6.	<sup>1</sup> H-NMR analysis of edeine A.	235
5-7.	Correlated spectroscopy- <sup>1</sup> H-NMR analysis of edeine A.	237
5-8.	Diagram of 2D thin layer chromatography of amino acid components of edeine.	240
5-9.	Reverse-phase HPLC analysis of edeines purified from cultures supplemented with [ <sup>14</sup> C]-tyrosine or [ <sup>14</sup> C]-serine.	243
5-10.	Purification of tyrosine $\alpha,\beta$ -amino mutase by DEAE-Sepharose anion exchange chromatography.	249
5-11.	Purification of edeine biosynthetic enzymes by Sephadex G100 size exclusion chromatography.	251
5-12.	Purification of edeine biosynthetic enzymes by DEAE-Sepharose anion exchange chromatography.	253
5-13a.	Possible mechanisms of tyrosine $\alpha,\beta$ -amino mutase.	259
5-13b.	Possible mechanisms of tyrosine $\alpha,\beta$ -amino mutase.	261
6-1.	Structures of potential HSD inhibitors.	273



## LIST OF SCHEMES

2-1.	The aspartate pathway in <i>S. cerevisiae</i> .	57
3-1.	Reaction scheme for a partial competitive inhibitor.	110
3-2.	General reaction scheme.	111
3-3.	Stereochemistry of hydride transfer by yeast HSD.	143
4-1.	Reaction scheme for a mechanism-based inactivator.	170
4-2.	Possible oxidation of ( <i>S</i> )-2-amino-4-oxo-5-hydroxypentanoic acid by yeast HSD in the presence of NAD(P) <sup>+</sup> .	197
4-3.	Possible mechanisms for NAD-RI-331 adduct formation.	198

## LIST OF ABBREVIATIONS

ACP	acyl carrier protein
ADP	adenosine diphosphate
AIDS	acquired immunodeficiency syndrome
AK	aspartate kinase (EC 2.7.2.4 )
AKHSD	aspartokinase-homoserine dehydrogenase (EC 2.7.2.4 and EC 1.1.1.3)
AMP	adenosine monophosphate
APAD	3-amino-pyridine adenosine dinucleotide
ASA	<i>L</i> -aspartate $\beta$ -semialdehyde
ASD	aspartate semialdehyde dehydrogenase (EC 1.2.1.11)
ATP	adenosine triphosphate
CAPS	3-[cyclohexylamino]-1-propanesulfonic acid
CHES	2-[N-cyclohexylamino]ethanesulfonic acid
DEPC	diethyl pyrocarbonate
DTT	dithiothreitol
DMSO	dimethyl sulfoxide
EDC	1-ethyl-3-[3-dimethylaminopropyl]-carbodiimide
FAD	flavin adenine dinucleotide
FMN	flavin mononucleotide

HEPES	N-[2-hydroxyethyl]piperazine-N'-[2-ethanesulfonic acid]
HIV	human immunodeficiency virus
HK	homoserine kinase (EC 2.7.1.39)
HPLC	high performance liquid chromatography
HSD	homoserine dehydrogenase (EC 1.1.1.3)
H <sub>2</sub> S	hydrosulfuric acid
Hse	homoserine
Ile	isoleucine
IPP	isopentenyl pyrophosphate
MES	2-[N-morpholino]ethane-sulfonic acid
Met	methionine
NAD <sup>+</sup>	nicotinamide adenine dinucleotide
NADP <sup>+</sup>	nicotinamide adenine dinucleotide phosphate
P <sub>i</sub>	inorganic phosphate
PLP	pyridoxal phosphate
PMSF	phenylmethanesulfonyl fluoride
PP <sub>i</sub>	inorganic pyrophosphate
RI-331	(S)-2-amino-4-oxo-5-hydroxypentanoic acid
SAM	S-adenosyl methionine
TAPS	N- <i>tris</i> [hydroxymethyl]methyl-3-amino-propanesulfonic acid
THF	tetrahydrofolate
Thr	threonine

TLC	thin layer chromatography
TNM	tetranitromethane
Tris	<i>tris</i> (hydroxymethyl)-aminomethane

## **CHAPTER 1**

### **Introduction**

## 1.1 Literature Review

### 1.1.1 Fungal disease

Hospital-acquired infections in general are a serious concern in healthcare today. Fungi are rapidly joining bacteria as a leading cause of nosocomial infections. *Candida albicans* was reported to be the fourth major cause of nosocomial infections (Stencel, 1999) and fungi accounted for 40% of deaths due to hospital-acquired infections (Sternberg, 1994). The dramatic increase in frequency of fungal infections was demonstrated in studies in which the number of infected patients doubled in just a decade (1980-1990) (Hazen, 1995; Sternberg, 1994; Viscoli *et al.*, 1997). Furthermore, the variety of species responsible for these infections is broadening, as illustrated with fungi of the genus *Candida*. The number of medically important *Candida* species increased from 5 in 1963 to greater than 17 in 1995 (Hazen, 1995). Fungal infections are also almost three times more fatal than bacterial and viral infections (Dixon *et al.*, 1996).

Several primary pathogens which infect healthy individuals such as *Coccidioides immitis* do exist, however, the majority of fungal infections are due to opportunistic pathogens which infect immunosuppressed patients (Dixon *et al.*, 1996). Consequently, increasing numbers of immunocompromised patients (AIDS, chemotherapy, organ transplant patients, low birth weight babies and the elderly) are the main reason for the higher incidence of fungal infections. Improved treatments against AIDS and cancer are leading to longer survival of immunocompromised individuals. In addition, aggressive

immunosuppressive therapy for organ recipients, exposure to broad-spectrum antibacterial agents and more invasive medical procedures are also predisposing patients to fungal infections (Georgopapadakou and Walsh, 1996; Hazen, 1995; Dixon *et al.*, 1996; Alexander and Perfect, 1997). Unfortunately, fungal infections in immunocompromised hosts are more often life-threatening (Viscoli *et al.*, 1997).

The important emerging fungal pathogens are *Candida albicans*, *Cryptococcus neoformans* and *Pneumocystis carinii* (Dixon *et al.*, 1996). Patients undergoing chemotherapy for cancer or immunosuppression for organ transplant are commonly infected by *Candida* or *Aspergillus* species (Armstrong, 1993; Alexander and Perfect, 1997). Systemic invasive candidiasis often results from infection of intravenous catheters or can simply be obtained through the gastrointestinal tract (Armstrong, 1993). *Candida* is one of the more important yeasts involved in bloodstream infections (Hazen, 1995) and the most frequent isolates are *C. albicans* and *C. tropicalis*, as well as *C. glabrata*, *C. parapsilosis*, *C. guilliermondii* and *C. krusei* (Hazen, 1995; Ribaud, 1997). *C. albicans* infections were discovered predominantly in solid tumor patients, whereas infections due to other *Candida* species were more prevalent among patients with haematological malignancies (Viscoli *et al.*, 1997). Lastly, mortality rates of hospitalised patients with candidiasis are approximately 50% (Ribaud, 1997).

On the other hand, invasive pulmonary aspergillosis is the leading cause of mortality in cancer patients (Viscoli *et al.*, 1997). Mortality rates are in the range of 60-85% and are caused mostly by *Aspergillus fumigatus* and *Aspergillus flavus* (Ribaud, 1997). Other diseases such as invasive mucormycosis also cause pulmonary or brain

lesions (Armstrong, 1993). A major complication in diagnosing invasive fungal disease is the difficulty in detecting these organisms in blood or sputum cultures. Sputum cultures are positive in only one third of cases of aspergillosis and blood cultures are positive for only around 50% patients with invasive fungal disease (Armstrong, 1993). Despite successful treatment of cancers, survival of the patient is frequently threatened by invasive fungal infections (Ribaud, 1997).

The largest group of immunocompromised patients are those infected with HIV (Myskowski *et al.*, 1997). These individuals are commonly afflicted by fungal diseases such as oral candidiasis, *Pneumocystis carinii* pneumoniae (PCP), cryptococcosis, coccidioidomycosis and histoplasmosis (Dixon *et al.*, 1996; Georgopapadakou and Walsh, 1996; Myskowski *et al.*, 1997). Ninety percent of AIDS patients will suffer from oropharyngeal or oesophageal candidiasis (thrush) (Alexander and Perfect, 1997), which is one of the first signs of HIV (Myskowski *et al.*, 1997). The more serious infections threatening AIDS patients, however, are the invasive fungal infections. Cryptococcal meningitis caused by the organism *Cryptococcus neoformans* is the most lethal infection for this group of individuals (Armstrong, 1993; Alexander and Perfect, 1997), whereas, PCP was found to be the most common cause of death among these patients (Georgopapadakou and Walsh, 1996).

Although infections by opportunistic pathogens are prevalent, an increasing number of infections are discovered to be caused by primary pathogens such as *Histoplasma capsulatum* or *Coccidioides immitis*. These infections are caused by soil fungi found in Central and South America, as well as in parts of North America



(Armstrong, 1993). As a consequence, histoplasmosis is the leading opportunistic infection in AIDS patients in Indianapolis (Sternberg, 1994). *H. capsulatum* is usually found in mycelial form in the soil but, upon infection, the yeast form prevails. In healthy individuals, this organism can cause problems ranging from mild flu-like symptoms to chronic lung disease. Since *H. capsulatum* can be dormant, most people are not aware of their infection until immunosuppression permits the infection to become a serious condition. Invasive histoplasmosis appears to be a threat predominantly to T cell-deficient individuals, and, more specifically, to individuals whose CD4+ T cell levels are less than 200 per microliter (Deepe, 1997).

In 1994, a ten-fold increase in the incidence of coccidioidomycosis occurred in California due to the release of *Coccidioides immitis* from the soil during the Northridge earthquake (Sternberg, 1994; Dixon *et al.*, 1996; Graybill, 1996). This fungus is similar to *H. capsulatum* in that it can infect healthy individuals and lay dormant until immunosuppression occurs (Armstrong, 1993). Furthermore, many other species are now emerging as serious hazards and, thus, are being isolated with higher frequency such as *Malassezia*, *Rhodotorula*, *Hansenula* and *Trichosporon* (Hazen, 1995).

In agriculture, fungi are the most important group of plant pathogens. Fungal diseases cause post-harvest spoilage resulting in crop losses worth billions of dollars annually. Crop destruction by fungi has led to serious food shortages in the past affecting large populations (Timberlake and Marshall, 1989). For example, *Pytophthora infestans* was responsible for the Irish potato famine in the nineteenth century (Kendrick, 1985). Recently, new strains of this organism has reemerged in Canada and the United States,

some of which were found to be resistant to current fungicides (Fry and Goodwin, 1997). Therefore, the control of fungal infections in crops all over the world is also a serious issue in agriculture.

### *1.1.2 Antifungal drugs in current use*

The major classes of antifungal agents in clinical use today are the polyenes, the azoles and the pyrimidine analogs. Others drugs such as morpholines, allylamines, thiocarbamates and griseofulvin are used mainly for the treatment of infections of the nail, skin and hair (dermatophytes) (Speed, 1996).

The polyene class of antifungal drugs include amphotericin B, nystatin and natamycin (Figure 1). Amphotericin B, a natural product from *Streptomyces* species, is often the drug of choice for serious invasive disease, whereas, nystatin and natamycin are used only in topical antifungal preparations (Bennett, 1990; Speed, 1996). These compounds are broad spectrum, fungicidal agents which act by binding ergosterol in the fungal cell membrane. The binding of polyenes leads to the disruption of the cell membrane and increased cell permeability causing cell death (Bennett, 1990; Georgopapadakou and Walsh, 1996; Hay, 1994). Oxidative damage by amphotericin B is also thought to be a very important factor in fungal cell toxicity (Hartsel and Bolard, 1996).

Amphotericin B is frequently used as a drug of last resort for many life-threatening invasive fungal infections. It is effective against organisms such as *Candida*,

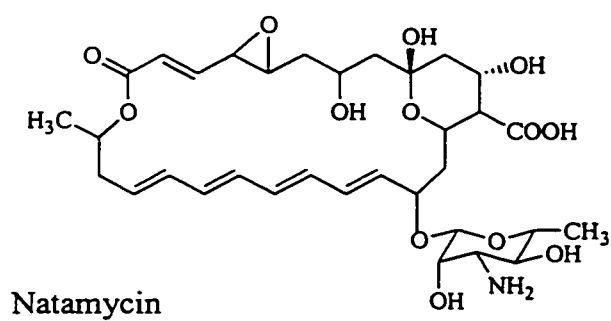
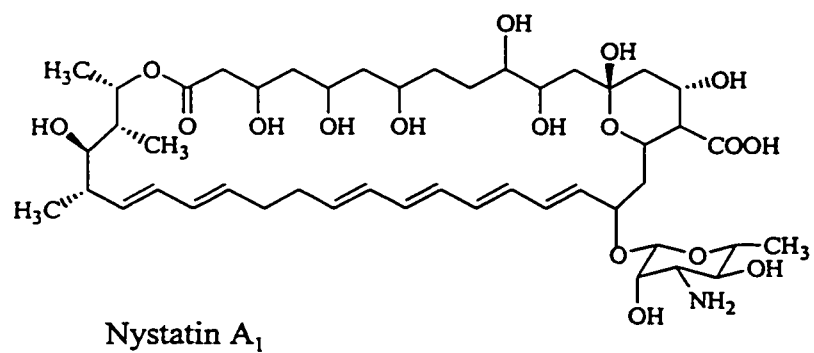
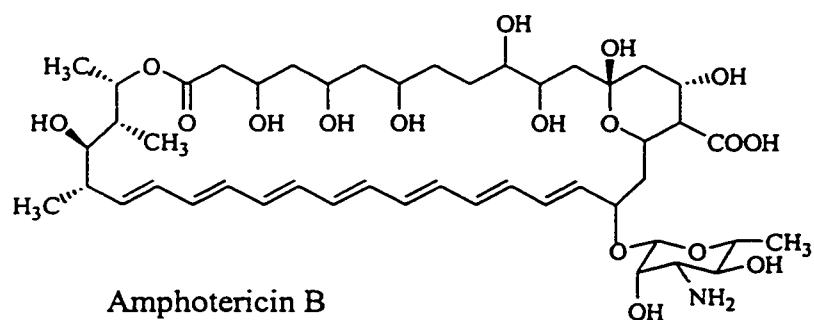


Figure 1. The polyene class of antifungal agents

*Cryptococcus*, *Aspergillus*, *Blastomyces*, *Histoplasma* and *Coccidioides* (Bennett, 1990; Kauffman and Carver, 1997a; Ribaud, 1997; Speed, 1996). The response rate for cancer patients suffering from invasive candidiasis is 50-75 % (Armstrong, 1993). Furthermore, amphotericin is often combined with the pyrimidine analog flucytosine (Figure 4) for treatment of cryptococcal meningitis (Armstrong, 1993; Viscoli *et al.*, 1997).

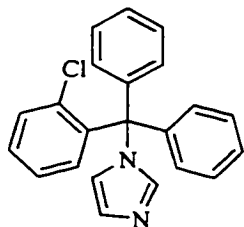
Although amphotericin B is customarily called the “gold” standard for antifungal therapy, its use is complicated by severe side effects. The lack of specificity of this drug results in high toxicity to mammalian cells. The immediate effects of amphotericin B administration are fever, chills and rigors. Other side effects include anaemia, nausea, phlebitis and hypertension (Bennett, 1990; Hartsel and Bolard, 1996; Hay, 1994; Ribaud, 1997; Speed, 1996). The most serious side effect of amphotericin B, however, is nephrotoxicity. Decreased kidney function usually appears later in the therapy and its risk increases with higher doses of amphotericin B (Hay, 1994; Speed, 1996).

In order to improve the specificity of amphotericin B and reduce its side effects, lipid formulations have been developed. Amphotericin B has been incorporated into liposomes, sheets of lipids or small lipid disks, thereby forming liposomal amphotericin B (AMBL) (AmBisome<sup>®</sup>), Amphotericin B lipid complex (ABLC) (Abelcet<sup>®</sup>) and amphotericin B colloidal dispersion (ABCD) (Amphocil<sup>®</sup>, Amphotec<sup>®</sup>), respectively. Lipid-associated amphotericin B delivery appears to drastically reduce toxicity, more importantly decreasing the occurrence of nephrotoxicity (Georgopapadakou and Walsh, 1996; Graybill, 1996; Hartsel and Bolard, 1996; Hay, 1994; Kauffman and Carver, 1997a). Moreover, liposomal amphotericin B formulations were effective against

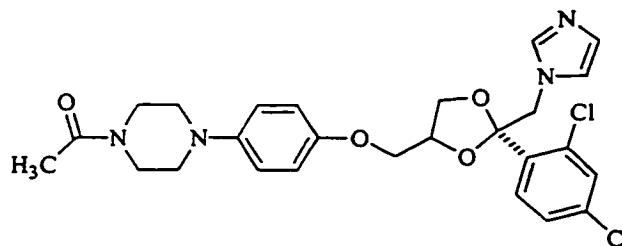
cryptococcal meningitis and severe aspergillosis (Hay, 1994). The mechanism for increased specificity, however, is unclear. Lipid-associated amphotericin B may have higher affinity for ergosterol than for cholesterol. Alternatively, amphotericin B may be gradually released from the lipid, thereby decreasing the number of non-specific interactions, or lipids may cause a more selective transfer to the fungal membrane (Hartsel and Bolard, 1996). The only disadvantage of using these preparations, however, is their manufacturing costs (Hay, 1994; Kauffman and Carver, 1997a). Chemical derivatives of amphotericin B, such as methyl esters, are also being examined for reduction in side effects (Hartsel and Bolard, 1996).

The azole class of antifungal drugs are likewise widely used against fungal infection. This class is composed of the imidazoles, which include clotrimazole, miconazole and ketoconazole, and the triazoles, which include fluconazole and itraconazole (Figure 2). Azoles, which act by inhibiting the biosynthesis of ergosterol, have broad spectrum, fungistatic activity. Inhibition of cytochrome P450-dependent sterol 14 $\alpha$ -demethylase (Figure 7) by azoles leads to depletion of ergosterol and accumulation of 14 $\alpha$ -methyl sterols, thereby disrupting the fungal cell membrane (Georgopapadakou and Walsh, 1996; Bennett, 1990; Kauffman and Carver, 1997a,b; Speed, 1996).

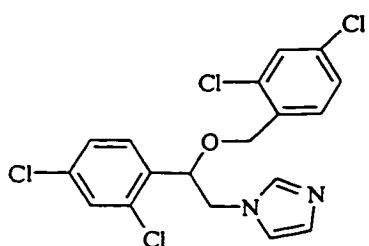
The newer azoles, fluconazole, itraconazole and ketoconazole, are used frequently to treat serious fungal infections, whereas miconazole and clotrimazole are used mostly for topical treatments. Fluconazole is an oral drug which is more effective than ketoconazole against invasive and mucocutaneous candidiasis, coccidioidal

**A. Imidazoles**

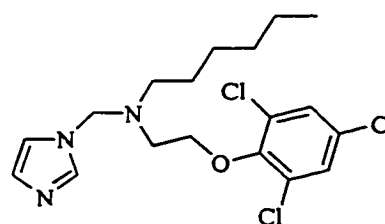
Clotrimazole



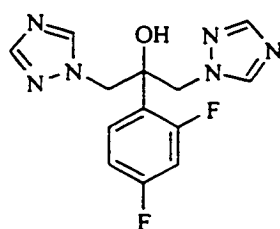
Ketoconazole



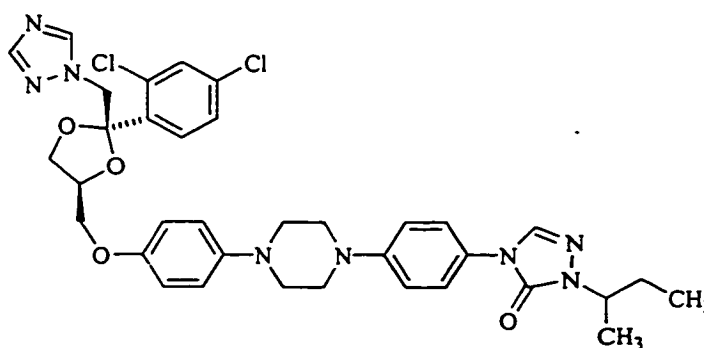
Miconazole



Prochloraz

**B. Triazoles**

Fluconazole



Itraconazole

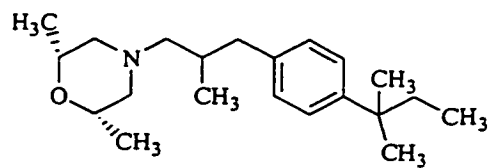
**Figure 2. The azole class of antifungal agents**

meningitis and cryptococcal meningitis (Bennett, 1990; Kauffman and Carver, 1997a,b). On the other hand, fluconazole is ineffective against aspergillosis or mucormycosis (Graybill,1996; Kauffman and Carver, 1997b; Speed, 1996). Unlike fluconazole, ketoconazole cannot be used against cryptococcal meningitis as it does not penetrate to the cerebral spinal fluid (Kauffman and Carver, 1997a,b). This drug is used mainly for mucocutaneous candidiasis, histoplasmosis, coccidioidomycoses and blastomycosis (Bennett, 1990; Kauffman and Carver, 1997a,b; Speed, 1996). Finally, itraconazole is the only azole active against *Aspergillus* (Graybill,1996; Speed, 1996). This drug is also used for non life-threatening histoplasmosis and blastomycosis (Kauffman and Carver, 1997a,b).

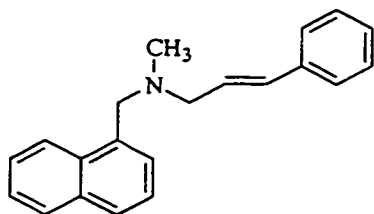
Triazoles are generally well tolerated drugs since they have lower affinity for mammalian cytochrome P450s (Hay, 1994). Some endocrinological disorders may occur due to their effect on steroid biosynthesis; however, side effects are usually limited to gastrointestinal discomfort, nausea, vomiting, headache and rash (Bennett, 1990; Kauffman and Carver, 1997b).

In addition, 14 $\alpha$ -demethylase is the primary site of action for important fungicides in agriculture (prochloraz (Figure 2), cyproconazole, tebuconazole). An estimated 1 million kg of azoles are used to treat cereal crops in the UK every year (Hollomon, 1993) and azoles make up 25% of fungicides in the world market (Joseph-Horne and Hollomon, 1997).

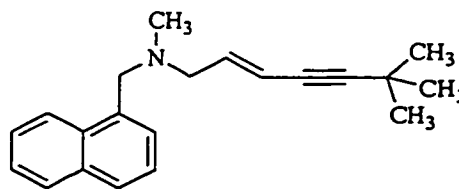
Ergosterol biosynthesis is an important target for antifungal activity as demonstrated by the azoles. Morpholines, allylamines and thiocarbamates likewise target

**A. Morpholines**

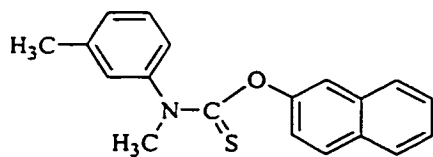
Amorolfine

**B. Allylamines**

Naftifine



Terbinafine

**C. Thiocarbamates**

Tolnaftate

**Figure 3. The morpholine, allylamine and thiocarbamate classes of antifungal agents**



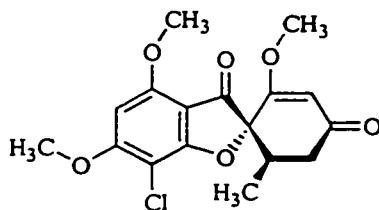
ergosterol biosynthesis, leading to the disruption of fungal cell membranes. Morpholines such as amorolfine (Figure 3) inhibit  $\Delta^{14}$  reductase and  $\Delta^7$ - $\Delta^8$  isomerase (Figure 7) (Georgopapadakou and Walsh, 1996), whereas allylamines (naftifine, terbinafine) and thiocarbamates (tolnaftate) (Figure 3) are reversible inhibitors of squalene-2,3-epoxidase (Figure 7) (Bennett, 1990; Georgopapadakou and Walsh, 1996). These agents, however, are used mostly for topical treatments of dermatophytes (Bennett, 1990; Hay, 1994; Speed, 1996) and morpholines are also used as agricultural fungicides (Georgopapadakou and Walsh, 1996).

Flucytosine is a pyrimidine analog (Figure 4) which is converted in fungi to 5-fluorouridine triphosphate and 5-fluorodeoxyuridine monophosphate (Alexander and Perfect, 1997). Subsequently, the nucleotide is incorporated into RNA, thereby causing RNA misreading. In addition, the deoxynucleotide is a potent inhibitor of thymidylate synthetase. Flucytosine is used mainly in combination with amphotericin B for cryptococcal meningitis and invasive candidiasis, since it has a limited spectrum of antifungal activity and a high occurrence of fungal resistance (Alexander and Perfect, 1997; Bennett, 1990; Georgopapadakou and Walsh, 1996). Toxicity from this drug is fairly low since mammalian cells cannot deaminate flucytosine. Nonetheless, administration of flucytosine may lead to nausea, vomiting and diarrhea (Bennett, 1990; Georgopapadakou and Walsh, 1996).

Lastly, griseofulvin (Figure 4) is another class of antifungal drugs, used primarily against dermatophytes. Its fungistatic activity is a result of inhibition of fungal mitosis and nucleic acid synthesis (Bennett, 1990; Speed, 1996).

**A. Pyrimidine analog**

Flucytosine

**B. Others**

Griseofulvin

**Figure 4. Other classes of antifungal agents**

In conclusion, serious life-threatening fungal infections are treated primarily with amphotericin B and azoles. Choices for antifungal therapy are very limited when compared to the number of antibacterial drugs available (Georgopapadakou and Walsh, 1996).

The usefulness of amphotericin B is restricted by its severe side effects, and the efficacy of azoles against fungal infections in medicine and agriculture is diminishing due to fungal resistance (Hollomon, 1993; Kauffman and Carver, 1997a,b). Therefore, it is evident that a shortage of selective effective antifungal drugs currently exists in both medicine and agriculture.

### *1.1.3 Antifungal drug resistance*

When fungal infections are not responsive to high concentrations of antifungal drugs, the fungus is said to be resistant. Primary or intrinsic resistance occurs without prior exposure to the drug, whereas secondary or acquired resistance develops after exposure to the drug (Alexander and Perfect, 1997). The use of antifungals is believed to create a selective pressure for resistant organisms (Klepser *et al.*, 1997).

Resistance to polyenes such as amphotericin B is relatively uncommon in medicine. Nonetheless, compounds which cause the depletion of ergosterol in the fungal cell membrane may also induce fungal resistance to polyenes (Alexander and Perfect, 1997; Klepser *et al.*, 1997; White, 1996). On the other hand, secondary resistance to flucytosine is very frequent. The mechanism of flucytosine resistance involves the loss of cytosine permease, cytosine deaminase or uridine monophosphate pyrophosphorylase, the

latter of which is most common in *C. albicans*. Resistance may also be a result of increased *de novo* pyrimidine synthesis in the fungi (Alexander and Perfect, 1997). Consequently, flucytosine is used chiefly in combination with other antifungal drugs (Alexander and Perfect, 1997; Bennett, 1990; Georgopapadakou and Walsh, 1996).

Fungal resistance to azoles is a currently emerging problem both in medicine and agriculture. Azole resistance initially appeared in agriculture in the early 1980s. Barley crops in Scotland and other areas of the U.K. were infected with resistant powdery mildews. Soon thereafter, azole resistance appeared in several other important plant pathogens (Hollomon, 1993). Clinically, azole resistance is increasingly more frequent, especially with *C. albicans* infections in HIV patients (Hitchcock, 1993; Kauffman and Carver, 1997a,b; Klepser *et al.*, 1997; White, 1996). Resistance is often a consequence of treatment or prevention of mucocutaneous candidiasis with low doses of fluconazole over a long period of time. Since azoles are merely fungistatic, host immunity plays an important role in eliminating the fungal infection. In the case of immunocompromised patients, infections often reoccur and are less susceptible to azoles than previously (Alexander and Perfect, 1997; Hitchcock, 1993). Some species of *Candida*, such as *C. glabrata* and *C. krusei*, are intrinsically resistant to several azoles and, therefore, must be treated by other classes of drugs (Alexander and Perfect, 1997; Kauffman and Carver, 1997a,b; White, 1996). Furthermore, resistance to one azole drug can have large implications, since it will usually lead to cross-resistance to other azoles (Hitchcock, 1993; Hollomon, 1993).

The molecular basis of azole resistance is currently not very well defined (Joseph-Horne and Hollomon, 1997). However, several mechanisms are believed to be involved. Point mutations in the target enzyme sterol P450 14 $\alpha$ -demethylase may lead to inactive enzyme or decreased inhibitor binding. Inactive enzyme, as with azole inhibition, causes the accumulation of methyl sterols, which is lethal. However, a suppressor mutation of  $\Delta^{5,6}$  sterol desaturase induces the accumulation of 14 $\alpha$ -methylfecosterol, which can substitute for ergosterol in the cell membrane. Organisms containing these mutations may demonstrate resistance to polyenes as sterol composition of the cell membrane would be altered. Nonetheless, these mutations are found only in laboratory strains and are generally not found in clinical isolates (Hitchcock, 1993; Joseph-Horne and Hollomon, 1997). On the other hand, some resistant strains of *C. albicans* and the phytopathogens *Ustilago maydis* and *Penicillium italicum* have demonstrated decreased affinity of the target enzyme for azoles (Hitchcock, 1993; Joseph-Horne *et al.*, 1995; Joseph-Horne and Hollomon, 1997). Overexpression of lanosterol P450<sub>14 $\alpha$ DM</sub> 14- $\alpha$ -demethylase may also lead to decreased susceptibility of fungi to azoles. Gene amplification of the target enzyme was discovered to be partially responsible for intrinsic resistance of *C. glabrata* (Hitchcock, 1993; Joseph-Horne and Hollomon, 1997).

In most cases, however, clinical azole resistance appears to correlate with decreased intracellular accumulation of the drug. This may result either from reduced fungal cell membrane permeability or overexpression of energy-dependent efflux pumps. The latter mechanism was found to be predominant in resistant *Candida* species. Two

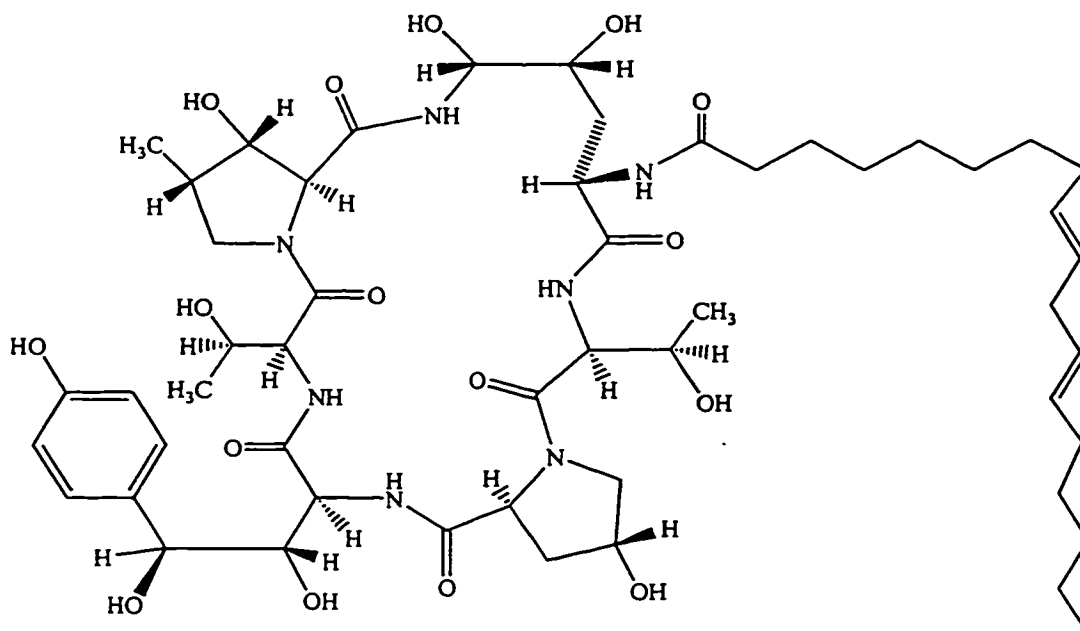
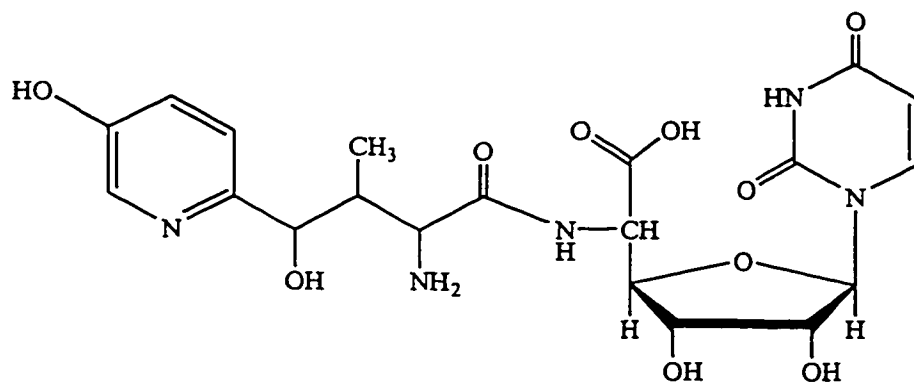
superfamilies of multidrug resistance proteins (MDR) are believed to be involved, ATP-binding cassette transporters (ABC transporters, CDR1) and major facilitators (BEN<sup>r</sup>). Energy is required in both cases, either in the form of ATP or a proton gradient (Alexander and Perfect, 1997; Klepser *et al.*, 1997; Joseph-Horne and Hollomon, 1997; White, 1996). The corresponding genes for these proteins (CDR1, BEN<sup>r</sup>) have been isolated from *C. albicans* (Alexander and Perfect, 1997) and were discovered to be overexpressed in fluconazole-resistant isolates obtained from AIDS patients (Joseph-Horne and Hollomon, 1997). CDR1 appears to transport most azole drugs, which would explain azole cross resistance (Klepser *et al.*, 1997; White, 1996). Moreover, cross resistance could occur with newly developed drugs if they are also substrates for these efflux pumps (White, 1996). Nonetheless, the development of novel antifungal drugs which attack different cellular sites in fungi and investigations into molecular mechanisms of antifungal resistance are critical in order to provide sufficient treatment for life-threatening fungal diseases.

#### *1.1.4 Search for new antifungal targets*

A number of fungal targets are currently being examined, however, the fungal cell wall and cell membrane continue to be the main focus of research. In order to design non-toxic antifungal drugs, it is important to select targets specific to fungi. These targets should also be essential for fungal viability, thereby creating fungicidal agents. The fungal cell wall is a good target for antifungal drugs, since it is both necessary for fungi

and lacking in mammals and plants (Georgopapadakou and Walsh, 1996; Gozalbo, 1993; Kurtz, 1998).

The major components of the fungal cell wall are  $\beta$ -glucan, chitin and mannoproteins.  $\beta$ -Glucan and chitin, which are homopolymers of glucose and N-acetylglucosamine, respectively, are responsible for the shape and strength of the cell wall. Biosynthesis of  $\beta$ -glucan can be blocked by echinocandins (Figure 5) (including pneumocandins and papulocandins), which are noncompetitive inhibitors of 1,3- $\beta$ -glucan synthase (Georgopapadakou and Walsh, 1996; Groll *et al.*, 1998; Kurtz, 1998). These compounds demonstrate fungicidal activity; however, they are not active against *C. neoformans* (Graybill, 1996; Kauffman and Carver, 1997a). Similarly, nikkomycins (Figure 5) and polyoxins are competitive inhibitors of chitin synthase (Georgopapadakou and Walsh, 1996; Groll *et al.*, 1998) and demonstrate narrow spectrum fungicidal activity (Alexander and Perfect, 1997; Graybill, 1996; Kauffman and Carver, 1997a). Lastly, mannoproteins form the outer layer of the cell wall, covering the fibrous  $\beta$ -glucan and chitin network (Groll *et al.*, 1998). These molecules are not believed to be good targets for antifungal drugs, since mannoproteins have a variety of structures and are not necessary for fungal viability (Kurtz, 1998). Nonetheless, pradimicins, which are fungicidal compounds, act by forming complexes with mannoproteins (Georgopapadakou and Walsh, 1996; Groll *et al.*, 1998; Kauffman and Carver, 1997a). Of these drugs, only echinocandins derivatives are currently under clinical trials (Georgopapadakou and Walsh, 1996; Kurtz, 1998). Furthermore, chitinase is being examined as a potential

**A. Echinocandin B****B. Nikkomycin Z****Figure 5. Antifungal agents targeting cell wall biosynthesis**



fungal target, as this enzyme is involved in cell wall elasticity (Georgopapadakou and Walsh, 1996).

The fungal cell membrane, on the other hand, is very similar to the mammalian membrane. Both are composed of phospholipids, sphingolipids and sterols (Georgopapadakou and Walsh, 1996; Groll *et al.*, 1998). The fungal cell membrane, however, contains ergosterol as opposed to cholesterol in the mammalian membrane. For this reason, ergosterol and its biosynthesis (Figures 6 and 7) have been a target of antifungal drugs for many years. Azoles block ergosterol biosynthesis at sterol 14 $\alpha$ -demethylase (Georgopapadakou and Walsh, 1996; Kauffman and Carver, 1997a,b; Speed, 1996), while allylamines/thiocarbamates and morpholines inhibit squalene epoxidase and  $\Delta^{14}$  reductase/ $\Delta^7$ - $\Delta^8$  isomerase, respectively (Georgopapadakou and Walsh, 1996). Other enzymes involved in ergosterol biosynthesis such as 2,3-oxidosqualene cyclase and  $\Delta^{24}$  methyltransferase may likewise prove useful as antifungal targets (Figure 6) (Georgopapadakou and Walsh, 1996; Groll *et al.*, 1998). Inhibitors of methyltransferase activity will likely be highly specific antifungal agents since this enzyme is lacking in mammals (Georgopapadakou and Walsh, 1996). Biosynthetic enzymes involved in presqualene steps (Figure 6), however, may not be favorable targets, since blocking these activities could also interfere with biosynthesis of essential terpenoids in mammals (Georgopapadakou and Walsh, 1996). Nonetheless, fluvastatin, which is a cholesterol-reducing agent and an inhibitor of hydroxymethylglutaryl-Coenzyme A reductase (HMG-CoA reductase) has demonstrated fungicidal activity *in vitro*. Fungicidal activity (*in vitro*) has also been shown with the squalene synthase

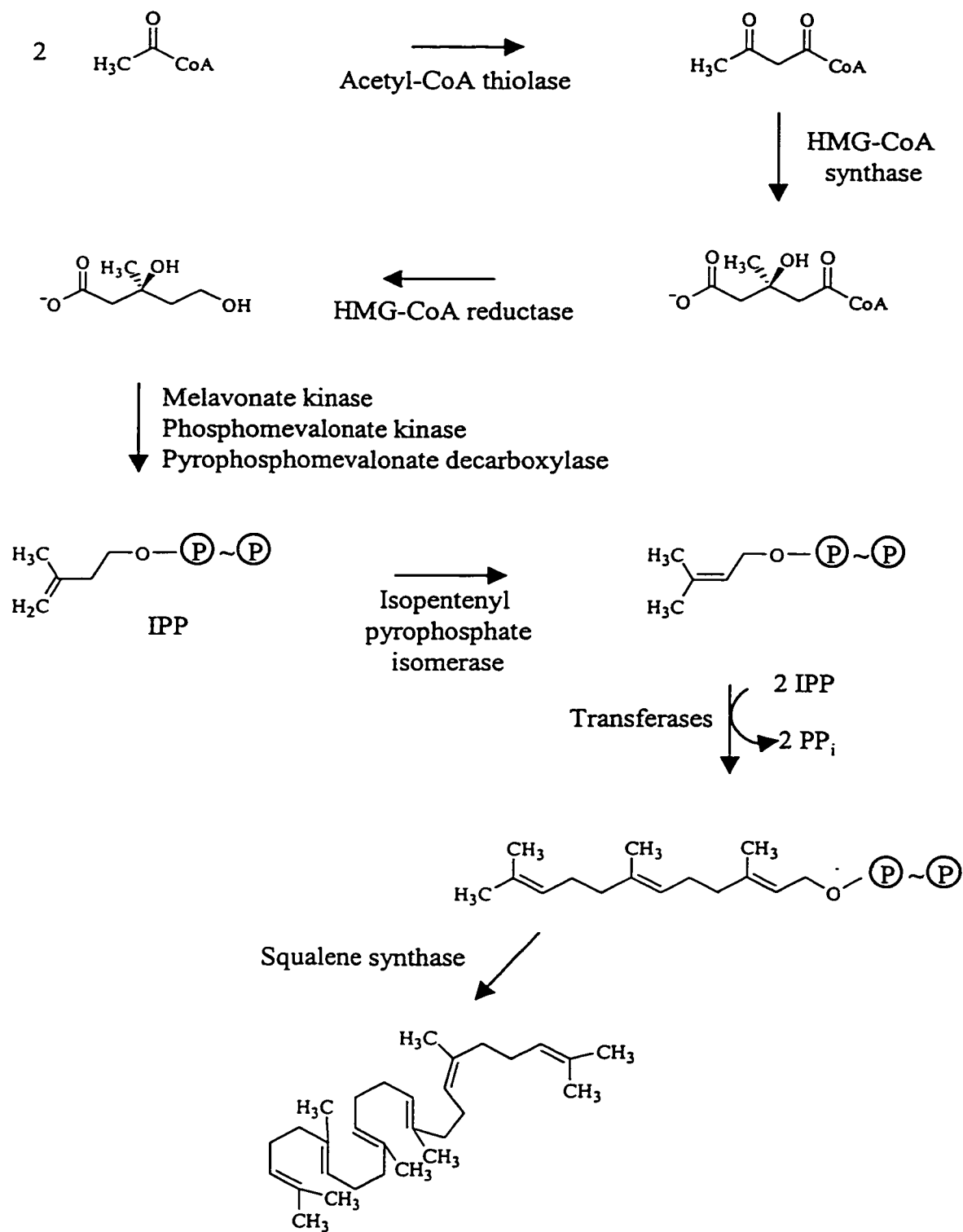


**Figure 6. The biosynthesis of squalene**

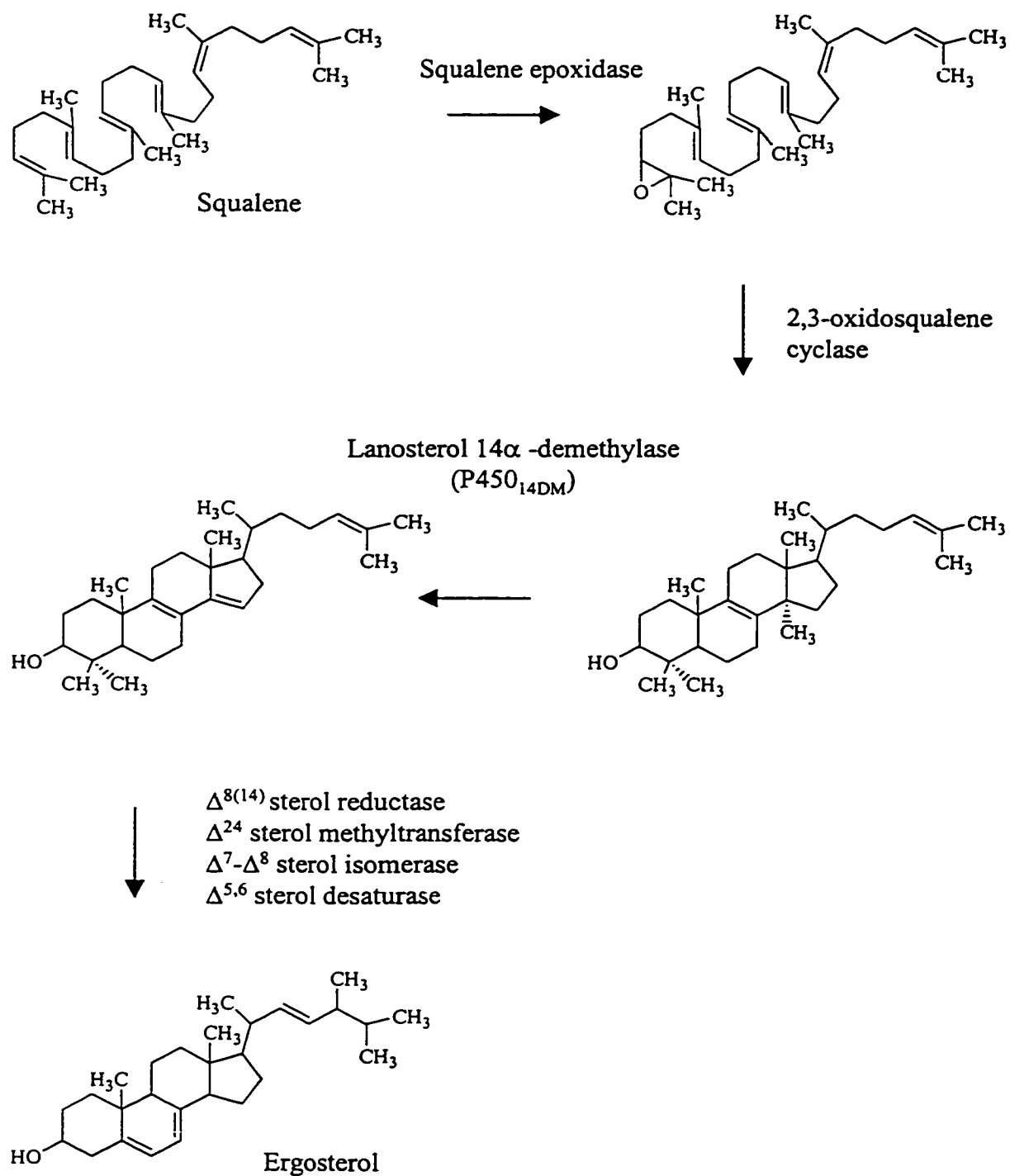


**Figure 7. The biosynthesis of ergosterol in fungi**

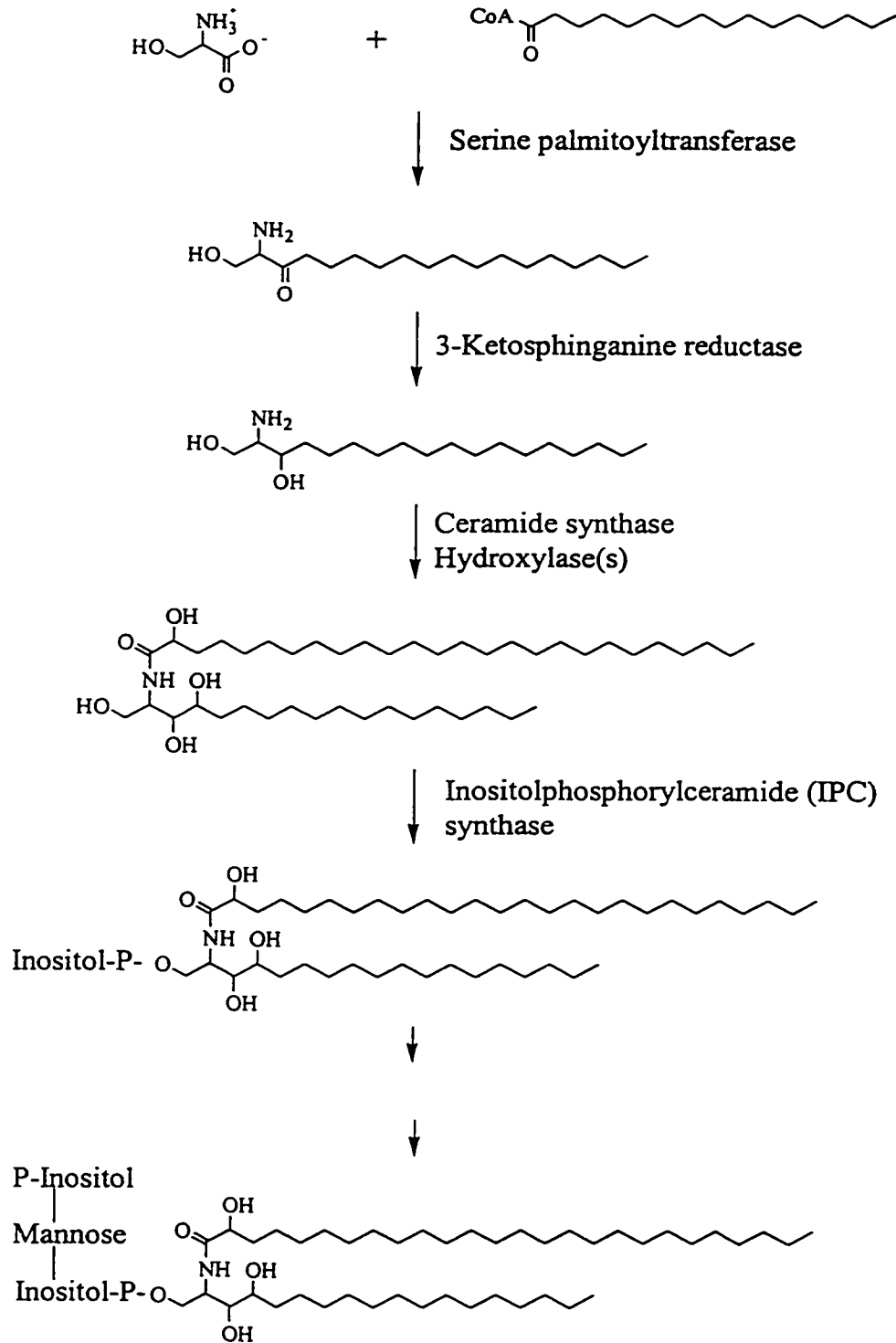


**Figure 8. The biosynthesis of sphingolipids**

inhibitors, zaragozic acids and squalostatins (Groll *et al.*, 1998). Therefore, ergosterol biosynthesis provides many targets for antifungal drugs. Another potential antifungal target is the biosynthesis of sphingolipids (Figure 8), which are essential components of both fungal and mammalian cell membranes. The first committed step in sphingolipid biosynthesis is the condensation of serine and palmitoyl CoA by serine palmitoyltransferase. This enzyme is inhibited by a number of natural products, such as sphingofungins (Georgopapadakou and Walsh, 1996; Groll *et al.*, 1998). Although these agents demonstrate broad spectrum antifungal activity (Groll *et al.*, 1998), sphingofungins also inhibit the mammalian enzyme (Zweerink *et al.*, 1992), thereby increasing the likelihood of human toxicity. On the other hand, aureobasidin A has little toxicity in mice (Endo *et al.*, 1997) and inhibits a different step in sphingolipid biosynthesis catalysed by inositolphosphorylceramide synthase (IPC synthase) (Groll *et al.*, 1998).

Aureobasidins have demonstrated antifungal activity *in vitro* against *Candida*, *Aspergillus*, *C. neoformans* and *H. capsulatum*, as well as *in vivo* against systemic candidiasis in mice (Endo *et al.*, 1997; Groll *et al.*, 1998). Since differences exist between fungal and mammalian sphingolipids, distinct steps in sphingolipid biosynthesis may be identified and determined to be good antifungal targets in the future (Georgopapadakou and Walsh, 1996).

Various fungal enzymes, such as H<sup>+</sup>-ATPase, DNA topoisomerases and fatty acid synthase, are also being examined to determine their potential as antifungal targets. H<sup>+</sup>-ATPase is a crucial component of the fungal cell membrane necessary to maintain the

transmembrane electrochemical proton gradient and intracellular pH (Georgopapadakou and Walsh, 1996; Seto-Young *et al.*, 1997). Omeprazole is a compound with antifungal activity which inhibits plasma membrane H<sup>+</sup>-ATPase by covalent interaction with the extracellular domains. Drugs attacking extracellular targets of fungi such as H<sup>+</sup>-ATPase would be advantageous, since the increased expression of multidrug efflux pumps would not confer fungal resistance (Seto-Young *et al.*, 1997). Folimycin is an antifungal agent which inhibits vesicular H<sup>+</sup>-ATPase, thereby causing disruption in protein trafficking. Nonetheless, it is unknown whether fungal and mammalian H<sup>+</sup>-ATPases are sufficiently distinct from each other to generate selective inhibition (Georgopapadakou and Walsh, 1996).

Fungal DNA topoisomerases, on the other hand, have demonstrated differing sensitivities to inhibitors when compared to mammalian topoisomerases (Shen and Fostel, 1994; Fostel *et al.*, 1996). Topoisomerase inhibitors have been used in the past as anticancer and antibacterial drugs. Therefore, compounds selective against fungal topoisomerases can likewise be used in antifungal therapies (Georgopapadakou and Walsh, 1996; Groll *et al.*, 1998; Shen and Fostel, 1994). DNA topoisomerases are ubiquitous enzymes responsible for DNA topology during DNA replication, transcription and recombination. Topoisomerase I which is ATP-independent is not essential for cell survival, whereas DNA topoisomerase II is essential and requires ATP and Mg<sup>2+</sup> (Shen and Fostel, 1994). DNA topoisomerase inhibitors cause cell death by stabilizing the covalent enzyme-DNA cleavage complex, which interferes with DNA replication (Fostel *et al.*, 1996; Groll *et al.*, 1998; Shen and Fostel, 1994). Drugs such as camptothecin and

etoposide have a greater effect on the mammalian enzymes, while podophyllotoxins and eupolauridine have larger effects on the fungal enzymes (Shen and Fostel, 1994). Currently, structural requirements for antifungal topoisomerase inhibitors are being determined (Fostel *et al.*, 1996).

Fatty acid synthase (*FAS2*) was shown to be required for virulence of *C. albicans* in a rat model of oropharyngeal candidiasis (Zhao *et al.*, 1996). When both *FAS2* genes were disrupted in *C. albicans*, the resulting strain could not cause infection in the rat model and infection could not be activated by the presence of free fatty acid. Fatty acid synthase is likewise blocked by the irreversible inhibitor cerulin. In addition, cerulin has no effect on human fatty acid synthase, demonstrating the specificity of this agent. Additional studies will determine the *in vivo* efficacy of this drug, as well as other natural product inhibitors of fatty acid synthase (Zhao *et al.*, 1996).

Recently, a gene (*INT1*) coding for a surface protein involved in virulence of *C. albicans* was identified (Gale *et al.*, 1998). Adhesion to epithelial cells and the induction of filamentous growth are believed to lead to virulence by *C. albicans*. Disruption of *INT1* in *C. albicans* produced an avirulent strain which demonstrated a 40 % decrease in adhesion to epithelial cells. On the other hand, the expression of *INT1* in *S. cerevisiae* caused adhesion onto epithelial cells (HeLa) and growth of highly polarized buds. Mice injected with *C. albicans* containing *INT1* died by day 11, whereas 90 % of mice injected with *C. albicans* containing the disrupted gene survived. This gene product (*int1p*) appears to be one of several adhesion molecules involved in virulence and may prove to be a good antifungal target (Gale *et al.*, 1998).

In addition to these targets, many other cellular processes in fungi are being investigated, such as protein synthesis, signal transduction, cell cycle regulation and the biosynthesis of nucleic acids, polyamines and amino acids, in order to determine their potential as antifungal targets (Georgopapadakou and Walsh, 1996; Groll *et al.*, 1998). As research into fungal infections increases, the number of antifungal targets will also expand. The identification of these targets and the increased understanding of their mechanisms will generate new classes of specific antifungal drugs. These agents will be critical for the treatment of fungal infections in the growing immunocompromised population, particularly in light of the current shortage of effective antifungal therapies.

#### 1.1.5 Discovery of (*S*)-2-amino-4-oxo-5-hydroxypentanoic acid

The natural product (*S*)-2-amino-4-oxo-5-hydroxypentanoic acid (RI-331) (Figure 9) from *Streptomyces* species was discovered a decade ago in a screening program for antifungal compounds. Experiments revealed that RI-331 had *in vitro* antifungal activity against several pathogens including *C. albicans* and *C. neoformans*,

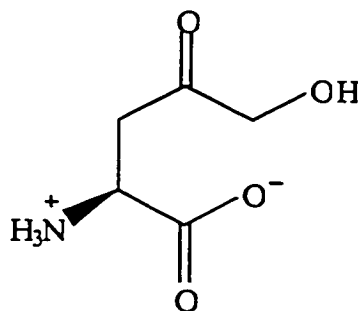


**Figure 9. Structure of (*S*)-2-amino-4-oxo-5-hydroxypentanoic acid (RI-331)**



but had no effect against *Aspergillus* sp. When administered to mice, RI-331 was rapidly absorbed orally and was well tolerated. No toxicity ( $LC_{50} > 5000$  mg/kg) or pathological or behavioural changes were demonstrated. Furthermore, survival rates for mice with systemic candidiasis increased with RI-331 treatment (100% with 100 mg/kg twice daily over 14 days) (Yamaguchi *et al.*, 1988). As a result, RI-331 has emerged as an important new lead compound in antifungal drug development and, therefore, its mode of action was investigated.

Studies into the mechanism of RI-331 revealed that it blocked the biosynthesis of the aspartate family of amino acids (methionine, isoleucine and threonine), consequently leading to the inhibition of protein synthesis. The target of RI-331 was determined to be the third enzyme in the pathway, homoserine dehydrogenase (HSD), which converts *L*-aspartate  $\beta$ -semialdehyde (ASA) to *L*-homoserine (Hse) (Figure 10). The aspartate pathway is absent in mammals, thereby explaining the high specificity of RI-331 (Yamaki *et al.*, 1990).

Further experiments demonstrated that inhibition of *Saccharomyces cerevisiae* HSD by RI-331 was noncompetitive with respect to either ASA or NADPH. Whereas in the reverse reaction ( $Hse + NADP^+ \rightarrow ASA + NADPH$ ), RI-331 inhibition was competitive with respect to Hse, implying that it is occupying the same binding site. In addition, the presence of the product,  $NADP^+$ , was essential for inhibition of HSD by RI-331 and inhibition was more pronounced in the reverse reaction than in the forward reaction. The authors stated that RI-331 inhibits yeast HSD by binding the enzyme- $NADP^+$  complex and that  $NADP^+$  is required for conformational change, thereby

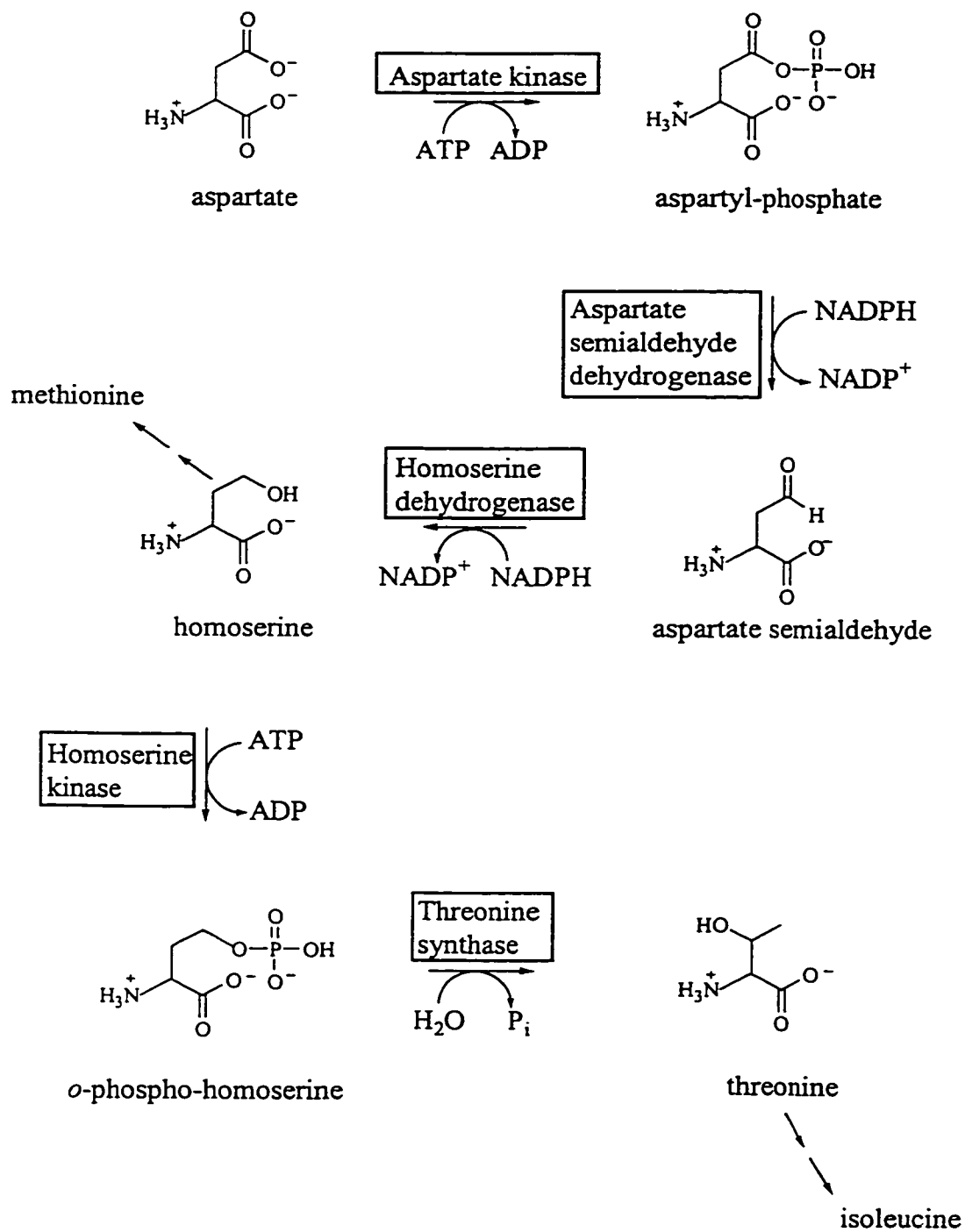


**Figure 10. The biosynthesis of the aspartate group of amino acids**

facilitating the binding of RI-331 (Yamaki *et al.*, 1992). However, the exact role of NADP<sup>+</sup> still remains unclear. A similar compound, 2-amino-4-oxo-5-chloropentanoic acid, also inactivates bacterial HSD. This affinity label formed an irreversible complex with HSD and also required the presence of NADP<sup>+</sup> (Hirth *et al.*, 1975).

Other antifungal agents targeting amino acid biosynthesis also exist. The agricultural pyrimidinamine fungicides (mepanipyridin, pyrimethanil and CGA 219417) were discovered to inhibit amino acid biosynthesis. Reversal of antifungal activity by the addition of *L*-methionine, suggested that the pyrimidinamines are inhibitors of methionine biosynthesis. Since the only methionine intermediate to reverse antifungal activity was homocysteine, cystathionine  $\beta$ -lyase (Figure 11) was determined to be the target for the pyrimidinamines. This enzyme converts cystathionine to homocysteine, which then becomes methylated to form methionine. (Masner *et al.*, 1994). In conclusion, the amino acid biosynthesis pathways, which are lacking in mammals, appear to be very promising targets for the future development of novel antifungal drugs. Consequently, the aspartate pathway was chosen for further study, in order to increase our understanding of these enzymes and, thereby, discover potent inhibitors.

#### *1.1.6 Aspartate pathway of amino acid biosynthesis*

Methionine, threonine and isoleucine are produced in bacteria, fungi and plants from the precursor amino acid, aspartate (Figure 10). Aspartate is generated by the transamination of oxaloacetate, an intermediate of the tricarboxylic acid cycle. The first committed step in the aspartate pathway is the phosphorylation of aspartate by

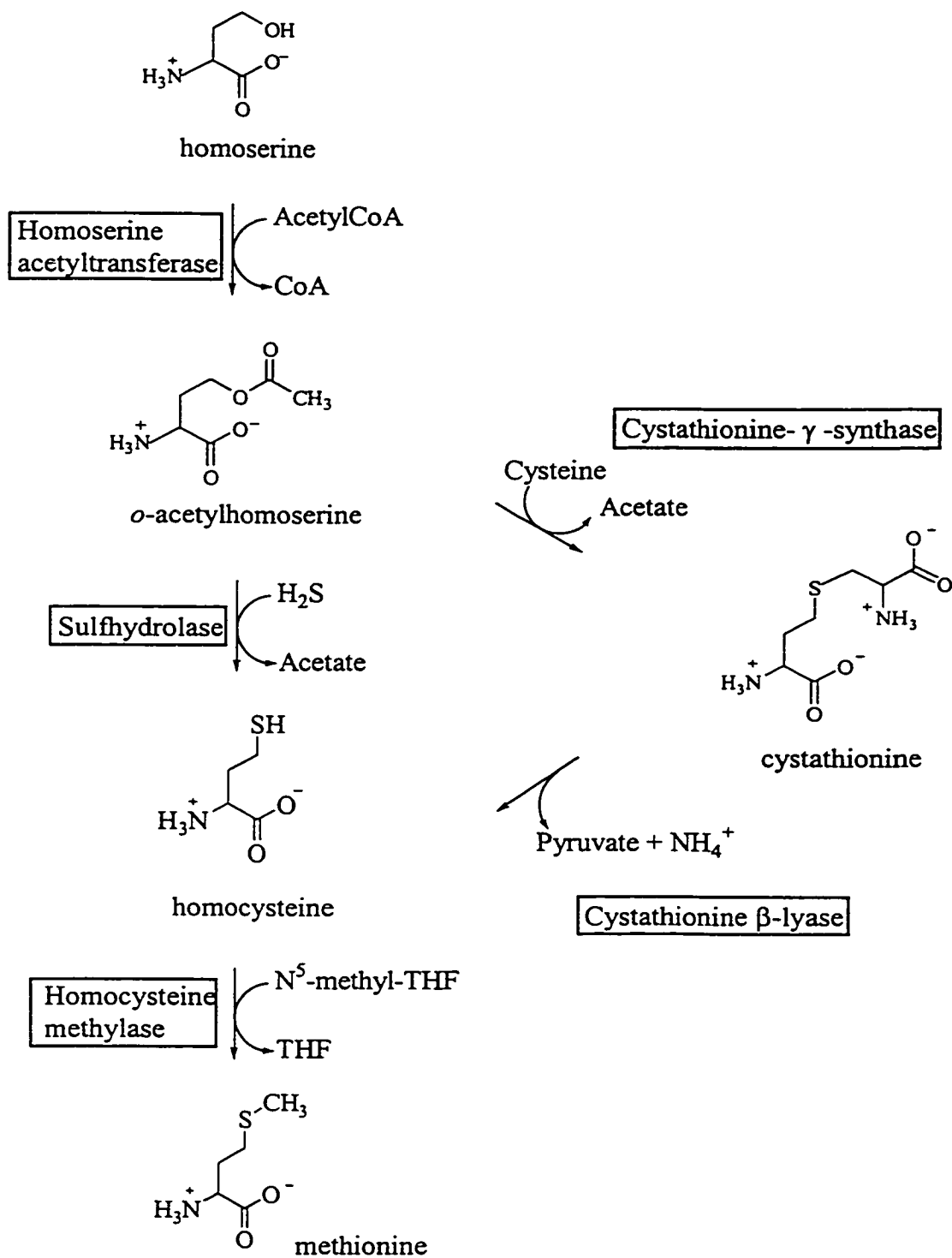


**Figure 11. The biosynthesis of methionine**

aspartate kinase (AK) (EC 2.7.2.4).  $\beta$ -Aspartyl-phosphate is then reduced to aspartate  $\beta$ -semialdehyde (ASA) in a NADPH-dependent fashion by aspartate semialdehyde dehydrogenase (ASD) (EC 1.2.1.11). This product is further reduced by homoserine dehydrogenase (HSD) (EC 1.1.1.3) to produce homoserine. At this point, the pathway branches. Methionine biosynthesis proceeds from homoserine, whereas phosphorylation of homoserine by homoserine kinase (HK) (EC 2.7.1.39) leads to the biosynthesis of threonine and isoleucine. In most fungi, lysine is produced from  $\alpha$ -ketoglutarate through the formation of saccharopine in a distinct pathway. However, in bacteria and plants, lysine biosynthesis begins with the condensation of aspartate  $\beta$ -semialdehyde and pyruvate. Therefore, in these organisms lysine may also be considered an end-product of the aspartate pathway. Finally, the aspartate pathway is absent in mammals and, therefore, the amino acids isoleucine, lysine, methionine and threonine must be obtained through the diet (Zubay, 1988). Thus, this pathway is an ideal target for antifungal agents.

#### *1.1.6.1 Escherichia coli enzymes of the aspartate pathway*

Research into the biosynthesis of the aspartate family of amino acids in *E. coli* has centered mostly on its regulation. Regulation can occur at two different levels. Certain components of the pathway may be regulated at the level of enzyme expression (repression) and/or at the level of enzyme activity (feed-back inhibition) (Ramos, *et al.*, 1991; Stadtman *et al.*, 1961). Since several amino acids are produced by the aspartate pathway, each end-product can cause downregulation of enzyme expression or activity at

different branchpoints. In addition, aspartate kinase, being the first step in this pathway, is a major site of regulation (Patte *et al.*, 1967; Stadtman *et al.*, 1961).

In *E. coli*, aspartate kinase exists in three different forms. Two of these isozymes, AK-HSD I and AK-HSD II, are bifunctional and include both aspartate kinase and homoserine dehydrogenase activities. It is believed that these activities are located in the amino-terminal domain and the carboxy-terminal domain, respectively, of the polypeptide (Zakin *et al.*, 1983). In contrast, the third isozyme, AK III, only contains aspartate kinase activity. These enzymes differ in their sensitivities to different amino acids. AK-HSD I is inhibited by threonine and repressed bivalently by threonine and isoleucine (Patte *et al.*, 1967). Inhibition by threonine is allosteric and competitive for AK with respect to both substrates and noncompetitive for HSD with respect to homoserine (Patte *et al.*, 1963; Stadtman *et al.*, 1961). The effect of threonine on HSD was demonstrated to be through AK, since agents which inactivate AK also abolish threonine inhibition of HSD (Veron *et al.*, 1973). The amino acids, cysteine and serine, have also been shown to inhibit HSD I. Since inhibition of HSD I by cysteine was competitive with respect to homoserine ( $K_i = 0.12$  mM) and heat treatment could desensitize HSD to threonine but not cysteine, cysteine and threonine are believed to occupy different sites on the enzyme. Although cysteine is not an end-product of the aspartate pathway, it is involved in a condensation reaction, leading to the formation of cystathionine in methionine biosynthesis (Datta, 1967). Serine is likewise not an end-product, however, it appears to be involved in the regulation of isoleucine biosynthesis from threonine (Hama *et al.*, 1990). In contrast, expression of AK-HSD II is repressed by

methionine, however, it is not inhibited by amino acids (Patte *et al.*, 1967). Lastly, AK III is regulated by repression and noncompetitive inhibition by the end-product, lysine (Patte *et al.*, 1967; Stadtman *et al.*, 1961).

Of these three enzymes, AK-HSD I is the most abundant in the *E. coli* K12 (Hama *et al.*, 1990) and, thus, has been the most studied. Through alternate substrate diagnostics, product inhibition and dead-end inhibition studies, the kinetic mechanism for the kinase activity was determined to be random order substrate binding, followed by an ordered release of the products, ADP and  $\beta$ -aspartyl phosphate, respectively. As for the dehydrogenase activity, initial experiments at pH 7.0 and 30°C suggested ordered binding of NADPH and aspartate  $\beta$ -semialdehyde, followed by the ordered release of homoserine and NADP<sup>+</sup> (Angeles and Viola, 1990). However, equilibrium isotope exchange studies at pH 9.0 and 37°C have determined the kinetic mechanism to be preferred order random, which may be a consequence of different reaction conditions (Wedler *et al.*, 1992). Determination of individual rate constants have shown that the kinetic mechanism is a result of the fact that dissociation of amino acids from the tertiary complex is faster than that of the cofactors (Wedler and Ley, 1993b). Furthermore, these experiments suggest that the chemical step is not rate-limiting (Wedler *et al.*, 1992).

The effects of threonine and cations on the kinetic mechanism of HSD I were also examined by equilibrium isotope exchange experiments. Threonine was found to partially inhibit HSD I catalysis without affecting substrate association and dissociation rates, thereby changing the kinetic mechanism to random order (Wedler and Ley, 1993b). AK-HSD activities are also known to be activated by monovalent cations such as Na<sup>+</sup>

and  $K^+$ . Although AK-HSD I has a higher affinity for  $Na^+$ , activation appears to be lower with  $Na^+$  than  $K^+$ . Likewise for threonine, substitution of  $Na^+$  for  $K^+$  appears to shift the kinetic mechanism of HSD I from preferred order random to nearly random. In contrast, however, this substitution changed rate constants for both catalysis and substrate association and dissociation. These effects are believed to result from conformational changes of AK-HSD I, where threonine prefers the T state (tense, less active) and  $K^+$  prefers the R state (relaxed, more active) (Wedler and Ley, 1993a).

As for the chemical mechanism of AK-HSD I, the identification of functional residues was attempted chiefly with the kinase activity. pH studies demonstrated the importance of a cationic acid with pK of 6.9 and a neutral acid with pK of 9.8 for AK activity. In chemical modification studies, reaction of AK-HSD I with diethyl pyrocarbonate (DEPC) resulted in loss of kinase activity, consistent with the modification of a histidine residue. Furthermore, protection from DEPC inactivation by aspartate implies this residue to be located in the substrate binding site. DEPC also inactivated HSD activity,. It was thought, however, to be a consequence of AK active site modification, since substrate protection was not competitive. N-Acetylimidazole and tetranitromethane, which modify tyrosine residues, also inactivated AK activity. Nevertheless, the effect of these reagents might be mostly structural, since only 3 of 6 tyrosine residues were protected by aspartate. As for HSD activity, the functional residues involved in catalysis have not been determined (Angeles *et al.*, 1989).

On the other hand, much less is known about AK-HSD II and AK III, since they are present at much lower levels in *E. coli* K12 (Hama *et al.*, 1990). AK-HSD II was



cloned and its amino acid sequence was discovered to be 31% identical to AK-HSD I (Zakin *et al.*, 1983). As for AK III, this enzyme was shown to be activated by cations such as  $K^+$  and  $NH_4^+$  (Funkhauser and Smith, 1974). AK III also demonstrated the same kinetic mechanism as the kinase activity of AK-HSD I (Shaw and Smith, 1977). The *E. coli* enzyme responsible for the second step in the aspartate pathway, aspartate  $\beta$ -semialdehyde dehydrogenase, has also been examined occasionally. Chemical modification and pH studies, as well as site-directed mutagenesis, reveal cysteine 135 to be involved in catalysis. Substitution of this residue by an alanine results in loss of enzyme activity. It is suggested that the mechanism of aspartate  $\beta$ -semialdehyde dehydrogenase is similar to that of glyceraldehyde-3-phosphate dehydrogenase and involves an attack by a cysteine thiolate to produce a thioester intermediate (Karsten and Viola, 1992). The information obtained from the *E. coli* enzymes of the aspartate pathway may increase our understanding of the homologous fungal enzymes and aid in the development of new antifungal drugs. Nevertheless, a more accurate model could be obtained by examining biosynthetic enzymes from *Saccharomyces cerevisiae*, a model fungus.

#### *1.1.6.2 Saccharomyces cerevisiae enzymes of the aspartate pathway*

Unlike in *E. coli*, the aspartate biosynthetic pathway in *S. cerevisiae* is composed of single separate proteins for aspartate kinase (AK), aspartate semialdehyde dehydrogenase (ASD) and homoserine dehydrogenase (HSD) activities. These enzymes were previously purified from yeast using a combination of heat treatment, acid treatment

and ammonium sulfate fractionation (Black and Wright, 1955a,b,c). More recently, the genes encoding these proteins have been cloned (Rafalski and Falco, 1988; Thomas *et al.*, 1993). Regulation of yeast AK and HSD by amino acids is slightly different from that in *E. coli* enzymes. AK, likewise, appears to be the major site of regulation. It is repressed bivalently by threonine and methionine and is subject to allosteric inhibition by threonine ( $K_i = 2.3$  mM) (Cherest *et al.*, 1971; Martinez-Force and Benitez, 1993; Ramos *et al.*, 1991). The threonine analog, hydroxynorvaline, also causes inhibition of AK activity (Ramos *et al.*, 1991). Threonine and methionine overproducing yeast mutants express AK which is insensitive to threonine (Martin-Rendon *et al.*, 1993; Martinez-Force and Benitez, 1993). In addition, yeast lacking the AK gene, *hom3*, contain no detectable aspartate kinase activity and require threonine and methionine for growth, suggesting the presence of only one AK enzyme (Rafalski and Falco, 1988).

Homoserine dehydrogenase (HSD) (*hom6*) expression in yeast is repressed by methionine and its activity is inhibited by methionine and threonine (Cherest *et al.*, 1971; Martinez-Force and Benitez, 1993). In some cases, methionine was a competitive inhibitor ( $K_i = 9.3$  mM) and threonine had no effect, while in other cases methionine caused noncompetitive inhibition ( $K_i = 139$  mM) and threonine caused competitive inhibition ( $K_i = 117$  mM) against homoserine (Martinez-Force and Benitez, 1993; Yumoto *et al.*, 1991). These values are significantly higher than the published  $K_m$  for homoserine (1.2 mM), suggesting that these amino acids are only weak inhibitors of yeast HSD (Yumoto *et al.*, 1991). Therefore, HSD is believed to play only a minor role in regulation of the aspartate pathway in *S. cerevisiae* (Martinez-Force and Benitez, 1993).

Several years ago, HSD was purified from yeast *as per* Black and Wright, 1955c with the addition of Matrex Gel Red A and Q-Sepharose chromatography. The resulting pure enzyme had a molecular weight of approximately 40 kD and was believed to be located in the cytoplasm (Yumoto *et al.*, 1991). The formation of dimers of identical subunits appeared to be critical for HSD activity, as determined by cross-linking analysis during enzyme renaturation. Yeast HSD was discovered to contain a NADP<sup>+</sup> consensus sequence, even though this enzyme is active with either NADH or NADPH (Yumoto *et al.*, 1991). In contrast, aspartate semialdehyde dehydrogenase (ASD) can only use NADPH or NADP<sup>+</sup> as a cofactor. Activity was highest for ASD at pH 8.0 for the forward reaction and pH 9.0 for the reverse reaction (Black and Wright, 1955b), whereas, HSD activity was greatest at pH 5.0 for NADPH and pH 6.8 for NADH in the forward direction (Black and Wright, 1955c). Salt concentration also affected HSD activity as demonstrated by a 1.5-fold increase in activity at 0.5 M KCl (Yumoto *et al.*, 1991).

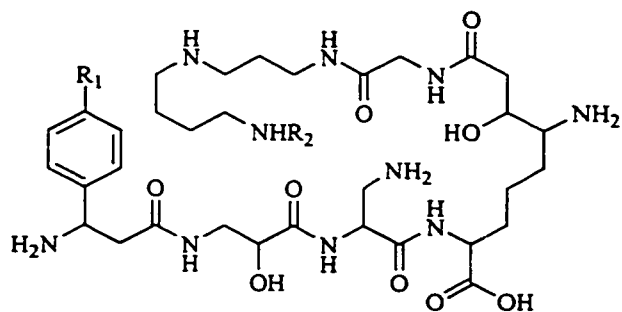
The yeast enzymes of the aspartate pathway have not been studied as extensively as the *E. coli* enzymes. The kinetic properties of AK, ASD and HSD from *S. cerevisiae* were examined in the 1950s and 1960s through Lineweaver-Burk plots. More recent investigations have focused mostly on the reverse reaction of HSD. Although understanding the *E. coli* enzymes gives insight into the mechanisms of the fungal counterparts, clearly, the enzymes from *S. cerevisiae* represent a better model of the aspartate pathway in pathogenic fungi. In addition, these enzymes are easily purified and their genes have been cloned, supplying sufficient quantities of the protein for study.

Investigations of AK, ASD and HSD from *S. cerevisiae* may lead to the future development of potent inhibitors, thereby generating specific antifungal agents.

#### *1.1.7 Biosynthesis of edeines in Bacillus brevis*

More than three decades ago, edeines secreted from *Bacillus brevis* Vm4 were discovered to possess antifungal and broad-spectrum antibacterial activity (Kurylo-Borowska, 1962). Edeines A and B (Figure 12) are short linear peptides composed of glycine, 2,3-diaminopropionic acid, spermidine or guanylspermidine, respectively, and the unusual amino acids, isoserine,  $\beta$ -tyrosine and 2,6-diamino-7-hydroxyazaleic acid (Hettinger and Craig, 1968; Hettinger *et al.*, 1968). Other edeine compounds were also discovered. Edeines D and F are identical to edeines A and B, respectively, with the exception of  $\beta$ -phenylalanine substituting for  $\beta$ -tyrosine (Figure 12) (Czerwinski *et al.*, 1983; Wojciechowska *et al.*, 1983). In the active isomers, isoserine is linked to the 2-amino group of 2,3-diaminopropionic acid, while the inactive isomers, such as edeine A<sub>2</sub> and B<sub>2</sub>, isoserine is linked to the 3-amino groups (Hettinger and Craig, 1970).

The mode of action of edeines was shown to be dependent on concentration. Low concentrations ( $10^{-6}$  M) are bacteriostatic and result in inhibition of DNA synthesis. At these concentrations, no effect was demonstrated on protein synthesis (Kurylo-Borowska, 1962). Further study determined that the inhibition of DNA synthesis by edeines is not a consequence of DNA binding nor of DNA degradation, but is due to inhibition of DNA polymerase II or III, as shown in *E. coli* (Kurylo-Borowska, 1964; Kurylo-Borowska and Szer, 1972). In contrast, edeine concentrations 100-fold higher are



Edeine	R <sub>1</sub>	R <sub>2</sub>
A	-OH	-H
B	-OH	-C(=NH)NH <sub>2</sub>
D	-H	-H
E	-H	-C(=NH)NH <sub>2</sub>

Figure 12. Structure of edeines produced from *Bacillus brevis* Vm4

bacteriocidal and cause inhibition of protein synthesis (Kurylo-Borowska and Szer, 1972). Unlike several ribosome-directed antibiotics which have affinity for the A-site (aminoacyl-t-RNA site) (Woodstock *et al.*, 1991), edeines block the P-site (peptidyl-t-RNA site) of the ribosome, thereby inhibiting the binding of the initiator aminoacyl-t-RNA (Szer and Kurylo-Borowska, 1972). Furthermore, protection of P-site-specific bases in 16S rRNA was demonstrated with edeines (Woodstock *et al.*, 1991).

In addition to antifungal and antibacterial activities, edeines were also found to possess antiviral and anticancer activities (Lacal *et al.*, 1980; Hill *et al.*, 1994). Mammalian cells demonstrate varying degrees of susceptibility to edeines (Kurylo-Borowska and Heany-Kieras, 1979). With some edeine-insensitive mammalian cells, edeines did not cross the plasma membrane. During the course of viral infection, however, permeability of these cells to edeines increased, protein synthesis was decreased and virus production was reduced (Lacal *et al.*, 1980). Edeines have also been reported to inhibit phosphatidylinositol-specific phospholipase C ( $IC_{50} = 16 \mu\text{M}$ ), an important enzyme in intracellular signal transduction. This effect may explain, in part, the inhibition by edeines of colony formation of human colon adenocarcinoma cells (Hill *et al.*, 1994). Nonetheless, edeines may not be clinically useful as they cause high toxicity in animal models (Kurylo-Borowska, 1962).

In addition to studying the mechanism of action of edeines, an understanding of the molecular mechanisms underlying edeine biosynthesis would also be helpful in the design of effective antibacterial and antifungal drugs. Edeines are synthesized non-ribosomally by a multienzyme complex (Kurylo-Borowska and Tatum, 1966; Kurylo-

Borowska and Sedkowska, 1974) similarly to other peptide antibiotics such as bacitracin, gramicidin S and tyrocidine (for a review see Kleinkauf and von Döhren, 1990). Generally, edeine synthesis involves the activation of amino acids by ATP, producing amino acid-AMP and pyrophosphate.



The activated amino acids are then attached to the multienzyme by thioester linkages. In the last step, a 4'-phosphopantetheine arm on the enzyme acts as an acceptor of the growing peptide and donor to the next thioester-linked amino acid, thereby forming the nascent peptide (Kleinkauf and von Döhren, 1990).

In 1974, Kurylo-Borowska and Sedkowska described the purification of 3 multienzyme fractions involved in edeine biosynthesis by DEAE-cellulose and Sephadex G-200 column chromatography. Of the three fractions (MW 210 kD (A), 180 kD (B) and 100 kD (C)), only fractions A and B were required for edeine synthesis. Fraction A was discovered to activate  $\beta$ -tyrosine, fraction B activated 2,3-diaminopropionic acid, isoserine, 2,6-diamino-7-hydroxyazaleic acid and glycine and fraction C also activated 2,3-diaminopropionic acid, isoserine and glycine. Both fractions A and B contained covalently bound 4'-phosphopantetheine, suggesting that edeine synthesis occurs bidirectionally (Kurylo-Borowska and Sedkowska, 1974). Unlike gramicidin S and tyrocidine synthesis, 2,6-diamino-7-hydroxyazaleic acid appears to be anchored to the multienzyme complex by the formation of an ester bond between the C-1 carboxyl group and a hydroxyl group on the enzyme. The remaining amino acids and spermidine are

subsequently added to the C-2 amine and C-9 carboxyl ends of 2,6-diamino-7-hydroxyazaleic acid until a complete molecule of edeine is formed (Kurylo-Borowska and Heaney-Kieras, 1982).

The biosynthesis of the unusual amino acid components of edeine, however, has not been determined with the exception of  $\beta$ -tyrosine. It appears that an enzyme, tyrosine  $\alpha,\beta$ -amino mutase (75 kD), is responsible for the generation of  $\beta$ -tyrosine from *L*-tyrosine in *B. brevis*. This activity was purified from *B. brevis* Vm4 some years ago by a combination of ammonium sulfate precipitation, Sephadex G200 chromatography and isoelectric focusing (Kurylo-Borowska and Abramsky, 1972). The authors stated that the only cofactor required for tyrosine  $\alpha,\beta$ -amino mutase activity was ATP. This requirement is unusual since ATP is not involved in the mechanisms of other known amino mutases. Therefore, tyrosine  $\alpha,\beta$ -amino mutase may have a unique reaction mechanism.

Lysine 2,3-aminomutase requires pyridoxal phosphate (PLP), iron and S-adenosyl methionine (SAM) for activity (Chirpich *et al.*, 1970), whereas leucine 2,3-aminomutase is adenosylcobalamin-dependent ( $B_{12}$ ) (Poston and Hemmings, 1979). Additionally, other enzymes, such as phenylalanine ammonia lyase and tyrosine ammonia lyase, make use of the electrophilic group dehydroalanine (Hanson and Havir, 1970). Tyrosine  $\alpha,\beta$ -amino mutase, nevertheless, demonstrated no requirement for any other cofactor than ATP, eliminated the mechanisms involving PLP, SAM or cobalamin (Kurylo-Borowska and Abramsky, 1972). Furthermore, tyrosine  $\alpha,\beta$ -amino mutase catalysis involves an exchange of  $\alpha$ -hydrogen, which does not occur with phenylalanine



ammonia lyase (Parry and Kurylo-Borowska, 1980). On the other hand, inhibition of tyrosine  $\alpha,\beta$ -amino mutase by carbonyl binding agents and  $\alpha$ -keto acids suggests the formation of a Schiff's base between the abstracted amino group and an active site residue. However, the role of ATP in this reaction mechanism remains unclear (Kurylo-Borowska and Abramsky, 1972).

Other experiments on tyrosine  $\alpha,\beta$ -amino mutase dealt with the abstraction of the amino group. Studies with [ $^{15}\text{N}$ ]-tyrosine revealed that only 10 % of the  $\beta$ -amino group originated from the  $\alpha$ -position. The source for the  $\beta$ -amino group was possibly  $\text{NH}_4\text{Cl}$  since it caused activation of tyrosine  $\alpha,\beta$ -amino mutase activity (Kurylo-Borowska and Abramsky, 1972). However, no further evidence of this has been shown.

In conclusion, edeines are highly useful compounds to study due to their variety of anti-infective activities (antibacterial, antifungal and antiviral). Investigations into the mode of action and the biosynthesis of such compounds will, therefore, yield a great deal of insight for the design of potent antibacterial and antifungal drugs in the future.

## 1.2 Purpose

The purpose of the work described in this thesis is to contribute to the development of novel specific antifungal agents by characterizing new antifungal targets and by studying the biosynthesis of natural antifungal drugs. The aspartate pathway is a promising new antifungal target since it is absent in mammals, eliminating the risk of drug toxicity. Homoserine dehydrogenase (HSD) was previously illustrated to be the target for the highly specific antifungal compound, RI-331. In order to develop effective inhibitors of fungal HSD, *S. cerevisiae* HSD was overproduced in *E. coli* and sufficient quantity was purified for kinetic and mechanistic evaluation. An increased understanding of fungal HSD will aid in the design of improved inhibitors. Simultaneously, several potentially inhibitory compounds were tested against yeast HSD activity. This survey could result in the discovery of a starting point in inhibitor design.

The second focus in this thesis involved the biosynthesis of a group of natural antifungal compounds. Edeines are linear peptides which demonstrate various activities including antibacterial, antifungal and antiviral. They are composed of several unique amino acids, such as  $\beta$ -tyrosine, isoserine and 2,6-diamino-7-hydroxyazaleic acid. Edeines belong to a group of peptide antibiotics which are synthesized non-ribosomally by multienzyme complexes. More interesting, however, is the synthesis of the unusual amino acid constituents such as  $\beta$ -tyrosine. The enzyme which produces  $\beta$ -tyrosine, tyrosine  $\alpha,\beta$ -amino mutase, has been studied previously, however, many aspects of its chemical mechanism are still unresolved. Therefore, an attempt was made at purifying tyrosine  $\alpha,\beta$ -amino mutase from *B. brevis* Vm4 in order to clarify its mechanism further.

Knowledge of the mechanism by which edeines are produced could prove beneficial in the design of similar antifungal compounds.

## **CHAPTER 2**

### **Characterization of Yeast Homoserine Dehydrogenase, an Antifungal Target**

**Suzanne L. Jacques, Catharine Pratt, Greg Broadhead,**

**Robert Kinach, John F. Honek and Gerard D. Wright**

## 2.1 Preface

Fungal amino acid biosynthesis was previously shown to be a target for the antifungal compound, RI-331. The antifungal activity of this compound is a result of inhibition of HSD, an enzyme involved in the biosynthesis of methionine, threonine and isoleucine. In order to develop other potent inhibitors of fungal HSD, a better understanding of this enzyme is required. Although a fair amount is known about the *E. coli* bifunctional enzyme, AK-HSD I, little is known of the properties of fungal HSD. The model enzyme, *S. cerevisiae* HSD, has been examined mostly for amino acid inhibition and some kinetic parameters were determined for the reverse, Hse oxidizing reaction. Furthermore, the functional amino acid residues involved in homoserine dehydrogenase activity of either enzyme have not been identified. Therefore, the focus of this paper was to fully characterize the kinetic properties of yeast HSD for both ASA reduction and Hse oxidation as a prerequisite for the determination of its chemical and kinetic mechanisms.

The results in this paper reveal that yeast HSD has high affinity for the nicotinamide cofactors and can work equally well with NADPH or NADH. Furthermore, the chemical mechanism appears to involve His309, since DEPC modification results in loss of activity and His309 to Ala mutation reduces the second order rate constant by almost two orders of magnitude. Following the completion of the research portion of this

thesis, the 3D structure of yeast HSD became available and revealed that His309 was, in fact, at the interface region of the HSD dimer.

All the experimental work described in this manuscript was performed by me with the exception of that summarized in Figure 1 and Table 1. The purification of wild type homoserine dehydrogenase (HSD) described in Figure 1 and Table 1 was performed by Catharine Pratt, a co-operative program student who worked under my supervision. She also sequenced pCP13 to confirm the absence of mutations and determined the molecular weight of wild type HSD by size exclusion chromatography. Greg Broadhead contributed to this work by purifying the HSD mutants, H79A and H309A. Dr. John Honek of the University of Waterloo provided advice and, with the assistance of Robert Kinach, furnished aspartate  $\beta$ -semialdehyde needed for the enzyme assays. Mass spectrometry was performed by Lorne Taylor at the University of Waterloo Biological Mass Spectrometry Laboratory.

## 2.2 Paper

### **Characterization of Yeast Homoserine Dehydrogenase, an Antifungal Target<sup>†</sup>**

Suzanne L. Jacques<sup>‡</sup>, Catharine Pratt<sup>‡</sup>, Greg Broadhead<sup>‡</sup>,  
Robert Kinach<sup>§</sup>, John F. Honek<sup>§</sup> and Gerard D. Wright<sup>\*†</sup>

<sup>‡</sup> Department of Biochemistry, McMaster University, Hamilton, ON, L8N 3Z5 and

<sup>§</sup> Department of Chemistry, University of Waterloo, Waterloo, ON, N2L 3G1

Running title: Chemical Modification and Mutagenesis of Yeast HSD

\*Corresponding author. Phone: (905) 525-9140, ext. 22943; Fax: (905) 522-9033;

Email: [wrightge@fhs.mcmaster.ca](mailto:wrightge@fhs.mcmaster.ca)

<sup>†</sup> This research was supported by a Natural Sciences and Engineering Research Council of Canada Strategic Grant and an Ontario Graduate Student Scholarship to S.L.J..

**Footnotes**

<sup>1</sup> Abbreviations: AKHSD, aspartokinase-homoserine dehydrogenase (EC 2.7.2.4 and EC 1.1.1.3); ASA, *L*-aspartate  $\beta$ -semialdehyde; CHES, 2-[N-cyclohexylamino]ethanesulfonic acid; DEPC, diethyl pyrocarbonate; DMSO, dimethylsulfoxide; EDC, 1-ethyl-3-[3-dimethylaminopropyl]-carbodiimide; HEPES, N-[2-hydroxyethyl]piperazine-N'-[2-ethanesulfonic acid]; HSD, homoserine dehydrogenase (EC 1.1.1.3); Hse, homoserine; MES, 2-[N-morpholino]ethane-sulfonic acid; PLP, pyridoxal phosphate; TAPS, N-tris[hydroxymethyl]methyl-3-amino-propanesulfonic acid; TNM, tetranitromethane.



## ABSTRACT

Chemical modification and site-directed mutagenesis were performed to probe the catalytic mechanism of *Saccharomyces cerevisiae* homoserine dehydrogenase (HSD), an enzyme required for the biosynthesis of Thr, Ile and Met from Asp, and a target for antifungal agents. Yeast HSD was overproduced in *Escherichia coli* and 25 mg of soluble dimeric enzyme was purified per liter of cell culture in two steps. HSD efficiently reduces aspartate semialdehyde to homoserine using either NADH or NADPH with  $k_{cat}/K_m$  on the order of  $10^{6-7} \text{ M}^{-1} \text{ sec}^{-1}$ . The rate constant of the reverse direction (homoserine oxidation) was also significant ( $k_{cat}/K_m \approx 10^{4-5} \text{ M}^{-1} \text{ sec}^{-1}$ ). The substrate, aspartate semialdehyde, demonstrated substrate inhibition ( $K_i = 3.79 \text{ mM}$ ) in the presence of cofactor NADH. Chemical modification of HSD with diethyl pyrocarbonate (DEPC) at pH 6.0 resulted in a loss of activity which could be obviated by the presence of substrates. UV difference spectra revealed an increase in absorbance at 240 nm for DEPC-modified HSD corresponding to the modification of 2 His per subunit. Amino acid sequence alignment of HSD from different sources illustrated the conservation of 2 His residues. These residues, His 79 and His 309, were substituted by Ala using site-directed mutagenesis. HSD H79A had steady-state kinetics similar to those of the wild type, while  $k_{cat}/K_m$  for HSD H309A decreased by almost two orders of magnitude. His 309 was therefore concluded to be important for enzyme activity. These results provide the first detailed analysis of a fungal HSD and consequently provide the necessary framework for future inhibitor design.

## INTRODUCTION

Clinical fungal infections have escalated dramatically in recent years (Sternberg, 1994). The rise in immunocompromised individuals (e.g., organ and marrow transplant recipients, AIDS patients) has resulted in a significant surge in life-threatening fungal infections (Georgopapadakou and Walsh, 1996). Treatment of these diseases is limited to very few agents: the polyenes (e.g., amphotericin), nucleotide analogues (e.g., 5-fluorouracil) and lanosterol 14 $\alpha$ -demethylase inhibitors (e.g., fluconazole) (Armstrong, 1993). As with all antimicrobial compounds, this limited number of agents is now being threatened by the emergence of drug resistant organisms (DeMuri and Hostetter, 1995). Antifungal-resistant plant pathogens are also a growing concern in agriculture (Hollomon, 1993). Crop damage due to pre- and post-harvest fungal infections results in dramatic losses throughout the world each year. Thus, there is heightened interest in the identification and exploitation of new antifungal targets and drugs.

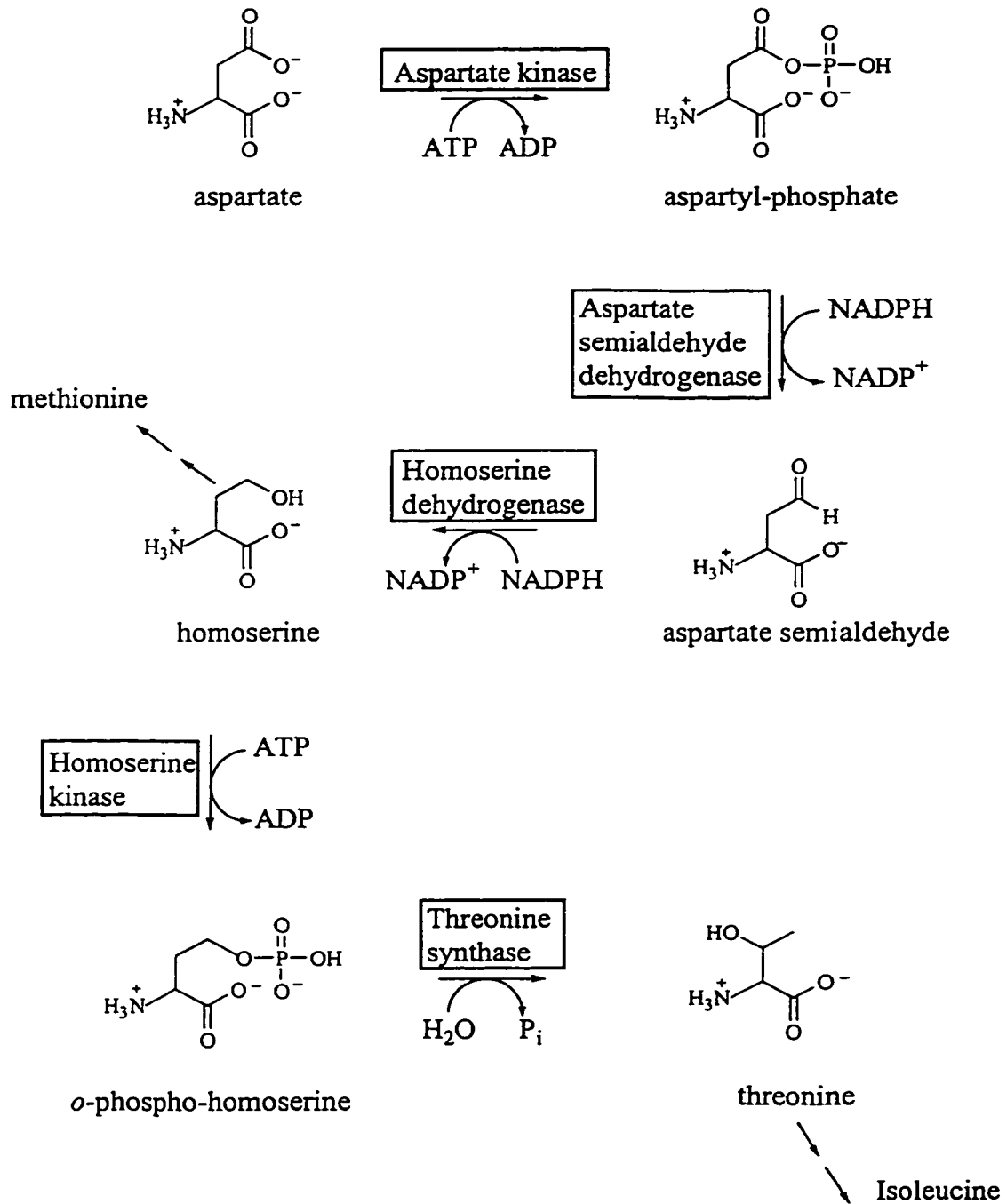
While sterol metabolism and the cell membrane continue to be useful targets, the identification of other important pathways is paramount for the development of new antifungal drugs. The biosynthesis of amino acids is one such target. The pyridinamine fungicides are thought to inhibit cystathionine- $\beta$ -lyase, an enzyme required for the biosynthesis of methionine (Masner *et al.*, 1994). Recently, it has been demonstrated that the biosynthetic enzyme homoserine dehydrogenase (HSD)<sup>1</sup> (EC 1.1.1.3) is the target for the antifungal natural product (*S*)-2-amino-4-oxo-5-hydroxypentanoic acid (Yamaguchi *et al.*, 1988; Yamaki *et al.*, 1992). HSD catalyzes a critical common step in the synthesis of

the amino acids threonine, isoleucine and methionine (Scheme 1), amino acids which are not synthesized by humans.

HSD was first characterized in yeast cell free extracts 41 years ago (Black and Wright, 1955) and a five-step purification yielding 12 mg of enzyme from 500 g of yeast cell paste was described more recently (Yumoto *et al.*, 1991). The gene encoding HSD in *Saccharomyces cerevisiae*, *hom6*, has been cloned and sequenced (Thomas *et al.*, 1993) and reveals a predicted 359 amino acid protein with a molecular weight of 38,505 Da, in good agreement with the size of 40,000 Da estimated from SDS-PAGE on the purified yeast enzyme (Yumoto *et al.*, 1991). The characterization of *S. cerevisiae* HSD has been relatively cursory, limited only to  $K_m$  determinations in the homoserine (Hse) oxidizing mode.

On the other hand, the *Escherichia coli* bifunctional enzyme aspartokinase-homoserine dehydrogenase 1 (AKHSD 1) has been studied in much more detail. Both kinase and dehydrogenase activities of this enzyme have been thoroughly characterized and the kinetic mechanisms determined (Angeles and Viola, 1990; Wedler *et al.*, 1992; Wedler and Ley, 1993a). Chemical modification and pH studies indicate that His and Tyr residues are involved in the kinase active site (Angeles *et al.*, 1989). The functional amino acid residues involved in the dehydrogenase activity of AKHSD I, however, have not yet been identified, thus the structural basis for substrate recognition and catalysis is unknown. Further exploration of HSD as a target for antifungal drugs requires a much more thorough delineation of enzyme action. We have therefore overexpressed the *S.*

*cerevisiae* enzyme in *E. coli*. This has permitted large scale purification for the analysis of the steady state kinetic properties of the enzyme and the identification of active site amino acid residues.



**Scheme 1. The aspartate pathway in *S. cerevisiae***

## MATERIALS AND METHODS

### *Chemicals*

Diethyl pyrocarbonate, *D*, *L*-Homoserine, *L*-homoserine, NADH, 2-[*N*-cyclohexylamino]ethanesulfonic acid (CHES), 1-ethyl-3-[3-dimethylaminopropyl]-carbodiimide, *N*-[2-hydroxyethyl]piperazine-*N'*-[2-ethanesulfonic acid] (HEPES), 2-[*N*-morpholino]ethane-sulfonic acid (MES), pyridoxal phosphate, *N*-tris[hydroxymethyl]methyl-3-amino-propanesulfonic acid (TAPS) and phenyl glyoxal were obtained from Sigma (St. Louis, MO). Reduced and oxidized forms of the nicotinamide coenzymes (NAD<sup>+</sup>, NADP<sup>+</sup>, NADPH) were purchased from Boehringer Mannheim (Laval, PQ). Methyl acetimidate was acquired from Pierce (Rockford, IL) and tetranitromethane was obtained from Aldrich (Milwaukee, WI).

### *Preparation of aspartate semialdehyde (ASA)*

*L*-ASA was prepared by a slight modification of the method of Tudor and coworkers (Tudor *et al.*, 1993). Briefly, *L*-allylglycine was converted first to the *N*-tert-butoxycarbonyl derivative and then to the *p*-methoxybenzyl ester by standard techniques. The resulting diprotected allylglycine derivative was then converted to *L*-ASA in two steps.

*L*-*N*-tert-Butoxycarbonylaspartic Acid  $\beta$ -Semialdehyde *p*-Methoxybenzyl Ester:  
*L*-*N*-tert-butoxycarbonylallylglycine *p*-methoxybenzyl ester (2.18 g; 6.48 mmol) in CH<sub>2</sub>Cl<sub>2</sub> (65 mL) was ozonized (1.5 hr) at -78 °C and excess ozone was removed with

argon. The protected amino acid ozonide was decomposed (-78 °C) by the addition of anhydrous triethylamine (2 equivalents) followed by stirring at 23 °C for 5 hours. Methylene chloride was removed *in vacuo* and the crude material was directly purified by flash silica gel chromatography using ethyl acetate as eluent to give the protected *L*-ASA as a clear oil, 941 mg (43% yield), Rf 0.65 (1 : 1 ethyl acetate : hexane) or Rf 0.42 (9:1 CHCl<sub>3</sub>:EtOAc). <sup>1</sup>H NMR (200 MHz, CDCl<sub>3</sub>): 1.41 (9H, s), 3.04 (2H, t), 3.79 (3H, s), 4.60 (1H, m), 5.12 (2H, s), 5.40 (1H, br, d), 6.88, 7.25 (4H, m), 9.71 (1H, s). IR (CHCl<sub>3</sub>): 3437, 3028, 2982, 1714, 1614, 1516 cm<sup>-1</sup>. MS (ESMS): m/z (%) = 338.18 (MH<sup>+</sup>, 100%), 282.05 (23%), 120.98 (52%); C<sub>17</sub>H<sub>23</sub>NO<sub>6</sub> requires 337.15.

*L*-Aspartic Acid β-Semialdehyde Hydrate Trifluoroacetate (*L*-ASA): A solution of protected semialdehyde (941 mg; 2.79 mmol) in CH<sub>2</sub>Cl<sub>2</sub> (20 mL) was cooled to 0°C. Trifluoroacetic acid (19 mL) was added under argon as the solution warmed to room temperature, and stirring was continued for an additional 2 hours. The solvent was removed *in vacuo* to give a yellow oily residue. This was partitioned between water (75 mL) and ethyl acetate (75 mL). The aqueous layer was separated and washed with ethyl acetate (2 x 75 mL). Removal of the water *in vacuo* gave the hydrated semialdehyde as an orange solid, 542 mg (78% yield). <sup>1</sup>H NMR (500 MHz, D<sub>2</sub>O): 2.10 (2H, m), 3.96 (1H, dd), 5.18 (1H, t). IR (KBr): 3429, 3120, 1688, 1645, 1400 cm<sup>-1</sup>; MS (ESMS): m/z (%) = 136.06 (M<sup>+</sup>; 50%), 118.07 (M-H<sub>2</sub>O; 100%); C<sub>4</sub>H<sub>10</sub>NO<sub>4</sub> requires 136.06.

*Preparation of hom6 overexpression construct*

*S. cerevisiae* DL1 served as the source for chromosomal DNA for PCR amplification of the *hom6* gene. The yeast were grown overnight at 30°C in 50 mL YPD, harvested by centrifugation and washed twice with cold sterile water. Cells were flash frozen, then ground with a mortar and pestle in liquid N<sub>2</sub> and resuspended in 5 mL lysis buffer (50 mM Tris-HCl pH 7.6, 5 mM EDTA, 150 mM NaCl, 5% SDS). Phenol:chloroform:isoamyl alcohol (25:25:1) (10 mL) was added to the lysed cells, mixed gently for 20 minutes at 30°C and centrifuged at 5000 x g for 10 min. The organic layer was re-extracted with 4 mL lysis buffer, the aqueous phases were pooled and extracted another 3 times with phenol:chloroform:isoamyl alcohol. Nucleic acids were subsequently precipitated by adding 0.1 volumes of 2 M potassium acetate and 2.5 volumes of absolute ethanol and storing overnight at -20°C. After centrifuging (4000 x g for 20 min), the pellet was washed with 70% ethanol and dried *in vacuo*. The pellet was then dissolved in 7 mL cold 3 M LiCl and stored for 2 days at 4 °C to precipitate RNA which was then removed by centrifugation at 5000 x g for 30 min. DNA was precipitated from the supernatant by adding 25 mL absolute ethanol and stored overnight at -20°C. After centrifugation at 4000 x g for 20 min, the pelleted chromosomal DNA was washed with 70% ethanol, dried and resuspended in 0.75 mL 10 mM Tris-HCl, 1 mM EDTA pH 8.0.

The HSD overexpression plasmid, pCP13, was prepared by PCR amplification of the *hom6* gene, encoding *S. cerevisiae* HSD (Thomas *et al.*, 1993). PCR primers were



designed to complement the 5' (5'-GCTCTAGACATATGAGCACTAAAGTTGTTAATG-3') and 3' (5'-CGGGATCCTCACTAAAGTCTTTGAGCAATCTTG-3') ends of the *hom6* open reading frame and to incorporate *Xba* I, *Nde* I (underlined and in bold, respectively, in the 5' primer) and *Bam*H I (underlined in the 3' primer) restriction sites for subcloning. The *hom6* gene was amplified from genomic DNA of *S. cerevisiae* DL1, using Vent DNA polymerase (New England Biolabs). The resulting 1.1 kb fragment was digested with *Nde* I and *Bam*H I and ligated into the expression vector pET-22b(+) (Novagen, Madison, WI) linearized with the same restriction endonucleases. This expression vector places the *hom6* gene under the control of the bacteriophage T7 promoter and the *lac* operator. The gene was completely sequenced to confirm the absence of mutations and the resulting recombinant plasmid, pCP13, was used to transform *E. coli* BL21 (DE3).

#### *Site-directed mutagenesis*

The recombinant plasmids, pHSD79 and pHSD309, encoding HSD H79A and HSD H309A mutants respectively, were prepared by the Quick Change protocol (Stratagene, LaJolla, CA). pHSD79 and pHSD309 were generated by native *Pfu* DNA polymerase (Stratagene, LaJolla, CA) using pCP13 as template and primers encoding the mutations (pHSD79: 5'-GGATGATTTAATTGCTGCTTTGAAGACTTCACC-3' and 5'-GGTGAAGTCTTCAAAGCAGCAATTAATCATCC-3'; pHSD309: 5'-GTACGATTACTCAGCCCCATTCGCATCATTG-3' and 5'-

CAATGATGCGAATGGGGCTGAGTAATCGTAC-3'; mutated bases are underlined) Following the reaction, the template (pCP13) was removed by digestion with *Dpn* I and the mixture was used to transform *E. coli* XL1-Blue. *Hom6* was sequenced in both constructs to determine the presence of the His→Ala mutation and to confirm the absence of other mutations. For overexpression, pHSD79 and pHSD309 were used to transform *E. coli* BL21 (DE3).

#### *Purification of HSD*

All purification steps were carried out at 4°C. Buffers were brought to the correct pH with HCl at room temperature.

An overnight culture of *E. coli* BL21 (DE3)/pCP13 (20 mL) served as inoculum for 2 L of Luria Broth containing 100 µg/mL ampicillin. The culture was grown at 37°C at 250 rpm to an absorbance of 0.4 at 600 nm. The cell culture was then cooled to 30°C in an ice bath and sterile isopropyl β-D-thiogalactopyranoside was added to a final concentration of 1 mM. The cells were grown for an additional 4 hr at 30°C at 250 rpm and then harvested by centrifugation at 5000 x g for 15 min. The cell pellet was washed with 25 mL of ice-cold 0.85% NaCl, then resuspended in 10 mL lysis buffer (10 mM HEPES pH 7.5, 1 mM EDTA, 1 mM phenylmethylsulfonyl fluoride, 1 mM β-mercaptoethanol) and lysed by three passages through a French pressure cell. Cell debris was removed by centrifugation at 10,000 x g for 20 min. The supernatant was applied to a Q-Sepharose Fast Flow (Pharmacia) column (2.5 x 11 cm), equilibrated with 10 mM

HEPES pH 7.5, 1 mM EDTA (buffer A). HSD did not bind and was washed from the column with 150 mL buffer A. Fractions containing HSD, as determined by enzyme assay, were pooled and concentrated to 2 mL using an Amicon PM30 Diaflo ultrafiltration membrane, followed by an Amicon Centriprep 10 concentrator. The concentrated protein was then applied to a Sephacryl S-200 (Pharmacia) column (2.5 x 110 cm) equilibrated with 10 mM TAPS pH 8.5. HSD-containing fractions were identified by activity assay, pooled and concentrated as described above. The purified enzyme was stored at 0°C or frozen in 5% glycerol at -20°C where it was stable for several months.

HSD mutants H79A and H309A were purified as described above from 1 L cultures of *E. coli* BL21 (DE3)/pHSD79 and *E. coli* BL21 (DE3)/pHSD309, respectively. To increase soluble expression of protein, the cultures were heat shocked at 45°C by the addition of 200 mL boiling Luria broth and then expression was induced with 0.5 mM isopropyl  $\beta$ -D-thiogalactopyranoside.

#### *Molecular Weight Determination of Purified Wild Type HSD*

Samples of purified wild type HSD were applied to a Superdex 200 column (HR 10/30) (Pharmacia) run at 0.4 mL/min in 50 mM HEPES pH 7.5, 1 mM EDTA. Carbonic anhydrase, bovine serum albumin,  $\beta$ -amylase, and blue dextran were used to construct the standard curve from which the native molecular weight of HSD was estimated.

The accurate molecular mass was determined by electrospray mass spectrometry

on a Fisons VG Quattro II instrument using CH<sub>3</sub>CN/H<sub>2</sub>O (1:1) with 0.1 % trifluoroacetic acid as solvent by L. Taylor at the University of Waterloo Biological Mass Spectrometry Laboratory.

### *Enzyme Assay*

During HSD purification, activity was measured in the reverse direction (*D,L*-Hse + NAD<sup>+</sup> → ASA + NADH) by continuously monitoring the increase in absorbance at 340 nm at room temperature (25°C) using a Cary 3E UV-vis spectrophotometer. The assay mixture contained 25 mM *D,L*-Hse, 0.2 mM NAD<sup>+</sup> and 100 mM Tris-HCl, pH 9.0 in a total volume of 995 μL. The reaction was initiated with 5 μL of partially purified enzyme.

For initial rates studies, both forward (ASA + NAD(P)H → Hse + NAD(P)<sup>+</sup>) and reverse reactions were monitored for the disappearance or the appearance of NAD(P)H at 340 nm. In the forward direction, the assay mixture contained 100 mM HEPES buffer, pH 7.5 and varying amounts of ASA and NAD(P)H in a total volume of 980 μL. ASA was held constant at 0.8 mM as a fixed second substrate, while NAD(P)H was held at 0.2 mM as a second substrate. In the reverse direction, the assay mixture contained 100 mM CHES, pH 9.5 and varying amounts of *L*-Hse and NAD(P)<sup>+</sup> in a total volume of 980 μL. *L*-Hse was held constant at 20 mM as a fixed second substrate, while NADP<sup>+</sup> and NAD<sup>+</sup> were held at 8.0 mM and 0.3 mM, respectively, as saturating substrates. When HSD mutants were assayed, NAD<sup>+</sup> concentration was held at 0.4 mM as a fixed second

substrate. The reaction was initiated by adding 20  $\mu\text{L}$  purified enzyme (wild type HSD: 0.1  $\mu\text{g}$  for the forward reaction, 1  $\mu\text{g}$  for the reverse reaction; HSD H79A: 0.33  $\mu\text{g}$  for the forward reaction, 1.5  $\mu\text{g}$  for the reverse reaction; HSD H309A: 8  $\mu\text{g}$  for the forward reaction, 33  $\mu\text{g}$  for the reverse reaction).

For measuring the effect of KCl on kinetic parameters, assays were prepared as above with varying concentrations of ASA, 0.2 mM NADH and 0, 100, 200, 300, 400, 500, 750 or 1000 mM KCl. The effect of KCl on the lag in the reaction progress curve was examined by assaying mixtures containing 1.6 mM ASA, 0.5 mM NADH, 100 mM HEPES pH 7.5 and varying levels of KCl. All assays were done in duplicate.

#### *Data Analysis*

Initial rates were obtained directly from the progress curves using the Cary 3.00 software and duplicate rates were analyzed by nonlinear least squares regression to equation 1 or 2 using Grafit 3.0 (Leatherbarrow, 1992). Parameters obtained from the best fit were reported with standard errors.

$$v = V_{max}S/(K_m + S) \quad (1)$$

$$v = V_{max}S/(K_m + S + S^2/K_i) \quad (2)$$

where  $v$  is the measured velocity,  $V_{max}$  is the maximal velocity,  $S$  is the varied substrate concentration,  $K_m$  is the Michaelis-Menten constant,  $K_i$  is the substrate inhibition constant.

First derivatives of the progress curve at high NADH concentration were fit to a

second order polynomial equation ( $y = ax^2 + bx + c$ ) by nonlinear least squares regression.

#### *Chemical modification studies of wild type HSD*

Chemical modification of wild type HSD was performed with several reagents to explore the participation of reactive amino acid side chains in catalysis. Purified HSD (0.7  $\mu\text{g}$ ) was incubated with 1.25 or 2.5 mM pyridoxal phosphate (PLP) in 100 mM  $\text{NaHCO}_3$ , pH 8.0, 2.5 mM 1-ethyl-3-[3-dimethylaminopropyl]-carbodiimide (EDC) in 100 mM MES, pH 6.0 or 2.5 mM methyl acetimidate in 100 mM  $\text{NaHCO}_3$ , pH 8.0 in a total volume of 100  $\mu\text{L}$  for 1 hour at 25°C. Phenyl glyoxal (10 mM) was added to 0.7  $\mu\text{g}$  purified HSD in 100 mM  $\text{NaHCO}_3$ , pH 8.0 in 100  $\mu\text{L}$  and allowed to react for 30 minutes at 25°C. HSD activity was measured as previously by adding 20  $\mu\text{L}$  modified HSD to an assay containing 0.8 mM ASA, 0.2 mM NADH and 100 mM HEPES, pH 7.5 and compared to control incubations containing no modifier. Substrate protection was determined by the addition of substrates to the HSD solution prior to the addition of PLP or phenyl glyoxal.

Diethyl pyrocarbonate (DEPC) and tetranitromethane (TNM) stock solutions were made in dimethyl sulfoxide (DMSO) and ethanol, respectively. Purified HSD (0.7  $\mu\text{g}$ ) was treated with 2.5 or 10 mM DEPC in 100 mM phosphate buffer, pH 6.0 or with 2.5 or 10 mM TNM in 100 mM  $\text{NaHCO}_3$ , pH 8.0 for 30 minutes at 25°C. DEPC/DMSO or TNM/ethanol (10  $\mu\text{L}$ ) were added to incubations having a total volume of 100  $\mu\text{L}$ .

Controls were prepared containing HSD in the appropriate buffer and 10  $\mu$ L DMSO or ethanol. These solvents had little effect on enzyme activity at this concentration. HSD activity was measured as described above and compared to controls. Substrate protection was determined by the addition of substrates to the HSD solution prior to the addition of DEPC or TNM.

Difference wavelength scans were performed with DEPC-treated HSD at 25°C. Wavelength scans were taken at between 220 and 350 nm of purified HSD (1.7 mg) in 100 mM phosphate buffer, pH 6.0, 10 % DMSO and subtracted from the same solution containing 2.5 mM DEPC. Scans were taken at 0.5, 1, 2, 3, 4, 6 and 8 minutes after the addition of DEPC and DMSO.

#### *Amino acid sequence alignment of HSD*

Amino acid sequences of HSD/AKHSD from various sources were obtained by searching the NCBI GenBank database. Sequence alignment was performed by ClustalW (<http://www2.ebi.ac.uk/clustalw/>) (Higgins *et al.*, 1994). The resulting phylogenetic tree and sequence alignment were viewed using TreeView version 1.5.2 (<http://taxonomy.zoology.gla.ac.uk/rod/treeview.html>) and GeneDoc version 2.3.0 (<http://cris.com/~Ketchup/genedoc.shtml>) respectively.

## RESULTS

### *Overproduction, purification and characterization of S. cerevisiae HSD*

In order to obtain an adequate supply of HSD for mechanistic and structural studies, we sought to prepare an overexpressing construct in *E. coli*. We therefore amplified the *hom6* gene from *S. cerevisiae* genomic DNA by PCR and inserted it into an appropriate vector, pET-22b, which places the gene downstream from an inducible bacteriophage T7 promoter and the optimal bacteriophage T7 gene 10 ribosome binding site. The resulting construct, pCP13, gave excellent overproduction of the yeast enzyme in *E. coli*. A rapid two step purification (anion exchange and size exclusion chromatography) gave over 25 mg of pure HSD per litre of cell culture (Table 1) (Figure 1).

The enzyme mass as determined by electrospray mass spectrometry was found to be  $38374.32 \pm 3.39$  Da in excellent agreement with the predicted mass of the enzyme lacking the N-terminal Met (38374.70). The enzyme purified from natural abundance in *S. cerevisiae* was reported to be a dimer (Yumoto *et al.*, 1991) and the recombinant enzyme also behaved as a dimer as indicated by size exclusion chromatography.

### *Steady state kinetics of wild type HSD*

The purified enzyme could be assayed in either the forward, Hse producing, or reverse, ASA producing, directions with ease. The pH optimum at saturating substrate

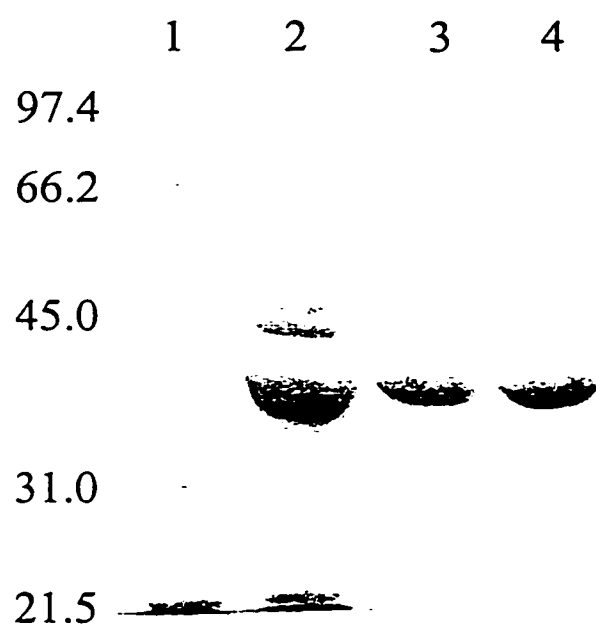


**Table 1. Purification of *S. cerevisiae* HSD from *E. coli* BL21(DE3)/pCP13**

Step	Protein (mg)	Activity (U) <sup>1</sup>	Specific Activity (U/mg)	Recovery (%)	Purification (n fold)
Cell lysate	470	2560	5.45	100	---
Q-Sepharose	110	2180	19.8	85	3.6
Sephacryl S-200	57	1340	23.7	52	4.4

<sup>1</sup> 1 U = enzyme required to reduce 1  $\mu$ mol of NAD<sup>+</sup>/min in the presence of 25 mM *D,L*-Hse at pH 9.0.

**Figure 1. Purification of *S. cerevisiae* HSD from *E. coli*/pCP13.** The SDS-polyacrylamide gel (11%) was stained with Coomassie blue R-250. Lanes: 1, molecular weight standards (kDa); 2, whole cell lysate; 3; Q Sepharose; 4, Sephacryl S-200.



concentrations in the forward direction was 7.5 while it was >9.5 in the reverse reaction. The forward reaction was favored, having  $k_{cat}/K_m$  equal to  $10^6$ - $10^7$   $M^{-1} s^{-1}$ , whereas the reverse reaction had  $k_{cat}/K_m$  equal to  $10^4$ - $10^5$   $M^{-1} s^{-1}$  (Table 2). In both cases, the non-phosphorylated nicotinamide was the preferred substrate having a 4-fold lower  $K_m$  and a 3-fold greater  $k_{cat}/K_m$  in the forward direction and a 14-fold lower  $K_m$  and a 15-fold greater  $k_{cat}/K_m$  in the reverse direction. The nicotinamide substrate also demonstrated an effect on the Michealis-Menten constant for *L*-Hse,  $K_{m,L-Hsc}$  was almost two-fold larger with  $NADP^+$  than  $NAD^+$ .

HSD was substrate inhibited in the forward reaction by ASA ( $K_i = 3.79$  mM) with NADH as the cofactor. Initial rates were also decreased by high concentrations ( $\geq 0.5$  mM) of either NADPH or NADH. However, these rates increased to a maximum value after a lag period lasting from 5-10 mins. The length of the lag phase appeared to decrease as KCl was added, but was not eliminated (Figure 2). Furthermore, the addition of monovalent cations ( $K^+$ ,  $Na^+$ ) increased both  $K_m$  and  $K_i$  for substrates in the forward reaction, but had no effect on  $k_{cat}$  (Figure 3).

#### *Chemical modification studies*

Chemical modification of amino acid residues in yeast HSD was performed to identify functional amino acid residues (Table 3). PLP, which reacts with Lys residues to form Schiff's bases, decreased HSD activity only to 75% after one hour and the presence

**Table 2. Steady state kinetic parameters for purified yeast HSD<sup>a</sup>**

HSD	Variable Substrate	Saturating Substrate	$K_m$ (mM)	$k_{cat}$ (s <sup>-1</sup> )	$k_{cat}/K_m$ (M <sup>-1</sup> s <sup>-1</sup> )	$K_i$ (mM)
Wild Type	<i>L</i> -ASA	NADPH	0.186 ± 0.012	530 ± 9	2.85 × 10 <sup>6</sup>	3.79 ± 0.87
	<i>L</i> -ASA	NADH	0.234 ± 0.030	563 ± 39	2.41 × 10 <sup>6</sup>	
	NADPH	<i>L</i> -ASA	0.028 ± 0.003	521 ± 15	1.86 × 10 <sup>7</sup>	
	NADH	<i>L</i> -ASA	0.007 ± 0.001	368 ± 11	5.26 × 10 <sup>7</sup>	
	<i>L</i> -Hse	NADP <sup>+</sup>	1.704 ± 0.164	17.2 ± 0.4	1.01 × 10 <sup>4</sup>	
	<i>L</i> -Hse	NAD <sup>+</sup>	1.034 ± 0.121	21.9 ± 0.6	2.12 × 10 <sup>4</sup>	
	NADP <sup>+</sup>	<i>L</i> -Hse	0.743 ± 0.118	16.6 ± 0.5	2.23 × 10 <sup>4</sup>	
	NAD <sup>+</sup>	<i>L</i> -Hse	0.052 ± 0.005	17.3 ± 0.5	3.33 × 10 <sup>5</sup>	
H79A	<i>L</i> -ASA	NADPH	0.159 ± 0.010	282 ± 5	1.77 × 10 <sup>6</sup>	1.69 ± 0.25
	<i>L</i> -ASA	NADH	0.239 ± 0.026	326 ± 21	1.36 × 10 <sup>6</sup>	
	NADPH	<i>L</i> -ASA	0.029 ± 0.001	262 ± 2	9.03 × 10 <sup>6</sup>	
	NADH	<i>L</i> -ASA	0.008 ± 0.001	175 ± 5	2.19 × 10 <sup>7</sup>	
	<i>L</i> -Hse	NAD <sup>+</sup>	0.263 ± 0.036	10.1 ± 0.3	3.84 × 10 <sup>4</sup>	
	NAD <sup>+</sup>	<i>L</i> -Hse	0.018 ± 0.002	11.7 ± 0.2	6.50 × 10 <sup>5</sup>	
H309A	<i>L</i> -ASA	NADPH	0.203 ± 0.010	14.1 ± 0.2	3.95 × 10 <sup>4</sup>	
	<i>L</i> -ASA	NADH	0.160 ± 0.022	7.5 ± 0.2	4.69 × 10 <sup>4</sup>	
	NADPH	<i>L</i> -ASA	0.023 ± 0.001	11.1 ± 0.1	4.83 × 10 <sup>5</sup>	
	NADH	<i>L</i> -ASA	0.007 ± 0.001	9.2 ± 0.3	1.31 × 10 <sup>6</sup>	
	<i>L</i> -Hse	NAD <sup>+</sup>	0.285 ± 0.031	0.89 ± 0.02	3.12 × 10 <sup>3</sup>	
	NAD <sup>+</sup>	<i>L</i> -Hse	0.021 ± 0.002	0.92 ± 0.02	4.38 × 10 <sup>4</sup>	

\* Reactions in the forward, NAD(P)H oxidizing direction was at pH 7.5 while the reverse, NAD(P)<sup>+</sup> reducing reactions were conducted at pH 9.5. Kinetic parameters were obtained by fitting data to equation (1), except in the case of variable ASA with saturating NADH which exhibited substrate inhibition and thus was fit to equation (2).

**Figure 2. Effect of KCl on progress curves of HSD activity at high NADH concentration.** Progress curves of the spectrophotometric assays at 340 nm were obtained with 1.6 mM ASA, 0.5 mM NADH, 100 mM HEPES pH 7.5 and 0.1  $\mu$ g HSD in the presence of 0 (— - -), 100 (— —), 200 (——), 400 (— - —) or 600 (- - - -) mM KCl. First derivatives (inset) were calculated using the Grafit 3.0 program, KCl concentrations are 0 (○), 100 (●), 400 (+) or 600 (•) mM.

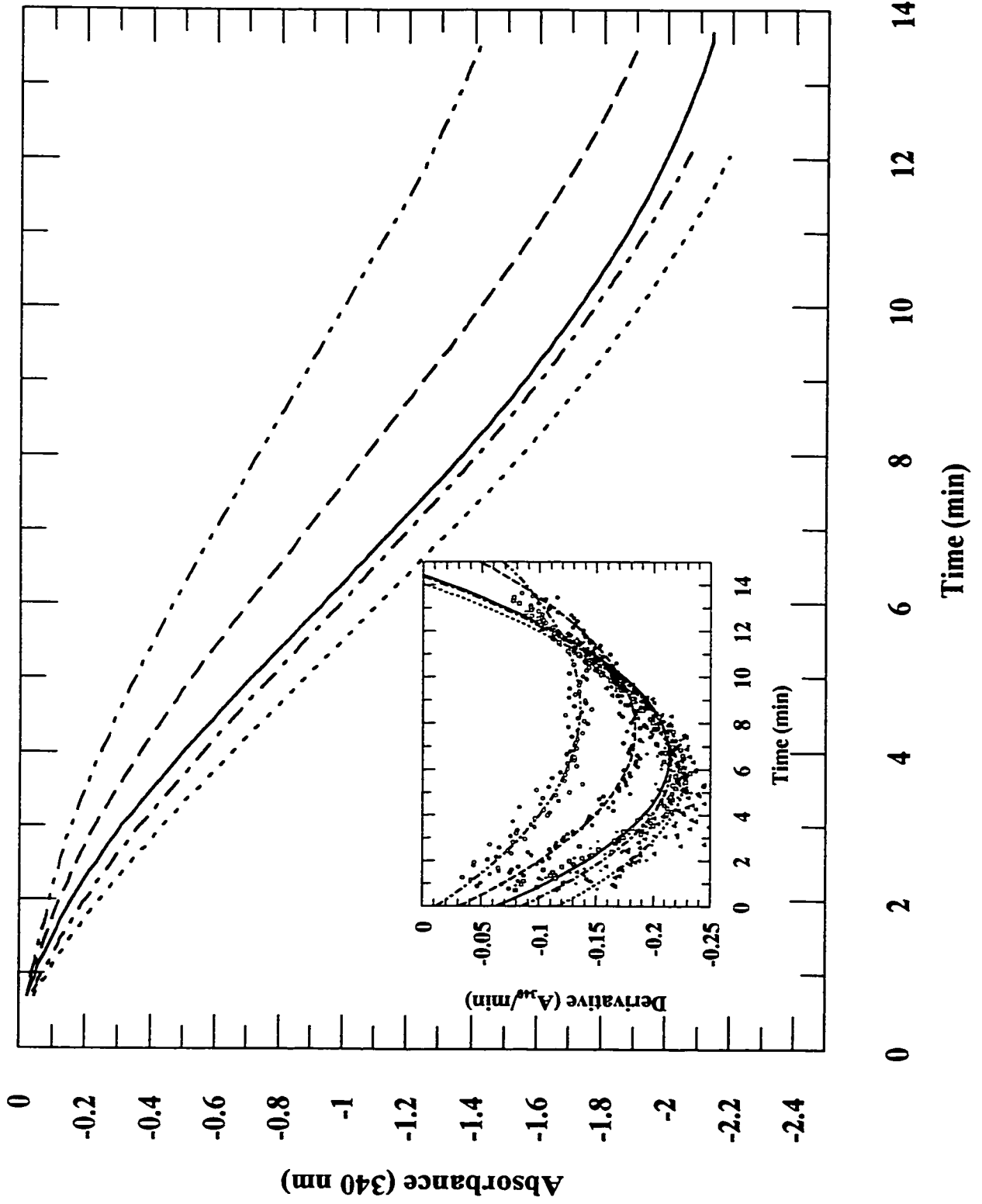
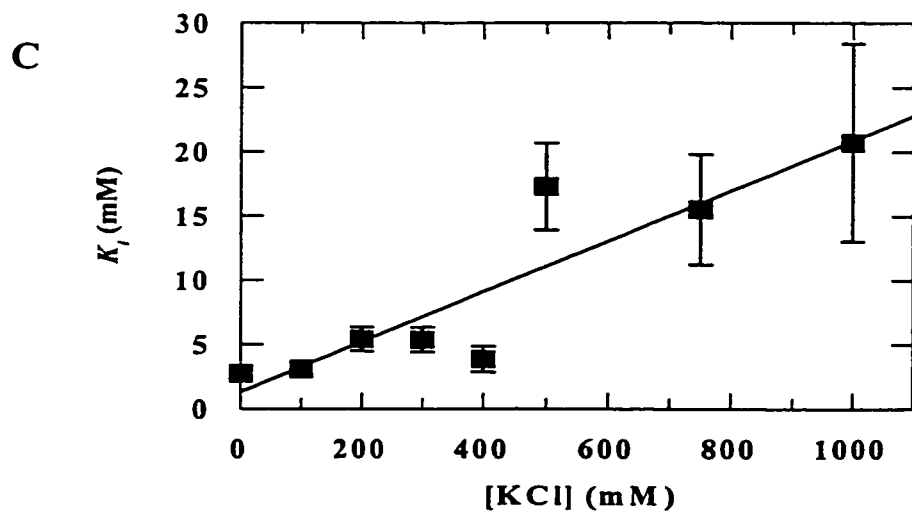
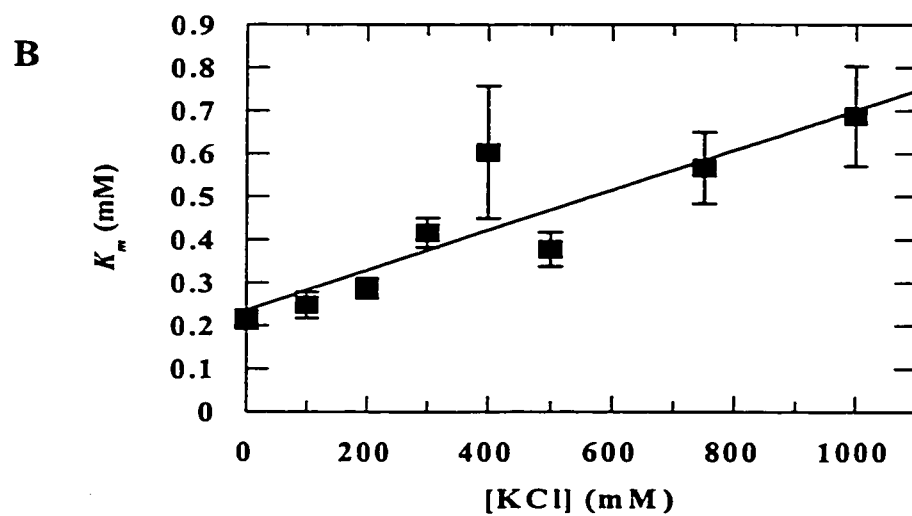
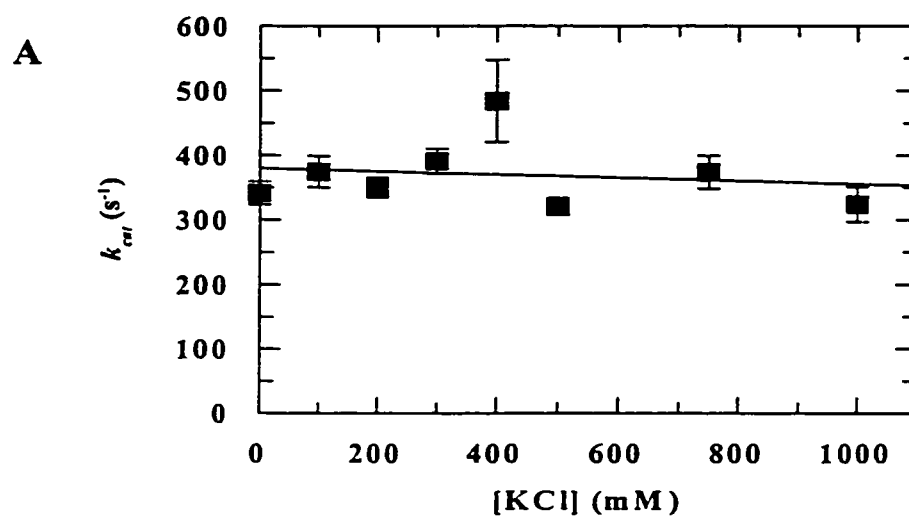




**Figure 3. Effect of KCl on kinetic parameters of yeast HSD.** ASA concentrations were varied at several fixed KCl concentrations in the presence of 0.2 mM NADH, 100 mM HEPES pH 7.5 and 0.1  $\mu$ g HSD.  $k_{cat}$  (A),  $K_m$  (B) and  $K_i$  (C) for ASA were obtained from best fits to eq. 2. Error bars represent the standard error for the best fit parameters. Lines represent the results of linear regression analyses of the parameters with respect to KCl concentrations.



of the cofactor  $\text{NAD}^+$  offered very little protection. Another Lys modifying reagent, methyl acetimidate, showed no effect on HSD activity after one hour incubation. Similarly, EDC, which reacts with carboxylate residues (Asp and Glu), also had very little effect on HSD activity. Modification of Arg residues with phenyl glyoxal decreased HSD activity to 63%, however, substrates did not protect HSD activity .

DEPC and TNM, which target His and Tyr residues respectively, demonstrated a more dramatic effect on HSD activity. Only 31 % and 42 % HSD activity remained after 30 minutes incubation with 2.5 mM DEPC or TNM and activity decreased further to 3 % and 19 % with 10 mM DEPC or TNM. Neither 5 mM  $\text{NAD}^+$  nor 5 mM *D, L*-Hse protected HSD from inactivation by TNM as activities remained the same. On the other hand, 5 mM  $\text{NAD}^+$  contributed some protection of HSD from DEPC inactivation (23% HSD activity) and 5 mM *D, L*-Hse offered almost complete protection (81% HSD activity). These results suggest that DEPC is the only reagent in those studies found to modify residues required by HSD for catalysis.

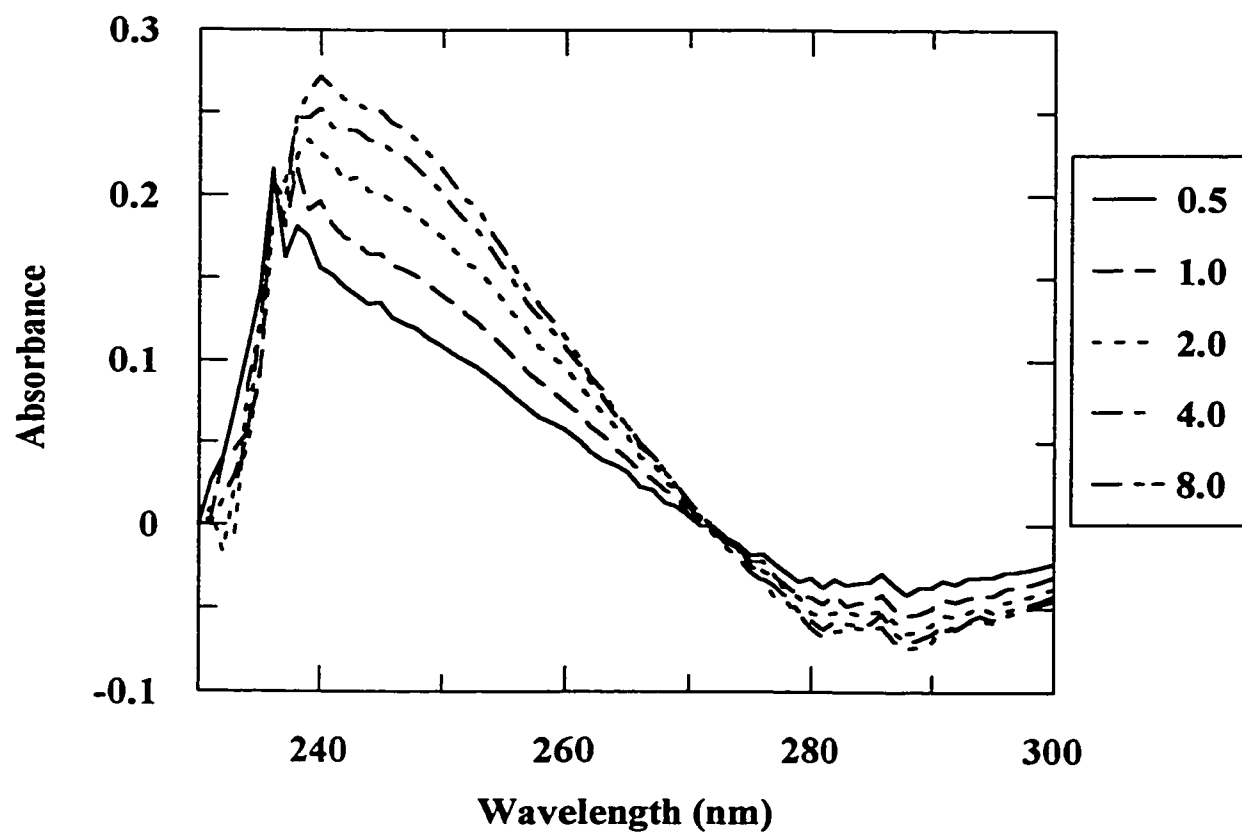
In order to determine whether DEPC inactivation of HSD was a result of His residue modification, DEPC inactivation was monitored as a function of wavelength (Figure 4). Difference spectra illustrated an increase in absorbance at 240 nm corresponding to the formation of N-carbethoxyhistidine and no significant change was visible at 278 nm corresponding to Tyr modification. Modification of His residues by DEPC should be reversible with the addition of neutral hydroxylamine; however, in control

**Table 3. Chemical modification of purified *S. cerevisiae* HSD**

Reagent (mM)		Target residues	Substrate (mM)		Residual HSD activity (%) <sup>a</sup>
phenyl glyoxal	10	Arg	—	—	62.5
	10		ASA NAD <sup>+</sup>	0.8 0.5	71.1
pyridoxal phosphate	1.25	Lys	—	—	80.5
	1.25		NAD <sup>+</sup>	1.0	84.4
	2.5		—	—	74.9
methyl acetimidate	2.5	Lys	—	—	96.2
1-ethyl-3-(3-dimethylaminopropyl)-carbodiimide (EDC)	2.5	Asp, Glu	—	—	82.4
diethyl pyrocarbonate	2.5	His, Tyr	—	—	31.3
	10		—	—	3.3
	10		NAD <sup>+</sup>	10	22.9
	10		<i>D, L</i> -Hse	5.0	80.5
tetranitromethane	2.5	Tyr	—	—	41.9
	10		—	—	18.9
	10		NAD <sup>+</sup>	5.0	25.8
	10		<i>D, L</i> -Hse	5.0	20.0

<sup>a</sup> HSD was incubated with chemical modifier for 30 minutes at room temperature (for phenyl glyoxal, DEPC and TNM) or for 1 hour at room temperature (for PLP, methyl acetimidate and EDC).

**Figure 4. Difference spectra for the modification of *S. cerevisiae* HSD by DEPC.** The increasing absorbance at 240 nm is representative of N-carboethoxyhistidine formation. The curves were obtained at 0.5, 1.0, 2.0, 4.0 and 8.0 minutes respectively, by incubating 1.7 mg HSD with 2.5 mM DEPC in 100 mM phosphate buffer, pH 6.0 and 10% DMSO at 25°C and subtracting the absorbance from the same solution containing no DEPC.



studies hydroxylamine alone inhibited HSD activity and reactivation of HSD could not be detected. The absorbance difference at 240 nm predicted the modification of 2 His per HSD subunit, using an extinction coefficient of  $3200 \text{ M}^{-1} \text{ cm}^{-1}$  (Miles, 1977).

*Amino acid sequence alignment and phylogenetic tree of HSD.*

As a means to identify conserved amino acid residues, the amino acid sequence of *S. cerevisiae* HSD was compared to sequences of HSD/AKHSD from various sources. The phylogenetic tree (Figure 5) illustrates that yeast HSD is most closely related to the bifunctional AKHSD family. This family includes AKHSD from *E. coli*, *H. influenzae*, *S. marcescens* and from plant sources (*D. carota*, *O. sativa* and *Z. mays*). The sequence alignment for HSD from this family (Figure 6) reveals a great deal of amino acid homology, including charged residues such as Lys, Asp, Arg. However, yeast HSD only contains three histidine residues, two of which are conserved. Histidine residue 79 is 83% conserved and His 309 is 100% conserved, whereas His 142 is not conserved at all.

*Steady-state kinetics of HSD H79A and HSD H309A mutants*

In order to determine the role of the conserved His residues, His→Ala mutations were introduced into yeast HSD. Both HSD H79A and HSD H309A mutants were purified and assayed in the forward and reverse directions. The replacement of His 79

**Figure 5. Phylogenetic tree of bacterial, fungal and HSD/AKHSD.** All amino acid sequences were obtained from the NCBI GenBank database and Genbank accession numbers are as follows: *Archaeoglobus fulgidus*-HSD (AE001039), *Bacillus subtilis*-HSD (J04034), *Corynebacterium glutamicum*-HSD (Y00546), *Daucus carota*-AKHSD (L11529), *E. coli*-AKHSD1 (J01709), *E. coli*-AKHSD2 (J01651), *Haemophilus influenzae*-AKHSD (U32694), *Helicobacter pylori*-HSD (AE000593), *Lactococcus lactis*-HSD (X96988), *Methanobacterium thermoautotrophicum*-HSD (AE000890), *Methanococcus jannaschii*-HSD (U67600), *Methylobacillus glycogenes*-HSD (D14071), *Mycobacterium tuberculosis*-HSD (Z73419), *Pseudomonas aeruginosa*-HSD (X65033), *Oryza sativa*-AKHSD (D78573), *S. cerevisiae*-HSD (X64457), *Serratia marcescens*-HSD (X60821), *Synechocystis sp.*-HSD (D64001), *Zea mays*-AKHSD1 (L33912), *Z. mays*-AKHSD2 (L33913). Amino acid sequence alignment was performed by ClustalW (<http://www2.edu./clustalw/>) (Higgins *et al.*, 1994) and the phylogenetic tree was illustrated by TreeDraw version 1.5.2. The scale represents the number of amino acid substitutions per site.



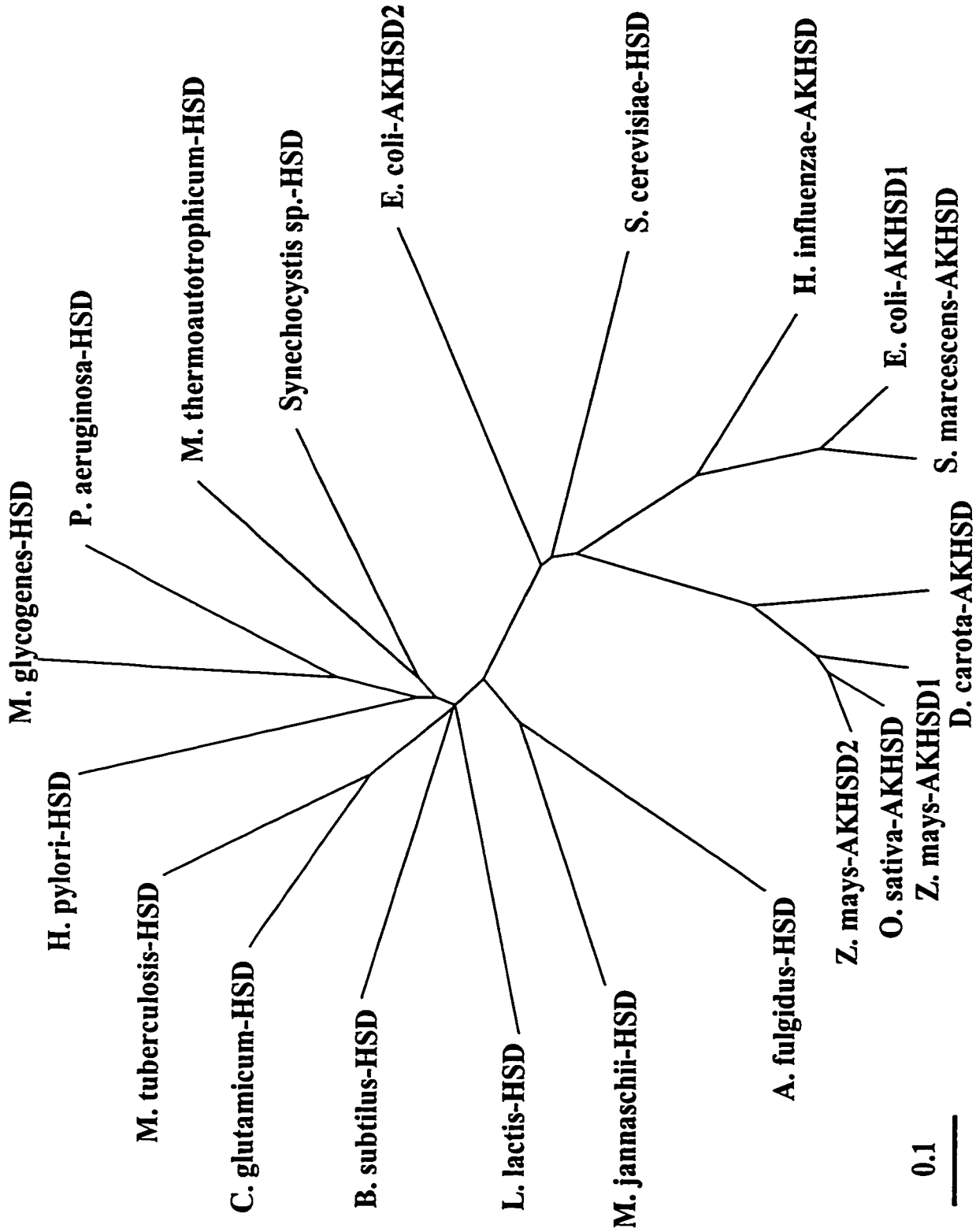


**Figure 6. Amino acid sequence alignment of *S. cerevisiae* HSD with the HSD domains of *E. coli* and plant enzymes.** All amino acid sequences were obtained from the NCBI GenBank database and Genbank accession numbers are as in Figure 5. Residues conserved in 80% or more of the sequences are shaded in grey. The positions of histidine residues in *S. cerevisiae* HSD are identified by arrows. Sequence alignment was performed by ClustalW (as in Figure 5) and was illustrated by GenDoc version 2.3.0.

\* 20 \* 40 \* 60 \* 80 \*  
 Osativa : -SKTTLAVGIIGPGLIGGTLDDQLKQDAAVLKENMNIIDLRVIGISGSRMHLSDIG-VDL-NQWKDLRKK-EAEPADLDSFVRHLSNHVFPNK  
 Zmays-HSD2 : -SKTTLAVGIIGPGLIGGALLNQLKQTAVALKENMNIIDLRVIGITGSSTMLLSDTG-IDL-TQWKQLQK-EAEPADIGSFVHHLSDNHVFPNK  
 Zmays-HSD1 : -SKTTLAVGIIGPGLIGRTLNLQKQDAAVLKENMNIIDLRVMGIAGSRTMLLSDIG-VDL-TQWKEKLOT-EAEPANLDFVHHLSENHFFPNR  
 Dcarota : -SRTTIAVGIIGPGLIGATLLDQLRDQAAILKENSKIDLRVMGITCSRTMLLSETG-IDL-SRWREVOKE-KGQTAGLEKFKVQHVGRGNHFFIPST  
 Scerevisia : MSTKVVNVAVIGAGVVGSAFLDQL- - -LAMKSTITYNL-VLLAEARSLISKDFSPLNVDKKAALAASTTKTLPDLDLIAHLKTS-PKP-V  
 Ecoli-HSD2 : -AEKRIGLVFGKGNIGSRWLELFAREQSTLSARTGFEFVLAVGVDSRRSLLSYDG-LDA-SRALAFFND-EAVEQEDESLEFLWMR-AHPYDDL



100 \* 120 \* 140 \* 160 \* 180  
 Osativa : VLVDCTADTYVACHYYDWLKKGIHVITPNKKANSGLDRLYLKRLTLQRASYTHYFYEATVGAGLP IISTLRGLLETDGKILRIEGIFSGTLSYI  
 Zmays-HSD2 : VLVDCTADTSVASHYYDWLKKGIHVITPNKKANSGLDQYLKRLTMQRASYTHYFYEATVGAGLP IISTLRGLLETDGKILRIEGIFSGTLSYI  
 Zmays-HSD1 : VLVDCTADTSVASHYYDWLKKGIHVITPNKKANSGLDRLYLKRLTLQRASYTHYFYEATVGAGLP IISTLRGLLETDGKILRIEGIFSGTLSYI  
 Dcarota : VIVDCTADSEVASHYHDWLCRGIHVITPNKKANSGLDQYLKRLALQRRSYTHYFYEATVAGLP IITLQGLLETDGKILRIEGIFSGTLSYI  
 Scerevisia : ILVDNTSSAYIAGFYTKFVENGISIATPNKKAFSSDLATWKALFSN-KPTNGFVYHEATVGAGLP IISFLREIIQTGDEVEKIEGIFSGTLSYI  
 Ecoli-HSD2 : VVLDVTAQQQLADQYLDFAHGFHVISANKLAGASDSNKYRQIHDAFEKTRHWLWLNATVAGLP INHTVTRDLIDSGDTILSISGIFSGTLSWL



\* 200 \* 220 \* 240 \* 260 \* 280  
 Osativa : FNNFEGTRT- - -FSNVVAEAKGAGTEPDRDDLSTGTDVARKV IILARESGLRLEL-SDIPVKSLLPEALRSCSSADEFMQKLPSPFDQDWDRO  
 Zmays-HSD2 : FNNFEGTRA- - -FSDVVAEAREAGTEPDRDDLSTGTDVARKVVVLARESGLRLEL-SDIPVKSLLVPEALRSCSSADEFMQKLPSPFDEDDWARQ  
 Zmays-HSD1 : FNNFEGART- - -FSDVVAEAKKAGTEPDRDDLSTGTDVARKV IILARESGLGLEL-SDIPVRSLVPEALRSCSSADEFMQKLPSPFDEDDWARE  
 Dcarota : FNNFKSTTP- - -FSEVVSEAKAAGTEPDRDDLSTGTDVARKV IILARGSGLKLEL-SDIPVQSLVPEALRGIASAEFFLLQLPQFDSDMTRK  
 Scerevisia : FNEFSTSQANDVKFSDVVVAKKLGTEPDRDDLSTGTDVARKV IIVGRIISGVEVESPTSFVQSLIPKPLESVKSADEFEKLSDYDKDLTLQL  
 Ecoli-HSD2 : FLQFDGSP- - -FTELVDQAWQGLTEPDRDDLSTGTDVSRKLVILAREAGYNIIEP-DQVRVESLVPAHCEG-GSIDHFFENGDELNEQMVQR

\* 300 \* 320 \* 340 \* 360 \*  
 Osativa : RDEAEAGEVLRVYGVVDVANRKRVELQRYKRDHPFAQLSGSDNIIAFTTSRYKEQPLIVRGPAGAEVTTAGGVFCDIILRLASYLGAPS  
 Zmays-HSD2 : RSDAEAGEVLRVYVGALDANRSGQVELRRYRRDHPFAQLSGSDNIIAFTTSRYKEQPLIVRGPAGAEVTTAGGVFCDIILRLASYLGAPS  
 Zmays-HSD1 : RKNAAAGEVLRVYGVVDVVS KKGQVELRAYKRDHPFAQLSGSDNIIAFTTSRYKQDQPLIVRGPAGAEVTTAGGVFCDIILRLSSYLGAPS  
 Dcarota : REDAENAGEVLRVYGVVDVANQGVVELKRYKKEHPFAQLSGSDNINAFTTERYNKQPPPIIRGPGAGAEVTTAGGVFCDIILRLASYLGAPS  
 Scerevisia : KKEAATENKVLRFI GKVDVATKTSVGI EKDYSHFPASLKGSDNVI SIKTKRYTN-PVVIQAGAGAAVTAAGVLGDVVKIAQRL- - -  
 Ecoli-HSD2 : LEAAREMGLVLRVYVARFDAN-GKARVGVAEVREDHPLRSLPCDNVFAIESRWYRDNPLVIRGPGAGRDVDTAGAIQISDINRLAQLL- - -



with Ala appeared to have little effect on HSD activity as steady state kinetics for HSD H79A were similar to wild type HSD (Table 2). Although  $k_{cat}$  for either direction was twofold lower for HSD H79A than wild type, rate constants ( $k_{cat}/K_m$ ) for HSD H79A were equal to  $10^6$ - $10^7$   $M^{-1} s^{-1}$  in the forward direction and  $10^4$ - $10^5$   $M^{-1} s^{-1}$  in the reverse direction as seen with the wild type enzyme. On the other hand, the catalytic efficiency for the HSD H309A mutant was reduced by almost two orders of magnitude.  $k_{cat}/K_m$  for HSD H309A were in the range of  $10^4$ - $10^6$   $M^{-1} s^{-1}$  for the forward reaction and  $10^3$ - $10^4$   $M^{-1} s^{-1}$  for the reverse reaction. Since both HSD mutants have Michaelis constants comparable to wild type, with the exception of lower values in the reverse direction, the reduced rate constants for HSD H309A is a consequence of severely lowered  $k_{cat}$  values. Turnover numbers for the forward reaction were reduced by approximately 40 times, whereas these numbers decreased by 20-fold for the reverse reaction. Lastly, substrate inhibition by ASA in the presence of NADH was not affected by mutation of His 79, however, inhibition was eliminated by mutation of His 309. These results suggest that histidine residue 309, and not His 79, is a critical residue for HSD catalysis.

## DISCUSSION

Prompted by the report that HSD was a potential target for antifungal compounds (Yamaki *et al.*, 1990; Yamaki *et al.*, 1992), we have initiated a study of the mechanism and structure of this enzyme from the yeast *S. cerevisiae*. Central to these studies was a requirement for an adequate supply of the enzyme in pure form. Attempts at purification of the enzyme from natural abundance in yeast proved unreliable and, therefore, it was overexpressed in *E. coli*. The expression construct, pCP13, gave sufficient quantities (>25 mg/L of cell culture) of pure, active dimeric HSD for mechanistic and crystallization (DeLaBarre *et al.*, 1998) studies.

The enzyme activity was readily measured in both the forward and reverse directions. Not surprisingly, the equilibrium appears to lie in the forward, physiologically relevant direction, as the second order rate constant  $k_{cat}/K_m$  for this reaction is  $10^2$  times larger. Both the phosphorylated and non-phosphorylated nicotinamide cofactors were good substrates, but NAD(H) was preferred. The substrates in the forward reaction have very low  $K_m$  values, which reflects very high affinities for the enzyme. Unlike previous results (Yamaki *et al.*, 1992), ASA was a substrate inhibitor of HSD only with NADH as the cofactor. If nicotinamide release is largely rate-limiting, as is the case for many dehydrogenases (Silverstein and Boyer, 1964; Iwatsubo and Pantaloni, 1967; Silverstein and Sulebele, 1969), substrate inhibition is a result of ASA binding to the E•NAD<sup>+</sup> complex, thereby forming an abortive ternary complex. Substrate inhibition may be more predominant with NADH as a result of higher affinity of HSD for the resulting NAD<sup>+</sup>

than  $\text{NADP}^+$ , which may be implied by the 14-fold lower  $K_m$  than  $\text{NADP}^+$ . This inhibition likely has little physiological relevance as it occurs at concentrations greater than  $4 K_m$ .

The back, Hse oxidizing, reaction obeyed typical Michaelis-Menten kinetics. However, in the forward reaction, oxidation at high  $\text{NAD(P)H}$  concentrations ( $\geq 0.5 \text{ mM}$ ,  $\geq 18\text{-}71 K_m$ ) resulted in a dramatic decrease in initial rate, which did not fit typical substrate inhibition equations. These rates did, however, increase over time. This phenomenon was independent of the commercial source of reduced cofactors. Preincubation of HSD with ASA did not result in enzyme inactivation. Thus, transient inactivation by a contaminant or through possible Schiff's base formation between HSD and ASA is unlikely. Formation of an adduct between the enolate of ketones or aldehydes and the C-4 of oxidized nicotinamide cofactors has some precedent (Everse *et al.*, 1971) and, indeed, these have been shown to be potent mechanism-based inhibitors of some dehydrogenases (Bull *et al.*, 1996). However, we see no evidence for novel adducts by anion exchange HPLC; in fact, only  $\text{NAD}^+$  and  $\text{NADH}$  are recovered. There was no observable reaction between ASA and  $\text{NAD}^+$  incubated in the absence or presence of HSD. It is therefore unlikely that the inhibition is due to formation of an ASA- $\text{NAD}^+$  adduct at the enzyme active site. Glutamate dehydrogenase has been shown to undergo dissociation of the active dimer into inactive monomer at high  $\text{NADH}$  concentrations (Frieden, 1959). We have not observed any dissociation of the dimer when incubated with inhibiting  $\text{NADH}$  concentrations by size exclusion chromatography or by native gel

electrophoresis (not shown). However, that some transient dissociation/association phenomenon is occurring which is not detectable by the methods we have used cannot be discounted. Horse liver alcohol dehydrogenase has demonstrated a similar lag in progress curves at high aldehyde concentrations. In this case, it was caused by the dismutation of the aldehyde substrate into acid and alcohol, which is invisible at 340 nm since  $\text{NAD}^+$  is not consumed (Henehan and Oppenheimer, 1993). This scenario, nonetheless, does not seem to apply to HSD. The fact that higher concentrations of KCl decreased the time of the lag observed, may point to a conformational component to this phenomenon. However, no changes in Trp fluorescence were visible when KCl was added to HSD, which suggests no major effect on protein conformation (at least as these would impact the local environments of the 2 Trp residues in HSD, data not shown). At this juncture, the precise nature of the rate lag remains unknown. However, as it occurs at very high nicotinamide concentrations (18-71  $K_m$ ), its biological significance is probably minimal.

Like *E. coli* AKHSD-1, yeast HSD is sensitive to  $\text{K}^+$  and  $\text{Na}^+$  ion concentrations. In the case of AKHSD-1,  $\text{K}^+$  is actually an activator and required for activity (Ogilvie *et al.*, 1975), while  $\text{Na}^+$  is an inhibitor of this activation (Wedler and Ley, 1993b). In contrast,  $\text{K}^+$  and  $\text{Na}^+$  ions have a similar effect on the *S. cerevisiae* HSD. Increased  $\text{K}^+$  or  $\text{Na}^+$  concentrations result in increased  $K_m$  for both ASA and NADH and increased substrate inhibition constant ( $K_i$ ) for ASA, but no effect was observed on  $k_{cat}$ . The structural reason for these effects is not known, but it does not appear to be due to

dramatic changes in quaternary structure, as assessed by Trp fluorescence.

The results of the chemical modification studies revealed that one or more histidine residues in HSD are important for catalytic activity. Of several reagents tested, only DEPC and TNM produced considerable inactivation of HSD. DEPC has been previously shown to modify histidine and tyrosine residues and, occasionally, cysteine and lysine residues (Miles, 1977), whereas TNM is frequently used as a nitration reagent specific for tyrosine residues at pH 8 (Sokolovski *et al.*, 1966). Although, the activity of DEPC-treated HSD could not be restored by the addition of neutral hydroxylamine due to a negative effect of hydroxylamine on HSD activity, the inactivation of HSD by DEPC is believed to occur as a result of His residue modification. UV difference spectra between native and DEPC-treated HSD illustrated an increase in absorbance at 240 nm, characteristic for the formation of N-carbethoxyhistidine. Whereas, no significant decrease in absorbance at 278 nm corresponding to modification of tyrosine residues was measured. Although, UV spectroscopy detected the modification of approximately 2 His residues /subunit, it was unclear whether 2 different His residues were modified or whether a disubstituted histidine was produced (Miles, 1977). In any case, it is obvious that inactivation of yeast HSD by DEPC is a consequence of carbethoxylation of His residue(s).

*D, L*-Hse protected HSD activity to a much greater extent than NAD<sup>+</sup>, suggesting that the important His residue(s) reside closer to the substrate binding site than the coenzyme binding site. This also appeared to be the case for pig heart malate



dehydrogenase (s-MDH) (Holbrook *et al.*, 1974) and chorismate mutase-prephenate dehydrogenase (Christendat and Turnbull, 1996). It is possible that DEPC is reacting with substrates. However, the concentration of DEPC was in excess of that for *D,L*-Hse and even with concentrations of DEPC as low as 2.5 mM activity of HSD was significantly inhibited. On the other hand, substrates had little effect on inactivation of yeast HSD by TNM.

The phylogenetic tree of HSD/AKHSD proteins from various species determined that *S. cerevisiae* HSD was more closely related to bifunctional AKHSD enzymes. Sequence alignments of the HSD portion of these enzymes revealed that 2 out of 3 His residues in HSD are conserved (His 79 and His 309). As a result, HSD His→Ala mutants were prepared by site-directed mutagenesis and steady state kinetics examined. Mutation of His 79 had little effect on HSD kinetic parameters. Rate constants ( $k_{cat}/K_m$ ) in both forward and reverse directions were in the same order of magnitude as wild type HSD and  $k_{cat}$  values were only twofold lower. In contrast, replacement of His 309 with Ala resulted in a dramatic decrease in catalytic efficiency and elimination of substrate inhibition.  $k_{cat}/K_m$  values for HSD H309A in both directions were almost two orders of magnitude lower as a result of severe decreases in  $k_{cat}$ . Turnover numbers for HSD H309A were about 40-fold lower than wild type in the forward direction and 20-fold lower in the reverse direction, suggesting that the mutation had a larger effect on the reduction of ASA.

Dehydrogenases are believed to promote hydride transfer by either of two

mechanisms: an active site residue such as His can act as a general acid/base to facilitate protonation or deprotonation of the oxygen group or, in the case of metallo dehydrogenases, a water molecule tightly coordinated to zinc can perform the same function (Oppenheimer and Handlon, 1992). However, mutation of catalytically important His residues in this context usually results in much more significant decreases in activity than we observed here, for example 600-fold for VanHst, an alpha ketoacid dehydrogenase (Marshall *et al.*, 1999). As noted above, after these experiments were completed, the 3D structure of the enzyme became available (B. DeLaBarre and A. Berghuis, personal communication). This structure revealed that His 309 was not adjacent to the enzyme active site, but rather was located at the dimer interface. Thus, this residue likely plays a critical role in maintaining protein structure in a catalytically competent form. On the other hand, several charged residues (Lys, Asp, Glu) are located in the active site. This is surprising in light of the fact that methyl acetimidate, PLP and EDC had little effect on enzyme activity.

In conclusion, yeast HSD has been highly expressed and efficiently purified such that mg quantities are now available for mechanistic and structural studies. Steady state parameters in the forward and backward directions have been accurately determined for the first time and His 309 was identified as an important HSD residue. These results provide the appropriate foundation for future examination of HSD as a possible target for new antifungal agents.

## REFERENCES

- Angeles, T. S., P. A. Smanik, C. L. Borders, Jr., and R. E. Viola (1989) Aspartokinase-homoserine dehydrogenase I from *Escherichia coli*: pH and chemical modification studies of the kinase activity, *Biochemistry*, **28**: 8771-8777.
- Angeles, T. S., and R. E. Viola (1990) The kinetic mechanism of the bifunctional enzyme aspartokinase-homoserine dehydrogenase I from *Escherichia coli*, *Arch. Biochem. Biophys.*, **283**: 96-101.
- Armstrong, D. (1993) Treatment of opportunistic fungal infections, *Clin. Infect. Dis.*, **16**: 1-9.
- Black, S., and N. G. Wright (1955) Homoserine dehydrogenase, *J. Biol. Chem.*, **213**: 51-60.
- Bull, H. G., M. Garcia-Calvo, S. Andersson, W. F. Baginski, H. K. Chan, D. E. Ellsworth, R. R. Miller, R. A. Stearns, R. K. Bakshi, G. H. Rasmusson, R. L. Tolman, R. W. Myers, J. W. Kozarich and G. S. Harris (1996) Mechanism-based inhibition of human steroid 5 $\alpha$ -reductase by finasteride: Enzyme-catalysed formation of NADP-dihydrofinasteride, a potent bisubstrate analog inhibitor, *J. Am. Chem. Soc.*, **118**: 2359-2365.
- Christendat, D., and J. Turnbull (1996) Identification of active site residues of chorismate mutase-prephenate dehydrogenase from *Escherichia coli*, *Biochemistry*, **35**: 4468-4479.
- DeLaBarre, B., S. L. Jacques, C. E. Pratt, D. Ruth, G. D. Wright, and A. M. Berghuis (1998) Crystallization and preliminary X-ray diffraction studies of homoserine dehydrogenase from *Saccharomyces cerevisiae*, *Acta Cryst. Sec. D*, **D54**: 413-415.
- DeMuri, G. P., and M. K. Hostetter (1995) Resistance to antifungal agents, *Ped. Clin. North Amer.*, **42**: 665-685.
- Everse, J., E. Cooper Zoli, L. Kahan and N. O. Kaplan (1971) Addition products of diphosphopyridine nucleotides with substrates of pyridine nucleotide-linked dehydrogenases, *Org. Chem.*, **1**: 207-233.
- Frieden, C. (1959) Glutamic dehydrogenase. I. The effect of coenzyme on the sedimentation velocity and kinetic behavior, *J. Biol. Chem.*, **234**: 809-814.

- Georgopapadakou, N. H., and T. J. Walsh (1996) Antifungal agents: Chemotherapeutic targets and immunologic strategies, *Antimicrob. Agents Chemother.*, **40**: 279-291.
- Henehan, G. T. M., and N. J. Oppenheimer (1993) Horse liver alcohol dehydrogenase-catalyzed oxidation of aldehydes: dismutation precedes net production of reduced nicotinamide adenine dinucleotide, *Biochemistry*, **32**: 735-738.
- Higgins, D., J. Thompson, T. Gibson, J. D. Thompson, D. G. Higgins, and T. J. Gibson (1994) Clustal W: improving the sensitivity of progressive multiple sequence alignment through sequence weighting, position-specific gap penalties and weight matrix choice, *Nucleic Acids Res.*, **22**: 4673-4680.
- Holbrook, J. J., A. Lodola, and N. P. Illsley (1974) Histidine residues and the enzyme activity of pig heart supernatant malate dehydrogenase, *Biochem. J.*, **139**: 797.
- Hollomon, D. W. (1993) Resistance to azole fungicides in the field, *Biochem. Soc. Trans.*, **21**: 1047-1051.
- Iwatsubo, M., and Pantaloni, D. (1967) Regulation of the activity of glutamate dehydrogenase by effectors GTP and ADP: Study by means of "stopped flow", *Bull. Soc. Chim. Biol.*, **49**: 1563-1572.
- Leatherbarrow, R. J. (1992) Grafit 3.0, Erithacus Software LTD., Staines, U.K.
- Marshall, C. G., M. Zolli and G. D. Wright (1999) Molecular mechanism of VanHst, an alpha-ketoacid dehydrogenase required for antibiotic resistance from a glycopeptide producing organism, *Biochemistry*, **38**: 8485-8491.
- Masner, P., P. Muster and J. Schmid (1994) Possible methionine biosynthesis inhibition by pyrimidinamine fungicides, *Pestic. Sci.*, **42**: 163-166.
- Miles, E. W. (1977) Modification of histidyl residues in proteins by diethylpyrocarbonate, *Methods Enzymol.*, **47**: 431-442.
- Ogilvie, J. W., L. P. Vickers, R. B. Clark, and M. M. Jones (1975) Aspartokinase I-homoserine dehydrogenase I of *Escherichia coli* K12 ( $\lambda$ ). Activation by monovalent cations and an analysis of the effect of the adenosine triphosphate-magnesium ion complex on this activation process, *J. Biol. Chem.*, **250**: 1242-1260.
- Oppenheimer, N. J., and A. L. Handlon (1992) in *The Enzymes* (Boyer, P. D., Ed.) Vol XX, Academic Press, New York, pp. 453-505

- Silverstein, E., and P. D. Boyer (1964) Equilibrium reaction rates and the mechanisms of liver and yeast alcohol dehydrogenase, *J. Biol. Chem.*, **239**: 3908-3914.
- Silverstein, E., and Sulebele, G. (1969) Catalytic mechanism of pig heart mitochondrial malate dehydrogenase studied by kinetics at equilibrium, *Biochemistry*, **8**: 2543-2550.
- Sokolovski, M., J. F. Riordan, and B. L. Vallee (1966) Tetranitromethane. A reagent for the nitration of tyrosyl residues in proteins, *Biochemistry*, **5**: 3582-3589.
- Sternberg, S. (1994) The emerging fungal threat, *Science*, **266**: 1632-1634.
- Thomas, D., R. Barbey and Y. Surdin-Kerjan (1993) Evolutionary relationships between yeast and bacterial homoserine dehydrogenases, *FEBS Lett.*, **323**: 289-293.
- Tudor, D. W., T. Lewis, and D. J. Robins (1993) *Synthesis*, 1061-1062.
- Wedler, F. C., B. W. Ley, S. L. Shames, S. J. Rembish and D. L. Kushmaul (1992) Preferred order random kinetic mechanism for homoserine dehydrogenase of *Escherichia coli* (Thr-sensitive) aspartokinase/homoserine dehydrogenase-I: Equilibrium isotope exchange kinetics, *Biochim. Biophys. Acta*, **1119**: 247-249.
- Wedler, F. C., and B. W. Ley (1993a) Kinetic and regulatory mechanisms for (*Escherichia coli*) homoserine dehydrogenase-I: Equilibrium isotope exchange kinetics, *J. Biol. Chem.*, **268**: 4880-4888.
- Wedler, F. C., and B. W. Ley (1993b) Homoserine dehydrogenase-I (*Escherichia coli*): Action of monovalent ions on catalysis and substrate association-dissociation, *Arch. Biochem. Biophys.*, **301**: 416-423.
- Yamaguchi, H., K. Uchida, T. Hiratani, T. Nagate, N. Watanabe and S. Omura (1988) RI-331, a new antifungal antibiotic, *Ann. N. Y. Acad. Sci.*, **544**: 188-191.
- Yamaki, H., M. Yamaguchi, H. Imamura, H. Suzuki, T. Nishimura, H. Saito and H. Yamaguchi (1990) The mechanism of antifungal action of (*S*)-2-amino-4-oxo-5-hydroxypentanoic acid, RI-331: The inhibition of homoserine dehydrogenase in *Saccharomyces cerevisiae*, *Biochem. Biophys. Res. Commun.*, **168**: 837-843.

- Yamaki, H., M. Yamaguchi, T. Tsuruo and H. Yamaguchi (1992) Mechanism of action of an antifungal antibiotic, RI-331, (*S*) 2-amino-4-oxo-5-hydroxypentanoic acid: Kinetics of inactivation of homoserine dehydrogenase from *Saccharomyces cerevisiae*, *J. Antibiotics*, **45**: 750-755.
- Yumoto, N., Y. Kawata, S. Noda and M. Tokushige (1991) Rapid purification and characterization of homoserine dehydrogenase from *Saccharomyces cerevisiae*, *Arch. Biochem. Biophys.*, **285**: 270-275.

## **CHAPTER 3**

**Homoserine Dehydrogenase from *Saccharomyces cerevisiae*:**

**Kinetic Mechanism and Stereochemistry**

**Suzanne L. Jacques and Gerard D. Wright**

### 3.1 Preface

In chapter 2, the kinetic properties and the chemical mechanism of *S. cerevisiae* HSD were examined. In order to further our knowledge of this fungal enzyme, this paper investigated the kinetic mechanism of yeast HSD and its stereochemistry. Earlier reports demonstrated that the kinetic mechanism of *E. coli* AKHSD I was preferred order random and that the hydride transfer occurred from the *pro-S* C-4 position of NADH. On the other hand, these issues were not previously examined for fungal HSD.

Surprisingly, the results in this chapter revealed that yeast HSD is very similar to *E. coli* AKHSD I. The kinetic mechanism for yeast HSD was likewise ordered and the stereochemistry also occurred at the *pro-S* C-4 position of NADH. Additional results from pH studies suggested basic groups were involved in substrate binding and several compounds were screened for inhibition of HSD activity. H-(1,2,4-triazol-3-yl)-*D,L*-alanine was discovered to be an effective inhibitor and, therefore, will prove useful as a lead compound for HSD inhibitor design. The results obtained in this paper complement the previous findings and will be very beneficial in the development of novel potent antifungal agents directed against yeast HSD.

I performed all the experimental work presented in this chapter. Dr. Honek of the University of Waterloo is gratefully acknowledged for providing most of the compounds screened for inhibition of yeast HSD presented in Appendix A.



### 3.2 Paper

**Homoserine Dehydrogenase from *Saccharomyces cerevisiae*:  
Kinetic Mechanism and Stereochemistry<sup>†</sup>**

Suzanne L. Jacques and Gerard D. Wright\*

Department of Biochemistry, McMaster University, Hamilton, ON,  
L8N 3Z5

Running title: Kinetic Mechanism of Yeast Homoserine Dehydrogenase

\*Corresponding author. Phone: (905) 525-9140, ext. 22943; Fax: (905) 522-9033;  
Email: [wrightge@fhs.mcmaster.ca](mailto:wrightge@fhs.mcmaster.ca)

<sup>†</sup> This research was supported by a Natural Sciences and Engineering Research Council of Canada Strategic Grant and an Ontario Graduate Student Scholarship to S.L.J..

**Footnotes**

<sup>1</sup> Abbreviations: AKHSD, aspartokinase-homoserine dehydrogenase (EC 2.7.2.4 and EC 1.1.1.3); ASA, *L*-aspartate  $\beta$ -semialdehyde; CAPS, 3-[cyclohexylamino]-1-propanesulfonic acid; CHES, 2-[N-cyclohexylamino]ethanesulfonic acid; HEPES, N-[2-hydroxyethyl]piperazine-N'-[2-ethanesulfonic acid]; HSD, homoserine dehydrogenase (EC 1.1.1.3); Hse, homoserine; RI-331, (*S*)-2-amino-4-oxo-5-hydroxypentanoic acid; TAPS, *N*-tris[hydroxymethyl]methyl-3-amino-propanesulfonic acid.

## ABSTRACT

Homoserine dehydrogenase (HSD), which is required for the synthesis of Thr, Ile and Met in fungi, is a potential target for novel antifungal drugs. In order to design effective inhibitors, the kinetic mechanism of *Saccharomyces cerevisiae* HSD and the stereochemistry of hydride transfer were examined. Product inhibition experiments revealed that yeast HSD follows an ordered Bi Bi kinetic mechanism, where NAD(P)H must bind the enzyme prior to aspartate semialdehyde (ASA) and homoserine (Hse) is released first followed by NAD(P)<sup>+</sup>. H-(1,2,4-triazol-3-yl)-*D,L*-alanine was an uncompetitive inhibitor of HSD with respect to NADPH ( $K_i = 3.04 \pm 0.18$  mM) and a noncompetitive inhibitor with respect to ASA ( $K_i = 1.64 \pm 0.36$  mM,  $K_i = 3.84 \pm 0.46$  mM), in agreement with the proposed substrate order. Both kinetic isotope and viscosity experiments provided evidence for a very rapid catalytic step and suggest nicotinamide release to be primarily rate limiting. Incubation of HSD with stereospecifically deuterated NADPD and subsaturating amounts of aspartate semialdehyde revealed that the *pro*-S NADPH hydride is transferred to the aldehyde. The pH dependence of steady state kinetic parameters indicate that ionizable groups with basic pKs may be involved in substrate binding. The results presented in this paper demonstrate that *S. cerevisiae* HSD shares significant similarities to *E. coli* AKHSD I. These findings provide the requisite foundation for future exploitation of fungal HSD in inhibitor design.

## INTRODUCTION

The last decade has seen a dramatic increase in the frequency and types of fungal infections as a result of increasing numbers of immunocompromised patients (Sternberg, 1994). However, the selection of non-toxic antifungal drugs available remains low and these are threatened by increasing fungal resistance (Graybill, 1996). The development of new antifungal agents is therefore critical. New drug targets, such as chitin synthase and  $\beta$ -1,3-glycan synthase in fungal cell wall biosynthesis and proton ATPases, are currently being studied (Georgopapadakou and Walsh, 1996)

Recently, a natural amino acid analog, (*S*)-2-amino-4-oxo-5-hydroxypentanoic acid (RI-331)<sup>1</sup> was found to be active against several pathogenic fungi by inhibiting homoserine dehydrogenase (HSD) (EC 1.1.1.3) (Yamaki *et al.*, 1990). This enzyme converts *L*-aspartate  $\beta$ -semialdehyde (ASA) to *L*-homoserine (*L*-Hse) in the aspartate pathway, which produces methionine, isoleucine and threonine. This biosynthetic pathway is absent in mammals, making it a good target for novel antifungal agents. In order to evaluate HSD as a drug target and design potent inhibitors, this enzyme needs to be well characterized and mechanistically understood. To this end, *Saccharomyces cerevisiae* HSD was overexpressed in *Escherichia coli* and purified, and the steady state kinetic parameters were obtained for both ASA reducing and Hse oxidizing directions (Jacques *et al.*, 1999 (Chapter2)).

Unlike the yeast enzyme, the *E. coli* enzyme AKHSD I has been well characterized. This enzyme is bifunctional, possessing both aspartate kinase (AK) and homoserine dehydrogenase (HSD) activities. The kinetic mechanism for the

dehydrogenase activity was determined to be preferred ordered random by equilibrium isotope exchange kinetics (Wedler *et al.*, 1992). Further experiments revealed that the order was a result of the amino acid dissociation from the ternary complex being more rapid than the cofactor (Wedler and Ley, 1993). The reaction rate was also limited by the dissociation of the cofactor (Wedler and Ley, 1993) and not by the chemical step (Wedler *et al.*, 1992). In addition, the stereochemistry of the hydride transfer was shown to be from the *pro-S* C-4 of NAD(P)H to the *pro-S* C-4 position on homoserine (Chang and Walsh, 1980). Although the functional amino acid residues involved in *E. coli* HSD activity have not yet been identified, a histidine residue (His 309) was demonstrated to be important in catalysis by yeast HSD (Jacques *et al.*, 1999 (Chapter 2)). Further characterization of *S. cerevisiae* HSD, presented in this paper, revealed the kinetic mechanism and stereochemistry of this enzyme. A full biochemical understanding of yeast HSD will prove useful in the development of novel, non-toxic antifungal agents, which are in great clinical demand at present.

## MATERIALS AND METHODS

### *Chemicals*

*L*-aspartate  $\beta$ -hydroxamate, 2-[*N*-cyclohexylamino]ethanesulfonic acid (CHES), 3-[cyclohexylamino]-1-propanesulfonic acid (CAPS), *L*-homoserine, *N*-[2-hydroxyethyl]piperazine-*N'*-[2-ethanesulfonic acid] (HEPES), *D,L*-hydroxynorvaline, *L*-methionine, NADH, *L*-threonine and *N*-tris[hydroxymethyl]methyl-3-aminopropanesulfonic acid (TAPS) were obtained from Sigma (St. Louis, MO). Reduced and oxidized forms of the nicotinamide coenzymes (NAD<sup>+</sup>, NADP<sup>+</sup>, NADPH) were purchased from Boehringer Mannheim (Laval, PQ). Glycerol and PEG 8000 was acquired from BDH (Toronto, ON) and H-(1,2,4-triazol-3-yl)-*D,L*-alanine from Bachem Bioscience (King of Prussia, PA). Trifluoromethionine was a generous gift from Dr. Honek, University of Waterloo. Fluconazole (Diflucan, Pfizer, 100 mg tablets) was purchased from McMaster University Hospital pharmacy (Hamilton, ON). 4*S*-d-NADPH and 4*R*-d-NADPH were prepared as previously described (Benson *et al.*, 1993) and purified by anion exchange chromatography on a Mono Q HR5/5 column (Pharmacia) (Orr and Blanchard, 1984). Fractions were collected and those with an  $A_{260\text{ nm}}/A_{340\text{ nm}}$  ratio of 2.8 or less were used for kinetic isotope effect experiments. *L*-aspartate  $\beta$ -semialdehyde (ASA) was synthesized and yeast homoserine dehydrogenase was purified from *E. coli* BL21 (DE3)/pCP13 as per Jacques *et al.*, 1999.

### *Enzyme assays*

Forward ( $\text{ASA} + \text{NAD(P)H} \rightarrow \text{Hse} + \text{NAD(P)}^+$ ) and reverse (Hse oxidizing) reactions were measured, as previously described (Jacques *et al.*, 1999) by continuously monitoring the disappearance or the appearance of NAD(P)H at 340 nm using a Cary 3E UV-vis spectrophotometer at room temperature (25 °C). For product inhibition studies, the assay mixture contained 100 mM HEPES buffer, pH 7.5 and varying amounts of ASA, NADPH and product (*L*-Hse or  $\text{NADP}^+$ ) in a total volume of 980  $\mu\text{L}$ . ASA was held constant at 0.130 mM as a fixed subsaturating second substrate or at 1.3 mM as a fixed saturating second substrate. NADPH was held at 20  $\mu\text{M}$  as a fixed subsaturating second substrate.

Compounds surveyed for HSD inhibition were added to assays containing 1.0 mM ASA, 0.2 mM NADH and 100 mM HEPES pH 7.5 for the forward reaction or 15 mM *L*-Hse, 0.4 mM  $\text{NAD}^+$  and 100 mM CHES pH 9.5 for the reverse reaction in a total volume of 980  $\mu\text{L}$ . For characterization of HSD inhibition, *L*-Met, *L*-Thr, *L*-aspartate  $\beta$ -hydroxamate and H-(1,2,4-triazol-3-yl)-*D,L*-alanine were added to assays containing 100 mM HEPES, pH 7.5 and variable amounts of ASA and NAD(P)H or 100 mM CHES, pH 9.5 and variable amounts of *L*-Hse and  $\text{NAD}^+$  in 980  $\mu\text{L}$  total volume. Fixed saturating substrates were held at 0.75 mM for ASA, 0.2 mM for NAD(P)H and 0.3 mM for  $\text{NAD}^+$ .

For the analysis of kinetic isotope effects, the high ASA concentration assays consisted of 100 mM HEPES pH 7.5, 1.2 mM ASA, 0.09 M KCl and appropriate amounts of deuterated NADPH and the low ASA concentration assays consisted of 100

mM HEPES pH 7.5, 0.130 mM ASA, 0.105 M KCl and appropriate amounts of deuterated NADPH in 980  $\mu$ L.

Viscosity experiments were performed in both forward and reverse directions. In the forward direction, HSD activity was measured, as a function of varying ASA or NADH concentrations in the presence of 0, 10, 20 and 30 % glycerol or 5 % PEG 8000. ASA was held at 0.8 mM as a fixed second substrate and NADH was held at 0.2 mM as a fixed second substrate. In the reverse direction, the assay mixture contained 100 mM CHES, pH 9.5 and varying amounts of *L*-Hse,  $\text{NAD}^+$  and glycerol (0, 10, 20 and 30 %) (or 5 % PEG 8000) in a total volume of 980  $\mu$ L. *L*-Hse was held constant at 15 mM as a fixed second substrate, while  $\text{NAD}^+$  was held at 0.4 mM as a fixed second substrate. The viscosity of assay solutions was determined in quadruplicate relative to assay mixtures lacking glycerol using an Ostwald viscometer at 25 °C.

Kinetic parameters for HSD were obtained at various pHs by measuring HSD activity, as above, at varying *L*-Hse or  $\text{NAD}^+$  concentrations in buffers of pH 7.0 to 11.0 in 0.25 and 0.5 pH intervals. The buffers were as follows: HEPES (pH 7.0-8.0), TAPS (pH 8.5-8.75), CHES (pH 9.0-10.0) and CAPS (pH 10.0-11.0). *L*-Hse was held fixed at 20 mM as a second saturating substrate and  $\text{NAD}^+$  was held at 0.4 mM as a fixed saturating substrate.

All assays were initiated by the addition of 20  $\mu$ L purified HSD (0.1  $\mu$ g for the forward reaction and 1  $\mu$ g for the reverse reaction) and were done in duplicate.



### Data Analysis

Initial rates were obtained directly from the progress curves using the Cary 3.00 software. Inhibition data was fitted by nonlinear least squares regression to equations 3, 4, 5, or 6 for competitive, uncompetitive, noncompetitive or partial competitive inhibition, respectively, using Grafit 3.0 (Leatherbarrow, 1992). Steady-state kinetic parameters for HSD were obtained from kinetic isotope effect data, viscosity experiment data and pH study data by nonlinear least squares regression to equation 1 or 2. Kinetic parameters obtained from the best fit were reported with standard errors.

$$v = V_{max}S/(K_m + S) \quad (1)$$

$$v = V_{max}S/(K_m + S + S^2/K_i) \quad (2)$$

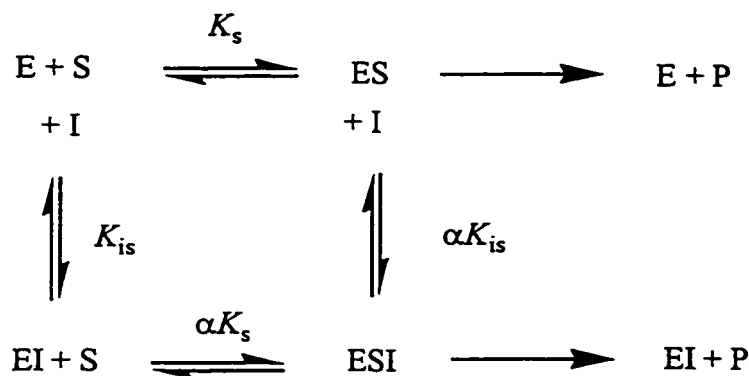
$$v = V_{max}S/(K_m(1 + I/K_{is}) + S) \quad (3)$$

$$v = V_{max}S/(K_m + S(1 + I/K_{ii})) \quad (4)$$

$$v = V_{max}S/(K_m(1 + I/K_{is}) + S(1 + I/K_{ii})) \quad (5)$$

$$v = V_{max}S/(K_m((1 + I/K_{is})/(1 + I/\alpha K_{is})) + S) \quad (6)$$

where  $v$  is the measured velocity,  $V_{max}$  is the maximal velocity,  $S$  is the varied substrate concentration,  $K_m$  is the Michealis-Menten constant,  $I$  is the inhibitor concentration,  $K_i$  is the substrate inhibition constant,  $K_{is}$  is the slope inhibition constant,  $K_{ii}$  is the intercept inhibition constant and  $\alpha$  is the correction factor for ES or EI in partial competitive inhibition (Scheme 1).

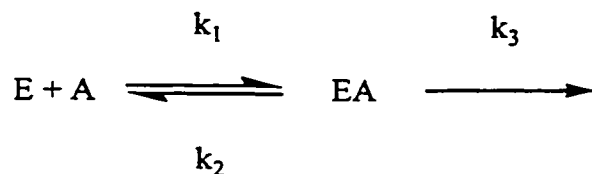


**Scheme 1. Reaction scheme for a partial competitive inhibitor**

Kinetic parameters ( $V_{max}/K_m$ ) obtained as a function of relative solution viscosity ( $\eta_{rel}$ ) were plotted as per equation 7.

$$1/(V_{max}/K_m[E]_0) = \eta_{rel}/k_1 + (k_2/k_3)/k_1 \quad (7)$$

where  $k_1$  is the rate of substrate binding,  $k_2$  is the rate of substrate dissociation and  $k_3$  is the rate of conversion, as shown in Scheme 2, and  $\eta_{rel}$  is relative viscosity (Cleland, 1986). From the results, the horizontal intercept was obtained by linear regression and was equal to  $k_2/k_3$ . The “stickiness” ratio ( $S_r$ ) for a substrate is equal to the forward and backward rates for the loss of the EA complex ( $k_2/k_3$ ). This value approaches zero for “nonsticky” substrates as their dissociation rates are usually larger than the rate of the catalytic step, whereas  $S_r$  is larger for “sticky” substrates which have substrate dissociation rates comparable or slower than the rate of the catalytic step.



**Scheme 2. General reaction scheme**

pH data demonstrating an increase in  $\log (V_{max}/K_m)_{app}$  with increasing pH were fit to equation 8 by nonlinear least squares regression using Grafit 3.0. Whereas pH data demonstrating a bell curve with pH were fit to equation 9. Equation 8 describes the titration of one ionizable group with an acidic pK and equation 9 describes a curve that has one ionizable group with an acidic pK and another ionizable group with a basic pK. The parameters ( $pK_a$  and  $pK_b$ ) were obtained along with standard errors.

$$\log (V_{max}/K_m)_{app} = \log((V_{max}/K_m)/(1 + H^+/K_a)) \quad (8)$$

$$\log (V_{max}/K_m)_{app} = \log((V_{max}/K_m)/(1 + H^+/K_a + K_b/H^+)) \quad (9)$$

where  $K_a$  and  $K_b$  are the ionization constants and  $H^+$  is the hydrogen ion concentration.

#### *Antifungal susceptibility assays*

An overnight *Candida albicans* or *Candida tropicalis* culture was diluted 20-fold or 40-fold, respectively, in YPD media (1 % yeast extract, 2 % peptone, 2 % dextrose) and 100  $\mu\text{L}$  was spread onto a YNB agar plate (0.67 % Difco yeast nitrogen base, 2 % dextrose, 1.5 % agar). Sterile filter disks were placed aseptically on the solid media and 15  $\mu\text{L}$  sample was added to each disk. The plates were then incubated overnight at 30  $^\circ\text{C}$ . A fluconazole tablet was ground up and dissolved in water to a

concentration of 2 mg/mL to use as a standard. The zone of growth inhibition was measured directly from the agar plate and is defined as the distance in mm between the edge of the filter disk and the outer edge of the area free from fungal growth.

## RESULTS

### *Product Inhibition*

Product inhibition was used in order to determine the kinetic mechanism of yeast HSD. With the fixed substrate at nonsaturating concentrations, the inhibition pattern by NADP<sup>+</sup> with respect to ASA was noncompetitive ( $K_{is} = 6.02 \pm 2.59$  mM,  $K_{ii} = 2.38 \pm 0.16$  mM), whereas it was partial competitive with respect to NADPH ( $K_{is} = 0.130 \pm 0.060$  mM,  $\alpha = 2.09 \pm 0.18$ ) (Table 1) (Figure 1). The inhibition pattern by *L*-Hse was noncompetitive with respect to ASA ( $K_{is} = 7.23 \pm 1.88$  mM,  $K_{ii} = 132 \pm 45$  mM) and with respect to NADPH ( $K_{is} = 28.9 \pm 9.8$  mM,  $K_{ii} = 18.6 \pm 2.0$  mM) (Figure 2). At saturating ASA concentrations, product inhibition by *L*-Hse with respect to NADPH displayed a noncompetitive inhibition pattern ( $K_{is} = 173 \pm 102$ ,  $K_{ii} = 45.6 \pm 5.3$  mM) (Figure 3).

### *Search for dead-end inhibitors and alternate substrates*

Only ASA and Hse were substrates for yeast HSD and no alternative substrates were found. Yeast HSD did not reduce 1.5, 15 or 30 mM acetaldehyde or butyraldehyde and did not oxidize 12.5 mM *D,L*-Ser, *D,L*-isoserine or *D,L*-hydroxynorvaline.

In addition, several amino acids, amino acid analogues and potential analogues were studied as possible inhibitors of HSD (see also Appendix A). *L*-Met and *L*-Thr, downstream products of the Asp pathway, weakly inhibited the reverse but not forward HSD reaction (Table 2). *L*-Met demonstrated noncompetitive inhibition with respect to *L*-Hse ( $K_{is} = 47.3 \pm 13.4$ ,  $K_{ii} = 186 \pm 27$  mM) and *L*-Thr competitive inhibition with

**Table 1. Kinetic constants for product inhibition of purified yeast HSD.**

Product	Variable Substrate	Fixed Substrate	Type of Inhibition	$K_i$ (mM)	$K_{ii}$ (mM)	Equation <sup>a</sup>
NADP <sup>+</sup>	ASA	NADPH <sup>b</sup>	NC	6.02 ± 2.59	2.38 ± 0.16	5
NADP <sup>+</sup>	NADPH	ASA <sup>b</sup>	C <sup>d</sup>	0.130 ± 0.060 ( $\alpha = 2.09 \pm 0.18$ )	—	6
<i>L</i> -Hse	ASA	NADPH <sup>b</sup>	NC	7.23 ± 1.88	132 ± 45	5
<i>L</i> -Hse	NADPH	ASA <sup>b</sup>	NC	28.9 ± 9.8	18.6 ± 2.0	5
<i>L</i> -Hse	NADPH	ASA <sup>c</sup>	NC	173 ± 102	45.6 ± 5.3	5

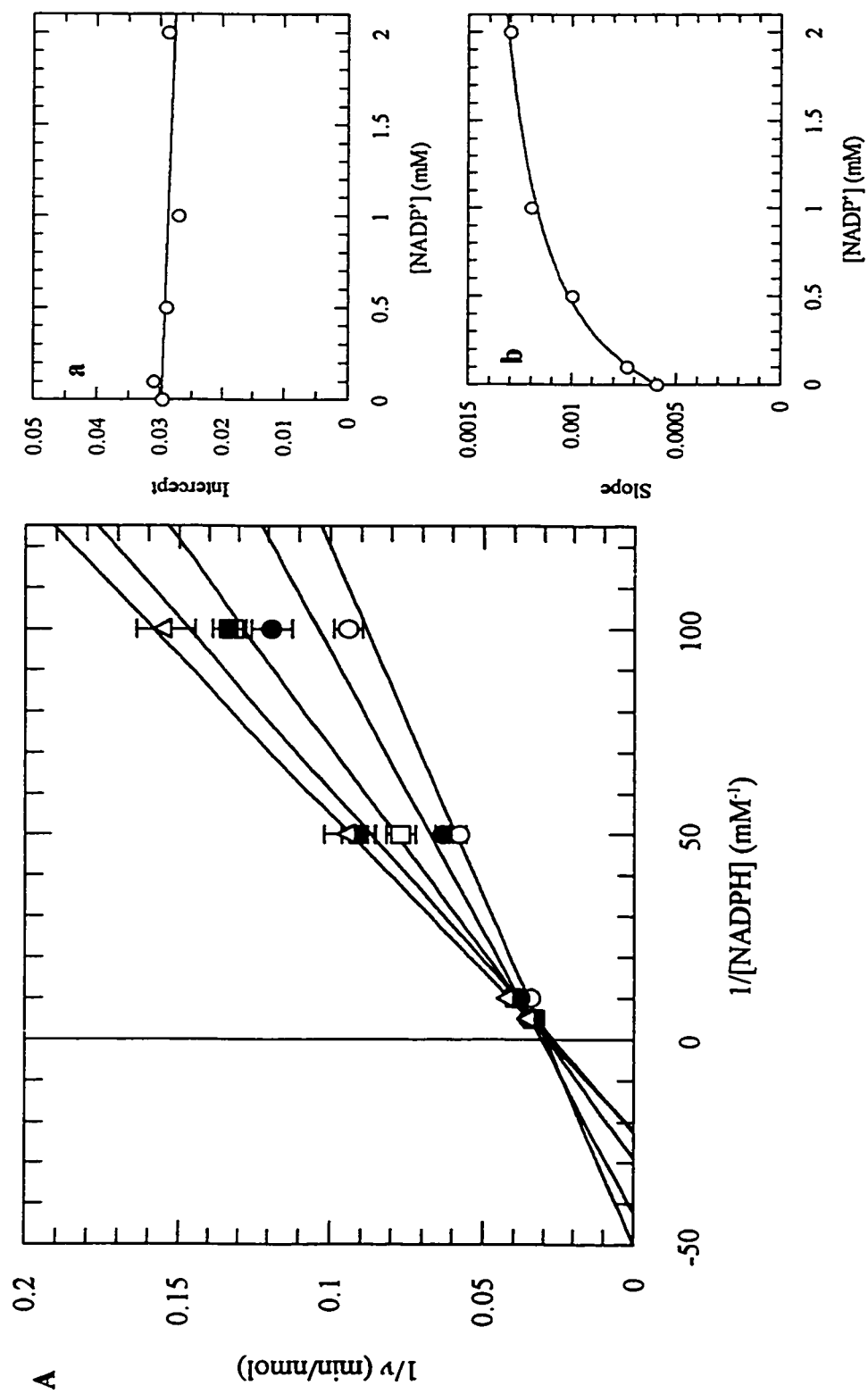
<sup>a</sup> -Data fit to equation number

<sup>b</sup> -Subsaturating concentrations (0.130 mM ASA or 20  $\mu$ M NADPH)

<sup>c</sup> -Saturating ASA concentration (1.3 mM)

<sup>d</sup> -Partial competitive, hyperbolic slope replot

**Figure 1. Product inhibition of HSD by NADP<sup>+</sup>.** (A) Partial competitive inhibition of NADPH. Double reciprocal plot with varying NADPH concentrations at 0 (○), 0.1 (●), 0.5 (□), 1.0 (■) and 2.0 (Δ) mM NADP<sup>+</sup>. ASA concentration was held constant at 0.130 mM (0.6  $K_m$ ). Data were fit to equation 6. *Inset (a)*, intercept replot of NADPH *versus* [NADP<sup>+</sup>]; *inset (b)*, slope replot of NADPH *versus* [NADP<sup>+</sup>]. (B) Noncompetitive inhibition of ASA. Double reciprocal plot with varying ASA concentrations at 0 (○), 0.2 (●), 1.0 (□), 2.0 (■) and 3.0 (Δ) mM NADP<sup>+</sup>. NADPH concentration was held constant at 20 μM ( $K_m$ ). Data were fit to equation 5.





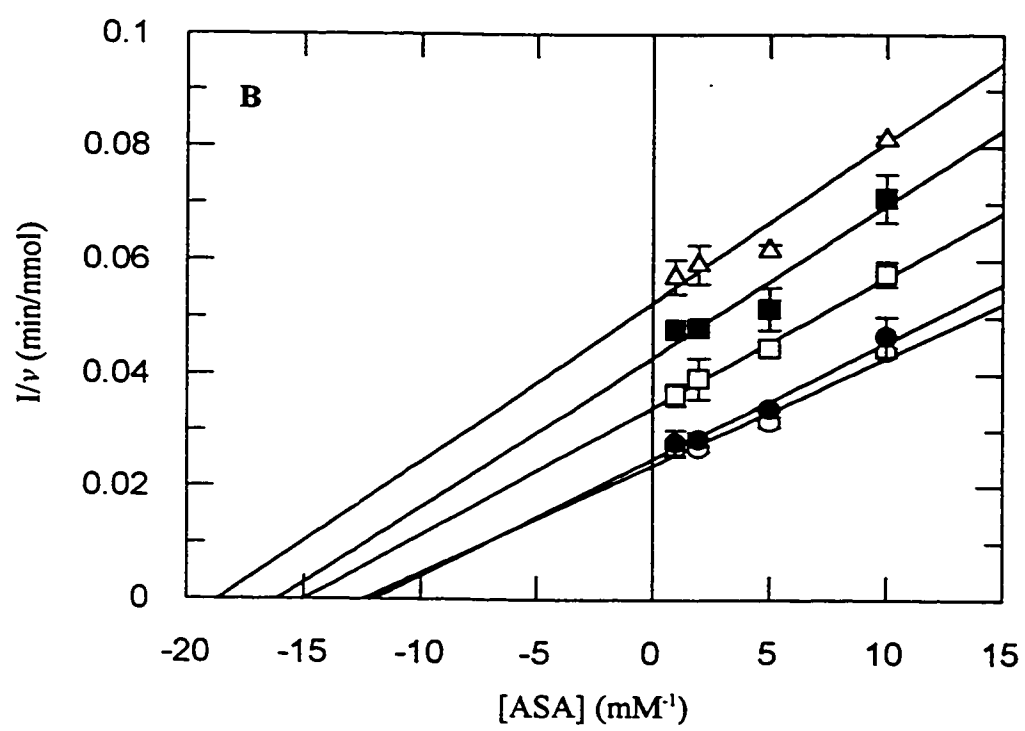


**Figure 2. Product inhibition of HSD by *L*-Hse.** (A) Noncompetitive inhibition of NADPH. Double reciprocal plot with varying NADPH concentrations at 0 (○), 5 (●), 10 (□), 30 (■) and 50 (Δ) mM *L*-Hse. ASA concentration was held constant at 0.130 mM ( $0.6 K_m$ ). Data were fit to equation 5. (B) Noncompetitive inhibition of ASA. Double reciprocal plot with varying ASA concentrations at 0 (○), 5 (●), 10 (□), 30 (■) and 50 (Δ) mM *L*-Hse. NADPH concentration was held constant at 20 μM ( $K_m$ ). Data were fit to equation 5.

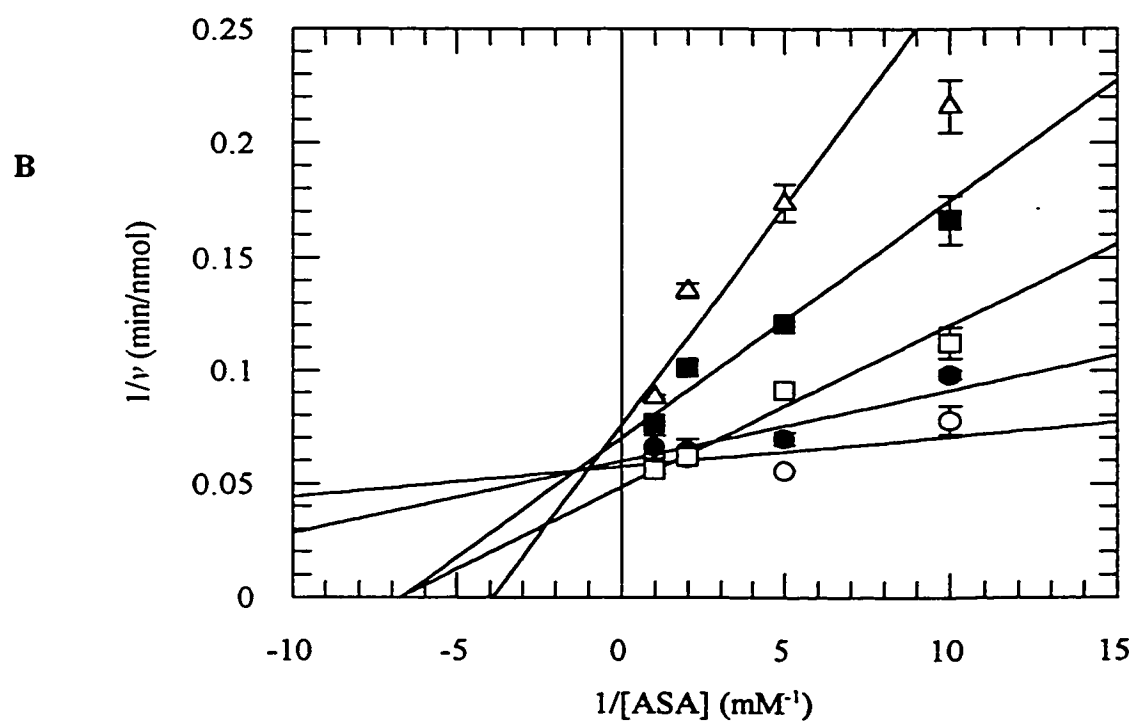
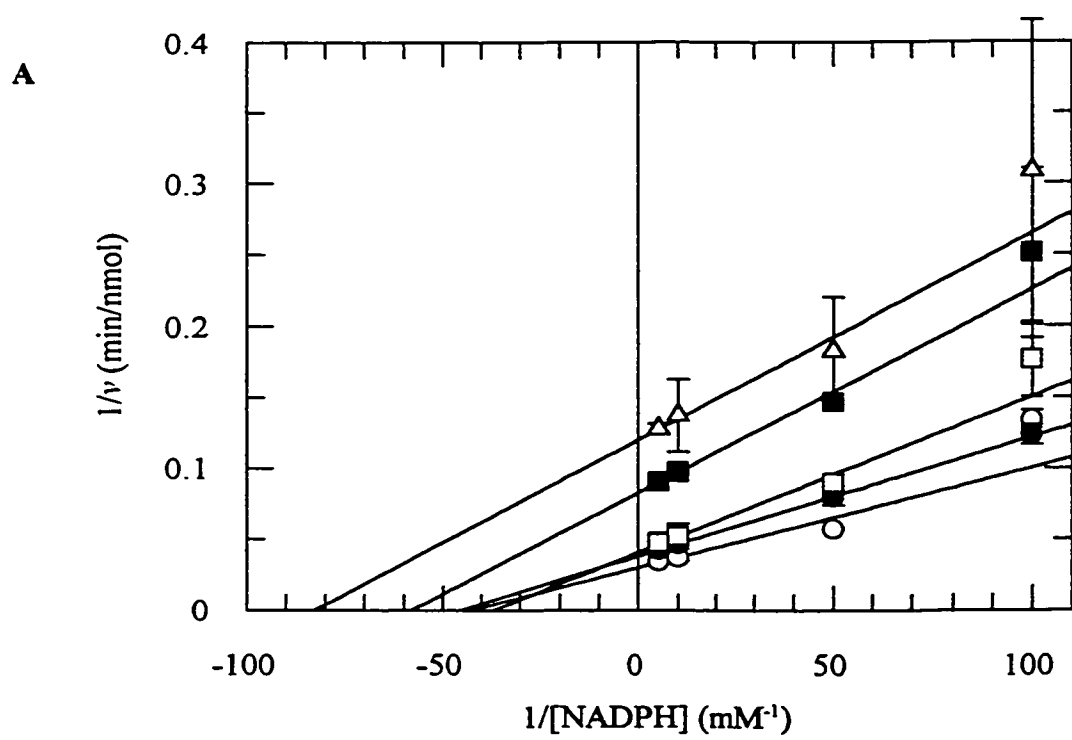
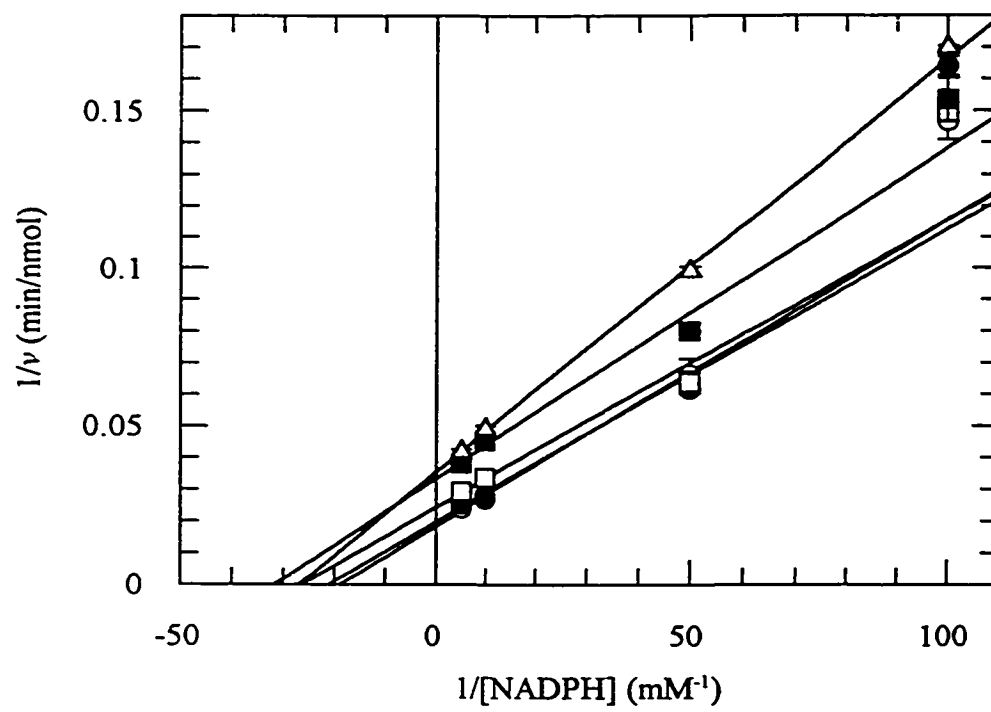


**Figure 3. Inhibition of HSD by *L*-Hse with respect to NADPH at saturating concentrations of ASA.** Double reciprocal plot with varying NADPH concentrations at 0 (○), 5 (●), 15 (□), 30 (■) and 50 (Δ) mM *L*-Hse. ASA concentration was saturating at 1.3 mM ( $6 K_m$ ). Data were fit to equation 5.



respect to *L*-Hse ( $K_i = 37.2 \pm 9.8$  mM). *L*-Aspartate  $\beta$ -hydroxamate (Figure 4), an analog of (*S*)-2-amino-4-oxo-5-hydroxypentanoic acid, was a good inhibitor of both forward and reverse reactions. Inhibition was noncompetitive against ASA ( $K_i = 0.77 \pm 0.15$ ,  $K_{ii} = 3.06 \pm 0.47$  mM) and competitive against *L*-Hse ( $K_i = 3.52 \pm 0.63$  mM). Trifluoromethionine (10 mM) and *D,L*-hydroxynorvaline (100 mM), an inhibitor of aspartate kinase, were weak inhibitors in the reverse direction (~ 20% inhibition at saturating *L*-Hse and NAD<sup>+</sup> concentrations, see Appendix A). H-(1,2,4-triazol-3-yl)-*D,L*-alanine (Figure 4) was a good inhibitor of HSD in both the forward and reverse directions. Further characterization of inhibition patterns revealed that H-(1,2,4-triazol-3-yl)-*D,L*-alanine demonstrated noncompetitive inhibition of HSD with respect to ASA ( $K_i = 1.64 \pm 0.36$  mM,  $K_{ii} = 3.84 \pm 0.46$  mM) and uncompetitive inhibition with respect to NADPH ( $K_{ii} = 3.04 \pm 0.18$  mM) (Table 2) (Figure 5).

Antifungal susceptibility assays revealed inhibition of growth of the pathogenic yeasts *Candida albicans* and *Candida tropicalis* on YNB agar media when *L*-aspartate  $\beta$ -hydroxamate (220  $\mu$ g) was added and not when H-(1,2,4-triazol-3-yl)-*D,L*-alanine (155  $\mu$ g) was added. *L*-Aspartate  $\beta$ -hydroxamate produced a partially cleared zone of 5 mm for *C. albicans* and 10 mm for *C. tropicalis*, compared to a partially cleared zone of 15 mm for 20  $\mu$ g the fluconazole for either *Candida*.

Table 2. Inhibition of purified yeast HSD.

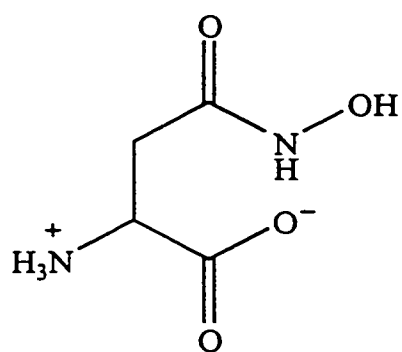
Inhibitor	Variable Substrate	Saturating Substrate	Type of Inhibition	$K_i$ (mM)	$K_{ii}$ (mM)	Equation <sup>a</sup>
<i>L</i> -Met <sup>b</sup>	<i>L</i> -Hse	NAD <sup>+</sup>	NC	47.3 ± 13.4	186 ± 27	5
<i>L</i> -Thr <sup>b</sup>	<i>L</i> -Hse	NAD <sup>+</sup>	C	37.2 ± 9.8	—	3
<i>L</i> -Asp β-hydroxamate	<i>L</i> -Hse	NAD <sup>+</sup>	C	3.52 ± 0.63	—	3
<i>L</i> -Asp β-hydroxamate	<i>L</i> -ASA	NADPH	NC	0.77 ± 0.15	3.06 ± 0.47	5
H-(1,2,4-triazol-3-yl)- <i>D,L</i> -alanine	ASA	NADH	NC	1.64 ± 0.36	3.84 ± 0.46	5
H-(1,2,4-triazol-3-yl)- <i>D,L</i> -alanine	NADPH	ASA	UC	—	3.04 ± 0.18	4

<sup>a</sup> -Data fit to equation number.

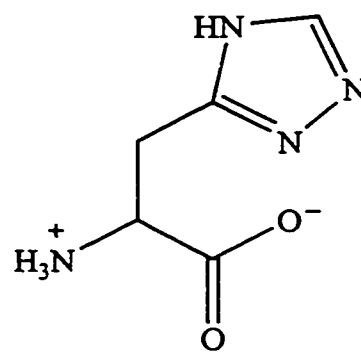
<sup>b</sup> -No inhibition of *L*-ASA at saturating NADH. Amino acids were added at 100 mM.

**Figure 4. Structures of yeast HSD inhibitors, *L*-aspartate  $\beta$ -hydroxamate and H-(1,2,4-triazol-3-yl)-*D,L*-alanine.**



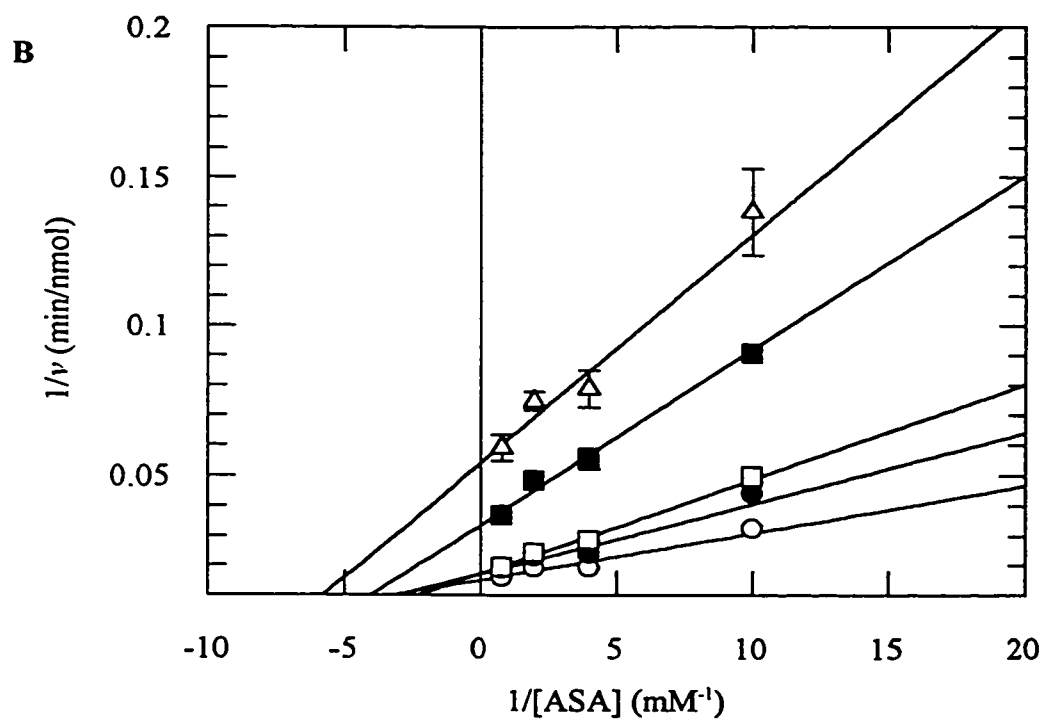
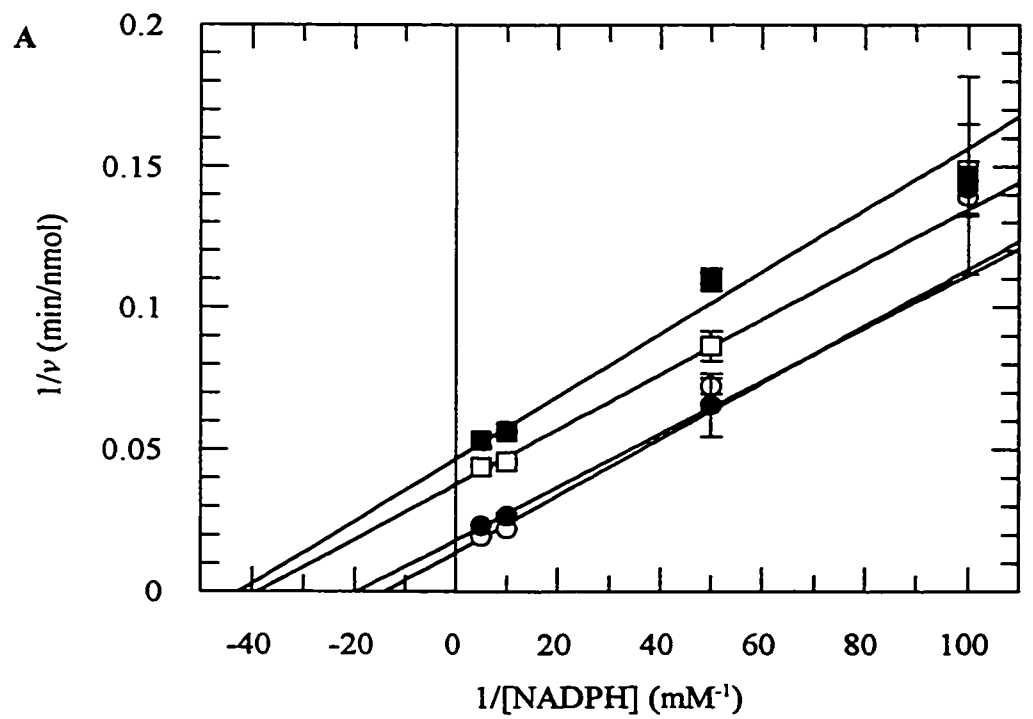


*L*-aspartate  $\beta$ -hydroxamate



(1,2,4-triazol-3-yl)-*D,L*-alanine

**Figure 5. Inhibition of HSD by H-(1,2,4-triazol-3-yl)-*D,L*-alanine.** (A) Uncompetitive inhibition of NADPH. Double reciprocal plot with varying NADPH concentrations at 0 (○), 1.0 (●), 5.0 (□), 7.5 (■) mM H-(1,2,4-triazol-3-yl)-*D,L*-alanine. ASA concentration was held constant at 0.75 mM ( $4 K_m$ ). Data were fit to equation 4. (B) Noncompetitive inhibition of ASA. Double reciprocal plot with varying ASA concentrations at 0 (○), 0.5 (●), 1.0 (□), 5.0 (■) and 7.5 (Δ) mM H-(1,2,4-triazol-3-yl)-*D,L*-alanine. NADH concentration was held constant at 0.2 mM ( $25 K_m$ ). Data were fit to equation 5.



### *Kinetic isotope effect*

The effect of incubating HSD, ASA and stereospecifically deuterated NADPH was determined at pH 7.5 and the values varied depending on the status of the ASA concentration (Table 3). At 1.2 mM ( $6 K_m$ ) ASA, no isotope effect ( $V_H/V_D$ ) was demonstrated with 4S-d-NADPH ( $1.0 \pm 0.05$ ), whereas 4R-d-NADPH produced an inverse effect ( $0.79 \pm 0.06$ ). At 0.130 mM ( $0.7 K_m$ ) ASA, a kinetic isotope effect was measured with 4S-d-NADPH ( $1.2 \pm 0.02$ ) and the inverse effect was modest for 4R-d-NADPH ( $0.97 \pm 0.02$ ).

### *Effects of Viscosity*

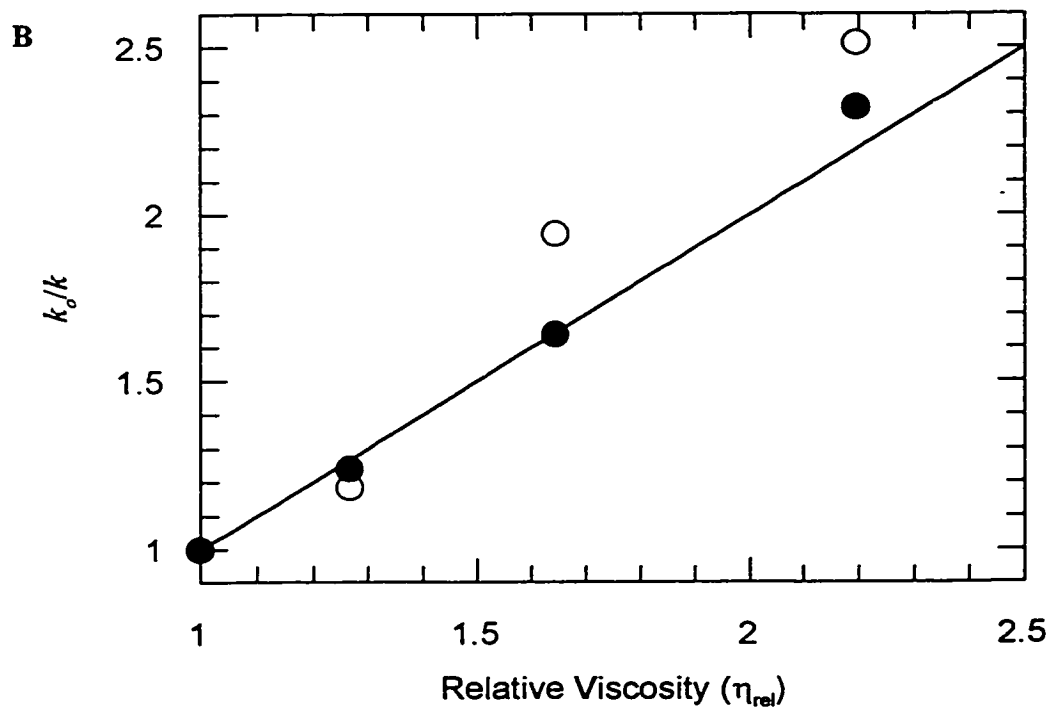
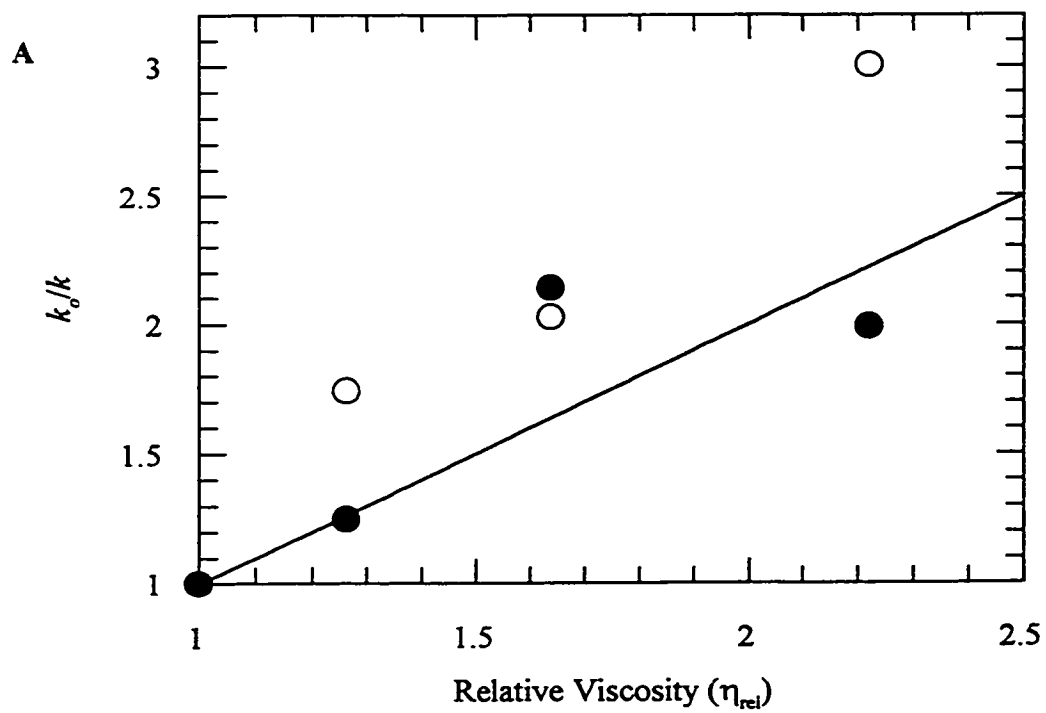
The effect of relative solvent viscosity ( $\eta_{rel}$ ) on the steady state parameters of HSD was examined in order to determine substrate “stickiness” in both forward and reverse directions. This evaluation was necessary since the use of “sticky” substrates in pH studies could lead to shifted pK measurements. Kinetic parameters of HSD were obtained in the presence of 0, 10, 20 and 30 % glycerol as a viscogen. In the forward direction,  $V_{max}/K_m$  for both ASA and NADH was greatly affected by solution viscosity (Figure 6) (Table 4).  $(V_{max}/K_m)_o/(V_{max}/K_m)^n$  were 1.54 and 1.33 respectively. In addition, stickiness ratios ( $S_r$ ) were correspondingly high at 3.71 and 3.56 (Table 5). Viscosity appeared to have a greater effect on the parameters for ASA than NADH.

$V_{max}/K_m$  for Hse and  $NAD^+$  in the reverse reaction were less affected by solvent viscosity (Figure 6) (Table 4).  $(V_{max}/K_m)_o/(V_{max}/K_m)^n$  for Hse was -0.17 and for  $NAD^+$

**Table 3. Kinetic isotope effects using stereospecifically deuterated NADPD**

Cofactor	ASA concentration	$V_H/V_D$
4 <i>S</i> -d-NADPH	$0.7 K_m$	$1.2 \pm 0.02$
4 <i>R</i> -d-NADPH	$0.7 K_m$	$0.97 \pm 0.02$
4 <i>S</i> -d-NADPH	$6 K_m$	$1.0 \pm 0.05$
4 <i>R</i> -d-NADPH	$6 K_m$	$0.79 \pm 0.06$

**Figure 6. Effect of relative viscosity on  $k_{cat}$  and  $k_{cat}/K_m$  for HSD.** In the forward, ASA reducing, direction, (A) ASA was varied in the presence of 0.2 mM NADH and (B) NADH was varied in the presence of 0.8 mM ASA. In the reverse, Hse oxidizing, direction, (C) *L*-Hse was varied in the presence of 0.4 mM NAD<sup>+</sup> and (D) NAD<sup>+</sup> was varied in the presence of 15 mM *L*-Hse. Open circles represent  $(k_{cat}/K_m)_o/(k_{cat}/K_m)$  and closed circles represent  $(k_{cat})_o/(k_{cat})$ . Lines have a slope of 1.



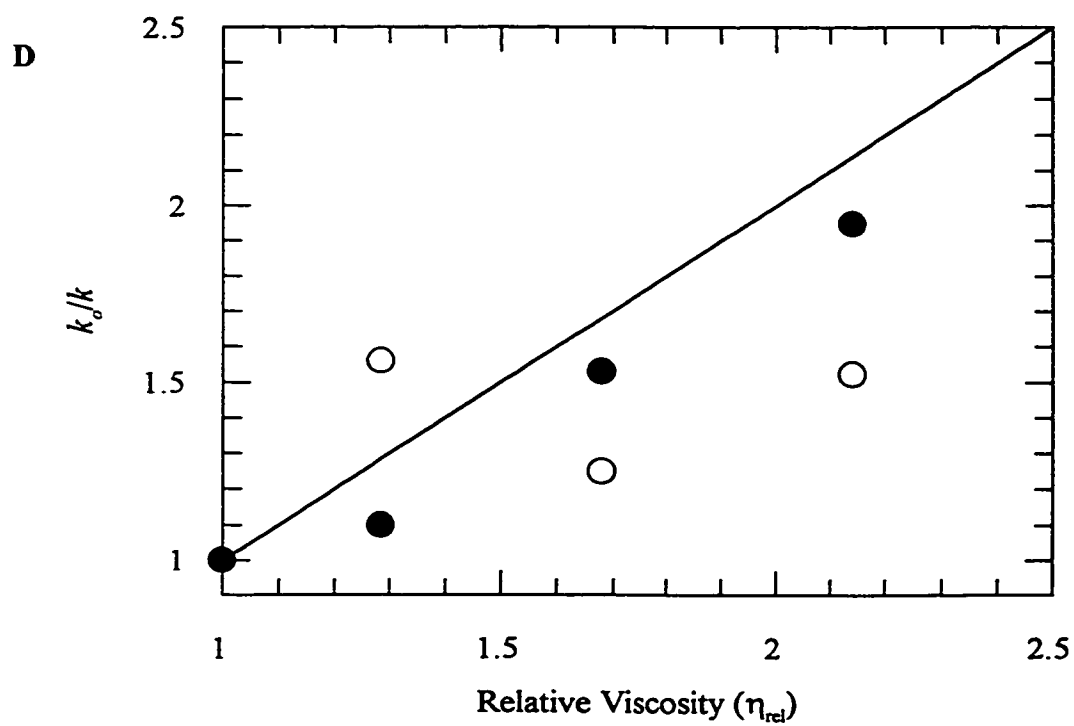
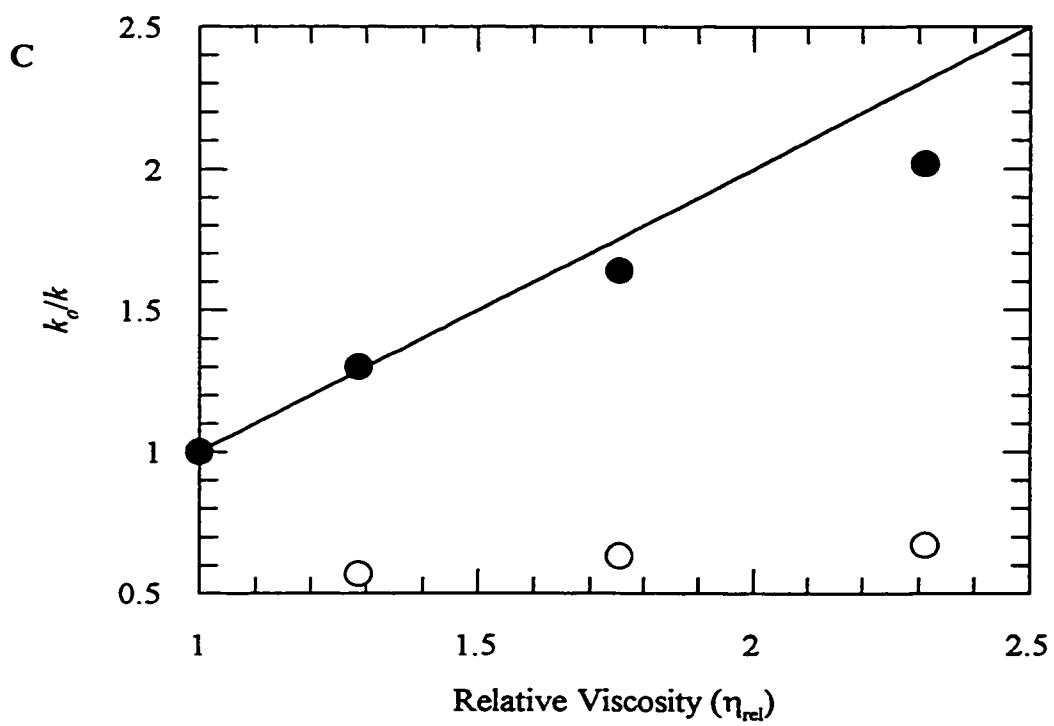




Table 4. Kinetic constants of yeast HSD as a function of relative viscosity ( $\eta_{rel}$ ).

Varied Substrate	Saturating Substrate	Relative viscosity ( $\eta_{rel}$ )	$k_{cat}$ ( $s^{-1}$ )	$k_{cat}/K_m$ ( $M^{-1}s^{-1}$ ) ( $\times 10^6$ )	$K_i$ (mM)
ASA	NADH	1.00	298 $\pm$ 26	1.96 $\pm$ 0.41	2.27 $\pm$ 0.50
		1.26	239 $\pm$ 18	1.13 $\pm$ 0.19	3.59 $\pm$ 0.83
		1.64	138 $\pm$ 12	0.96 $\pm$ 0.23	13.7 $\pm$ 10.0
		2.22	150 $\pm$ 9	0.65 $\pm$ 0.09	5.52 $\pm$ 1.42
		2.50*	353 $\pm$ 22*	1.98 $\pm$ 0.29*	2.75 $\pm$ 0.47*
NADH	ASA	1.00	182 $\pm$ 3	37.1 $\pm$ 3.8	
		1.27	147 $\pm$ 4	31.3 $\pm$ 5.4	
		1.64	111 $\pm$ 2	19.1 $\pm$ 1.7	
		2.20	78.4 $\pm$ 2.0	14.8 $\pm$ 2.0	
		2.50*	166 $\pm$ 3*	39.5 $\pm$ 3.8*	
L-Hse	NAD <sup>+</sup>	1.00	34.4 $\pm$ 1.2	0.0286 $\pm$ 0.0046	
		1.29	26.5 $\pm$ 0.6	0.0501 $\pm$ 0.0054	
		1.75	21.1 $\pm$ 1.0	0.0451 $\pm$ 0.0096	
		2.31	17.0 $\pm$ 0.7	0.0424 $\pm$ 0.0077	
NAD <sup>+</sup>	L-Hse	1.00	30.0 $\pm$ 1.1	0.573 $\pm$ 0.075	
		1.28	27.3 $\pm$ 1.4	0.368 $\pm$ 0.062	
		1.68	19.6 $\pm$ 0.4	0.460 $\pm$ 0.036	
		2.14	15.4 $\pm$ 0.1	0.375 $\pm$ 0.012	

\* Assays performed with PEG 8000 instead of glycerol.

**Table 5. “Stickiness” parameters of yeast HSD substrates**

Varied Substrate	Reaction	$((k_{cat})_o/(k_{cat}))^n$	$((k_{cat}/K_m)_o/(k_{cat}/K_m))^n$	Stickiness Ratio ( $S_r$ )
ASA	Forward	0.88	1.54	3.71
NADH		1.12	1.33	3.56
<i>L</i> -Hse	Reverse	0.76	-0.17	0.17
NAD <sup>+</sup>		0.85	0.30	0.35

was 0.30. Stickiness ratios ( $S_r$ ) were 0.17 and 0.35, respectively (Table 5). Although  $S_r$  for  $\text{NAD}^+$  is higher than  $L$ -Hse, it is still 10 fold lower than the values for ASA and NADH.

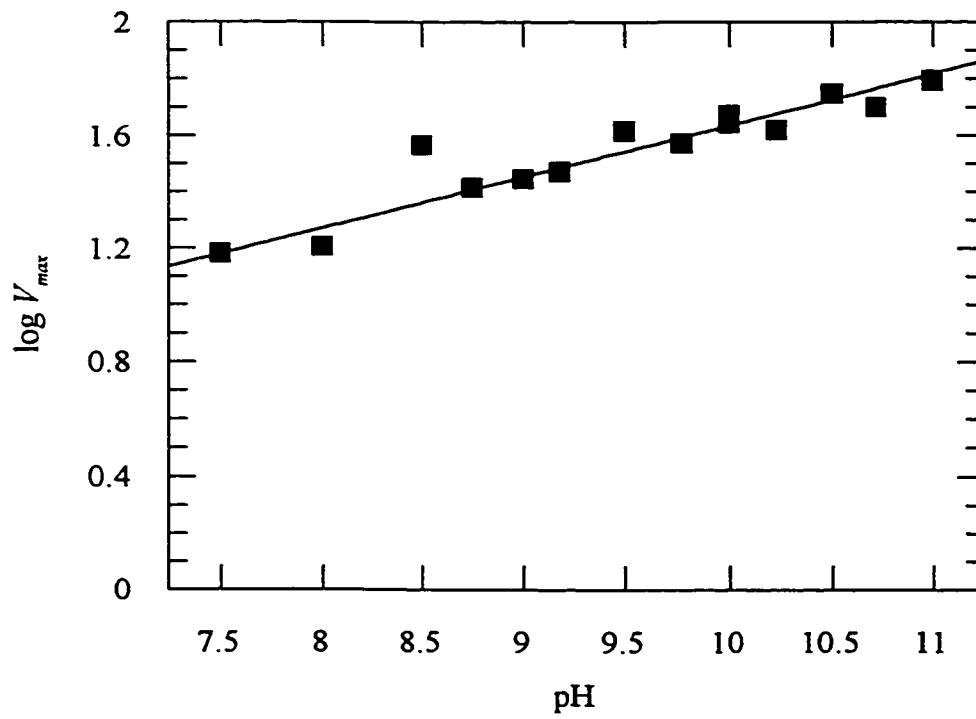
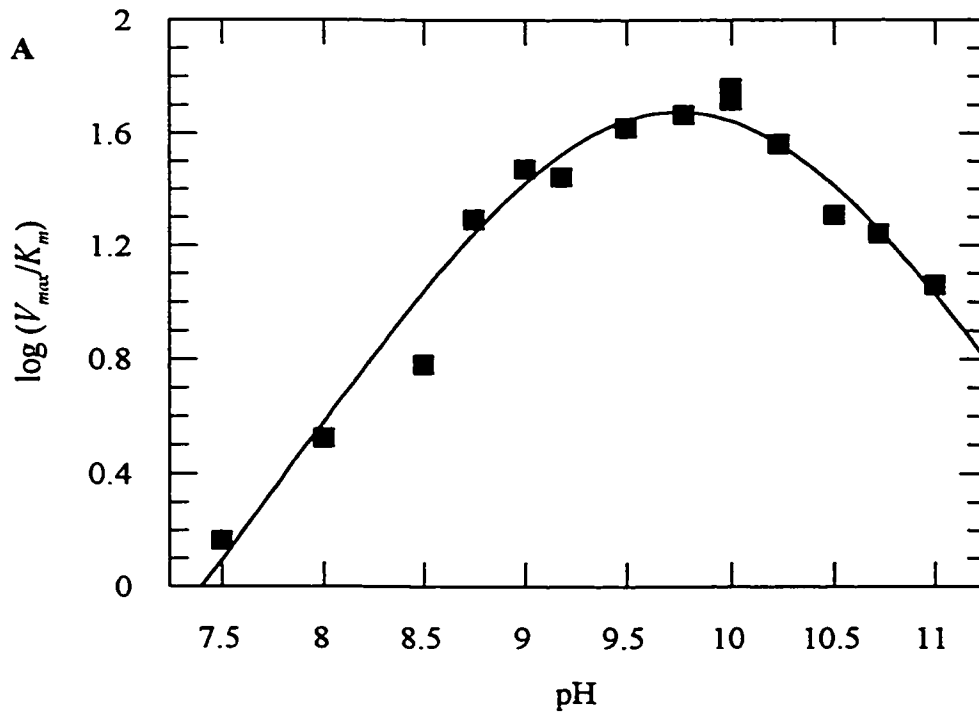
The rate limiting step can also be determined by looking at the effect of viscosity on rate constants. When any substrate was varied, in either direction,  $(k_{cat})_o/(k_{cat})^n$  increased proportionally with relative viscosity (Figure 6) (Table 4). Slopes  $(k_{cat})_o/(k_{cat})^n$  were between 0.76 and 1.12 (Table 5). On the other hand, viscosity had little effect on the substrate inhibition constant ( $K_i$ ) for ASA (Table 4).

The effect of the macroviscogen PEG 8000 was determined in order to distinguish between effects due to changes in global viscosity and effects due to changes in the rate of diffusion. PEG 8000 had no effect on first or second order rate constants determined for ASA and NADH in the forward direction (Table 4).

### *Effects of pH*

The effects of pH on steady state parameters for “nonsticky” substrates were measured in order to study the role of ionizable groups in catalysis and/or substrate binding.  $\log V_{max}$  for  $L$ -Hse and  $\text{NAD}^+$  increased linearly with pH (Figure 7).  $\log (V_{max}/K_m)$  for  $\text{NAD}^+$  increased with pH until pH 9.5, while  $\log (V_{max}/K_m)$  versus pH for  $L$ -Hse was bell shaped, dropping below pH 9.5 and above pH 10.0. Assuming two ionization groups for  $L$ -Hse and one ionization group for  $\text{NAD}^+$ , the  $\text{pK}_a$  and  $\text{pK}_b$  were determined to be  $9.32 \pm 0.15$  and  $10.17 \pm 0.20$ , respectively, for  $L$ -Hse and the  $\text{pK}_a$  for  $\text{NAD}^+$  was  $8.46 \pm 0.13$  (Table 6).

**Figure 7. Effect of pH on steady state parameters ( $V_{max}$  and  $V_{max}/K_m$ ) of HSD. (A) *L*-Hse was varied at fixed 0.4 mM  $\text{NAD}^+$  and B)  $\text{NAD}^+$  was varied at fixed 20 mM *L*-Hse. The lines represent the results from fitting by nonlinear least squares to equation 8 or 9 for  $\log(V_{max}/K_m)$  profiles or from linear fitting for  $\log(V_{max})$  profiles.**



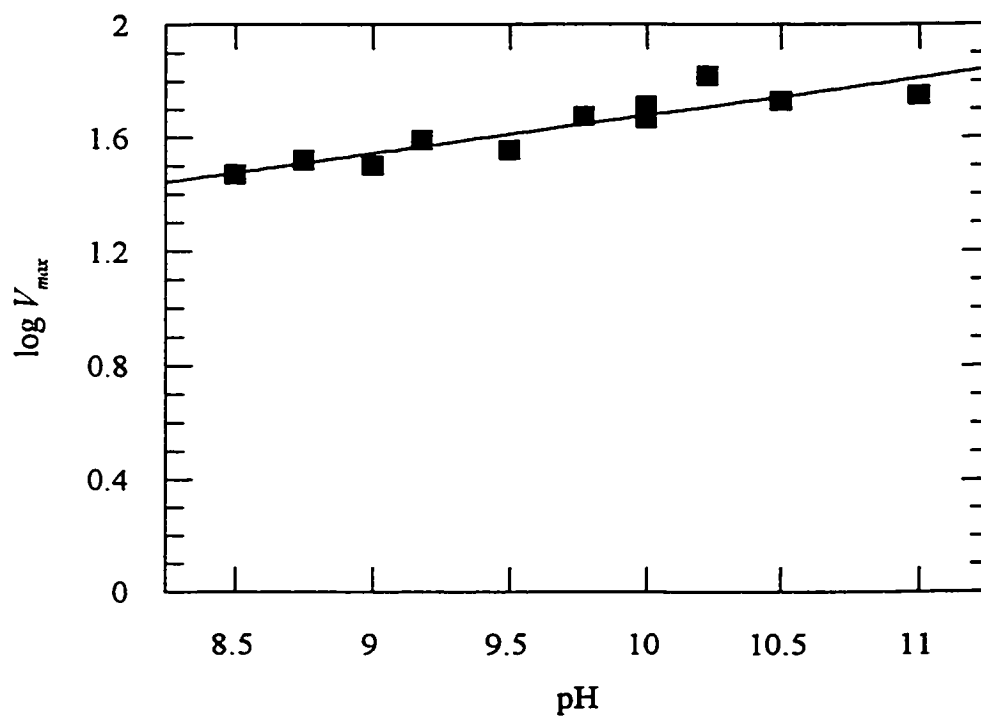
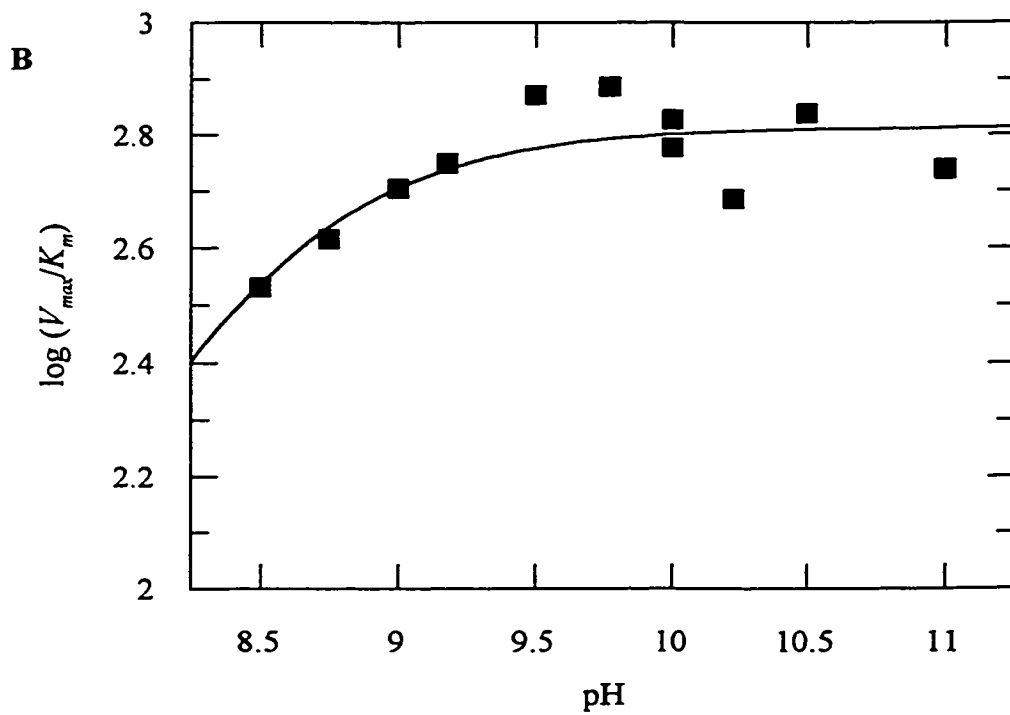


**Table 6. Summary of pK values for yeast HSD**

Parameter	pK <sub>a</sub>	pK <sub>b</sub>
$(V_{max}/K_m)_{L-Hse}$	9.32 ± 0.15	10.17 ± 0.20
$(V_{max}/K_m)_{NAD^+}$	8.46 ± 0.13	

## DISCUSSION

We have previously reported the overexpression and purification of *S. cerevisiae* homoserine dehydrogenase and obtained steady state kinetic parameters for both the ASA reducing (forward) direction and the Hse oxidizing (reverse) directions (Jacques *et al.*, 1999 (Chapter 2)). With an ample supply of HSD, a study into the kinetic mechanism and stereochemistry was initiated. This information is necessary in order to design potent inhibitors of HSD, which could lead to the discovery of novel antifungal agents.

As expected, yeast HSD appears to operate through a sequential kinetic mechanism, since the double reciprocal plot of initial velocities produced a set of intersecting lines indicative of the formation of a ternary complex (data not shown). Product inhibition of HSD by NADP<sup>+</sup> and *L*-Hse was employed to differentiate between random and ordered mechanisms. Random substrate binding and product release would result in either no inhibition or competitive inhibition patterns by these products. Noncompetitive inhibition patterns resulting from inhibition of NADPH by *L*-Hse and inhibition of ASA by NADP<sup>+</sup> or *L*-Hse at subsaturating levels of fixed second substrate indicate an ordered substrate binding and product release.

Competitive inhibition of NADPH by NADP<sup>+</sup> suggests that these cofactors are binding the free enzyme form and therefore, these cofactors are the first substrate to bind and the last product to be released. Partial competitive inhibition may be a result of one cofactor binding site affecting the dissociation constant ( $K_s$  or  $K_i$ ) at the other cofactor binding site as shown in Scheme 1. Yeast HSD was previously shown to be a dimer



(Jacques *et al.*, 1999 (Chapter 2); Yumoto *et al.*, 1991), thereby making this scheme feasible.

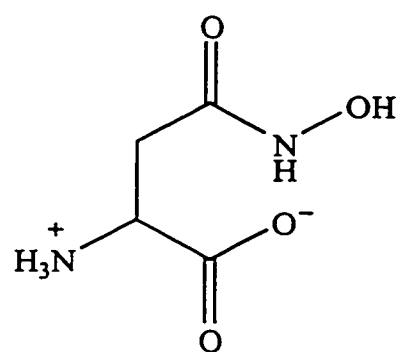
An ordered Bi Bi kinetic mechanism would consequently involve the enzyme binding NAD(P)H and then ASA, followed by the release of Hse and then NAD(P)<sup>+</sup> as products. The same mechanism has been attributed to *E. coli* AKHSD I (Angeles and Viola, 1990). An ordered mechanism, however, would produce an uncompetitive pattern for the inhibition of NADPH by *L*-Hse at high ASA concentration, as opposed to the noncompetitive inhibition pattern which resulted. Nonetheless, inhibition constants for *L*-Hse at high ASA concentration were 2.5-6 fold higher than at subsaturating ASA concentration ( $K_{i_s} = 173 \pm 102$ ,  $K_{i_i} = 45.6 \pm 5.3$ ). Consequently, determination of the kinetic mechanism of yeast HSD by other means such as alternate substrate diagnosis or dead-end inhibition was necessary.

On the other hand, an ordered Bi Bi mechanism could not readily be confirmed by the use of alternate substrate diagnostics or dead-end inhibition. Alternate substrates for yeast HSD were not found, as yeast HSD only converted ASA or Hse. S-methyl-cysteine did not inhibit yeast HSD, in spite of the fact that S-methyl-cysteine sulfoxide was a competitive inhibitor for *E. coli* AKHSD I with respect to ASA (Angeles and Viola, 1990). Without this inhibition or any other competitive inhibitor of ASA, substrate order could not be verified directly. However, we found that H-(1,2,4-triazol-3-yl)-*D,L*-alanine was a noncompetitive inhibitor of ASA ( $K_{i_s} = 1.64 \pm 0.36$  mM,  $K_{i_i} = 3.84 \pm 0.46$  mM) and an uncompetitive inhibitor of NADPH ( $K_{i_i} = 3.04 \pm 0.18$  mM). This pattern of inhibition agrees with the proposed substrate order, as this compound will bind

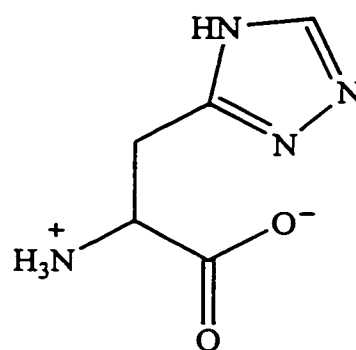
either the E•NADPH or the E•NADPH•ASA complexes. Although, both *L*-aspartate  $\beta$ -hydroxamate and H-(1,2,4-triazol-3-yl)-*D,L*-alanine were good inhibitors, only *L*-aspartate  $\beta$ -hydroxamate demonstrated *in vivo* antifungal activity against *C. albicans* and *C. tropicalis*.

Kinetic isotope experiments were highly informative. First, the kinetic isotope effect was much lower at saturating concentrations of ASA than at subsaturating concentrations and hydride transfer was only partially rate limiting at lower ASA concentrations. This is consistent with a fast catalytic step and a rate limiting product release. Product release appears to be rate-limiting for several dehydrogenases (Bush *et al.*, 1973; Iwatsubo and Pantaloni, 1967; Silverstein and Sulebele, 1969). Previous kinetic isotope exchange experiments on AKHSD I likewise point to slow cofactor dissociation compared to dissociation of the amino acid product (Wedler and Ley, 1993).

Second, only the *pro-S* deuterated nicotinamide gave a positive kinetic isotope effect. This demonstrates the stereospecificity of hydride transfer to be from the *pro-S* C-4 nicotinamide hydrogen to the aldehyde (Scheme 3). This specificity is also found in the *E. coli* AKHSD I enzyme (Chang and Walsh, 1980). Furthermore, KIE experiments revealed a significant inverse  $\alpha$ -secondary effect. This suggests that, in the transition state, the  $\alpha$ -secondary C-4 hydrogen is stiffly bonded and its motion is coupled to hydride transfer (Cleland, 1982). All dehydrogenase reactions are believed to involve coupling of



*L*-aspartate  $\beta$ -hydroxamate



(1,2,4-triazol-3-yl)-*D,L*-alanine

**Scheme 3. Stereochemistry of hydride transfer by yeast HSD**

both primary and  $\alpha$ -secondary hydrogen motions as a result of hydrogen tunneling (Cleland, 1986; Hermes, *et al.*, 1984).

Viscosity experiments also provided evidence for a fast catalytic step. The effect of relative solvent viscosity was used as a measure for substrate “stickiness”. Substrate “stickiness” is a result of low rate of substrate dissociation as compared to rate of catalysis. If the rate of catalysis is fast compared to substrate dissociation, viscosity will affect the overall rate by slowing the diffusion of substrates. As there was no effect of viscosity on the substrate inhibition constant ( $K_i$ ) for ASA, glycerol, the viscogen used in these studies, does not interfere with the binding of ASA to yeast HSD and precludes the requirement for a poor substrate control. Furthermore, the macroviscogen PEG 8000 had no effect on kinetic parameters and therefore, viscosity effects were not due to global viscosity changes.

Stickiness ratios ( $S_r$ ) and slopes  $[(V_{max}/K_m)_\sigma/(V_{max}/K_m)]^n$  suggest that the substrates for the forward reaction (ASA and NADH) are “sticky” substrates, as a result of fast catalysis. When the products, *L*-Hse and  $\text{NAD}^+$ , were used as substrates in the reverse reaction (Hse oxidizing), however, relative viscosity affected  $V_{max}/K_m$  to a much lesser extent.  $[(V_{max}/K_m)_\sigma/(V_{max}/K_m)]^n$  and  $S_r$  for *L*-Hse approached zero, hence, *L*-Hse can be termed a “nonsticky” substrate. Although, the stickiness ratio ( $S_r$ ) for  $\text{NAD}^+$  was 10 times lower than that for NADH, the parameters for  $\text{NAD}^+$  were not completely unaffected by relative viscosity. Since physiologically both *L*-Hse and  $\text{NAD}^+$  are generated as products, rates of dissociation from HSD are expected to be relatively high. On the other hand, the slight effect of viscosity on  $\text{NAD}^+$  may suggest a much slower rate

of dissociation implying that product release is rate limiting. If nicotinamide release is largely rate limiting, substrate inhibition may result from ASA binding to the E•NAD<sup>+</sup> complex, thereby forming an abortive ternary complex. Furthermore, the effect of viscosity on  $k_{cat}$  indicates a diffusion-controlled rate limiting step, providing additional support for rate limiting product release.

The role of ionizable groups in catalysis and/or substrate binding was probed by pH studies. The increase in maximal reaction rate ( $V_{max}$ ) with pH for the reverse reaction was conceivably caused by the favorable deprotonation of *L*-Hse, since the  $pK_a$  for the hydroxyl group on *L*-Hse is ~14. The effect of pH on  $V_{max}/K_m$  produced a bell curve with  $pK$  of 9.3 and 10.2 for *L*-Hse, whereas increasing pH produced an increase in  $\log(V_{max}/K_m)$  for NAD<sup>+</sup> with an inflection at 8.5.  $pK$  values obtained for both *L*-Hse and NAD<sup>+</sup> are involved primarily in substrate binding; however, they may not necessarily reflect only HSD amino acid residues. *L*-Hse also has an amino group with  $pK_a$  of ~9. Since amino acids in solution are zwitterions, it is plausible that the protonation or deprotonation of the amino group on *L*-Hse would lead to a loss of hydrogen bonding or important ionic interactions, respectively, required for binding. On the other hand, basic residues such as histidine, lysine or tyrosine residues of yeast HSD, could also be involved in substrate-enzyme interactions based on these results. Upon completion of the research component of this work, the X-ray structure of yeast HSD was determined (B. DeLaBarre and A. Berghuis, personal communication). Inspection of the active site region reveals Lys 223 as a possible candidate amino acid residue.

In conclusion, these results illustrate that yeast HSD is very similar to the *E. coli* enzyme, AKHSD I. Both demonstrate ordered mechanisms, where the nicotinamide substrate is bound prior to the amino acid substrate and the nicotinamide product is released after the amino acid product. Kinetic isotope effect experiments and viscosity data demonstrated that the catalytic event is rapid with respect to the principal rate limiting step, NAD(P)<sup>+</sup> release. Isotope experiments also determined that the hydride is transferred from the *pro-S* C-4 position of NAD(P)H, as the case with *E. coli* AKHSD I. Finally, ionizable groups with basic pKs are involved in substrate binding and basic pH increases reaction rates by facilitating the deprotonation of Hse. These results now serve as the basis for further inhibitor design and evaluation.

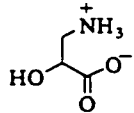
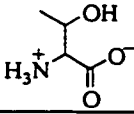
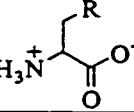
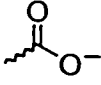
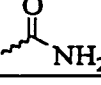
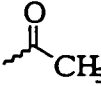
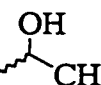
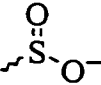
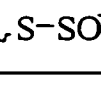
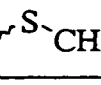
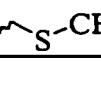
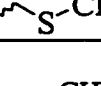
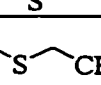

## REFERENCES

- Angeles, T. S., and R. E. Viola (1990) The kinetic mechanism of the bifunctional enzyme aspartokinase-homoserine dehydrogenase I from *Escherichia coli*, *Arch. Biochem. Biophys.*, **283**: 96-101.
- Benson, T. E., Marquardt, J. L., Marquardt, A. C., Etkorn, F. A., and Walsh, C. T. (1993) Overexpression, purification, and mechanistic study of UDP-N-acetylenolpyruvylglucosamine reductase, *Biochemistry* **32**: 2024-2030.
- Bush, K., V. J. Shiner, Jr. and H. R. Mahler (1973) Deuterium isotope effects on initial rates of liver alcohol dehydrogenase reaction, *Biochemistry*, **12**: 4802-4805.
- Chang, M. N., and Walsh, C. (1980) Stereochemical analysis of the homoserine dehydrogenase reaction and preparation of chiral 4-deuteriohomoserines, *J. Am. Chem. Soc.*, **102**: 2499-2501.
- Cleland, W. W. (1982) Use of isotope effects to elucidate enzyme mechanisms, *CRC Crit. Rev. Biochem.*, **13**: 385-428.
- Cleland, W. W. (1986) Enzyme kinetics as a tool for determination of enzyme mechanisms, in: *Investigation of Rates and Mechanisms of Reactions, Part 1*, (C. F. Bernasconi, Ed.) 4th Ed., Wiley, New York, pp. 791-870.
- Georgopapadakou, N. H., and T. J. Walsh (1996) Antifungal agents: Chemotherapeutic targets and immunologic strategies, *Antimicrob. Agents Chemother.*, **40**: 279-291.
- Graybill, J. R. (1996) The future of antifungal therapy, *Clin. Infect. Dis.*, **22**: S166-S178.
- Hermes, J. D., S. W. Morrical, M. H. O'Leary, and W. W. Cleland (1984) Variation of transition-state structure as a function of the nucleotide in reactions catalyzed by dehydrogenases. 2. Formate dehydrogenase, *Biochemistry*, **23**: 5479-5488.
- Houston, M. E., and Honek, J. F. (1989) *J. Chem. Soc. Chem. Commun.*, 761-762.
- Iwatsubo, M., and Pantaloni, D. (1967) Regulation of the activity of glutamate dehydrogenase by effectors GTP and ADP: Study by means of "stopped flow", *Bull. Soc. Chim. Biol.*, **49**: 1563-1572.
- Jacques, S.L., C. Pratt, G. Broadhead, R. Kinach, J. F, Honek and G. D. Wright (1999) Characterization of yeast homoserine dehydrogenase, an antifungal target (Chapter 2).

- Leatherbarrow, R. J. (1992) Grafit 3.0, Erithacus Software LTD., Staines, U.K.
- Orr, G. A., and Blanchard, J. S. (1984) High-performance ion-exchange separation of oxidized and reduced nicotinamide adenine dinucleotide, *Anal. Biochem.*, **142**: 232-234.
- Silverstein, E., and Sulebele, G. (1969) Catalytic mechanism of pig heart mitochondrial malate dehydrogenase studied by kinetics at equilibrium, *Biochemistry*, **8**: 2543-2550.
- Sternberg, S. (1994) The emerging fungal threat, *Science*, **266**: 1632-1634.
- Wedler, F. C., and B. W. Ley (1993) Kinetic and regulatory mechanisms for (*Escherichia coli*) homoserine dehydrogenase-I: Equilibrium isotope exchange kinetics, *J. Biol. Chem.*, **268**: 4880-4888.
- Wedler, F. C., B. W. Ley, S. L. Shames, S. J. Rembish and D. L. Kushmaul (1992) Preferred order random kinetic mechanism for homoserine dehydrogenase of *Escherichia coli* (Thr-sensitive) aspartokinase/homoserine dehydrogenase-I: Equilibrium isotope exchange kinetics, *Biochim. Biophys. Acta*, **1119**: 247-249.
- Yamaki, H., M. Yamaguchi, H. Imamura, H. Suzuki, T. Nishimura, H. Saito and H. Yamaguchi (1990) The mechanism of antifungal action of (*S*)-2-amino-4-oxo-5-hydroxypentanoic acid, RI-331: The inhibition of homoserine dehydrogenase in *Saccharomyces cerevisiae*, *Biochem. Biophys. Res. Commun.*, **168**: 837-843.
- Yumoto, N., Y. Kawata, S. Noda and M. Tokushige (1991) Rapid purification and characterization of homoserine dehydrogenase from *Saccharomyces cerevisiae*, *Arch. Biochem. Biophys.*, **285**: 270-275.



**APPENDIX A****List of compounds surveyed for HSD inhibition**

	Compound	R group	Concentration (mM)	Reaction <sup>b</sup>	Inhibition (%)
1			100 100	F R	0 13
2			100	F	0
3			10	F	0
4			10	F	0
5 <sup>c</sup>			10 1	F R	0 0
6			100 100	F R	0 20
7 <sup>c</sup>			10 1	F R	0 0
8 <sup>c</sup>			1 1	F R	0 0
9 <sup>c</sup>			10 1	F R	9 2
10			100	F	0
11 <sup>d</sup>			1 10	F R	0 19
12 <sup>d</sup>			1 10	F R	0 5
13 <sup>d</sup>			1 1	F R	0 0

	Compound	R group	Concentration (mM)	Reaction <sup>b</sup>	Inhibition (%)
14			10 10	F R	77 0
15 <sup>c</sup>			10 10	F R	15 10
16			10 10	F R	0 10
17 <sup>c</sup>			10 10	F R	0 2
18 <sup>c</sup>			10 10	F R	10 11
19 <sup>c</sup>			10 1	F R	0 0
20 <sup>c</sup>			1 1	F R	5 0
21 <sup>c</sup>			1 1	F R	0 3
22 <sup>c</sup>			1	R	0
23 <sup>c</sup>			10 1	F R	0 0
24 <sup>d</sup>			1 10	F R	0 16

- a-** Compounds were added to assays containing 1.0 mM ASA, 0.2 mM NADH and 100 mM HEPES pH 7.5 or 15 mM *L*-Hse, 0.4 mM NAD<sup>+</sup> and 100 mM CHES pH 9.5 and reaction was initiated with 0.1 or 1 μg purified HSD, respectively.
- b-** F- Inhibition measured in the forward reaction, R- in the reverse reaction.
- c-** Preincubation with HSD (30 min, RT) had no effect at 1 mM in the forward direction.
- d-** As in c, in both forward and reverse directions.

## **CHAPTER 4**

**(S) 2-amino-4-oxo-5-hydroxypentanoic acid (RI-311),  
an Antifungal Compound, is a Mechanism-Based Inactivator of  
*Saccharomyces cerevisiae* Homoserine Dehydrogenase**

**Suzanne L. Jacques, Kirk Green and Gerard D. Wright**

#### 4.1 Preface

Chapters 2 and 3 investigated the properties of the fungal model enzyme, *S. cerevisiae* HSD, to facilitate the design of effective inhibitors. The paper in this chapter, on the other hand, focused on the properties of RI-331 and its mode of action. In previous reports, this antifungal compound was identified as an inhibitor of yeast HSD. The presence of NADP<sup>+</sup> was shown to be crucial for inhibition, however, the purpose of NADP<sup>+</sup> was ambiguous.

The results obtained in this paper clearly demonstrated that RI-331 is, in fact, a mechanism-based inactivator. RI-331 appears to react with the cofactor in an HSD-dependent manner producing a tight-binding adduct. Although mechanism-based inactivators generally produce their effect by covalent modification of the active site, other examples of inactivator-nicotinamide adducts exist and are described as excellent inhibitors of dehydrogenases/reductases. The elucidation of the mechanism of HSD inactivation by RI-331 will give significant insight in the development of novel antifungal drugs targeting fungal HSD.

All the experimental work presented in this chapter was performed by me, with the exception of the acquisition of the mass spectrometry data. These results were obtained by Dr. Kirk Green at the McMaster Regional Centre for Mass Spectrometry and Dr. Jian Chen at the University of Waterloo Biological Mass Spectrometry Laboratory.

## 4.2 Paper

**(S) 2-amino-4-oxo-5-hydroxypentanoic acid (RI-331),  
an antifungal compound, is a mechanism-based inactivator of  
*Saccharomyces cerevisiae* homoserine dehydrogenase<sup>†</sup>**

Suzanne L. Jacques, Kirk Green and Gerard D. Wright<sup>\*</sup>

Department of Biochemistry, McMaster University, Hamilton, ON, L8N 3Z5

Running title: RI-331 inactivation of yeast homoserine dehydrogenase

Key words: RI-331, Homoserine dehydrogenase, *Saccharomyces cerevisiae*,  
Antifungal agents

<sup>\*</sup>Corresponding author. Phone: (905) 525-9140, ext. 22943; Fax: (905) 522-9033;  
Email: [wrightge@fhs.mcmaster.ca](mailto:wrightge@fhs.mcmaster.ca)

<sup>†</sup> This research was supported by a Natural Sciences and Engineering Research Council of Canada Strategic Grant and an Ontario Graduate Student Scholarship to S.L.J.

**Footnotes**

<sup>1</sup>Abbreviations: ACP, acyl carrier protein; APAD, 3-amino-pyridine adenosine dinucleotide; ASA, *L*-aspartate  $\beta$ -semialdehyde; HEPES, N-[2-hydroxyethyl]piperazine-N'-[2-ethanesulfonic acid]; HSD, homoserine dehydrogenase (EC 1.1.1.3); Hse, *L*-homoserine; RI-331, (*S*)-2-amino-4-oxo-5-hydroxypentanoic acid; TAPS, N-tris[hydroxymethyl]methyl-3-amino-propanesulfonic acid.



## ABSTRACT

The antifungal compound RI-331 ((*S*)-2-amino-4-oxo-5-hydropentanoic acid) was shown to inhibit yeast homoserine dehydrogenase (HSD), which is responsible for the conversion of *L*-aspartate  $\beta$ -semialdehyde to *L*-homoserine in the aspartate biosynthetic pathway. Inhibition of HSD by RI-331, however, required the presence of NADP<sup>+</sup>. In this paper, we examined the mode of action of RI-331 and the role of NAD(P)<sup>+</sup>. The kinetics of inactivation of purified yeast HSD by RI-331 were pseudo-first order with time and were saturated at high inactivator concentrations.  $k_{inact} = 0.216 \text{ min}^{-1}$  and  $K_I = 5.14 \text{ mM}$  were calculated in the presence of 0.5 mM NAD<sup>+</sup>. Although inactivation of yeast HSD by RI-331 appears to be irreversible, no covalent modification of HSD could be detected by positive ion electrospray mass spectrometry. On the other hand, [<sup>14</sup>C]-NAD<sup>+</sup> was invariably associated with inactivated HSD. The amount of enzyme that bound radiolabeled NAD<sup>+</sup> clearly correlated with the extent of inactivation by RI-331 and the stoichiometry was 1:1. Lastly, neutral electrospray mass spectrometry of RI-331 inactivated HSD measured a mass corresponding to HSD dimer bound to 2 RI-331 and 2 NAD<sup>+</sup> (78 333 Da). RI-331 demonstrated many properties of a mechanism-based inactivator. However, instead of inactivating yeast HSD by covalent modification, RI-331 appears to be forming a tight-binding adduct with NAD(P)<sup>+</sup> in an HSD-dependent manner. The tight-binding properties of the inhibition suggest that the adduct resembles the transition state. RI-331 is a good model for the design of potent antifungal compounds targeting other fungal dehydrogenases.

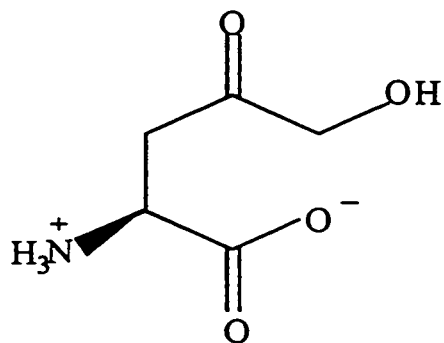
## INTRODUCTION

Fungal pathogens are rapidly becoming a serious health threat as the population of immunocompromised individuals increases and the current antifungal therapies become ineffective due to fungal resistance (Graybill, 1996). As a consequence, the discovery of new targets for antifungal drugs is essential. Much attention has been placed on the biosynthesis of the fungal cell wall, as well as the components of the plasma membranes. Other promising fungal targets include DNA topoisomerases, elongation factor 2 (EF-2), regulation of cell cycle and virulence factors (for reviews see Georgopapadakou and Walsh, 1996; Groll *et al.*, 1998).

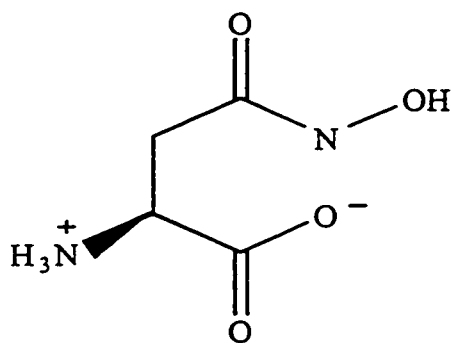
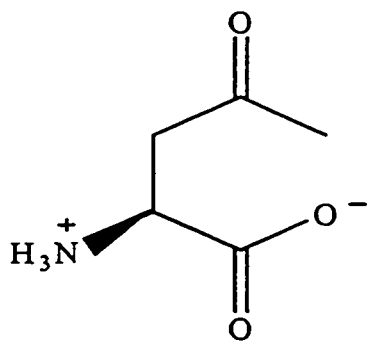
A decade ago, the natural product (*S*)-2-amino-4-oxo-5-hydropentanoic acid (RI-331)<sup>1</sup> (Figure 1) from *Streptomyces* species was discovered to have *in vitro* antifungal properties against several important yeasts such as *Candida albicans* and *Cryptococcus neoformans*. Treatment of mice with systematic candidiasis using RI-331 increased survival rates (100% with 100 mg/kg twice daily over 14 days) and demonstrated no toxicity (LC<sub>50</sub> > 5000 mg/kg) (Yamaguchi *et al.*, 1988). RI-331 was reported to inhibit the biosynthesis of the aspartate family of amino acids (methionine, isoleucine and threonine), consequently leading to the inhibition of protein synthesis. The target of RI-331 was determined to be the third enzyme in the pathway, homoserine dehydrogenase (HSD) (EC 1.1.1.3) (Yamaki *et al.*, 1990) (Figure 2). HSD is responsible for the conversion of *L*-aspartate  $\beta$ -semialdehyde (ASA) to *L*-homoserine (Hse). The aspartate pathway is absent in mammals, thus making it a good target for novel antifungal agents.

Previously, inhibition of *Saccharomyces cerevisiae* HSD by RI-331 was found only in the presence of the product, NADP<sup>+</sup>, or in the reverse direction (Hse + NADP<sup>+</sup> → ASA + NADPH) (Yamaki *et al.*, 1992). RI-331 was believed to inhibit HSD by binding the enzyme-NADP<sup>+</sup> complex. NADP<sup>+</sup> was postulated to be required for conformational change, thereby facilitating the binding of RI-331. However, the requirement for NADP<sup>+</sup> still remains unclear. In order to address this issue, *S. cerevisiae* HSD was purified from overexpressing *Escherichia coli* (Jacques *et al.*, 1999 (Chapter 2)) and its inactivation by RI-331 was carefully examined. The results presented in this paper suggest that RI-331 is a mechanism-based inactivator. RI-331 causes inactivation of HSD by reacting with the cofactor NAD(P)<sup>+</sup> and, consequently, forming a transition-state analog capable of very tight binding.

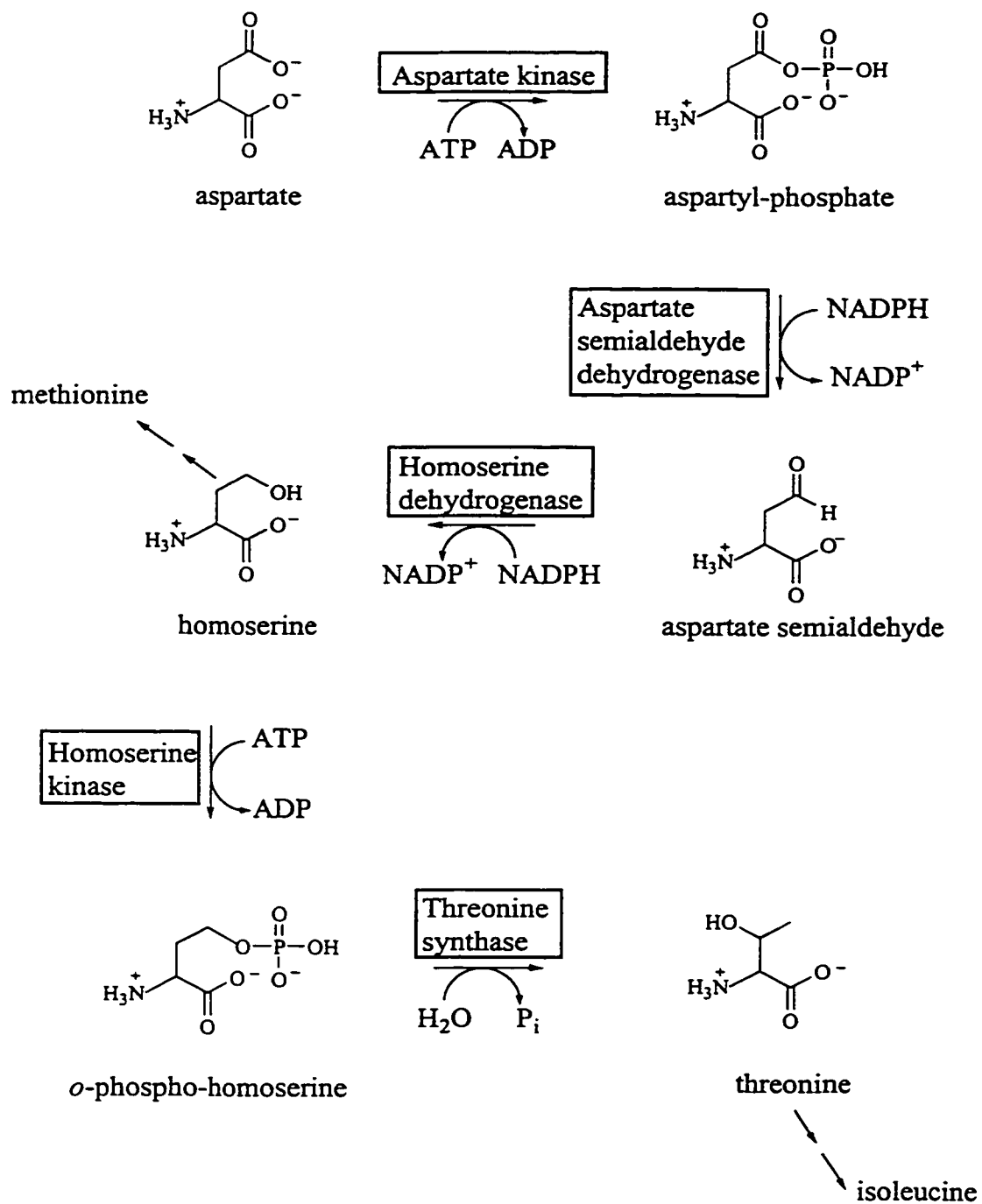
**Figure 1. Structures of (*S*)-2-amino-4-oxo-5-hydroxypentanoic acid (RI-331), *L*-aspartate  $\beta$ -hydroxamate and 4-oxo-*L*-norvaline.**



RI-331

*L*-aspartate  $\beta$ -hydroxamate4-oxo-*L*-norvaline

**Figure 2. The aspartate pathway of amino acid biosynthesis.**



## MATERIALS AND METHODS

### *Chemicals*

3-Amino-pyridine adenine dinucleotide (APAD), *D,L*-arginine, *L*-aspartate  $\beta$ -hydroxamate, *N*-[2-hydroxyethyl]piperazine-*N'*-[2-ethanesulfonic acid] (HEPES),  $\beta$ -mercaptoethanol, NADH, phenyl glyoxal, reduced glutathione and [2-hydroxy-1,1-bis(hydroxymethyl)-ethylamino]-1-propanesulfonic acid (TAPS) were obtained from Sigma (St. Louis, MO). NAD<sup>+</sup> was purchased from Boehringer Mannheim (Laval, PQ) and [<sup>14</sup>C]-NAD<sup>+</sup> was purchased from NEN Dupont (Wilmington, DE). *L*-aspartate  $\beta$ -semialdehyde was prepared as previously described (Jacques *et al.*, 1999 (Chapter 2)). (*S*)-2-amino-4-oxo-5-hydroxypentanoic acid (RI-331) and 4-oxo-*L*-norvaline were generous gifts from Dr. John Honek, University of Waterloo, Waterloo, ON, Canada. Yeast homoserine dehydrogenase (HSD) was purified from *Escherichia coli* BL21 (DE3)/pCP13 as Jacques *et al.*, 1999 (Chapter 2).

### *Inactivation kinetics*

Yeast HSD (1.2  $\mu$ g, 0.12  $\mu$ M) was incubated with various concentrations (0, 0.12, 0.6, 1.2, 2.4 and 4.8 mM) of RI-331 in the presence of 0.5 mM NAD<sup>+</sup> and 100 mM HEPES pH 7.5 at room temperature (25°C) in a final volume of 250  $\mu$ L. At several timepoints, 20  $\mu$ L preincubation mixture was added to 980  $\mu$ L assay mixture containing 0.2 mM NADH, 0.8 mM ASA and 100 mM HEPES pH 7.5. HSD activity was measured at room temperature in the forward (ASA + NADH  $\rightarrow$  Hse + NAD<sup>+</sup>) direction by continuously monitoring the disappearance of NADH at 340 nm using a Cary 3E UV-vis



spectrophotometer. Activity assays were performed in duplicate. Initial rates were obtained directly from the progress curves using the Cary 3.00 software. Percent residual activity was calculated with respect to HSD activity at time = 0.  $k_{\text{obs}}$  was determined for each RI-331 concentration by linear regression of log % residual activity versus time data. These rates were subsequently fitted to equation (1) by nonlinear least-squares regression using Grafit 3.0 (Leatherbarrow, 1992). The parameters obtained from the best fit were reported with standard errors.

$$k_{\text{obs}} = k_{\text{inact}} I / (K_I + I) \quad (1)$$

Inactivation of yeast HSD was also performed by first incubating 4 mM RI-331 and 4 mM NAD<sup>+</sup> together in 100 mM HEPES, pH 7.5 at room temperature overnight. The mixture was then added to 0.7 μg HSD (0.18 μM) and 100 mM HEPES, pH 7.5 to a concentration of 1 mM each. HSD samples were assayed for activity as above to determine the rate of inactivation.

In addition, *L*-aspartate β-hydroxamate and 4-oxo-*L*-norvaline were tested for inactivation of yeast HSD. *L*-aspartate β-hydroxamate (5 mM) was added to 1.2 μg HSD (0.12 μM), 0.5 mM NAD<sup>+</sup> and 100 mM HEPES, pH 7.5. 4-oxo-*L*-norvaline (2 mM) was added to 1.4 μg HSD (0.37 μM), 0.5 mM NAD<sup>+</sup> and 100 mM HEPES, pH 7.5. Samples were taken from the preincubation mixtures at various timepoints, assayed for residual HSD activity and rates of inactivation were calculated as above.

### *Substrate Protection*

HSD inactivation was performed as described above in the presence of 0, 0.15, 2.0 and 4.0 mM ASA. The preincubation mixture contained 1.2  $\mu\text{g}$  HSD (0.12  $\mu\text{M}$ ), 2.4 mM RI-331, 0.5 mM  $\text{NAD}^+$  and 100 mM HEPES pH 7.5. Residual HSD activity was measured and inactivation rates were obtained as above.

### *Effect of trapping agents*

HSD (1.2  $\mu\text{g}$ , 0.12  $\mu\text{M}$ ) was inactivated as described above with 2.4 mM RI-331 and 0.5 mM  $\text{NAD}^+$  in 100 mM HEPES, pH 7.5 in the presence of 0.8 mM reduced glutathione, 4 mM  $\beta$ -mercaptoethanol or 10 mM *D,L*-arginine. Residual HSD activity was measured and inactivation rates were obtained as above. Recovery of HSD activity by the addition of  $\beta$ -mercaptoethanol was tested by first inactivating 1.2  $\mu\text{g}$  HSD (0.12  $\mu\text{M}$ ) with 2 mM RI-331 and 0.5 mM  $\text{NAD}^+$  in 100 mM HEPES, pH 7.5 at room temperature, then adding 3.9 mM  $\beta$ -mercaptoethanol and measuring residual HSD activity at various times as above.

### *Effect of RI-331 in the presence of APAD*

HSD (1.2  $\mu\text{g}$ , 0.12  $\mu\text{M}$ ) was incubated as previously in a mixture containing 0.45 mM APAD instead of  $\text{NAD}^+$ , 2.4 mM RI-331 and 100 mM HEPES pH 7.5. Residual HSD activity was measured and the rate of inactivation was determined as above.

*[<sup>14</sup>C]-NAD<sup>+</sup> studies*

To study the role of NAD<sup>+</sup> in HSD inactivation by RI-331, HSD (37 μM) was incubated with 0.36 mM RI-331 or without RI-331 in the presence of 0.26 mM [<sup>14</sup>C]-NAD<sup>+</sup> (1.1 X 10<sup>12</sup> cpm/mol) and 100 mM HEPES, pH 7.5 at room temperature for 3 days. HSD activity was measured as previously to assure full inactivation. Excess reagents were removed by diluting the mixtures with 100 mM HEPES, pH 7.5 and reconcentrating the enzyme using an UltraFree 10 kD cutoff concentrator. After repeating this 5 times, 373 μM cold NAD<sup>+</sup> was added to the mixtures to compete off the enzyme-bound [<sup>14</sup>C]-NAD<sup>+</sup>. The release of [<sup>14</sup>C]-NAD<sup>+</sup> was monitored at room temperature over 28 days by periodically taking 100 μL samples, removing HSD by filtration through a Microcon 10 kD cutoff membrane, adding 3 mL scintillation fluid and measuring free [<sup>14</sup>C]-NAD<sup>+</sup> by liquid scintillation counting.

After 20 days, both inactivated and control HSD were analyzed by gel filtration. Samples (500 μL) were injected onto a Sephadex G25 column (Pharmacia, HR 5/10) equilibrated with distilled water and 250 μL fractions were eluted at a flow rate of 0.5 mL/min. Fractions were then counted for [<sup>14</sup>C]-NAD<sup>+</sup>.

Furthermore, the binding of [<sup>14</sup>C]-NAD<sup>+</sup> to HSD was monitored during inactivation by RI-331. HSD (37 μM) was incubated with 0.28 mM RI-331 and 0.28 mM NAD<sup>+</sup> (1.2 X 10<sup>12</sup> cpm/mol) in 10 mM TAPS, pH 8.5 and 250 μL samples were removed at several times during inactivation of HSD. The samples were then dialyzed in 2 L 10 mM TAPS, pH 8.5 at 4°C for over 24 hours with three buffer changes. Subsequently, the

samples were counted for [ $^{14}\text{C}$ ]-NAD $^+$ , assayed for HSD activity as previously and HSD concentration measured by absorbance at 280 nm (1 AU = 1.1 mg/mL).

#### *Dialysis of HSD inactivated by RI-331 and NAD $^+$*

HSD (0.35 mg, 36  $\mu\text{M}$ ) was inactivated with 0.2 mM RI-331 and 0.16 mM NAD $^+$  in 10 mM TAPS pH 8.5 (250  $\mu\text{L}$  total volume) overnight at room temperature along with a control sample without RI-331. HSD activity was measured as previously to assure full inactivation. The mixtures were then dialyzed in 2 L 20 mM HEPES pH 7.5 for 3 days at 4°C with three buffer changes. HSD activity was monitored by adding 20  $\mu\text{L}$  dialyzed mixture diluted 10-300 times with 10 mM TAPS pH 8.5 to 980  $\mu\text{L}$  assay mixture containing 0.2 mM NADH, 0.8 mM ASA and 100 mM HEPES pH 7.5. Subsequently, the inactivated HSD and control samples were then left at room temperature for 2 days and HSD activity was remeasured.

#### *Mass spectrometry*

Positive ion electrospray mass spectrometry of RI-331-inactivated HSD was performed by Dr. Kirk Green at the McMaster Regional Centre for Mass Spectrometry. HSD was denatured with 5 % CH $_3$ CN and injected on a Micromass Quattro-LC instrument using CH $_3$ CN/H $_2$ O (1:1) as a solvent by. Positive ion electrospray mass spectrometry of phenyl glyoxal-inactivated HSD was performed by Dr. Jian Chen at the University of Waterloo Biological Mass Spectrometry Laboratory on a Fisons VG Quattro II instrument using CH $_3$ CN/H $_2$ O (1:1) with 0.1 % trifluoroacetic acid as a solvent.

Samples were prepared by incubating HSD (1 mg, 100  $\mu$ M) with either 0.5 mM NAD<sup>+</sup>, or 0.58 mM RI-331 and 0.5 mM NAD<sup>+</sup>, or 50 mM phenyl glyoxal in 10 mM TAPS, pH 8.5 overnight at room temperature. After HSD activity was tested as previously to determine the extent of inactivation, HSD was purified from excess reagents by gel filtration. Mixtures were injected onto a Sephadex G25 column (Pharmacia, HR 5/10) equilibrated with distilled water and 250  $\mu$ L fraction were eluted at 0.5 mL/min. Purification was monitored by absorbance at 280 nm and high absorbance fractions were analyzed by mass spectrometry.

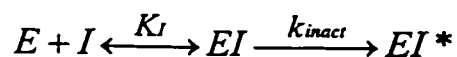
#### *Purification of NAD-RI-331 adduct*

HSD (39  $\mu$ M) was incubated with 0.50 mM RI-331 or without RI-331 in the presence of 0.26 mM [<sup>14</sup>C]-NAD<sup>+</sup> ( $1.2 \times 10^{12}$  cpm/mol) and 100 mM HEPES, pH 7.5 at room temperature for 2 days. HSD activity was measured as previously described to assure full inactivation. Excess reagents were then removed by dilution and concentration 5 times as above. The mixtures (1 mL) were then concentrated to 100  $\mu$ L and added to 100  $\mu$ L methanol to release the adduct by denaturation of HSD. After removing the precipitated protein by centrifugation, 100  $\mu$ L supernatant was injected onto a Superdex-Peptide column (Pharmacia HR 10/30) equilibrated with distilled water. The 250  $\mu$ L fractions were eluted at 0.5 mL/min and monitored for absorbance by a Dionex PD40 diode array detector and for [<sup>14</sup>C]-NAD<sup>+</sup> by radiolabel counting.

## RESULTS

### *Inactivation kinetics*

Inactivation of yeast HSD by RI-331 was examined by measuring HSD activity after preincubation of the enzyme (0.12  $\mu\text{M}$ ) with 0.5 mM  $\text{NAD}^+$  and various concentrations of RI-331 at room temperature (25°C) for a specified period of time. Since  $\text{NAD}^+$  and  $\text{NADP}^+$  were shown earlier to perform equally well in HSD catalysis (Chapter 2),  $\text{NAD}^+$  was used in these assays for convenience. RI-331 demonstrated both time and concentration-dependent inactivation of HSD (Figure 3). The extent of HSD inactivation by RI-331 increased over time in a pseudo-first order manner and the observed rates of inactivation ( $k_{\text{obs}}$ ) increased with RI-331 concentration. The observed rates were calculated to be 0.0119, 0.0308, 0.0475, 0.0727 and 0.111  $\text{min}^{-1}$  for 0.12, 0.6, 1.2, 2.4 and 4.8 mM RI-331, respectively. HSD alone displayed a minimal decrease in activity at room temperature (0.0065  $\text{min}^{-1}$ ). High concentrations of RI-331 appeared to saturate HSD as rates of inactivation did not increase linearly (Figure 4). The maximal rate of inactivation ( $k_{\text{inact}}$ ) was determined to be  $0.216 \pm 0.015 \text{ min}^{-1}$  (Scheme 1) and the dissociation constant ( $K_I$ ) was  $5.14 \pm 0.59 \text{ mM}$  from nonlinear least-squares regression to equation 1.



**Scheme 1. Reaction scheme for a mechanism-based inactivator**

When RI-331 and  $\text{NAD}^+$  (4 mM each) were incubated together prior to HSD inactivation, the rate of inactivation for a final concentration of 1 mM each was 0.0384

**Figure 3. Time-dependent inactivation of yeast HSD by RI-331.** Residual HSD activity was measured at specific times after HSD (0.12  $\mu$ M) incubation with 0 (O), 0.12 ( $\bullet$ ), 0.6 ( $\square$ ), 1.2 ( $\blacksquare$ ), 2.4 ( $\Delta$ ) and 4.8 mM ( $\blacklozenge$ ) RI-331 in the presence of 0.5 mM NAD<sup>+</sup> and 100 mM HEPES pH 7.5 at room temperature (25°C). Lines represent the results of linear regressions.

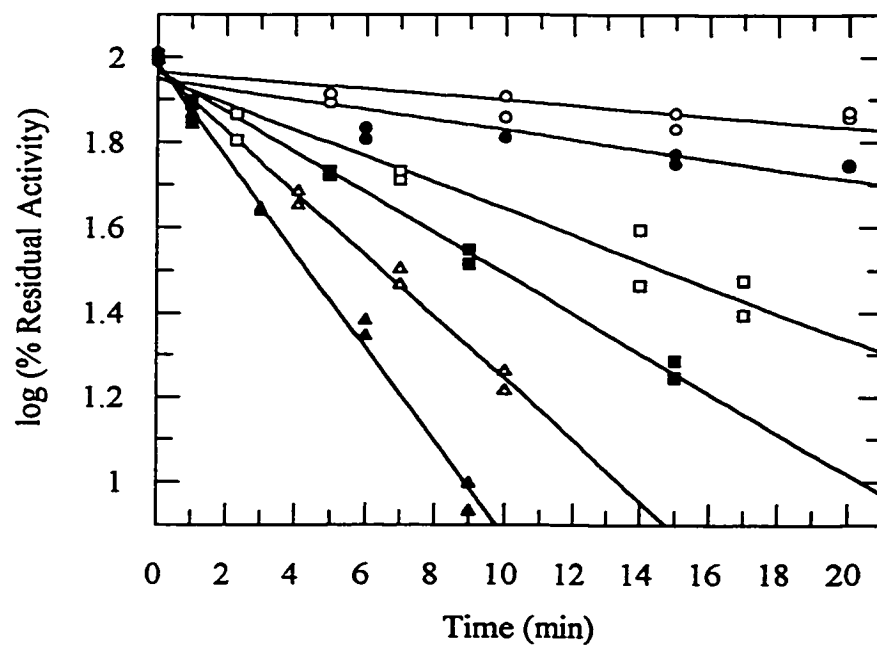
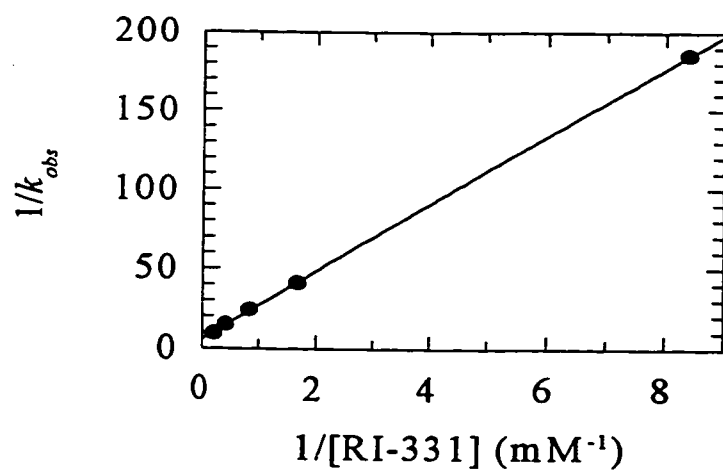
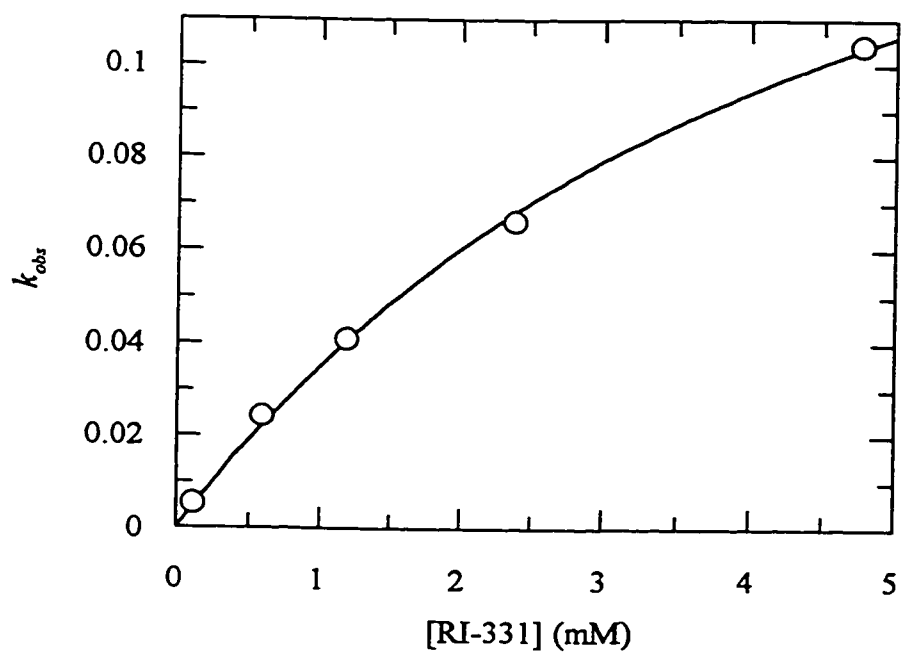




**Figure 4. Saturation of RI-331 inactivation of yeast HSD.**  $k_{obs}$  versus RI-331 concentration data were fit to equation 1 by nonlinear least-squares regression using Grafit 3.0. The inactivation parameters  $k_{inact} = 0.195 \pm 0.026 \text{ min}^{-1}$  and  $K_I = 3.30 \pm 0.81 \text{ mM}$  were obtained. *Inset:* Double reciprocal plot of  $k_{obs}$  versus RI-331 concentration data.



min<sup>-1</sup> (Table 1). This value is comparable to the rate obtained for 1.2 mM RI-331 above (0.0475 min<sup>-1</sup>) and is equal to the expected value for 1 mM RI-331 (0.0352 min<sup>-1</sup>). Therefore, no increase in inactivation rate was observed by preincubating RI-331 and NAD<sup>+</sup> prior to inactivation of HSD.

Two other structurally related compounds, *L*-aspartate β-hydroxamate and 4-oxo-*L*-norvaline (Figure 1), were also examined for time-dependent inactivation of HSD in the presence of 0.5 mM NAD<sup>+</sup>. The observed rates (Table 1) are shown to be negligible and therefore no inactivation of HSD activity was demonstrated with these compounds. *L*-aspartate β-hydroxamate was previously shown to be an inhibitor of yeast HSD for either ASA reduction ( $K_{ii} = 0.77 \pm 0.15$ ,  $K_{ii} = 3.06 \pm 0.47$  mM) or homoserine oxidation ( $K_{ii} = 3.52 \pm 0.63$  mM). On the other hand, 4-oxo-*L*-norvaline demonstrated no inhibitory activity (Chapter 2, Appendix A).

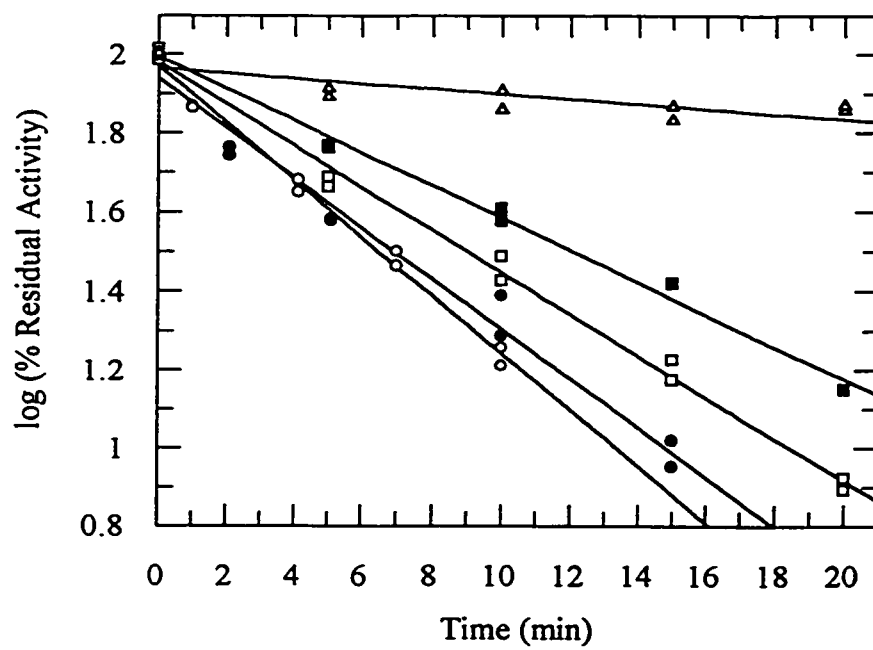
### *Substrate protection*

Substrate protection of yeast HSD from RI-331 inactivation was performed by the addition of various concentrations of ASA to the preincubation mixture containing 2.4 mM RI-331, 0.5 mM NAD<sup>+</sup> and 0.12 μM HSD. As illustrated in Figure 5, inactivation of HSD by RI-331 decreased with increasing ASA concentrations. The observed inactivation rates were calculated to be 0.0727, 0.0634, 0.0532, 0.0409 min<sup>-1</sup> for 0, 0.15, 2.0 and 4.0 mM ASA respectively.

**Table 1. Observed inactivation rates ( $k_{obs}$ ) of yeast HSD**

Conditions	$k_{obs}$ (min <sup>-1</sup> )
0 mM RI-331 and 0.5 mM NAD <sup>+</sup>	0.0065 ± 0.0015
+ 5 mM <i>L</i> -aspartate β-hydroxamate	0.0035 ± 0.0014
+ 2 mM 4-oxo- <i>L</i> -norvaline	0.0010 ± 0.0010
2.4 mM RI-331 and 0.5 mM NAD <sup>+</sup>	0.0530 ± 0.0014
+ 1 mM reduced glutathione	0.0651 ± 0.0023
+ 4 mM β-mercaptoethanol	0.0613 ± 0.0020
+ 10 mM <i>D,L</i> -arginine	0.0565 ± 0.0018
2.4 mM RI-331 and 0.5 mM APAD	0.0057 ± 0.0019
preincubated 1 mM RI-331 and 1 mM NAD <sup>+</sup>	0.0384 ± 0.005

**Figure 5. Substrate protection from RI-331 inactivation of yeast HSD.** HSD (0.12  $\mu$ M) was incubated with 2.4 mM RI-331, 0.5 mM NAD<sup>+</sup> and 100 mM HEPES pH 7.5 in the presence of 0 (●), 0.15 (□), 2.0 (■) and 4.0 ( $\Delta$ ) mM ASA or with only 0.5 mM NAD<sup>+</sup> and 100 mM HEPES, pH 7.5 (O) at room temperature. Residual HSD activity was measured at specific times. Lines represent the results of linear regressions.



### *Effect of trapping agents*

Trapping agents were added to the preincubation mixture to determine whether reactive species are released from the active site prior to inactivation of HSD. Reduced glutathione (0.8 mM) and  $\beta$ -mercaptoethanol (4 mM) were used as electrophile trapping agents and *D,L*-arginine (10 mM) was added to trap glyoxal compounds. As shown in Table 1, these compounds had little effect on the rate of inactivation of RI-331. In addition, HSD activity could not be recovered by the addition of 3.9 mM  $\beta$ -mercaptoethanol after its inactivation by RI-331 and  $\text{NAD}^+$ .

### *Role of $\text{NAD(P)}^+$ and stoichiometry*

Previous results (Yamaki *et al.*, 1992) demonstrated that  $\text{NADP}^+$  was necessary for RI-331 inhibition of yeast HSD activity. Likewise, inactivation of HSD by RI-331 was seen only when  $\text{NAD}^+$  was added (data not shown). The presence of oxidized nicotinamide may promote inactivation of HSD either by causing a conformational change, which could facilitate RI-331 binding, or by acting as a cofactor in the conversion of RI-331 to a reactive species. In order to answer this question, 0.45 mM 3-amino-pyridine adenosine dinucleotide (APAD), a nonreactive  $\text{NAD}^+$  analog, was incubated with 0.12  $\mu\text{M}$  HSD and 2.4 mM RI-331. No inactivation of HSD was observed, as the rate of inactivation was comparable to that in the absence of RI-331 (Table 1). Consequently, a reactive form of  $\text{NAD(P)}^+$  is essential and appears to be involved in the conversion of RI-331 to an inhibitory form.

The role of  $\text{NAD(P)}^+$  was probed further by inactivating HSD with RI-331 in the presence of [ $^{14}\text{C}$ ]-labeled  $\text{NAD}^+$ . After removing excess reagents by dilution and ultrafiltration, the amount of enzyme-bound [ $^{14}\text{C}$ ]- $\text{NAD}^+$  was measured by gel filtration (Sephadex G25) followed by radiolabel counting. In the inactive sample, all the remaining [ $^{14}\text{C}$ ]- $\text{NAD}^+$  coeluted with HSD producing a ratio of 1.2 mol bound  $\text{NAD}^+$  per mol HSD (Figure 6). In the control sample (HSD + [ $^{14}\text{C}$ ]- $\text{NAD}^+$ ), however, the majority of [ $^{14}\text{C}$ ]- $\text{NAD}^+$  eluted with a larger volume (7 mL) indicating it was unbound and a ratio of 0.2 mol bound  $\text{NAD}^+$  per mol HSD was measured.

In a subsequent experiment, samples were taken as HSD was being inactivated by RI-331 and [ $^{14}\text{C}$ ]- $\text{NAD}^+$ . After the removal of excess reagents by dialysis in 10 mM TAPS, pH 8.5, the samples were measured for incorporation of [ $^{14}\text{C}$ ]- $\text{NAD}^+$ , tested for residual HSD activity and measured for protein concentration. As shown in Figure 7, the amount of HSD-associated [ $^{14}\text{C}$ ]- $\text{NAD}^+$  correlated well with the extent of HSD inactivation. In addition, the stoichiometry was calculated to be 1 mol [ $^{14}\text{C}$ ]- $\text{NAD}^+$  / 1 mol HSD at 100 % inactivation, thereby supporting the preceding experiment. The results clearly show that a form of  $\text{NAD}^+$  is bound to HSD during inactivation of yeast HSD by RI-331.



**Figure 6. Gel filtration analysis of yeast HSD inactivated with RI-331 and [<sup>14</sup>C]-NAD<sup>+</sup>.** HSD (37 μM) was incubated with 0.36 mM RI-331 and 0.26 mM [<sup>14</sup>C]-NAD<sup>+</sup> (1.1 X 10<sup>12</sup> cpm/mol) (solid line) or with 0.26 mM [<sup>14</sup>C]-NAD<sup>+</sup> (1.1 X 10<sup>12</sup> cpm/mol) alone (dotted line) in 100 mM HEPES, pH 7.5 at room temperature. After removal of excess reagents, 373 μM cold NAD<sup>+</sup> was added and 500 μL samples were injected onto Sephadex G25 column (Pharmacia, HR 5/10) equilibrated with distilled water. Fractions (250 μL) were eluted at 0.5 mL/min and measured for [<sup>14</sup>C]-radiolabel.

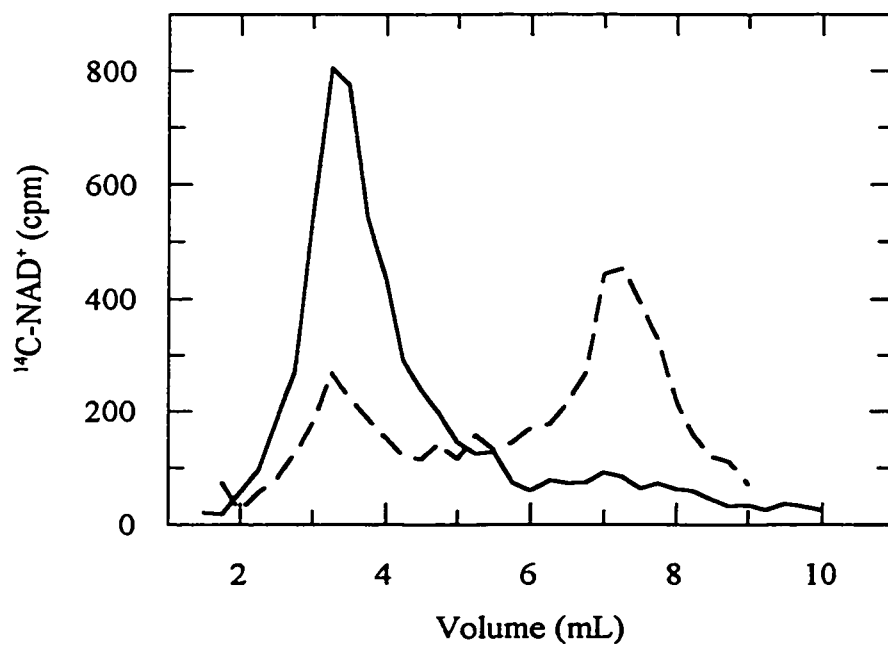
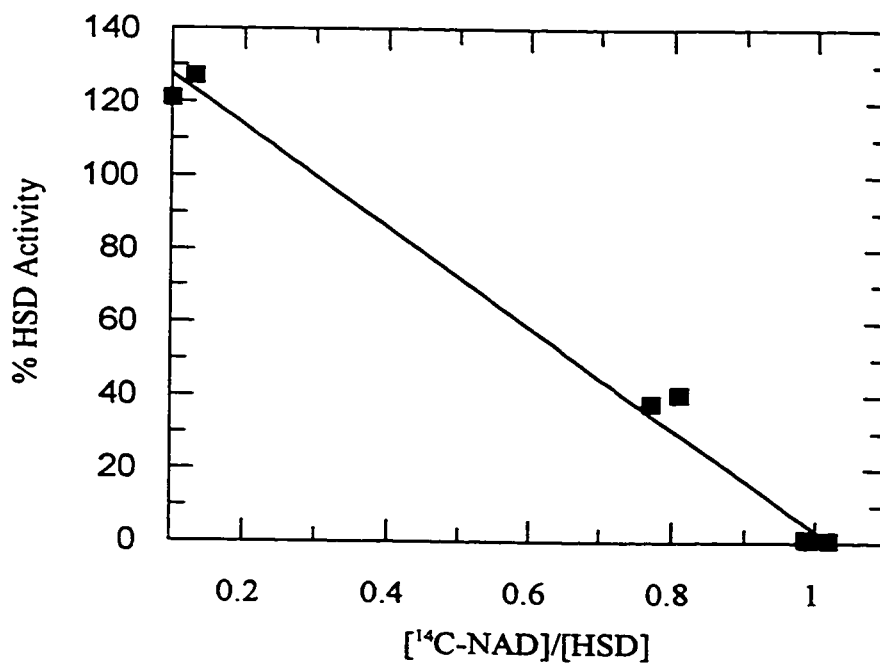


**Figure 7. Incorporation of [<sup>14</sup>C]-NAD<sup>+</sup> during inactivation of yeast HSD by RI-331.** HSD (37 μM) was incubated with 0.28 mM RI-331 and 0.28 mM [<sup>14</sup>C]-NAD<sup>+</sup> (1.2 x 10<sup>12</sup> cpm/mol) in 10 mM TAPS, pH 8.5 at room temperature. Samples were removed during inactivation, dialyzed in 10 mM TAPS, pH 8.5, measured for [<sup>14</sup>C]-NAD<sup>+</sup>, assayed for HSD activity and HSD concentration was measured. The line represents the results of a linear regression on the % HSD activity *versus* [<sup>14</sup>C]-NAD<sup>+</sup>/[HSD] data.

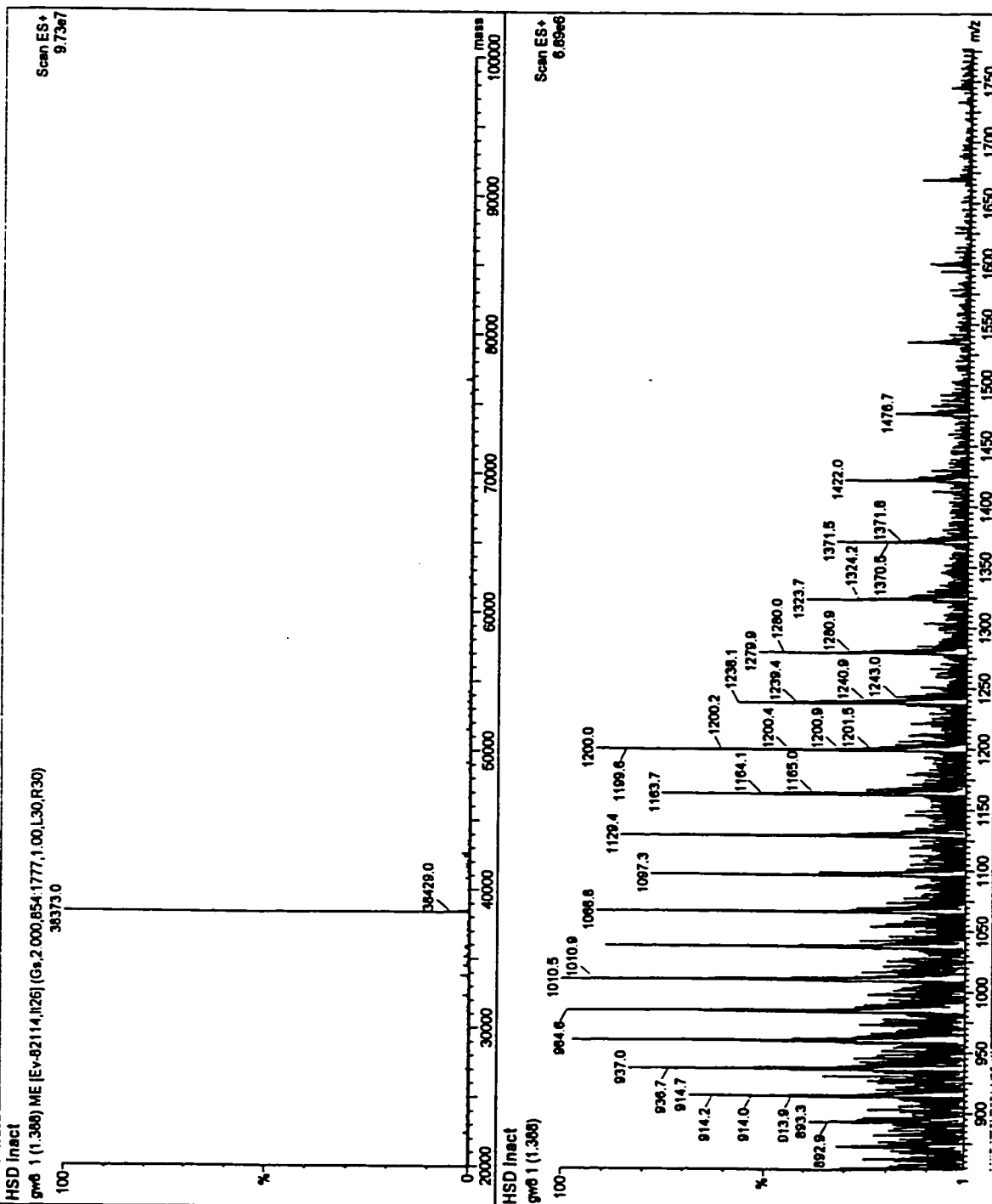


*Irreversibility and mass spectrometry*

The reversibility of RI-331 inactivation of yeast HSD was examined by measuring the reappearance of HSD activity after purification of inactivated HSD from excess reagents. HSD completely inactivated by RI-331 and  $\text{NAD}^+$  was dialyzed over three days in 20 mM HEPES, pH 7.5, with several buffer changes without any recovery of enzyme activity. Additional incubation at room temperature did not result in HSD reactivation. Likewise, HSD inactivated in the presence of [ $^{14}\text{C}$ ]- $\text{NAD}^+$ , quenched with 373  $\mu\text{M}$  unlabeled  $\text{NAD}^+$  and incubated at room temperature did not release any [ $^{14}\text{C}$ ]- $\text{NAD}^+$  over 28 days. Consequently, RI-331 inactivation of HSD appears to be irreversible.

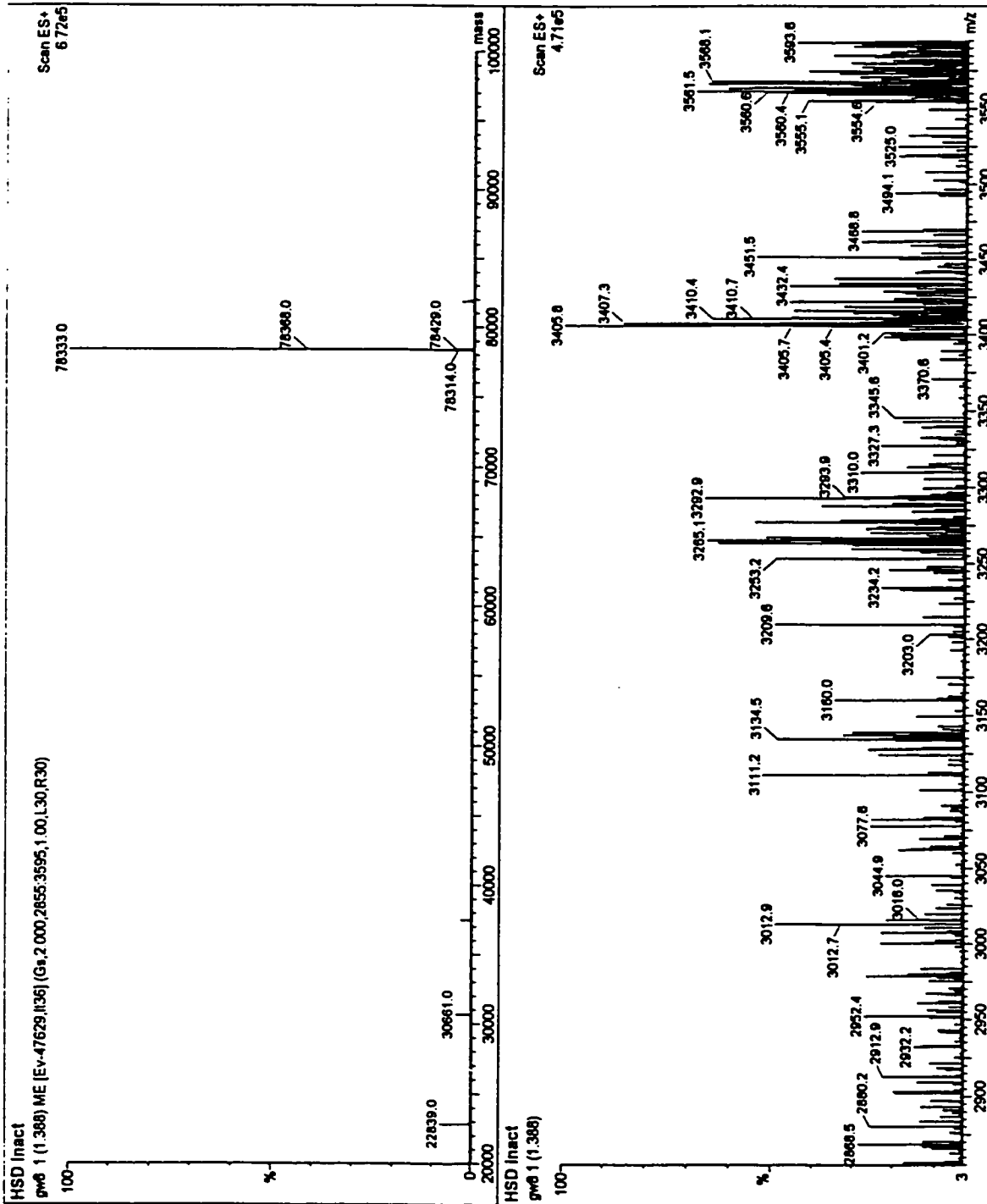
Electrospray mass spectrometry was employed to determine whether the inactivation was a result of covalent modification of yeast HSD. For comparison, HSD was inactivated by phenyl glyoxal and electrospray mass spectrometry revealed 5 different species corresponding to HSD covalently modified by 2, 3, 4, 5, or 6 phenyl glyoxal molecules (Figure 8C). On the other hand, HSD inactivated with RI-331 did not appear to be covalent since no modification of the monomeric molecule was demonstrated (38 373 Da) (Figure 8A). At high mass/charge ratios ( $m/z$ ), however, a molecular mass of 78 333 Da was obtained, corresponding to two RI-331 molecules and two  $\text{NAD}^+$  molecules bound to the HSD dimer ( $2 \times (38\ 375\ \text{Da} + 147\ \text{Da} + 663\ \text{Da})$ ) (Figure 8B). These results indicate that RI-331 inactivation is a consequence of the formation of a NAD-RI-331 complex capable of irreversible binding to yeast HSD.

**Figure 8. Positive ion mass spectrometry of A) RI-331-inactivated HSD, low m/z; B) RI-331-inactivated HSD, high m/z; and C) phenyl glyoxal-inactivated HSD.** HSD (1 mg, 100  $\mu$ M) was incubated with either 0.5 mM NAD<sup>+</sup>, or 0.58 mM RI-331 and 0.5 mM NAD<sup>+</sup>, or 50 mM phenyl glyoxal in 10 mM TAPS, pH 8.5 at room temperature. HSD was purified from excess reagents by gel filtration (Sephadex G25, Pharmacia, HR 5/10). Samples were analyzed on a Micromass Quattro-LC instrument after denaturation with 5 % CH<sub>3</sub>CN using CH<sub>3</sub>CN/H<sub>2</sub>O (1:1) as a solvent by Dr. Kirk Green at the McMaster Regional Centre for Mass Spectrometry (RI-331-inactivated HSD) except for phenyl glyoxal-inactivated HSD, which was analyzed on a Fisons VG Quattro II instrument using CH<sub>3</sub>CN/H<sub>2</sub>O (1:1) with 0.1 % trifluoroacetic acid as solvent by Dr. Jian Chen at the University of Waterloo Biological Mass Spectrometry Laboratory.

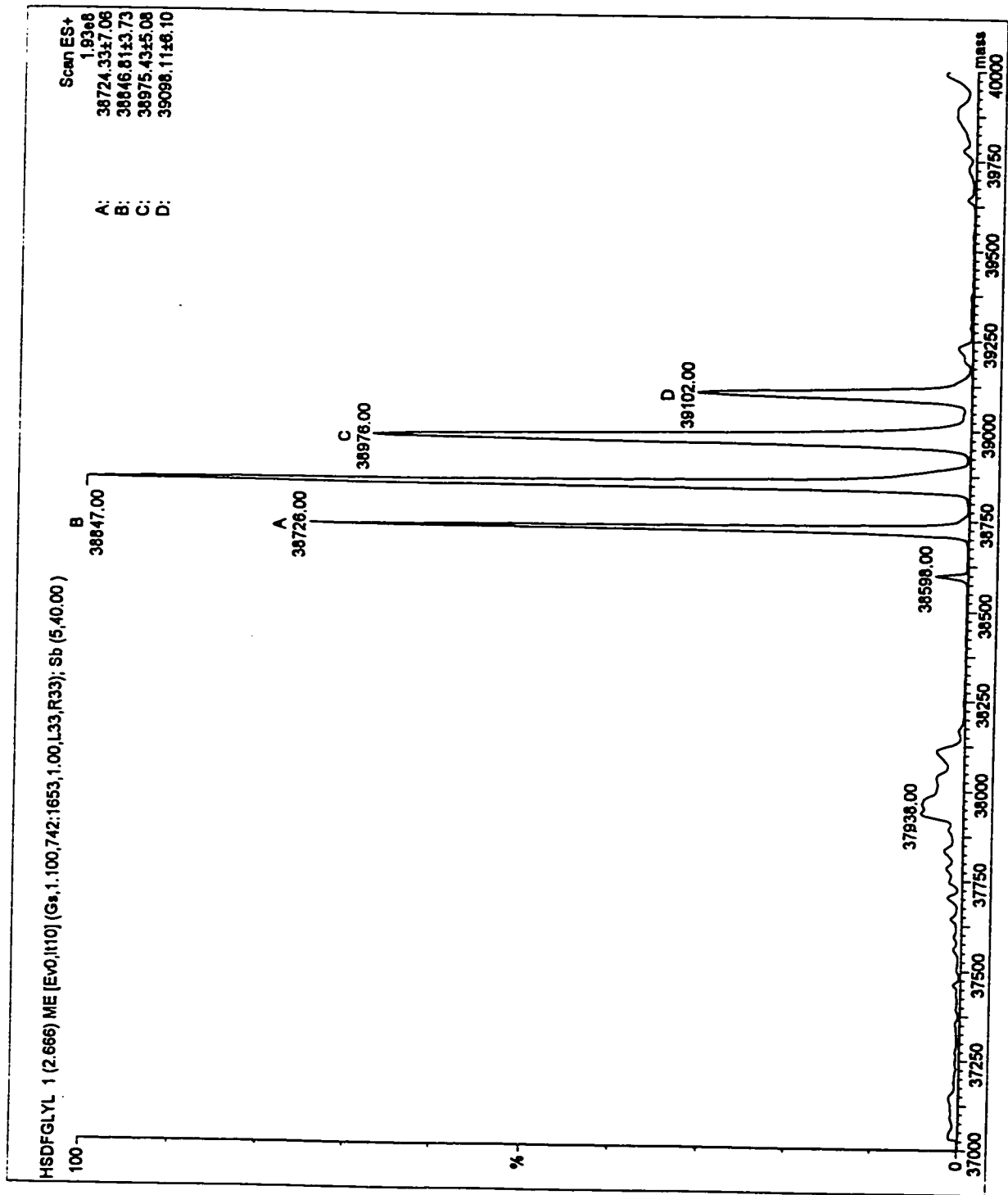


A

B





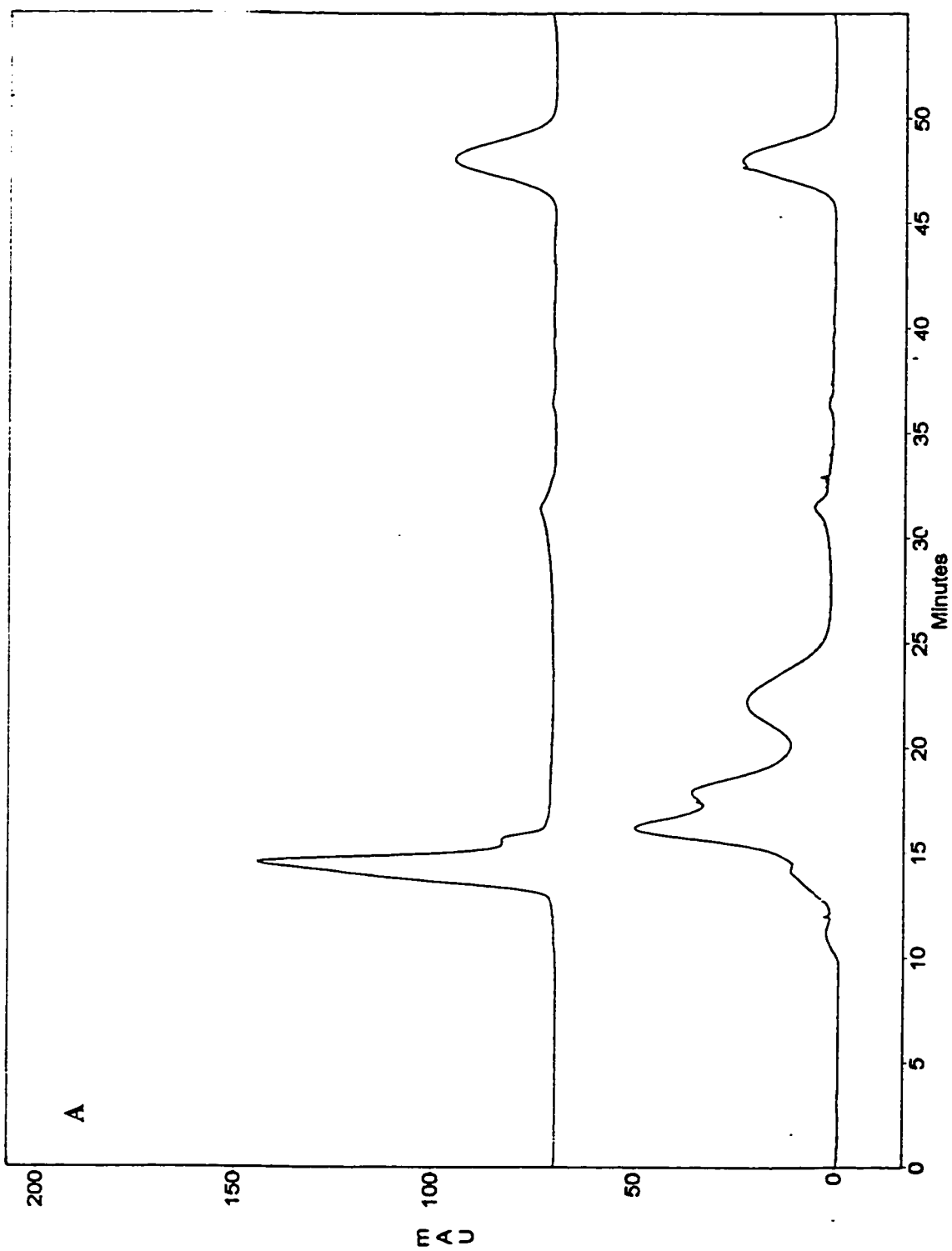


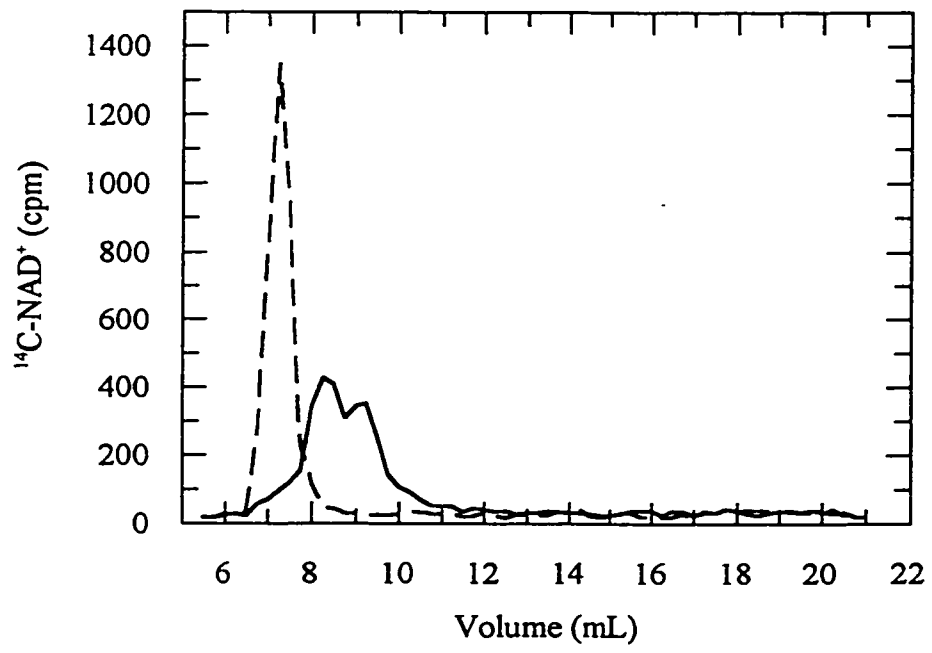
*Purification of NAD-RI-331 adduct*

Attempts were made to purify the NAD-RI-331 adduct by size-exclusion chromatography. RI-331-inactivated HSD was prepared in the presence of [ $^{14}\text{C}$ ]-NAD $^+$ , purified and concentrated using an UltraFree concentrator. The concentrated inactivated HSD was then denatured by 50% methanol to release the adduct and the centrifuged solution was applied onto a Superdex-Peptide column (Pharmacia, HR 10/30). Purification was monitored by a Dionex PD40 diode array detector and radiolabel counting (Figure 9). Both absorbance and radiolabel profiles demonstrate that NAD $^+$  was converted to smaller species during the inactivation process, which is in disagreement with the formation of a NAD-RI-331 adduct. Other attempts to purify a complex capable of HSD inhibition were also futile. It is apparent that the unbound NAD-RI-331 complex is sensitive to degradation and the smaller compounds illustrated in the chromatograms are degradation products.

**Figure 9. Purification of NAD-RI-331 adduct by size exclusion chromatography.**

HSD (39  $\mu\text{M}$ ) was incubated with 0.50 mM RI-331 or without RI-331 in the presence of 0.26 mM [ $^{14}\text{C}$ ]-NAD $^{+}$  ( $1.2 \times 10^{12}$  cpm/mol) and 100 mM HEPES, pH 7.5 at room temperature. After excess reagents were removed and HSD was denatured by 50 % methanol, samples was injected onto a Superdex-Peptide column (Pharmacia, HR 10/30) equilibrated with distilled water. Fractions (250  $\mu\text{L}$ ) were eluted at 0.5 mL/min and monitored for absorbance by a Dionex PD40 diode array detector (A) and for [ $^{14}\text{C}$ ]-NAD $^{+}$  by radiolabel counting (B).



**B**

## DISCUSSION

Fungal amino acid biosynthesis appears to be an effective new target for antifungal therapy as illustrated by the antifungal effects of (*S*)-2-amino-4-oxo-5-hydropentanoic acid (RI-331) (Yamaki *et al.*, 1990). The requirement of NAD(P)<sup>+</sup> for HSD inactivation by RI-331 reveals an interesting mechanism of action. In this paper, we examined the mode of action of RI-331 on yeast HSD in order to clarify the necessity for the oxidized cofactor.

Earlier work described RI-331 as a mixed inhibitor of yeast HSD in the forward direction ( $K_i = 2$  mM) and competitive inhibitor in the reverse direction ( $K_i = 0.025$  mM) (Yamaki *et al.*, 1992). Here, we illustrated that RI-331 possesses many properties of a mechanism-based inactivator. These inactivators are unreactive compounds which are converted by the enzyme to a reactive species, capable of inactivating the enzyme, usually by covalent modification, prior to leaving the active site (Silverman, 1995).

Like mechanism-based inactivators, RI-331 demonstrated time-dependent pseudo-first order inactivation of yeast HSD activity. Furthermore, inactivation was concentration-dependent and exhibited saturation kinetics. A maximal inactivation rate ( $k_{inact}$ ) of  $0.216 \pm 0.015$  min<sup>-1</sup> and an inhibition constant ( $K_i$ ) of  $5.14 \pm 0.59$  mM was obtained in the presence of 0.5 mM NAD<sup>+</sup>. Inactivation by RI-331 decreased significantly when the substrate ASA was added to the preincubation mixture. These results suggest that inactivation of HSD is occurring at the active site. On the other hand, the addition of nucleophiles such as reduced glutathione or  $\beta$ -mercaptoethanol did not

affect the rate of inactivation, indicating that a reactive intermediate was not released from the active site before inactivation of HSD.

Inactivation of yeast HSD by RI-331 was experimentally irreversible, considering HSD activity could not be recovered after extensive dialysis. Irreversible inactivation is usually as a result of covalent modification of the enzyme. Nevertheless, no covalent modification of yeast HSD could be detected by positive ion electrospray mass spectrometry.

The previous report stated that RI-331 may be binding the enzyme-NADP<sup>+</sup> complex and that the cofactor may be required for a conformational change necessary for RI-331 binding (Yamaki *et al.*, 1992). However, RI-331 did not inactivate HSD in the presence of the nonreactive NAD<sup>+</sup> analog, APAD, which also binds HSD ( $K_i = 0.22$  mM) (DeLaBarre *et al.*, 1998). This suggests that the presence of a catalytically competent oxidized nicotinamide (NAD<sup>+</sup> or NADP<sup>+</sup>) is essential for inactivation of yeast HSD by RI-331 and that inactivation likely occurs as a result of a catalytic event. Finally, the stoichiometry of [<sup>14</sup>C]-NAD<sup>+</sup> interaction with yeast HSD was 1:1 when measured after dialysis or gel filtration. Radiolabelled NAD<sup>+</sup> was found to remain associated with HSD after inactivation by RI-331 and the amount of radiolabelled NAD<sup>+</sup> correlated well with the extent of inactivation. Hence, it is evident that NAD(P)<sup>+</sup> is included in the inactivation complex.

Two mechanisms are possible to describe inactivation of yeast HSD by RI-331, both of which account for the necessity of NAD(P)<sup>+</sup>. Firstly, HSD may catalyze the NAD(P)<sup>+</sup>-dependent oxidation of RI-331 to form a glyoxal intermediate (Scheme 2)

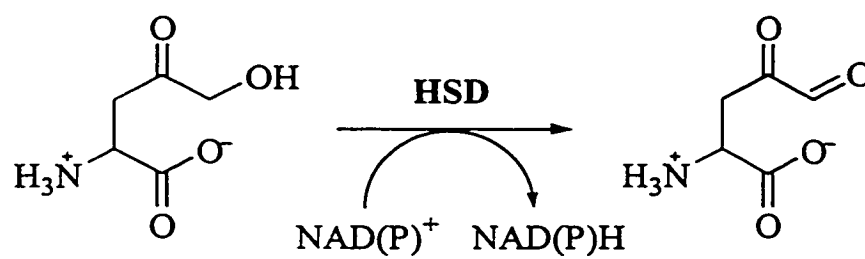
capable of reacting with active site arginine residues. Secondly, RI-331 may react with NAD(P)<sup>+</sup> in an HSD-dependent manner producing a NAD(P)-RI-331 adduct (Scheme 3).

Phenyl glyoxal was shown previously to inactivate HSD, although the effect was modest and no substrate protection was observed (Jacques *et al.*, 1999 (Chapter 2)). Inactivation of HSD by phenyl glyoxal was a consequence of covalent modification as observed by positive ion electrospray mass spectrometry. However, covalent modification of HSD was not observed upon inactivation by RI-331. Furthermore, the addition of arginine, as a trapping agent, had no effect on inactivation by RI-331. Therefore, the formation of a glyoxal intermediate appears to be unlikely.

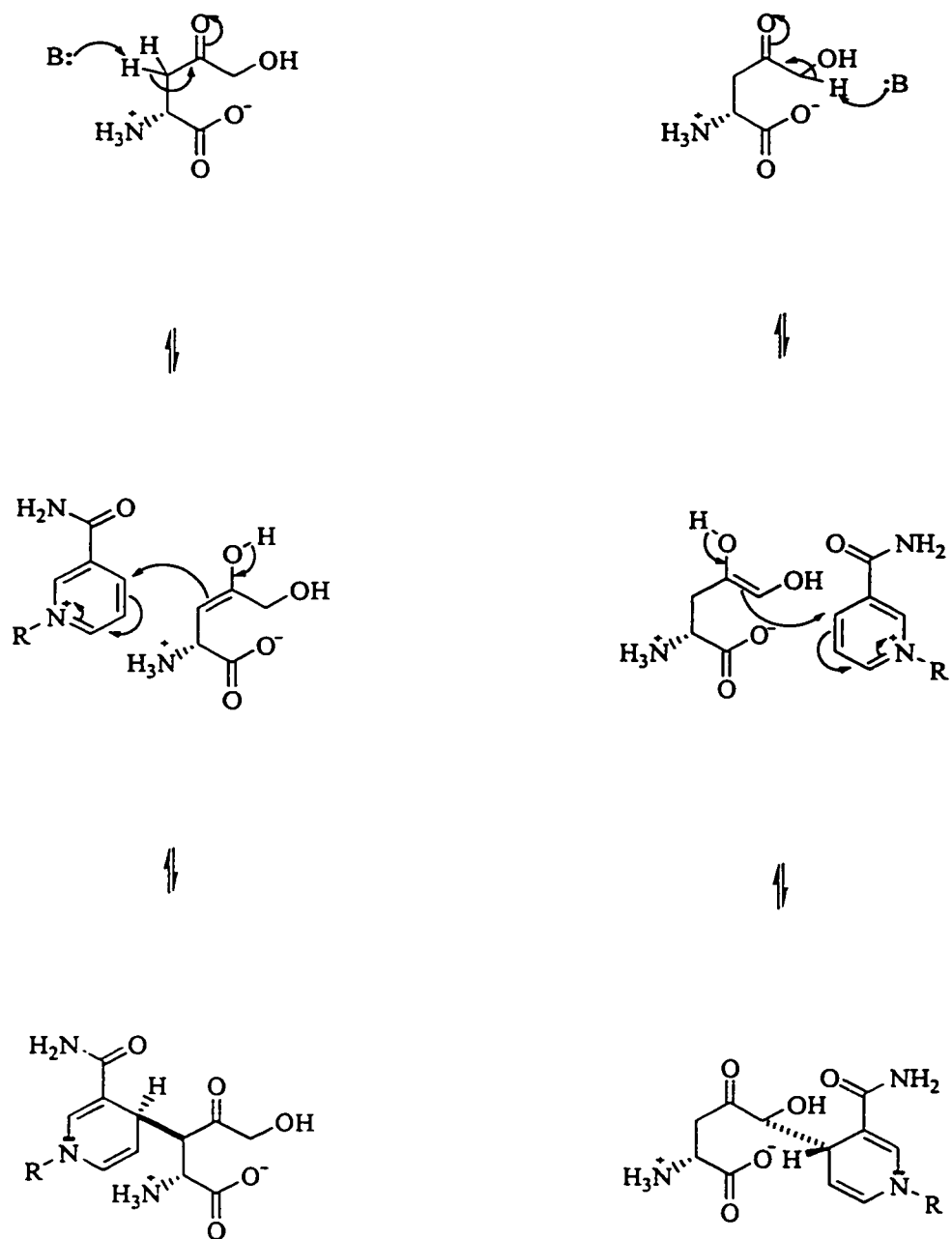
In contrast, the persistent association of NAD<sup>+</sup> with RI-331-inactivated HSD points to the formation of a tight-binding NAD(P)-RI-331 adduct. In fact, an enzyme-bound NAD-RI-331 adduct was detected by electrospray mass spectrometry of inactivated HSD (78 333 Da) under conditions designed to identify non-covalent interactions. Given the tight-binding phenomena, this adduct could be acting as a transition state analog and, consequently, would be expected to bind very tightly to the active site of HSD. Adduct formation appears to require HSD since preincubation of RI-331 and NAD<sup>+</sup> had no effect on the rate of inactivation.

Inactivation of nicotinamide-dependent dehydrogenases/reductases by NAD(P) adducts has been reported earlier. The antitubercular drug, isoniazid, has been shown by x-ray crystallography and mass spectrometry to be covalently-linked to NAD in the active





**Scheme 2.** Possible oxidation of (*S*)-2-amino-4-oxo-5-hydroxypentanoic acid by yeast HSD in the presence of NAD(P)<sup>+</sup>.



**Scheme 3. Possible mechanisms for NAD-RI-331 adduct formation.**

site of long-chain enoyl-acyl carrier protein (ACP) reductase in *M. tuberculosis* (Rozwarsky *et al.*, 1998). Similarly, inactivation of human steroid  $5\alpha$ -reductase by finasteride was demonstrated to be as a result of an enzyme-bound NADP-dihydrofinasteride adduct (Bull *et al.*, 1996). Several examples have also been illustrated with dehydrogenases such as lactate dehydrogenase (Everse *et al.*, 1971).

The production of a NAD(P)-RI-331 adduct may occur through the formation of an enolate at C-3 or C-5 of RI-331, as shown in Scheme 3. It is difficult to state which occurs in reality since neither *L*-aspartate  $\beta$ -hydroxamate nor 4-oxo-*L*-norvaline (Figure 1) are inactivators of yeast HSD. Nevertheless, if enolization takes place at C-3 of RI-331, then these compounds could also be inactivators of HSD. Therefore, the current evidence may suggest that the NAD(P)-RI-331 adduct is produced by the formation of an enolate at C-5 of RI-331, followed by its attack of the pyridine ring of NAD(P)<sup>+</sup>. As is the case with isoniazid inactivation of enoyl-ACP reductase (Rozwarski *et al.*, 1998), RI-331 likely attacks NAD(P)<sup>+</sup> from the same side as the substrates. Since hydride transfer arises from the *pro-S* C-4 H of NADPH, suggesting ASA is located on the *si*-face (Jacques and Wright, 1999 (Chapter 3)), then it can be concluded that attack by the RI-331 enolate also occurs from the *si*-face of NAD(P)<sup>+</sup>.

Finally, efforts were made to purify the NAD(P)-RI-331 adduct in order to clearly identify its structure. Unfortunately this complex proved to be unstable when HSD was denatured. Similarly the NADP-dihydrofinasteride adduct was unstable and decomposed easily to dihydrofinasteride (Bull *et al.*, 1996).

In conclusion, RI-331 was determined to be a mechanism-based inactivator of yeast HSD. Catalytically competent NAD(P)<sup>+</sup> is essential for RI-331 inactivation and appears to be part of the inactivating complex. The results in this paper suggest that the presence of NAD(P)<sup>+</sup> is required for the formation of a NAD(P)-RI-331 adduct. In addition, irreversible inactivation of HSD by RI-331 indicates that this is a very tight-binding compound with yeast HSD. Mechanism-based inactivators are very useful drugs since they are very specific and potent. RI-331 becomes a good model for the design of potent inhibitors of nicotinamide-dependent dehydrogenase and reductases. Similar inactivators of other fungal dehydrogenases could also prove to be excellent antifungal drugs.

## REFERENCES

- Bull, H. G., M. Garcia-Calvo, S. Andersson, W. F. Baginski, H. K. Chan, D. E. Ellsworth, R. R. Miller, R. A. Stearns, R. K. Bakshi, G. H. Rasmusson, R. L. Tolman, R. W. Myers, J. W. Kozarich and G. S. Harris (1996) Mechanism-based inhibition of human steroid 5 $\alpha$ -reductase by finasteride: Enzyme-catalysed formation of NADP-dihydrofinasteride, a potent bisubstrate analog inhibitor, *J. Am. Chem. Soc.*, **118**: 2359-2365.
- DeLaBarre, B., S. L. Jacques, C. Pratt, D. R. Ruth, G. D. Wright, and A. M. Berghuis (1998) Crystallization and preliminary X-ray diffraction studies of homoserine dehydrogenase from *Saccharomyces cerevisiae*, *Acta Cryst.*, **D54**: 413-415.
- Everse, J., E. Cooper Zoli, L. Kahan and N. O. Kaplan (1971) Addition products of diphosphopyridine nucleotides with substrates of pyridine nucleotide-linked dehydrogenases, *Org. Chem.*, **1**: 207-233.
- Georgopapadakou, N. H., and T. J. Walsh (1996) Antifungal agents: Chemotherapeutic targets and immunologic strategies, *Antimicrob. Agents Chemother.*, **40**: 279-291.
- Graybill, J. R. (1996) The future of antifungal therapy, *Clin. Infect. Dis.*, **22**: S166-S178.
- Groll, A. H., A. J. De Lucca and T. J. Walsh (1998) Emerging targets for the development of novel antifungal therapeutics, *Trends in Microbiology*, **6**: 117-124.
- Jacques, S.L., C. Pratt, G. Broadhead, R. Kinach, J. F. Honek and G. D. Wright (1999) Characterization of yeast homoserine dehydrogenase, an antifungal target (Chapter 2).
- Jacques, S. L. and G. D. Wright (1999) Homoserine dehydrogenase from *Saccharomyces cerevisiae*: Kinetic mechanism and stereochemistry (Chapter 3)
- Leatherbarrow, R. J. (1992) Grafit 3.0, Erithacus Software LTD., Staines, U.K.
- Rozwarski, D. A., G. A. Grant, D. H. R. Barton, W. R. Jacobs Jr., and J. C. Sacchettini (1998) Modification of the NADH of the isoniazid target (InhA) from *Mycobacterium tuberculosis*, *Science*, **279**: 98-102.
- Silverman, R. B. (1995) Mechanism-based enzyme inactivators, *Meth. Enzymol.*, **249**: 240- 283.
- Yamaguchi, H., K. Uchida, T. Hiratani, T. Nagate, N. Watanabe, and S. Omura (1988) RI-331, a new antifungal antibiotic, *Ann. N. Y. Acad. Sci.*, **544**: 199-190.

- Yamaki, H., M. Yamaguchi, H. Imamura, H. Suzuki, T. Nishimura, H. Saito, and H. Yamaguchi (1990) The mechanism of antifungal action of (*S*)-2-amino-4-oxo-5-hydroxypentanoic acid, RI-331: The inhibition of homoserine dehydrogenase in *Saccharomyces cerevisiae*, *Biochem. Biophys. Res. Comm.*, **168**: 837-843.
- Yamaki, H., M. Yamaguchi, T. Tsuruo, and H. Yamaguchi (1992) Mechanism of action of an antifungal antibiotic, RI-331, (*S*) 2-amino-4-oxo-5-hydroxypentanoic acid: Kinetics of inactivation of homoserine dehydrogenase from *Saccharomyces cerevisiae*, *J. Antibiotics*, **45**: 750-755.

## **CHAPTER 5**

### **Purification of Edeines and the Biosynthetic Enzymes, Tyrosine $\alpha,\beta$ -Amino Mutase and Edeine Synthetase, from *Bacillus brevis* Vm4**

## 5.1 Preface

The papers in chapters 2, 3 and 4 characterized a new antifungal target, yeast HSD, and its inactivator, RI-331, in an effort to design new specific antifungal agents inhibiting fungal amino acid biosynthesis. In this chapter, however, the biosynthesis of the natural antifungal compounds, edeines, which could also be useful in the development of new antifungal drugs, was investigated. Edeines, which are produced from *Bacillus brevis*, are linear peptides composed of several unnatural amino acids, such as  $\beta$ -tyrosine. These compounds have demonstrated antibacterial, antifungal and antiviral activities and, therefore, are of great interest. Edeines are synthesized non-ribosomally by a multienzyme complex, edeine synthetase. Although an earlier report described the biosynthesis of  $\beta$ -tyrosine by tyrosine  $\alpha,\beta$ -amino mutase; many questions remained about its chemical mechanism. Therefore, this chapter chronicles the efforts made at purifying tyrosine  $\alpha,\beta$ -amino mutase in order to fully analyze the chemical mechanism of this enzyme and its kinetic properties. Although, it was apparent that  $\beta$ -tyrosine is produced from tyrosine in *B. brevis*, tyrosine  $\alpha,\beta$ -amino mutase could not be detected. On the other hand, edeine synthetase was easily purified by previous methods.

All the experimental work presented in this chapter was performed by me, with the exception of the acquisition of the mass spectrometry data and the NMR data. Mass spectrometry results were obtained by Dr. Richard Smith at the McMaster University Regional Centre for Mass Spectrometry and the NMR data were obtained by Dr. Don Hughes at the McMaster University NMR facility.



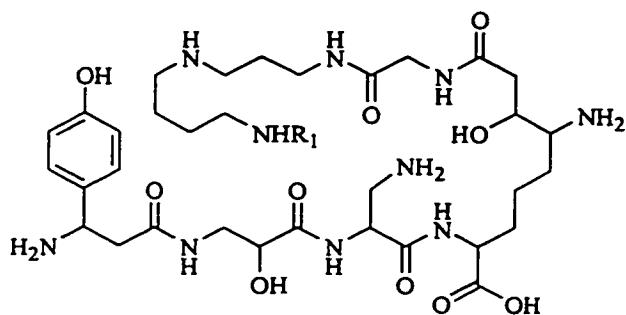
## 5.2 Introduction

Presently, bacterial and fungal infections are becoming increasingly difficult to treat as a result of the lack of potent, specific antimicrobial agents. Thus, new drugs attacking new bacterial and fungal targets need to be discovered. Edeines (Figure 1), which are linear peptides produced by *Bacillus brevis* Vm4, are interesting compounds since they demonstrate various activities such as antibacterial, antifungal and antiviral (Kurylo-Borowska, 1962; Lacal *et al.*, 1980). Their mode of action is two-fold. Low concentrations of edeines ( $10^{-6}$  M) cause inhibition of DNA synthesis, whereas concentrations 100-fold higher also result in inhibition of protein synthesis (Kurylo-Borowska and Szer, 1972). Edeines were discovered to have affinity for the P-site (peptidyl-t-RNA site) on ribosomes and, therefore, block the binding of the initiator aminoacyl-t-RNA (Kurylo-Borowska and Szer, 1972; Woodstock *et al.*, 1991).

Edeine A is composed of spermidine, glycine and 2,3-diaminopropionic acid, as well as unique amino acids such as isoserine,  $\beta$ -tyrosine and 2,6-diamino-7-hydroxyazaleic acid (Hettinger and Craig, 1968). Other edeines also exist, such as edeine B which contains guanylspermidine instead of spermidine (Figure 1) (Hettinger *et al.*, 1968). Investigation into the biosynthesis of edeines and of the unique amino acid constituents may lead to the design of new effective antibacterial and antifungal drugs.

Tyrosine  $\alpha,\beta$ -amino mutase (75 kD), the enzyme which converts *L*-tyrosine to  $\beta$ -tyrosine, was previously purified from *B. brevis* Vm4 by ammonium sulfate precipitation,

**Figure 1. Structure of edeines**



Edeine	$\text{R}_1$
A	-H
B	$-\text{C}(=\text{NH})\text{NH}_2$

Sephadex G200 chromatography and isoelectric focusing (Kurylo-Borowska and Abramsky, 1972). The only cofactor required for tyrosine  $\alpha,\beta$ -amino mutase activity was ATP<sup>1</sup>, which suggests that this enzyme has a mechanism distinct from other amino acid mutases.

Tyrosine  $\alpha,\beta$ -amino mutase activity is inhibited by carbonyl binding agents and  $\alpha$ -keto acids, suggesting the formation of a Schiff's base between the abstracted amino group and an active site residue (Kurylo-Borowska and Abramsky, 1972). Studies with [<sup>15</sup>N]-tyrosine revealed that only 10 % of the  $\beta$ -amino group originated from the  $\alpha$ -position. The source for the  $\beta$ -amino group was possibly NH<sub>4</sub>Cl since it caused activation of tyrosine  $\alpha,\beta$ -amino mutase activity (Kurylo-Borowska and Abramsky, 1972). However, no further evidence of this has been reported. Lysine 2,3-aminomutase requires pyridoxal phosphate, iron and S-adenosyl methionine (SAM) for activity, whereas leucine 2,3-aminomutase is adenosylcobalamin-dependent (B<sub>12</sub>) (Chirpich *et al.*, 1970; Poston and Hemmings, 1979). Other enzymes which remove ammonia groups from amino acids (without readdition of NH<sub>3</sub> to the molecule), such as phenylalanine ammonia lyase and tyrosine ammonia lyase, make use of the electrophilic group dehydroalanine (Hanson and Havir, 1970). Catalysis by tyrosine  $\alpha,\beta$ -amino mutase, however, resulted in  $\alpha$ -hydrogen exchange, which does not occur with phenylalanine ammonia lyase (Parry and Kurylo-Borowska, 1980).

As a result, investigation of the source of the  $\beta$ -amino group, as well as the fate of the  $\alpha$ -amino group, is necessary. Since the participation of ATP in a mutase reaction

is unusual, it is important to understanding the role ATP plays in the mechanism of tyrosine  $\alpha,\beta$ -amino mutase. The purpose of this project was, therefore, to purify and study tyrosine  $\alpha,\beta$ -amino mutase in order to obtain a greater understanding of its chemical mechanism.

**Footnotes**

<sup>1</sup>Abbreviations: ATP, adenosine triphosphate; DTT, dithiothreitol; FAD, flavin adenine dinucleotide; FMN, flavin mononucleotide; HEPES, N-[2-hydroxyethyl]piperazine-N'-[2-ethanesulfonic acid]; HPLC, high performance liquid chromatography; NAD<sup>+</sup>, nicotinamide adenine dinucleotide; PLP, pyridoxal phosphate; PMSF, phenylmethanesulfonyl fluoride; Tris, *tris*(hydroxymethyl)-aminomethane; SAM, S-adenosyl methionine; TLC, thin layer chromatography.

## 5.3 Materials and methods

### 5.3.1 Materials

#### *Chemicals*

Adenosylcobalamin (B<sub>12</sub>), ATP, bovine serum albumin, *N*-bromosuccinamide, chloramphenicol, cobalt chloride, cupric acetate, 2,3-diaminopropionic acid, FAD, ferric chloride, ferrous ammonium sulfate, FMN, *N*-[2-hydroxyethyl]piperazine-*N'*-[2-ethanesulfonic acid] (HEPES), 8-hydroxyquinoline, inorganic pyrophosphatase, pyridoxal phosphate, reduced glutathione, spermidine, sodium dithionite, sodium fluoride, sodium dihydrogen pyrophosphate and the amino acids (except for glycine and  $\beta$ -tyrosine) were obtained from Sigma (St. Louis, MO). DNase I, isotridecyl-poly(ethylene-glycolether)<sub>n</sub>, lysozyme, NAD<sup>+</sup> and Tris were purchased from Boehringer Mannheim (Laval, PQ). Glycine was obtained from Bioshop Canada (Burlington, ON) and magnesium acetate from Fisher Scientific (Fairlawn, NJ). [<sup>14</sup>C]-Tyrosine (0.45 Ci/mmol, 0.1 mCi/mL), [<sup>14</sup>C]-serine (0.17 Ci/mmol, 0.1 mCi/mL) and [<sup>32</sup>P]-sodium pyrophosphate (33 Ci/mmol, 10 mCi/mL) were purchased from NEN DuPont (Wilmington, DE).  $\beta$ -Tyrosine was prepared by Dr. G. Wright according to the method of Rodionov *et al.*, 1958 [<sup>1</sup>H-NMR (NaOD/D<sub>2</sub>O)  $\delta$  6.90 (d, 2H, J = 8 Hz), 6.38 (d, 2H, J = 8 Hz), 3.90 (t, 1H, J = 7 Hz), 2.30 (d, 2H, J = 7 Hz)]. S-adenosyl methionine was a generous gift from Dr. J. Honek, University of Waterloo.

### *Media*

PY medium was composed of 1 % peptone, 0.5 % yeast extract, 0.5 % NaCl, 50  $\mu\text{g/mL}$   $\text{MgCl}_2$  and 30  $\mu\text{g/mL}$   $\text{MnCl}_2$  adjusted to pH 7.2. M9 minimal medium was composed of 0.75 % NaCl, 0.2 % glucose, 1.64 mg/mL  $\text{KH}_2\text{PO}_4$ , 4.1 mg/mL *L*-glutamic acid, 0.91 mg/mL glycine, 60  $\mu\text{g/mL}$   $\text{MgSO}_4$ , 6  $\mu\text{g/mL}$   $\text{MnCl}_2$ , 25  $\mu\text{g/mL}$   $\text{FeSO}_4$ , 19  $\mu\text{g/mL}$   $\text{ZnCl}_2$  and 1.9  $\mu\text{g/mL}$  cupric acetate adjusted to pH 7.4 .

### *5.3.2 Methods*

#### *Bacillus brevis* growth

*Bacillus brevis* Vm4 was grown in PY medium or M9 minimal medium at 30°C with 250 rpm agitation.

#### *Purification of edeines*

The purification protocol of edeines from *B. brevis* cultures is a modification of the procedure from Kurylo-Borowska and Heany-Kieras, 1983. AG50W-X8 resin ( $\text{H}^+$  form, 100-200 mesh; BioRad) (40 g/L) was added to 4 L spent PY medium supernatant from a *B. brevis* culture and stirred for 30 minutes at 4°C. The exchange resin was filtered from the supernatant and washed with 1 L distilled water. The pH was adjusted to 7.0 by the addition of 1 M potassium hydrogen phosphate ( $\text{K}_2\text{HPO}_4$ ) and the resin was filtered and washed with 5 L distilled water until the wash had no absorbance at 272 nm. The resuspended resin was poured into a column (2.5 cm dia., 37 cm high) and the



edeines were eluted with a 400 mL 0-0.5 M ammonium hydroxide gradient. Edeines were found to elute at around 0.15 M ammonium hydroxide. Fractions (2.5 mL) were collected and absorbance was determined at 272 nm to detect the presence of edeines. Fractions were pooled and lyophilized (approximately 2 g light brown material).

Dry material was dissolved in 2 mL distilled water (1 g/mL) and applied in 0.5 mL aliquots to a Sephadex G25 column (1.5 cm dia., 85 cm high; Pharmacia) using distilled water as the mobile phase (1.5 mL/min) and 2.5 mL fractions were collected. The fractions from the first peak which contained antibacterial activity were combined and lyophilized to produce a total of 220 mg of light brown material.

The solid product was dissolved in distilled water, 50  $\mu$ L (0.2 mg/mL), injected onto a Mono S column (HR 5/5, Pharmacia) and washed with 5 mL distilled water before eluting with an 0-0.5 M ammonium formate gradient over 25 mL followed by a 0.5-1.0 M ammonium formate gradient over 5 mL with a flow rate of 1 mL/min. The elution of edeines was monitored by absorbance at 280 nm and 1 mL fractions were collected. Two peaks were pooled separately and lyophilized to a clear film.

Further purification for NMR and mass spectrometry was performed by reverse phase high performance liquid chromatography (HPLC). Samples (10  $\mu$ L) were injected onto a reverse phase column (CSC, Spherisorb ODS2, 250 x 4.6 mm) equilibrated in 0.1% TFA. Edeines were eluted at a flow rate of 0.5 mL/min using an acetonitrile (0.06% TFA) gradient: 0-30% over 25 minutes, 30% for 5 minutes and 30-100% over 5 minutes. Absorbance was monitored at 214 and 272 nm and 0.5 mL fractions were

collected. Approximately 5 mg of edeine A or edeine B was purified from 4 L of spent media.

*Susceptibility assays on Bacillus subtilis*

An overnight *B. subtilis* culture was diluted two-fold in PY medium and 70  $\mu\text{L}$  was spread onto a M9 minimal medium agar plate. Sterile filter disks were placed aseptically on the solid medium and a 15  $\mu\text{L}$  sample was added to each disk. Plates were then incubated overnight at 37°C. The zone of growth inhibition was measured directly from the agar plate and is defined as the distance in mm between the edge of the filter disk and the outer edge of the area free from bacterial growth.

*Sagakuchi reaction for detection of the guanadinium group*

Purified edeine (30  $\mu\text{L}$ ) was diluted to 0.5 mL, 1 mL reagent I (0.02% 8-hydroxyquinoline in 3N NaOH) was added and the mixture was incubated at ambient temperature for three minutes. Subsequently, 0.5 mL 0.1% *N*-bromosuccinimide in distilled water was added and the absorbance at 500 nm was determined in the following 5-30 minutes. *L*-Arginine (0.1 mM in 0.5 mL) was used as a positive control.

*NMR and mass spectrometry analyses of edeine*

$^1\text{H}$ -NMR and correlated spectroscopy- $^1\text{H}$ -NMR analyses were performed with pure edeine A dissolved in  $\text{D}_2\text{O}$  (Cambridge Isotopes, Andover, MA) on a 500 MHz Bruker instrument by Don Hughes at the McMaster University NMR facility.

The molecular mass of edeines A and B were determined by electrospray mass spectrometry on a Fisons platform quadrupole instrument using CH<sub>3</sub>CN/H<sub>2</sub>O (1:1) with 0.4 % trifluoroacetic acid as a solvent by Dr. Richard Smith at the McMaster University Mass Spectrometry facility.

#### *Hydrolysis of edeine A and B*

Approximately 2 mg of edeine A or edeine B obtained from Mono S chromatography were dissolved in 200 µL of fresh 6 N HCl. Each solution was sealed in a glass tube under a vacuum and placed at 110°C for 17 hours. Samples were then evaporated to dryness before being analyzed by 2D thin layer chromatography and reverse phase HPLC (same HPLC conditions as for the tyrosine α,β-amino mutase activity assay described below).

#### *2D thin layer chromatography*

Hydrolyzed edeine samples were dissolved in 40 µL distilled water and 5 µL was spotted on the corner of a 20x20 cm silica plate. The silica plate was developed with solvent system I (butanol-acetic acid-water (60:20:30)), air dried and then developed in solvent system II (butanol-acetic acid-water-pyridine (60:30:50:20)) (Roncari *et al.*, 1966). Spots were visualized by UV light and by spraying with 0.1% ninhydrin in ethanol and developing with a heat gun. Glycine, isoserine, spermidine, β-tyrosine and 2,3-diaminopropionic acid (10 µL of 1 mg/mL solution) were also chromatographed as standards.

### *Production of [<sup>14</sup>C]-labeled edeines*

PY medium (5 mL) was inoculated with 50  $\mu$ L saturated *B. Brevis* Vm4 culture and grown for 6 hours at 30 °C. Chloramphenicol (17  $\mu$ L of 30 mg/mL) was then added to the culture to inhibit ribosomal peptide synthesis, followed by 50  $\mu$ L 25 mM [<sup>14</sup>C]-labeled tyrosine or [<sup>14</sup>C]-labeled serine (ethanol solution) (1.25  $\mu$ Ci). The culture was incubated at 30°C for 18 hours.

Edeine was partially purified by passing the supernatants from the above cultures through an AG50W-X8 column (1.75 cm dia., 15 cm high). After the sample was applied, 100 mL distilled water was added to wash impurities from the column. Edeines were then eluted with 0.3 M ammonium hydroxide. Fractions were collected and edeines were detected by spotting on filter paper and spraying with 0.1% ninhydrin. Fractions were also assessed for [<sup>14</sup>C]-radiolabel by adding scintillation fluid to 1 mL fraction and counting in a liquid scintillation counter. Samples were analyzed by reverse-phase HPLC (same HPLC conditions as for tyrosine  $\alpha,\beta$ -amino mutase activity described below).

### *Purification of biosynthetic enzymes*

Unless otherwise specified, all purification steps were carried out at 4°C. *Bacillus brevis* Vm4 was grown in PY medium for 5 to 22 hours at 30°C. The cells were then harvested by centrifugation at 5000 x g for 15 minutes and washed with ice-cold 0.85 % NaCl or 50 mM Tris (or HEPES), pH 7.6 and 1 mM  $\beta$ -mercaptoethanol.

### i) Cell lysis

The resulting cell pellet was lysed by several methods. For cell lysis using French press, the pellet was resuspended in lysis buffer (2 mL/g pellet) (50 mM Tris, pH 7.6, 1 mM EDTA, 100 mM NaCl, 0.1 mM dithiotreitol (DTT), 1 mM phenylmethylsulfonyl fluoride (PMSF)) followed by four passages through a French pressure cell at 20 000 psi. Alternatively, the cell pellet was treated with 1 mg/mL lysozyme in 50 mM Tris (or HEPES), pH 7.6, 25 % sucrose, 1 mM DTT, 1mM EDTA (1-2 mL/g pellet) for 1 hour at 0°C, PMSF was added to 1 mM and the mixture was passed through a French pressure cell three times. Occasionally, 1 mg DNase I was added after lysis by French press and incubated for 15 minutes at 30°C.

For cell lysis by osmotic shock, the washed pellet (4.3 g) was resuspended in 10 mL cold 25 mM Tris, pH 7.6, 5 % sucrose, 1 mM DTT, 1 mM EDTA, 0.3 mg/mL lysozyme and 0.1 % isotridecyl-poly(ethylene-glycolether)<sub>n</sub> and incubated for 1 hour at 0°C with occasional mixing. Osmotic shock was initiated with the addition of 100 mL ice-cold 10 mM MgSO<sub>4</sub>, 1 mM DTT and 1 mg DNase I. The mixture was then incubated at 30°C for 15 minutes with agitation.

For cell lysis by alumina grinding, the washed pellet (2.3 g) was ground with 0.5 g alumina in liquid nitrogen. The frozen powder was then added to 5 mL cold 50 mM Tris, pH 7.6, 1 mM β-mercaptoethanol and vortexed.

For cell lysis by bead mill (Biospec Bead Beater), the washed pellet (100-200 g) was resuspended in 500 mL cold buffer (50 mM Tris, pH 7.6, 1 mM β-mercaptoethanol) and added to the bead mill container with approximately 150 mL glass beads. Extra

buffer was then added to fill the container. Cells were lysed by 15 on/off cycles (30 seconds on, 1 minute off) of the bead mill at 0°C.

Once *B. brevis* cells were lysed, cell debris was removed by centrifugation at 10 000 x g for 20 minutes. When cells were lysed by bead mill, the glass beads were first collected by centrifugation at 5000 x g for 15 minutes, followed by centrifugation of the supernatant to remove cell debris. The crude lysate was then assayed for enzyme activity or used in subsequent purification steps.

#### ii) Chromatography

Purification of tyrosine  $\alpha,\beta$ -amino mutase was attempted by anion exchange chromatography on a DEAE-Sepharose column. DNase I treated crude lysate (approximately 5 mg) was applied onto DEAE-Sepharose Fast Flow (1 cm dia., 11 cm height; Pharmacia) equilibrated with 50 mM HEPES, pH 7.5, 1 mM EDTA and 0.1 mM DTT. The column was washed for 13 minutes at a flow rate of 1 mL/min and then protein was eluted with a 0-0.5 M NaCl gradient over 30 minutes. The gradient was then increased to 1 M over 10 minutes and the column was washed with 1 M NaCl for 10 minutes. Proteins were detected by absorbance at 280 nm and 1 mL fractions were collected. Fractions were then assayed for tyrosine  $\alpha,\beta$ -amino mutase activity.

#### iii) Ammonium sulfate fractionation

For fractionation by ammonium sulfate precipitation, fine ammonium sulfate powder was added slowly with continuous stirring to the cell lysate to 25 % saturation. After 30 minutes, the precipitate was collected by centrifugation at 10 000 x g for 20 minutes. Ammonium sulfate was then added to the supernatant to 55 % saturation as

previously and the precipitate collected. The two precipitate pellets were dissolved in 100 mM Tris, pH 7.6 and dialyzed along with the high salt supernatant against 50 mM Tris, pH 7.6, 1 mM  $\beta$ -mercaptoethanol. When *B. brevis* was lysed in the presence of DTT, EDTA and NaCl, the ammonium sulfate pellets were dialyzed in 50 mM Tris, pH 7.6, 0.1 mM DTT and 1 mM EDTA.

Proteins found in the 25-55 % ammonium sulfate fraction were further purified by size exclusion chromatography or by anion exchange chromatography. The dialyzed protein fraction (15 mL, approx. 200 mg) was applied onto a Sephadex G100 column (2.5 cm dia., 117 cm height; Pharmacia) and eluted with 50 mM Tris, pH 7.6, 1 mM  $\beta$ -mercaptoethanol at 1 mL/min. Proteins were detected by absorbance at 280 nm and 8 mL fractions were collected. Fractions were assayed for tyrosine  $\alpha,\beta$ -amino mutase activity and isoserine-dependent ATP- $^{32}$ PP<sub>i</sub> exchange activity.

Alternatively, 30 mL dialyzed 25-55 % ammonium sulfate fraction (approx. 400 mg) was injected onto a DEAE-Sepharose Fast Flow column (1 cm dia., 11 cm height; Pharmacia) equilibrated with 100 mM Tris, pH 7.6, 2 mM DTT. After washing the column with buffer for 48 minutes, proteins were eluted stepwise with 0.3 and 1 M KCl in buffer at 4 mL/min. Proteins were detected by absorbance at 280 nm and 1.5 mL fractions were collected. Fractions were assayed for tyrosine  $\alpha,\beta$ -amino mutase activity and isoserine-dependent ATP- $^{32}$ PP<sub>i</sub> exchange activity.

#### iv) Protein extraction of cell debris pellets

Cell debris pellets produced from cell lysis by French press or alumina grinding were extracted with 50 mM Tris, pH 7.6, 500 mM KCl, 1 mM  $\beta$ -mercaptoethanol to

remove loosely associated proteins and centrifuged at 10 000 x g for 30 minutes. These extracts, as well as the pellets resuspended in 50 mM Tris, pH 7.6, 1 mM  $\beta$ -mercaptoethanol, were assayed for tyrosine  $\alpha,\beta$ -amino mutase activity.

v) Modified purification protocol from Chirpich *et al.*, 1970

A modification of the lysine 2,3-aminomutase purification and assay was also attempted (Chirpich *et al.*, 1970). All steps were performed with minimal exposure to air oxygen by keeping all solutions sealed under argon. The harvested cells were washed with cold degassed 30 mM Tris, pH 7.6, 1 mM DTT, and 0.01 mM pyridoxal phosphate (PLP). The cell pellet was resuspended in cold degassed buffer (1-2 mL/g pellet) (25 mM Tris, pH 7.6, 25 % sucrose, 1 mM EDTA, 10 mM DTT and 0.1 mM PLP) and treated with lysozyme (1 mg/mL) for 1 hour at 0°C. PMSF (1 mM) was then added and the mixture was passed three times through the French pressure cell. After centrifugation at 10 000 x g for 20 minutes, the supernatant was activated and assayed as described below.

*Tyrosine  $\alpha,\beta$ -amino mutase assay*

Crude lysate or partially purified protein (0.1-1 mg) was added to assay mixtures containing 50 mM Tris or HEPES, pH 8.8, 40 mM  $MgCl_2$ , 10 mM ATP, 0.2 mM  $NH_4Cl$ , 0.4 mM [ $^{14}C$ ]-tyrosine (or 1 mM [ $^{14}C$ ]-serine to assay serine amino mutase) (0.034  $\mu Ci$ ) in a total volume of 100  $\mu L$  and incubated at 30°C for 2 hours. Assay mixtures were then analyzed immediately for  $\beta$ -tyrosine or placed at -20°C until analyses were performed. The formation of  $\beta$ -tyrosine was measured by reverse-phase HPLC or paper electrophoresis. Protein samples boiled for 5 minutes were used as negative controls.



In order to test the effect of certain metals, cofactors and reducing agents on tyrosine  $\alpha,\beta$ -amino mutase activity, 5 mM  $\text{CoCl}_2$ , 5 mM cupric acetate, 5 mM  $\text{FeCl}_3$ , + 10 mM sodium dithionite, 5  $\mu\text{M}$  adenosylcobalamin ( $\text{B}_{12}$ ), 0.1 mM FAD + 0.1 mM FMN + 1 mM  $\text{NAD}^+$ , 1 mM PLP, 100  $\mu\text{M}$  S-adenosyl methionine (SAM), 10 mM DTT were added separately to the above assays before the reaction was started by the addition of protein solution.

The activation and assay protocol used for lysine 2,3-amino mutase (Chirpich *et al.*, 1970) was attempted in order to detect tyrosine  $\alpha,\beta$ -amino mutase activity. Under an argon atmosphere, crude lysate (0.8 mg) was activated in 42 mM Tris, pH 8.8, with freshly made 50  $\mu\text{M}$  PLP, 12.5 mM reduced glutathione, 1 mM  $\text{Fe}(\text{NH}_4)_2(\text{SO}_4)_2$ , and 1 mM sodium dithionite in a total volume of 120  $\mu\text{L}$ . The mixture was incubated at 37 °C for 1 hour and added to assays. The assays were performed as previously with the following changes: 25 mM Tris, pH 8.8, addition of 3.8  $\mu\text{M}$  SAM and 1 mM sodium dithionite and assays were kept sealed under argon.

#### *Separation of tyrosine and $\beta$ -tyrosine*

When assay mixtures were analyzed by HPLC, 20  $\mu\text{L}$  samples were injected onto a reverse-phase HPLC column (BioSil C18 HL 90-5S, 250 x 4.6 mm, BioRad) and run isocratically with 5 % acetonitrile, 0.1 % trifluoroacetic acid at a flow rate of 1 mL/min. The detector was set at 280 nm and 1 mL fractions were collected for liquid scintillation counting (retention time for  $\beta$ -tyrosine, 10 minutes; for tyrosine, 14 minutes).

To analyze assay mixtures by paper electrophoresis, a 2  $\mu\text{L}$  sample was spotted, along with standards (1  $\mu\text{L}$  each of a 1 mg/mL solution), onto a wetted 5.5 x 15 cm Whatman 3MM paper with ends immersed in formic acid/acetic acid/water (1:4:45) (pH 2). Samples were placed across an electric field at 200 V, 5 mA for 45 minutes and migrated towards the anode (migration distance for  $\beta$ -tyrosine, 4.8 cm; for tyrosine, 3.6 cm; for isoserine, 5.8 cm; for serine, 4.2 cm). The dried paper was sprayed with 0.1 % ninhydrin in ethanol and spots were developed with a heat gun.  $\beta$ -Tyrosine and isoserine produced yellow spots, while tyrosine and serine produced purple spots. The paper was also exposed to film to visualize radiolabeled spots.

*Isoserine-dependent ATP-<sup>32</sup>PP<sub>i</sub> exchange assay*

Partially purified protein (>100  $\mu\text{g}$ ) was added to assays (total volume 250  $\mu\text{L}$ ) containing 80 mM Tris, pH 8.0, 0.02 mM EDTA, 4 mM magnesium acetate, 1 mM DTT, 2 mM ATP, 1 mM NaF, 1 mM *D,L*-isoserine, 80  $\mu\text{g/mL}$  bovine serum albumin, 4 mM  $\text{Na}_2\text{H}_2\text{P}_2\text{O}_7$ , and 0.09  $\mu\text{Ci/assay}$   $\text{Na}_4^{32}\text{P}_2\text{O}_7$ , and incubated at 35°C for 30 minutes (Kurylo Borowska and Sedkowska, 1974). The reaction was terminated by the addition of 100  $\mu\text{L}$  0.35 M  $\text{Na}_2\text{H}_2\text{P}_2\text{O}_7$ , 10.5 % perchloric acid and 3 % (w/v) charcoal. Charcoal was collected on 2.5 cm glass filter disks (Whatman GF-C), washed with 30 mL distilled water and counted in a liquid scintillation counter.

### *Labeling of edeine synthetase with [<sup>14</sup>C]-tyrosine*

An attempt was made to label edeine synthetase by adding ammonium sulfate precipitation purified protein (0.8 mg) to an assay containing 50 mM Tris, pH 8.8, 40 mM MgCl<sub>2</sub>, 1 mM DTT, 0.2 mM NH<sub>4</sub>Cl, 10 mM ATP, 0.4 mM <sup>14</sup>C-tyrosine (0.034 μCi) and inorganic pyrophosphatase (0.5 μL, approximately 1U) in 100 μL total volume. Assays were incubated at 30°C and stopped at 0, 15, 30 and 60 minutes by the addition of 100 μL 2X SDS-PAGE loading buffer. Proteins in the assays (20 μL) were separated on a 9 % SDS-polyacrilamide gel. The gel was stained with Coomassie brilliant blue, soaked in Entensify radiolabel intensifying solution(NEN DuPont, Boston, MA), dried and exposed to film.

### *Preparation of B. brevis protein electroblot for N-terminal sequencing*

Crude lysate (approximately 18 μg) prepared from *B. brevis* was loaded onto a 9 % SDS polyacrylamide gel and separated. Proteins were electroblotted onto a PVDF membrane in 25 mM ethanolamine, 25 mM glycine and 15 % methanol overnight at 30 V and 4 °C. Proteins on the membrane were detected by Ponceau S stain and analyzed by N-terminal sequencing on a Porton Gas-phase Microsequencer, model 2090, with online PTH analysis by T. S. Chen at the peptide sequence analysis facility of the University of Toronto.

## 5.4 Results

### 5.4.1 Production of edeines from *Bacillus brevis*

Saturation of *Bacillus brevis* Vm4 growth was reached at approximately 8 hours (Figure 2). Edeines production was confirmed by susceptibility assays on *B. subtilis* and occurred during early stationary phase, between 10-12 hours growth. Peptone appears to be an essential nutrient for edeine production as shown in Table 1. No edeines were produced in media lacking peptone. Growth was greatly reduced in M9 minimal media unless peptone and/or yeast extract was added.

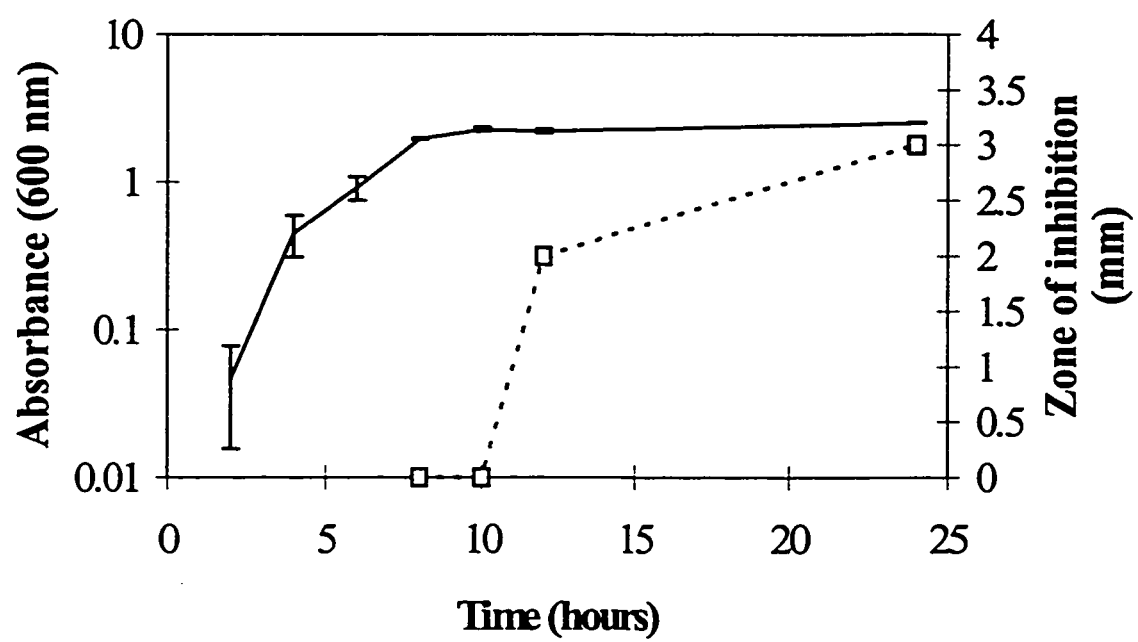
**Table 1. Minimal media requirements for production of edeines.**

Media	Added Nutrients	Growth ( $A_{600}$ )	Zone of Inhibition (mm)
M9 minimal	—	0.8 <sup>b</sup>	0
M9 minimal	1% peptone	> 2	1.5
M9 minimal	0.5% yeast extract	> 2	0
M9 minimal	1% peptone + 0.5% yeast extract	> 2	9
M9 minimal	0.3 mg/mL tyrosine + serine + DAPA <sup>a</sup>	0.5 <sup>b</sup>	0
M9 minimal	0.3 mg/mL $\beta$ -tyrosine + serine + DAPA <sup>a</sup>	0.2 <sup>b</sup>	0
M9 minimal	0.3 mg/mL $\beta$ -tyrosine	0	—
M9 minimal	0.3 mg/mL isoserine	0.3 <sup>b</sup>	0
M9 minimal	0.3 mg/mL DAPA <sup>a</sup>	0.8 <sup>b</sup>	0
PY	—	> 2	4.5

<sup>a</sup> -2,3-diaminopropionic acid

<sup>b</sup> -after 3 days of growth

**Figure 2. Growth curve for *Bacillus brevis* and production of edeines.** *B. brevis* was grown in PY media at 30°C and samples were removed at indicated times for absorbance readings and supernatants were tested for edeine by susceptibility assay on *B. subtilis*. The full line represents absorbance and the broken line and open squares represent zone of inhibition. Error bars represent the variation between 2 experiments.



#### 5.4.2 Purification and characterization of edeines A and B

Purification of edeines from *Bacillus brevis* spent PY media was achieved by batch adsorption on AG50W-X8 anion exchange resin, size exclusion chromatography, Mono S cation exchange chromatography and reverse-phase HPLC. Spent medium was mixed with AG50W-X8 resin and edeines were eluted using an ammonium hydroxide gradient. Edeines were eluted at approximately 0.15 M  $\text{NH}_4\text{OH}$ . Purification by a Sephadex G25 size exclusion column produced three fractions (Figure 3), the first of which demonstrated antibiotic activity measured by susceptibility assays (Peak 1). The next step consisting of Mono S chromatography using an ammonium formate gradient produced two peaks with antibiotic activity (Figure 4). As edeines can contain either spermidine (edeine A) or guanylspermidine (edeine B), the presence of a guanidinium group was measured using the Sakaguchi reaction. A positive test, such as with arginine, results in the development of a red-orange color. Only peak B from Mono S chromatography resulted in a positive reaction. Therefore, peaks A and B correspond to edeine A and edeine B, respectively. Further purification of each edeine was accomplished by reverse-phase HPLC with an acetonitrile gradient (Figure 5). Edeine A eluted with a retention time of 17.5 minutes, whereas edeine B eluted at 19 minutes.

**Figure 3. Purification of edeines from spent media by Sephadex G25 size exclusion chromatography.** A concentrated edeines sample eluted from AG50W-X8 resin was applied onto a Sephadex G25 column (1.5 cm dia., 85 cm height; Pharmacia) and eluted with distilled water. Antimicrobial activity was found only in peak #1.



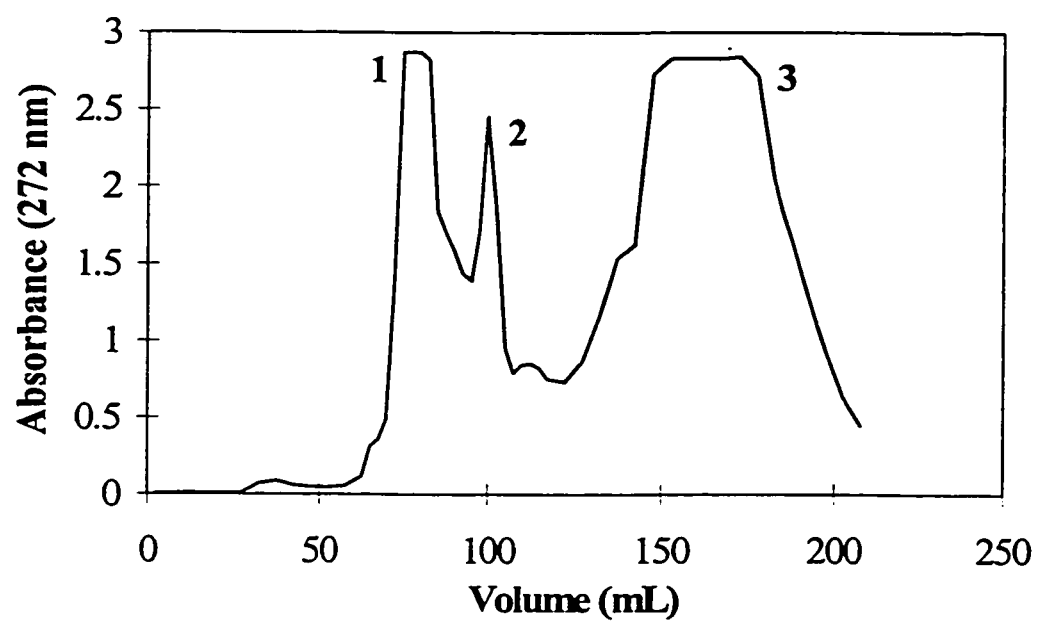


**Figure 4. Purification of edeines by Mono S cation exchange chromatography.**

Lyophilized material from Sephadex G25 column was dissolved and applied onto a Mono S column (HR 5/5, Pharmacia) and edeines were eluted with ammonium formate. Peaks A and B were determined to be edeine A and edeine B, respectively, by Sakaguchi reaction.

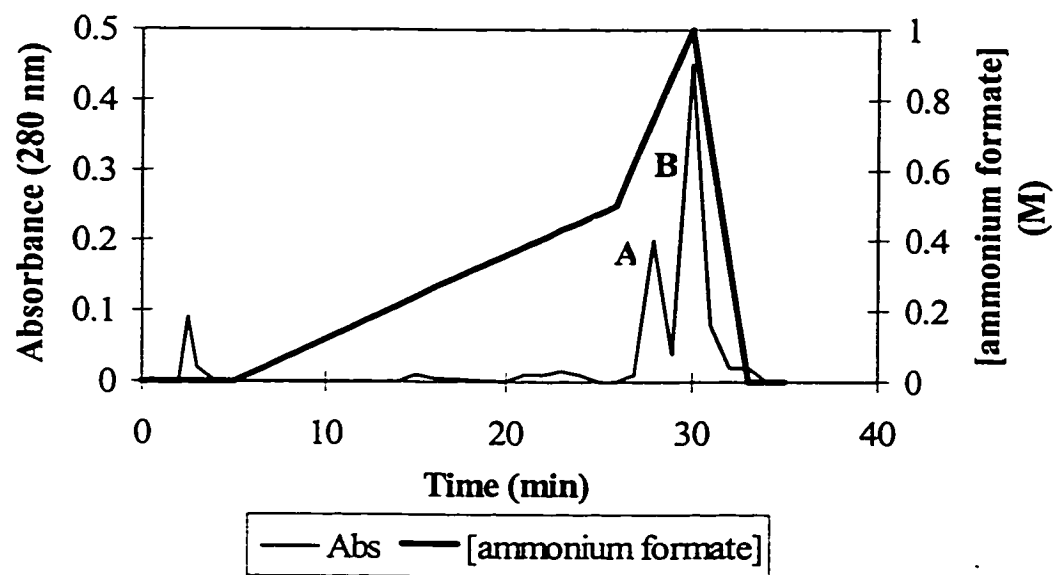
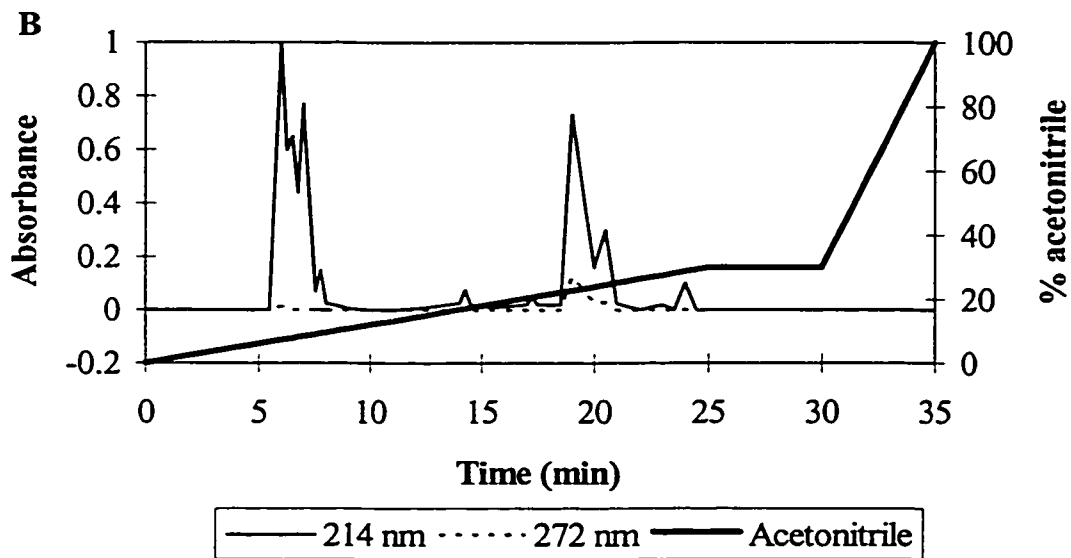
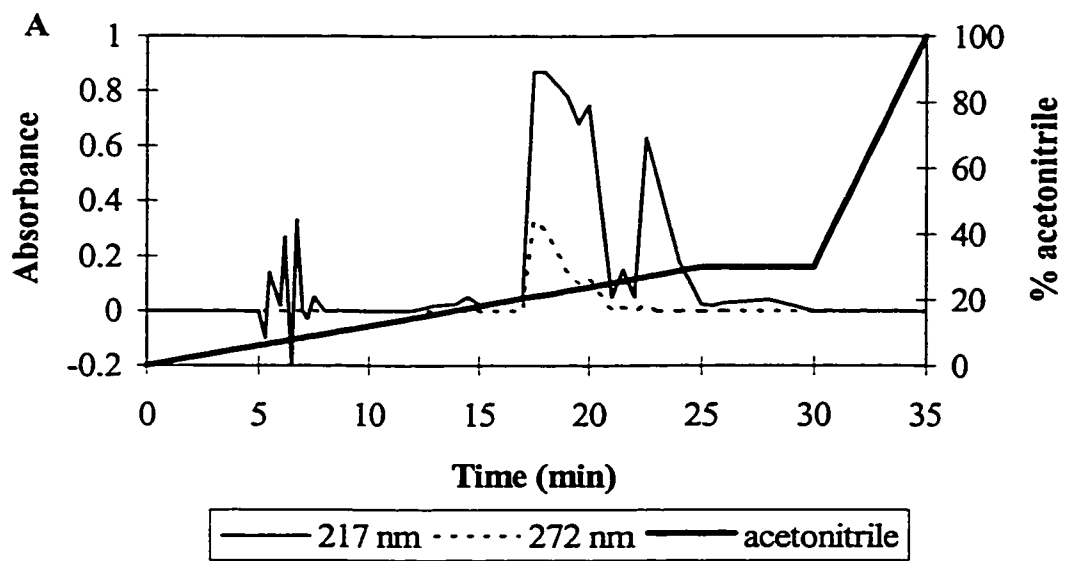


**Figure 5. Purification of edeines A and B by reverse-phase HPLC.** (A) Edeine A or (B) edeine B were further purified on a reverse-phase column (CSC, Spherisorb ODS2, 250 x 4.6 mm) using an acetonitrile gradient. Absorbance was monitored at both 214 and 272 nm. Retention times: 17.5 minutes, edeine A; 19 minutes, edeine B.



Molecular masses of purified edeine A and B were determined by electrospray mass spectrometry and experimental values are shown to be in agreement with expected molecular weights of 755.4 and 797.4 g/mol, respectively (Table 2). Edeine B also produced several additional peaks, likely due to impurities. Furthermore,  $^1\text{H-NMR}$  and Correlated spectroscopy- $^1\text{H-NMR}$  analyses of purified edeine A revealed aromatic protons ( $\delta = 6.8$  and  $7.2$  ppm) belonging to  $\beta$ -tyrosine (Figure 6 and 7). These resonances are different from the standard  $\beta$ -tyrosine due to the use of different solvents ( $\text{D}_2\text{O}$  vs  $\text{NaOD}$ ).

**Table 2. Electrospray mass spectrometry analysis of purified edeines.**

Compound	Mass (m/z)	Relative Intensity (%)
Background	429.1	15
	577.3	100
	594.1	7.5
Edeine A	429.3	14
	577.2	100
	578.2	38
	592.3	31
	755.4*	46
	756.5	22
Edeine B	460.0	64
	475.4	22
	494.4	27
	551.3	53
	577.3	100
	595.4	21
	634.2	69
	684.4	43
	729.0	23
	797.4*	36

Values with \* are equal to expected molecular masses.

**Figure 6.  $^1\text{H-NMR}$  analysis of edeine A.** Edeine A, purified by reverse-phase HPLC, was dissolved in  $\text{D}_2\text{O}$  and analysed on a 500 MHz Bruker instrument by Dr. Don Hughes at the McMaster University NMR facility.



WRIGHTED.001  
 AU PROG:  
 PRESAT .AU  
 DATE 17-8-94

SF 500.137  
 SY 83.0  
 O1 8788.739  
 SI 32768  
 TD 16384  
 SH 3472.222  
 HZ/PT .212

PH 9.4  
 RD 0.0  
 AQ 2.359  
 RG 40  
 NS 88  
 TE 297

FW 4400  
 O2 9031.049  
 DP 26L P0

LB -1.500  
 GB .200  
 CX 25.00  
 CY 0.0  
 F1 7.591P  
 F2 .649P  
 HZ/CM 118.880  
 PHM/CM .278  
 SF 6770.42

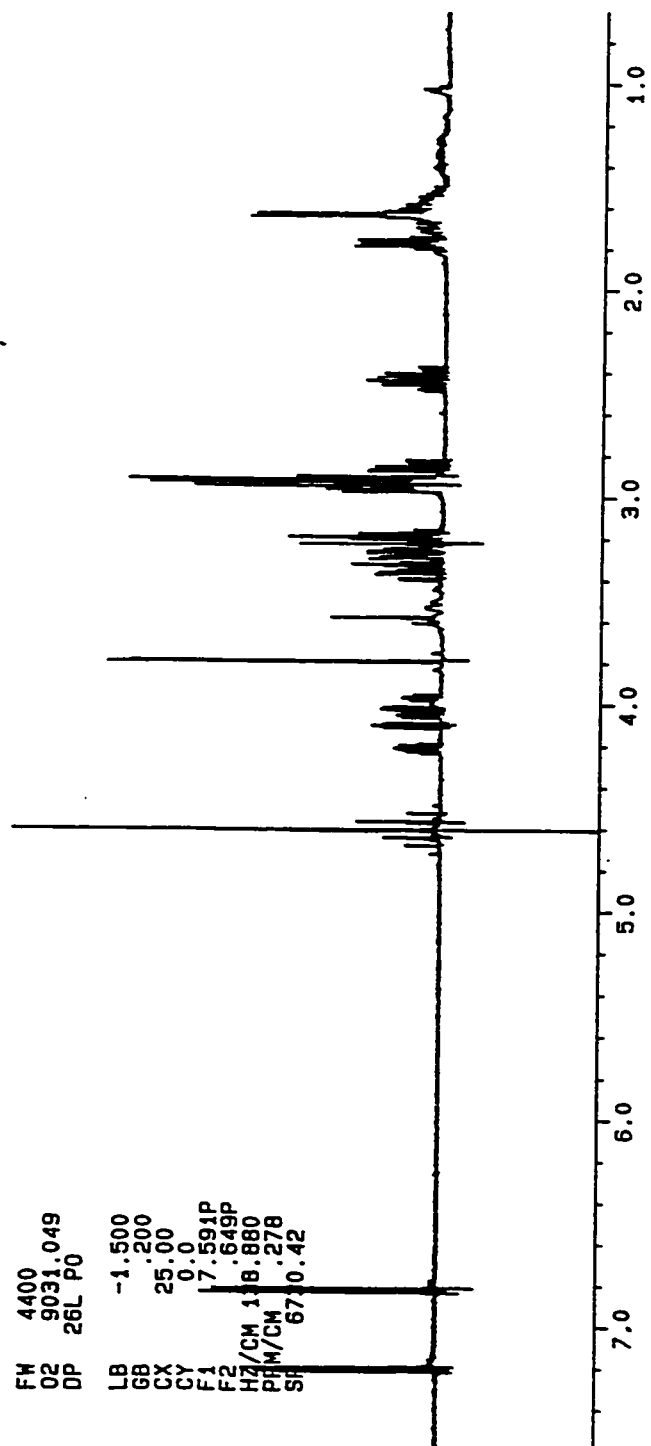
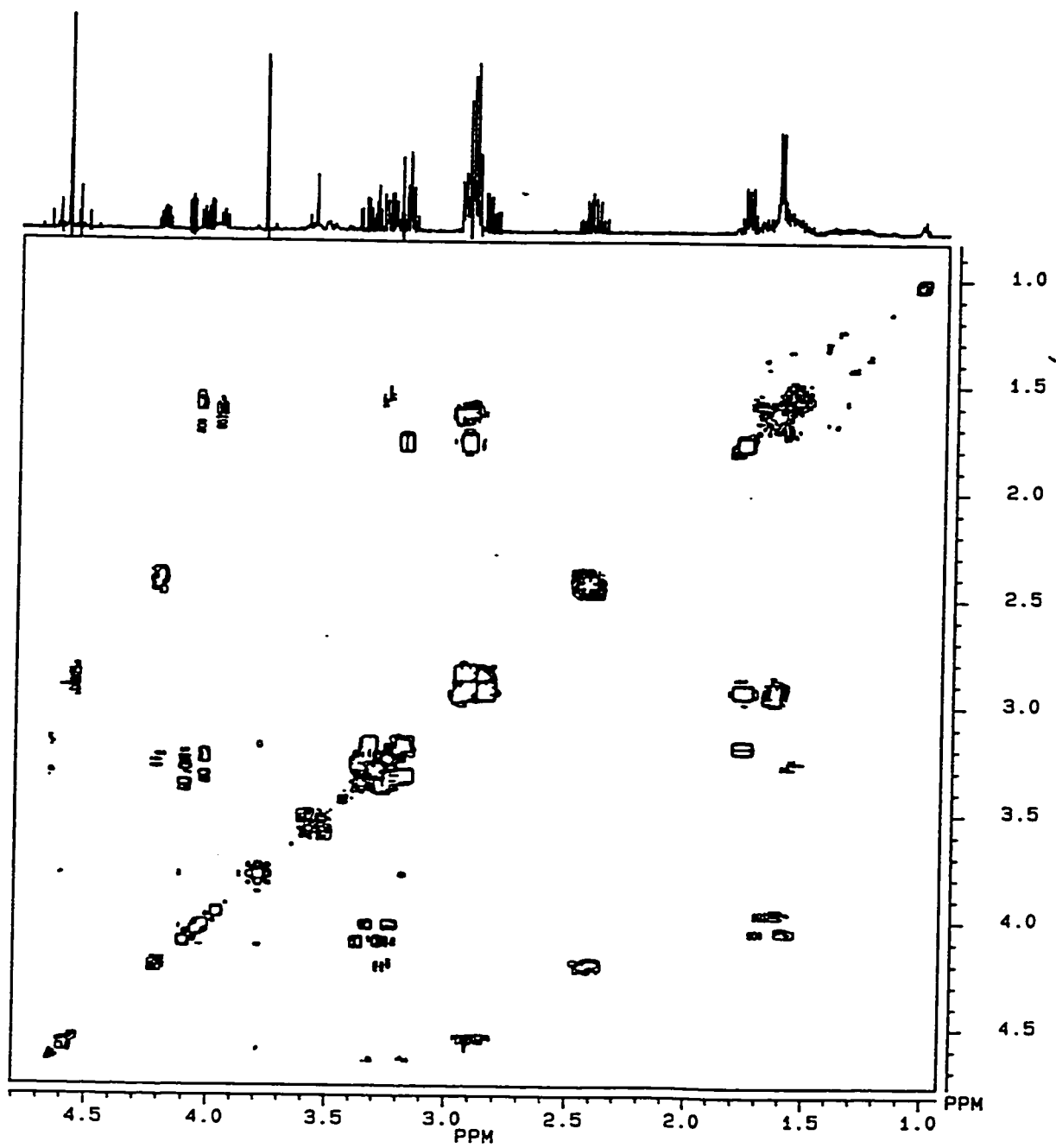




**Figure 7. Correlated spectroscopy-<sup>1</sup>H-NMR analysis of edeine A.** Edeine A, purified by reverse-phase HPLC, was dissolved in D<sub>2</sub>O and analysed on a 500 MHz Bruker instrument by Dr. Don Hughes at the McMaster University NMR facility.



Acid hydrolysis and 2D thin layer chromatography (TLC) of pure edeine A or edeine B produced spots possessing  $R_f$  values and ninhydrin colors similar to those of the expected amino acid components (Figure 8) (Table 3).  $R_f$  values for spot #1 of edeine A hydrolysate or edeine B hydrolysate appear to coincide with those for the  $\beta$ -tyrosine standard. Furthermore, reverse-phase HPLC analysis of edeine hydrolysates produced a peak at 10 minutes corresponding to  $\beta$ -tyrosine. Peptone and yeast extract were also analysed similarly by 2D TLC and reverse-phase HPLC to search for  $\beta$ -tyrosine. No spots corresponding to  $\beta$ -tyrosine were visible from the 2D TLC of peptone or yeast extract. Furthermore, reverse-phase HPLC could not detect the presence of  $\beta$ -tyrosine in either extract.

To determine whether  $\beta$ -tyrosine and isoserine in edeines are produced from tyrosine and serine, *B. brevis* was grown in PY media containing [ $^{14}\text{C}$ ]-tyrosine or [ $^{14}\text{C}$ ]-serine. Media was applied to a AG50W-X8 column, washed and edeines were eluted with 0.3 M ammonium hydroxide. Reverse-phase HPLC of the eluate produced a radiolabeled peak with a retention time of 16 minutes corresponding to edeines (Figure 9), whether media was supplemented with [ $^{14}\text{C}$ ]-tyrosine or [ $^{14}\text{C}$ ]-serine. Differences in retention times between [ $^{14}\text{C}$ ]-tyrosine or [ $^{14}\text{C}$ ]-serine labeled edeine were a result of different column loading.

**Figure 8. Diagram of 2D thin layer chromatography of amino acid components of edeine.** 1, tyrosine (purple); 2, 2,3-diaminopropionic acid (orange); 3, isoserine (dark yellow); 4, spermidine (brown); 5, 2,6-diamino-7-hydroxyazaleic acid (no standard); 6, glycine (purple). Solvent system I consisted of n-butanol-acetic acid-water (60:20:30). Solvent system II consisted of n-butanol-acetic acid-water-pyridine (60:30:50:20)

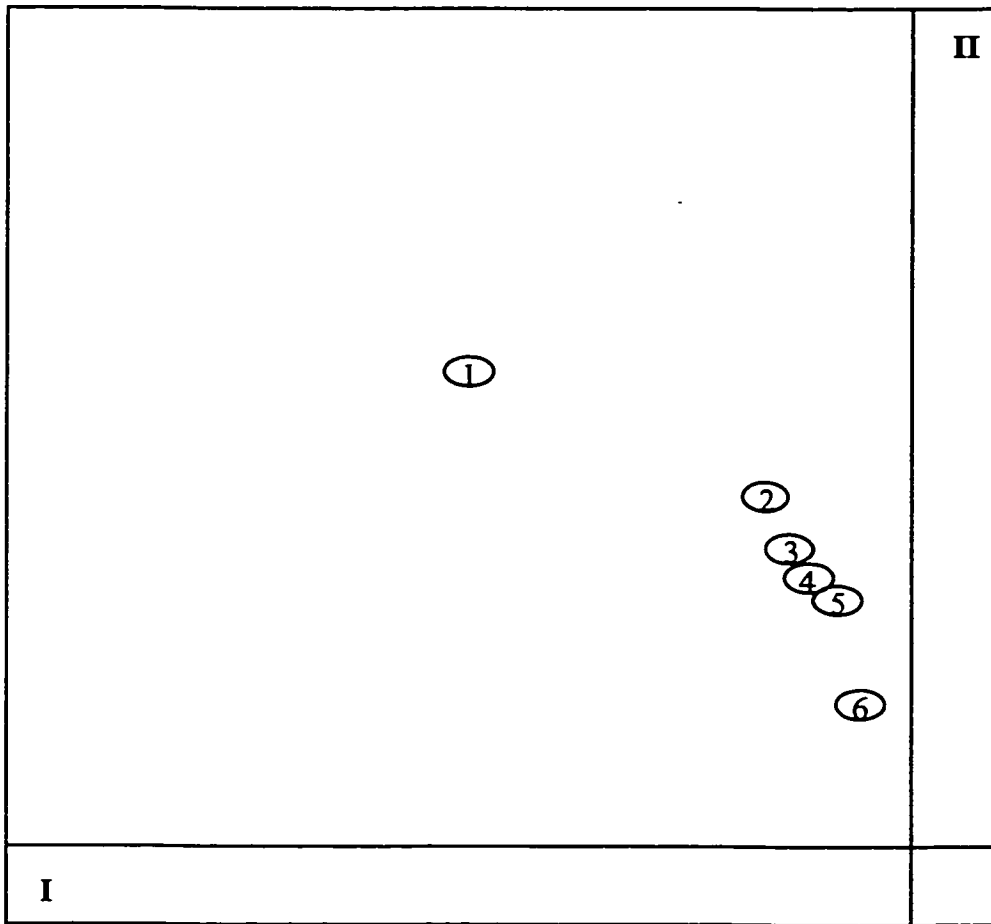


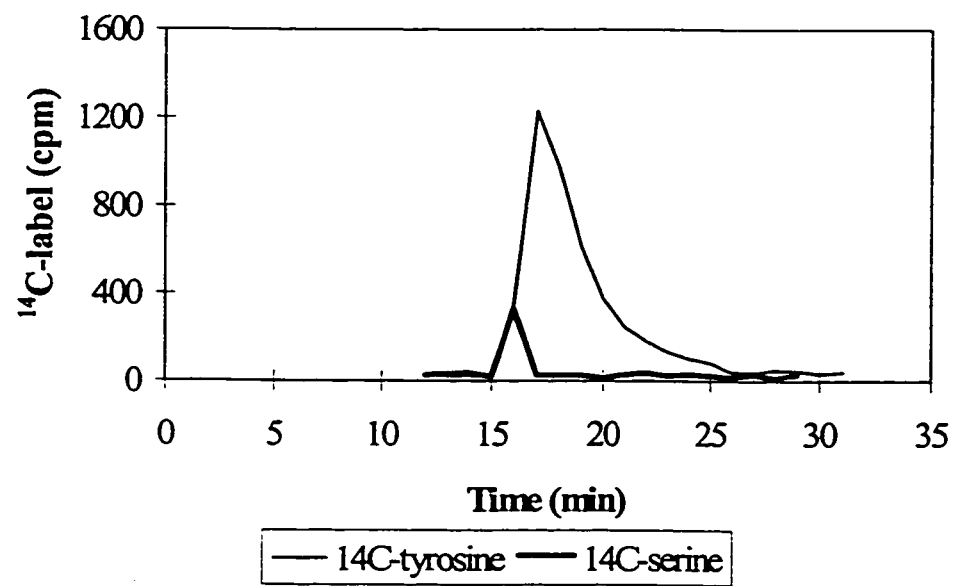
**Table 3.  $R_f$  for 2D thin layer chromatography of component amino acids and hydrolysed edeines.**

Compound	$R_f$ I <sup>a</sup>	$R_f$ II <sup>a</sup>	Ninhydrin Color
$\beta$ -tyrosine	0.54	0.64	yellow
diaminopropionic acid	0.23	0.45	orange
isoserine	0.20	0.40	dark yellow
spermidine	0.16	0.38	brown
glycine	0.08	0.26	purple
hydrolysed edeine A			
1	0.45	0.53	yellow
2	0.13	0.40	orange
3	0.12	0.34	dark yellow
4	0.11	0.32	brown
5	0.10	0.30	orange red
6	0.06	0.20	purple
hydrolysed edeine B			
1	0.42	0.54	yellow
2	0.15	0.38	orange
3	0.11	0.33	dark yellow
4	0.11	0.31	brown
5	0.10	0.30	orange
6	0.06	0.23	purple

<sup>a</sup> -Solvent system I consisted of n-butanol-acetic acid-water (60:20:30).

-Solvent system II consisted of n-butanol-acetic acid-water-pyridine (60:30:50:20).

**Figure 9. Reverse-phase HPLC analysis of edeines purified from cultures supplemented with [<sup>14</sup>C]-tyrosine or [<sup>14</sup>C]-serine.** Edeines purified by AG50W-X8 column were analysed on a reverse phase column (BioSil C18HL 90-5S, 250 x 4.6 mm, BioRad) with 5 % acetonitrile and 0.1 % trifluoroacetic acid. Fractions (1 mL) were collected for liquid scintillation counting. Differences in retention times appear to be a result of different column loading.





#### 5.4.3 Purification of tyrosine $\alpha,\beta$ -amino mutase from *Bacillus brevis*

Purification of tyrosine  $\alpha,\beta$ -amino mutase was attempted by several methods. Initially, *Bacillus brevis* Vm4 cultures were harvested during late log phase of growth (10 hours), before the appearance of edeines. The cells were lysed by French press and the crude lysate was fractionated by ammonium sulfate precipitation. Assays of all fractions, including crude lysate, revealed no formation of  $\beta$ -tyrosine by paper electrophoresis and/or reverse-phase HPLC. Therefore, no tyrosine  $\alpha,\beta$ -amino mutase activity was detected.

In order to obtain tyrosine  $\alpha,\beta$ -amino mutase activity, *B. brevis* cultures were harvested at different times of growth. However, activities were not detected from cultures harvested between 5 and 22 hours.

Various methods of cell lysis were also examined since these bacteria have thick cell walls, including an S-layer. The S-layer (or surface layer) is the outermost layer of many gram-positive and gram-negative bacteria and is composed of proteins or glycoproteins arranged in a crystalline array (Neidhardt *et al.*, 1990; Tsuboi *et al.*, 1988). Osmotic shock, bead mill, alumina grinding and a combination of lysozyme treatment and French press were tested. All methods resulted in sufficient cell lysis with the exception of osmotic shock, which produced a dilute lysate. Nonetheless, no tyrosine  $\alpha,\beta$ -amino mutase activity could be detected from all lysates or ammonium sulfate fractions of these lysates.

In addition, different buffers were used during cell washes, cell lysis and dialysis of ammonium sulfate pellets in an effort to detect activity. Generally, Tris was the

buffering agent in these solutions. However, HEPES buffers were also utilized to eliminate the possibility of negative effects from Tris on tyrosine  $\alpha,\beta$ -amino mutase activity. In the first step, *B. brevis* cells were washed with either 0.85 % NaCl or 50 mM Tris (or HEPES), pH 7.6 and 1 mM  $\beta$ -mercaptoethanol. During cell lysis, different components were added to the lysis buffer, such as NaCl, EDTA, PMSF, DTT or  $\beta$ -mercaptoethanol. Dialysis of ammonium sulfate pellets was performed in 50 mM Tris, pH 7.6 and 1 mM  $\beta$ -mercaptoethanol or 50 mM Tris, pH 7.6, 0.1 mM DTT and 1 mM EDTA. In these experiments no tyrosine  $\alpha,\beta$ -amino mutase activity was measured, therefore, altering buffer composition was not helpful in detecting activity.

With the possibility that tyrosine  $\alpha,\beta$ -amino mutase was insoluble and associated with membranes, the cell debris pellet was extracted with high salt buffer (50 mM Tris, pH 7.6, 500 mM KCl, 1 mM  $\beta$ -mercaptoethanol). This extract and the pellets resuspended in buffer were assayed. Nonetheless, tyrosine  $\alpha,\beta$ -amino mutase activity was not detected in these fractions.

Simultaneously, different assay conditions for tyrosine  $\alpha,\beta$ -amino mutase activity were tested. Since other mutases such as leucine 2,3-aminomutase and lysine 2,3-aminomutase require cofactors for activity (Chirpich *et al.*, 1970; Poston and Hemmings, 1979), a variety of cofactors and activators were added to the tyrosine  $\alpha,\beta$ -amino mutase assay. Supplementing assays with metals, such as  $\text{CoCl}_2$  (5 mM), cupric acetate (5 mM), or  $\text{FeCl}_3$  (5 mM) + sodium dithionite (10 mM), had no effect. Likewise, tyrosine  $\alpha,\beta$ -amino mutase activity was not detected after the addition of various

cofactors such as adenosylcobalamin ( $B_{12}$ ) (5  $\mu$ M), SAM (100  $\mu$ M), PLP (1 mM) and a mixture of FAD (0.1 mM), FMN (0.1 mM) and  $NAD^+$  (1 mM) to assays. Similar results were also obtained in the presence of the reducing agent DTT.

Furthermore, purification of tyrosine  $\alpha,\beta$ -amino mutase was attempted using a modified version of the protocol for lysine 2,3-aminomutase (Chirpich *et al.*, 1970). Purification and assays were performed under semi-anaerobic conditions by using degassed solutions and keeping all mixtures sealed under argon. *B. brevis* cells were washed with a buffer containing DTT (1 mM) and PLP (0.01 mM) and then lysed by French press after lysozyme pretreatment. PLP (0.1 mM) was also added to the lysis buffer and DTT concentration was increased to 10 mM. Crude lysate was then incubated for 1 hour at 37°C with PLP (50  $\mu$ M), reduced glutathione (12.5 mM),  $Fe(NH_4)_2(SO_4)_2$  (1 mM) and sodium dithionite (1 mM) prior to activity assays. Tyrosine  $\alpha,\beta$ -amino mutase assays were performed as previously with the addition of 3.8  $\mu$ M SAM and 1 mM sodium dithionite. However, analysis of these assays by paper electrophoresis and reverse-phase HPLC revealed no activity. In addition to tyrosine  $\alpha,\beta$ -amino mutase assays, protein fractions were also tested for serine aminomutase activity. The formation of isoserine from [ $^{14}C$ ]-serine was monitored by paper electrophoresis and, similarly, no activity was detected.

Since amino acids activated by ATP are subsequently covalently bound to the pantothenic acid arm of edeine synthetase during edeine biosynthesis, the labeling of this enzyme was attempted by incubating protein with [ $^{14}C$ ]-tyrosine, ATP and

pyrophosphatase. This mixture was then separated by SDS-polyacrylamide gel electrophoresis. Upon exposure to film, no radiolabeled protein bands were visible.

When proteins are expressed in the cell in small quantities, several purification steps may be required before any enzyme activity can be measured. Therefore, *B. brevis* crude lysate was applied to a DEAE-Sepharose column and proteins were elute with a NaCl gradient (Figure 10) When fractions were tested for tyrosine  $\alpha,\beta$ -amino mutase activity, once more none was detected.

Lastly, samples of *B. brevis* Vm4 were obtained from Dr. Kurylo-Borowska and purification of tyrosine  $\alpha,\beta$ -amino mutase was performed as per Kurylo-Borowska and Abramsky,1972. Cells (270 g) were washed and resuspended with 50 mM Tris, pH 7.6 and 1 mM  $\beta$ -mercaptoethanol, followed by cell lysis with a bead mill. Lysed cells were then treated with DNase I and cell debris was removed by centrifugation. The resulting crude lysate was fractionated by ammonium sulfate precipitation and the 25-55 % saturation fraction was further purified after dialysis by size exclusion chromatography (Sephadex G100) (Figure 11) or anion exchange chromatography (DEAE-Sepharose) (Figures 12). No tyrosine  $\alpha,\beta$ -amino mutase activity nor serine aminomutase activity was detected when fractions from these columns were assayed.

**Figure 10. Purification of tyrosine  $\alpha,\beta$ -amino mutase by DEAE-Sephrose anion exchange chromatography.** Crude lysate from *Bacillus brevis* was applied onto a DEAE-Sephrose Fast Flow column (1 cm dia., 11 cm height; Pharmacia) and eluted with NaCl in 50 mM HEPES, pH 7.5, 1 mM EDTA and 0.1 mM DTT.

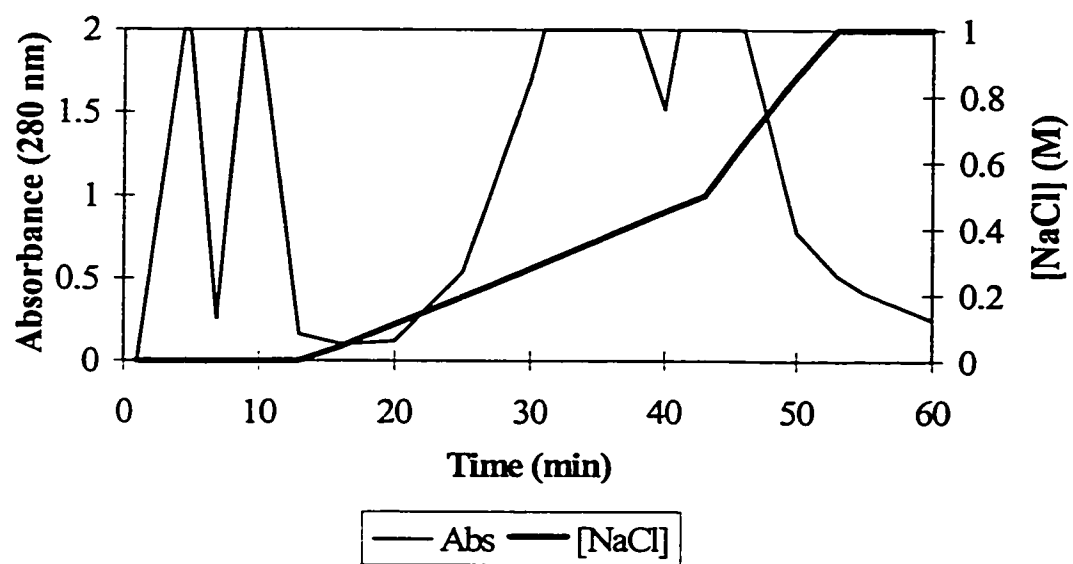


**Figure 11. Purification of edeine biosynthetic enzymes by Sephadex G100 size exclusion chromatography.** The dialyzed 25-55 % ammonium sulfate fraction from *Bacillus brevis* crude lysate was applied onto a Sephadex G100 column (2.5 cm dia., 117 cm height; Pharmacia) and eluted with 50 mM Tris, pH 7.6, 1 mM  $\beta$ -mercaptoethanol. Protein was monitored by absorbance at 280 nm and edeine synthetase activity was detected with the isoserine-dependent ATP- $^{32}$ PP<sub>i</sub> exchange assay.

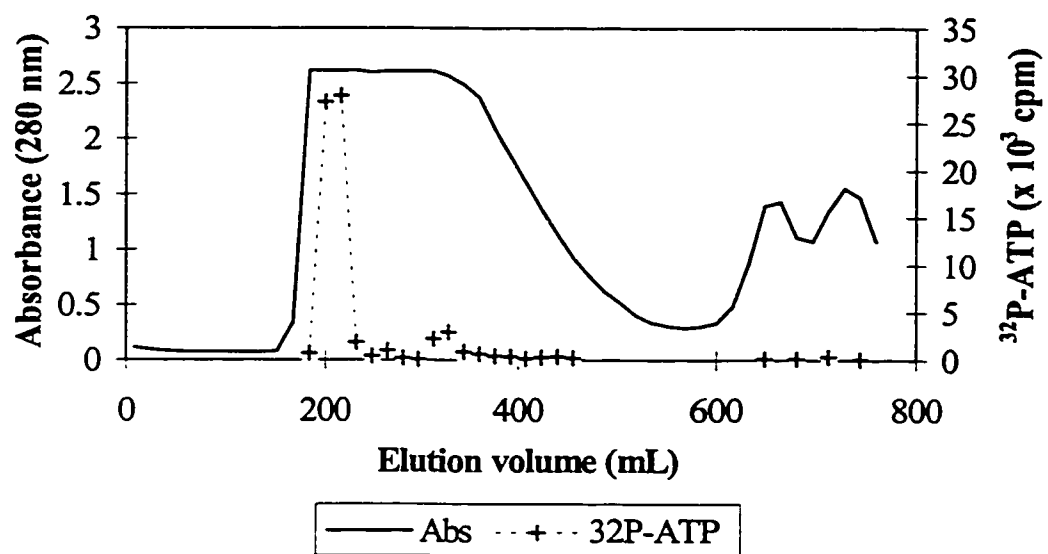
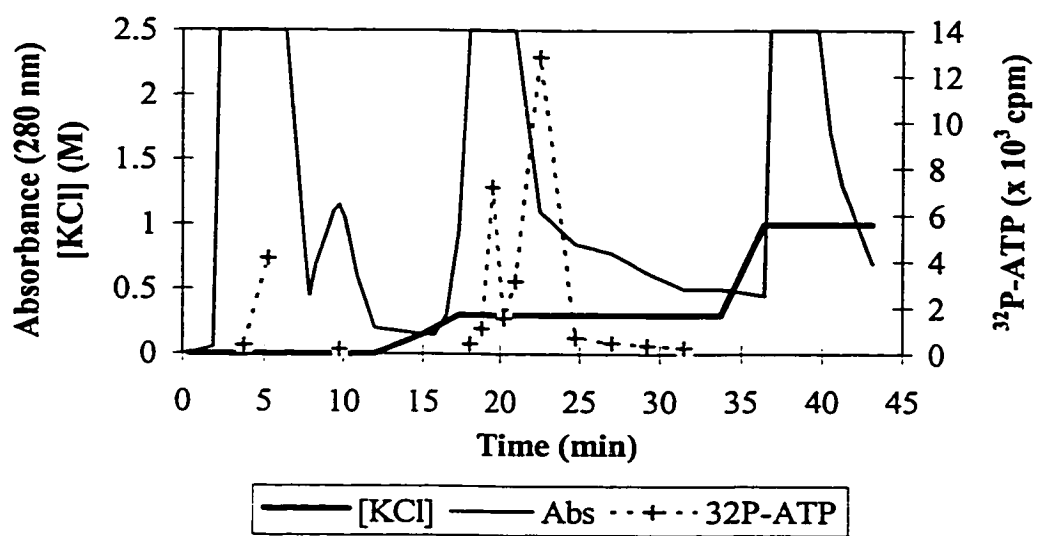




**Figure 12. Purification of edeine biosynthetic enzymes by DEAE-Sephacel anion exchange chromatography.** The dialyzed 25-55 % ammonium sulfate fraction from *Bacillus brevis* crude lysate was applied onto a DEAE-Sephacel Fast Flow column (1 cm dia., 11 cm height; Pharmacia) and eluted with KCl in 100 mM Tris, pH 7.6, 2 mM DTT. Protein was monitored by absorbance at 280 nm and edeine synthetase activity was detected with the isoserine-dependent ATP-<sup>32</sup>PP<sub>i</sub> exchange assay.



In order to detect the presence of any enzyme involved in edeine biosynthesis, fractions from these columns were tested for edeine synthetase activity using an isoserine-dependent ATP-<sup>32</sup>PP<sub>i</sub> exchange assay. This assay relies on the equilibrium of amino acid activation with ATP by edeine synthetase and measures the formation of <sup>32</sup>P-ATP.



ATP-<sup>32</sup>PP<sub>i</sub> exchange activity was discovered after purification by either column. A peak demonstrating exchange activity eluted from the Sephadex G100 column after 200 mL buffer (Figure 11). This elution occurred soon after the void volume. Several peaks containing edeine synthetase exchange activity were also obtained from DEAE-Sepharose chromatography (Figure 12). Some activity (30 % of maximum) was measured in the unbound fraction, probably a consequence of loading a large amount of protein. Whereas, two peaks containing more ATP-<sup>32</sup>PP<sub>i</sub> exchange activity were eluted from this column with 0.3 M KCl.

Two protein bands (140 and 160 KD) on a SDS-polyacrylamide gel, believed to correspond to edeine synthetase, were electroblotted onto PVDF for N-terminal sequencing. The resulting amino acid sequences were EEAATTVAPKMDRAFEK and PKAGVYVGSYYP, respectively. However, these sequences were discovered to be homologous to the middle wall and outer wall proteins, components of the S-layer in *B. brevis* (Mooi *et al.*, 1986; Tsuboi *et al.*, 1988). These proteins are also reported to have molecular weights of 130 and 150 KD (Yamada *et al.*, 1981).

## 5.5 Discussion

The purpose of this project was to study tyrosine  $\alpha,\beta$ -amino mutase, an enzyme involved in the biosynthesis of edeines in *Bacillus brevis* Vm4. Prior to purification of this enzyme, the secretion of edeines by *B. brevis* was examined and  $\beta$ -tyrosine was verified to be a constituent amino acid of edeine. In this study, *B. brevis* demonstrated usual bacterial growth kinetics and edeines were detected during early stationary phase. This suggests that expression of the edeine biosynthetic machinery of *B. brevis* is maximal at the time preceding stationary phase and that purification of these enzymes in late log phase should be fruitful. Furthermore, media requirements for edeine production by *B. brevis* were examined and peptone was found to be essential. The exact factor that is required from this extract was not determined.

Previous methods of edeine purification from *B. brevis* cultures (Kurylo-Borowska and Heaney-Kieras, 1983) were optimized to supply pure edeine A and fairly pure edeine B. The addition of Mono S cation exchange chromatography and reverse-phase HPLC allowed a greater separation of edeine A and edeine B. The purity of edeine A was demonstrated by mass spectrometry which also confirmed the molecular masses of both edeine A and B. Further analysis of edeines by  $^1\text{H-NMR}$ , Correlated spectroscopy- $^1\text{H-NMR}$  and acid hydrolysis proved the presence of  $\beta$ -tyrosine in these peptides. The source of  $\beta$ -tyrosine in PY media was pursued. However, this unusual amino acid could not be detected in either peptone or yeast extract. On the other hand, [ $^{14}\text{C}$ ]-tyrosine or [ $^{14}\text{C}$ ]-serine added to the media appears to have been incorporated into edeines. Thus, tyrosine and serine must be converted to  $\beta$ -tyrosine and isoserine, respectively, and then

incorporated into edeines. This suggests that *B. brevis* Vm4 possesses the catalytic ability to convert these amino acids and, therefore, should express tyrosine  $\alpha,\beta$ -amino mutase activity.

Since the existence of tyrosine  $\alpha,\beta$ -amino mutase activity appears evident and purification of this activity was previously reported (Kurylo-Borowska and Abramsky, 1972), attempts were made to purify this enzyme using similar methods. Despite great efforts, tyrosine  $\alpha,\beta$ -amino mutase activity could not be measured from protein fractions prepared from *B. brevis* Vm4 under a variety of conditions. Cultures at different stages of growth were harvested and lysed by several different methods, including osmotic shock, alumina grinding, glass bead mill, French press and lysozyme treatment followed by French press. All fractions were assayed including high salt buffer extracts of cell debris pellets and resuspended cell debris pellets, in the event that this enzyme was associated with membranes.

In addition, tyrosine  $\alpha,\beta$ -amino mutase activity assay conditions were altered. Since many amino mutases require factors such as iron, cobalamin and PLP for activity (Chirpich *et al.*, 1970; Poston and Hemmings, 1979), several cofactors, metals and reducing agents were tested. *B. brevis* crude lysate was also prepared and assayed under anaerobic conditions as for lysine 2,3-aminomutase (Chirpich *et al.*, 1970) and yet no tyrosine  $\alpha,\beta$ -amino mutase activity was measured. Ammonium sulfate fractionation, size exclusion chromatography and anion exchange chromatography were also performed in case partial purification is required before tyrosine  $\alpha,\beta$ -amino mutase activity can be measured, however, no activity was obtained.

As tyrosine  $\alpha,\beta$ -amino mutase activity could not be detected, assays for serine aminomutase and edeine synthetase were performed. The only activity detected in the course of this study was edeine synthetase, using the isoserine-dependent ATP- $^{32}\text{P}_i$  exchange assay. Our interests, however, were in the biosynthesis of the unusual amino acid,  $\beta$ -tyrosine, and in the determination of the chemical mechanism of tyrosine  $\alpha,\beta$ -amino mutase. Two different mechanisms are possible as illustrated in Figure 13a. Either mechanism may be initiated by Schiff's base formation between the amino group and pyridoxal phosphate (Baker *et al.*, 1973) or a Michael addition of the amino group to a dehydroalanine residue (Hanson and Havir, 1972). Mechanism A occurs with abstraction of only the  $\beta$ -hydrogen and, therefore, no exchange of the  $\alpha$ -hydrogen is possible, whereas, mechanism B occurs with sequential abstraction of  $\alpha$ -hydrogen and  $\beta$ -hydrogen. Recently, it has been suggested that the first step for histidine ammonia lyase and phenylalanine ammonia lyase is a Friedel-Crafts-like electrophilic substitution, as illustrated in Figure 13b (Mechanism C) (Rétey, 1996). Instead of reacting with the amino group, the dehydroalanine residue participates in an electrophilic attack of the aromatic ring. Other possible mechanisms may involve free radical formation as with cobalamin- and metals-assisted catalysis (Walsh, 1979). None of these mechanisms, however, explain the requirement for ATP. Nonetheless, as no tyrosine  $\alpha,\beta$ -amino mutase activity could be found, the project was terminated.

**Figure 13a. Possible mechanisms of tyrosine  $\alpha,\beta$ -amino mutase**

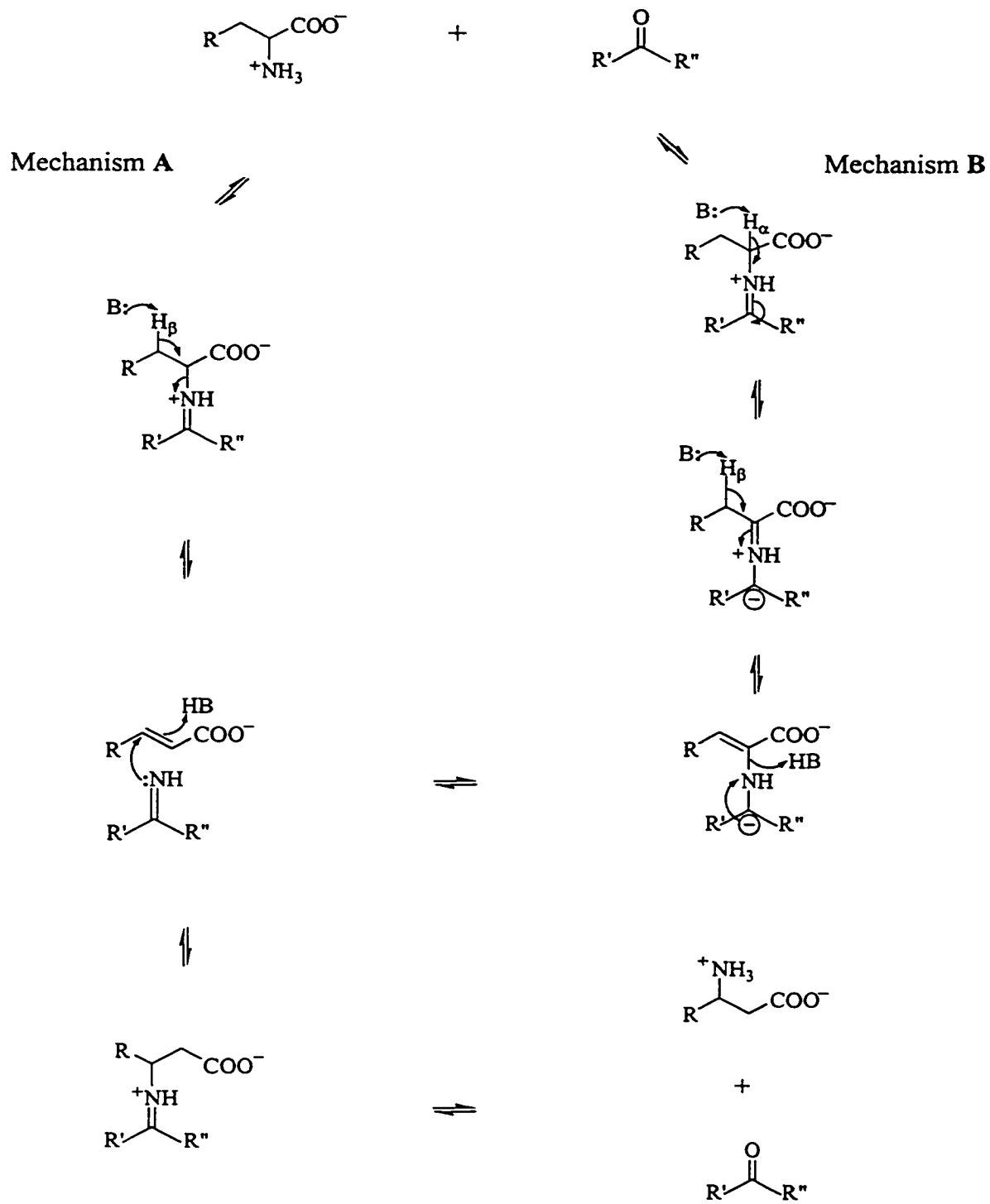
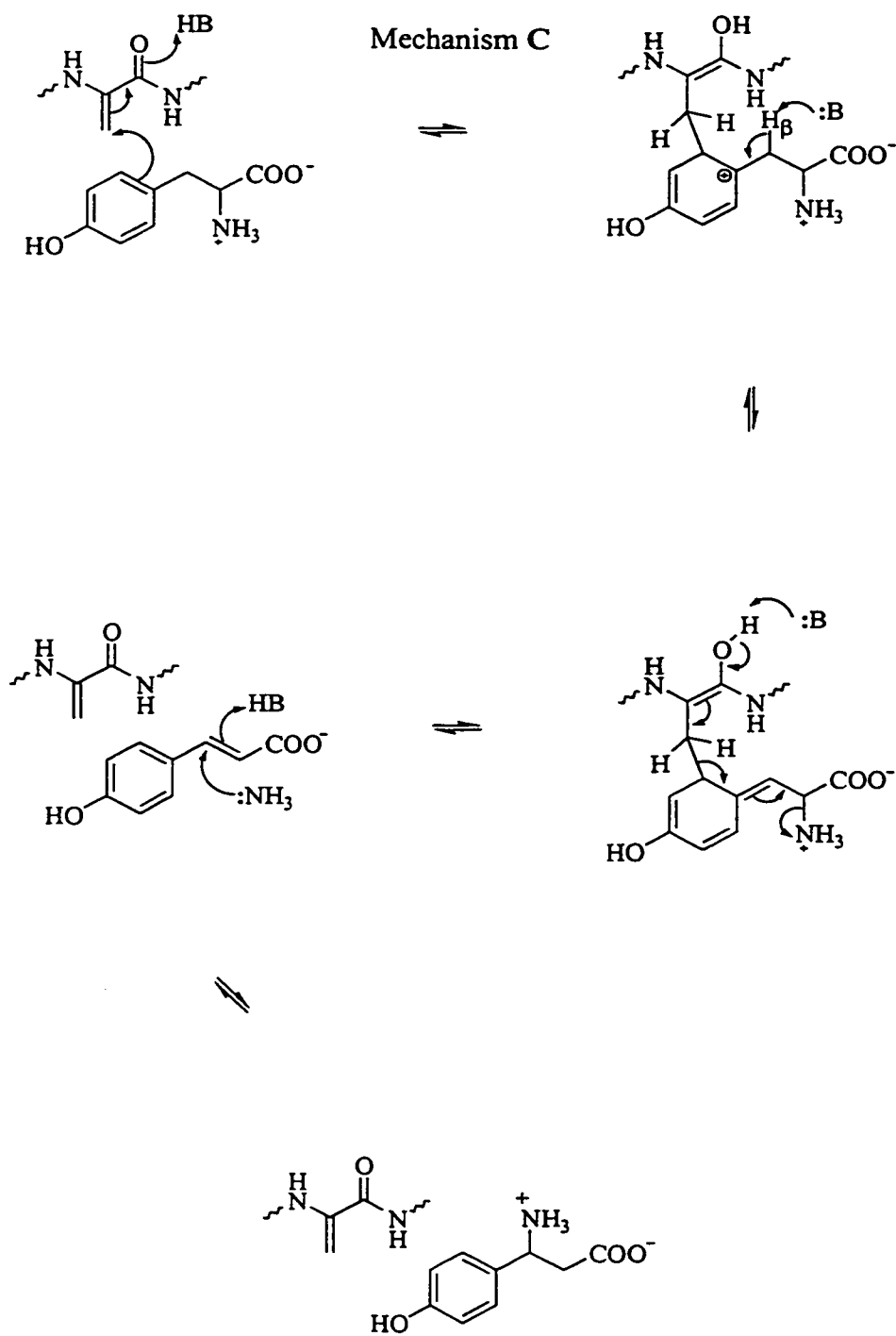




**Figure 13b. Possible mechanisms of tyrosine  $\alpha,\beta$ -amino mutase**



Kurylo-Borowska, who had previously purified this enzyme (Kurylo-Borowska and Abramsky, 1972), stated that harvesting large *B. brevis* cultures (>20 L) and cell lysis by alumina grinding were essential in order to successfully purify tyrosine  $\alpha,\beta$ -amino mutase. Nevertheless, these conditions were believed to be reproduced without any success. Difficulty in measuring tyrosine  $\alpha,\beta$ -amino mutase activity may occur if reaction rates are especially slow or if specific activity is very low. These possibilities are likely since, previously,  $\beta$ -tyrosine had to be partially purified from tyrosine  $\alpha,\beta$ -amino mutase assays and concentrated before analysis in order to detect activity (Kurylo-Borowska and Abramsky, 1972).

Future experiments, involving the purification of tyrosine  $\alpha,\beta$ -amino mutase, may be more successful if tyrosine  $\alpha,\beta$ -amino mutase were cloned and overproduced. Sufficient quantities of tyrosine  $\alpha,\beta$ -amino mutase could, therefore, be obtained for mechanistic studies. Biosynthesis genes for other peptide antibiotics produced in *Bacillus*, such as gramicidin S and tyrocidine, are clustered into polycistronic transcription units (Nakano and Zuber, 1990). Thus, the cloning of the edeine synthetase genes could lead to the discovery of the tyrosine  $\alpha,\beta$ -amino mutase gene. The edeine synthetase gene might be obtained by a number of methods, including screening a library with a degenerate hybridization probe corresponding to the N-terminal protein sequence, screening an expression library with antibodies to edeine synthetase or by PCR using primers corresponding to areas of high homology in other peptide synthetase genes. The discovery of an edeine biosynthetic gene cluster would prove very useful not only for the

study of tyrosine  $\alpha,\beta$ -amino mutase, but also to investigate other enzymes involved in edeine biosynthesis.

## 5.6 References

- Baker, J. J., C. van der Drift and T. C. Stadtman (1973) Purification and properties of  $\beta$ -lysine mutase, a pyridoxal phosphate and B<sub>12</sub> coenzyme dependent enzyme, *Biochemistry*, **12**: 1054-1063.
- Chirpich, T. P., V. Zappia, R. N. Costilow and H. A. Barker (1970) Lysine 2,3-aminomutase: Purification and properties of a pyridoxal phosphate and S-adenosylmethionine activated enzyme, *J. Biol. Chem.*, **245**: 1778-1789.
- Hanson, K. R., and E. A. Havir (1970) L-phenylalanine ammonia-lyase. IV. Evidence That the prosthetic group contains a dehydroalanyl residue and mechanism of action, *Arch. Biochem. Biophys.*, **141**: 1-17.
- Hanson, K. R., and E. A. Havir (1972) The enzymic elimination of ammonia, in *The Enzymes* (P. D. Boyer, ed.), Vol. VII, Academic Press, New York, pp. 75-166.
- Hettinger, T. P. and L. C. Craig (1968) Edeine II: The composition of the antibiotic peptide edeine A, *Biochemistry*, **7**: 4147-4153.
- Hettinger, T. P., Z. Kurylo-Borowska and L. C. Craig (1968) Edeine III: The composition of the antibiotic peptide edeine B, *Biochemistry*, **7**: 4153-4160.
- Kurylo-Borowska, Z. (1962) On the mode of action of edeine, *Biochim. Biophys. Acta*, **61**: 897-902.
- Kurylo-Borowska, Z. and T. Abramsky (1972) Biosynthesis of  $\beta$ -tyrosine, *Biochim. Biophys. Acta*, **264**: 1-10.
- Kurylo-Borowska, Z. and J. Heaney-Kieras (1983) Edeine A, edeine B, and guanidospermidine, *Methods Enzymol.*, **94**: 441-451.
- Kurylo-Borowska, Z., and W. Szer (1972) Inhibition of bacterial DNA synthesis by edeine: Effect on *Escherichia coli* mutants lacking DNA polymerase I, *Biochim. Biophys. Acta*, **287**: 236-245.
- Kurylo-Borowska, Z. and J. Sedkowska (1974) Biosynthesis of edeine: Fractionation and characterization of enzymes responsible for biosynthesis of edeine A and B, *Biochim. Biophys. Acta*, **351**: 42-56.
- Lacal, J. C., D. Vazquez, J. M. Fernandez-Sousa and L. Carrasco (1980) Antibiotics that specifically block translation in virus-infected cells, *J. Antibiotics*, **33**: 441-446.
- Mooi, F. R., I. Claassen, D. Bakker, H. Kuipers and F. K. de Graaf (1986) Regulation

- Mooi, F. R., I. Claassen, D. Bakker, H. Kuipers and F. K. de Graaf (1986) Regulation and structure of an *Escherichia coli* gene coding for an outer membrane protein involved in export of K88ab fimbrial subunits, *Nucleic Acids Res.*, **14**: 2443-2457.
- Nakano, M. M., and P. Zuber (1990) Molecular biology of antibiotic production in *Bacillus*, *Crit Rev. Biotechnol.*, **10**: 223-240.
- Neidhardt, F. C., J. L. Ingraham and M. Schaechter (1990) *Physiology of the bacterial cell: A molecular approach*, Sinauer Associates, Inc., Sunderland, MA, pp. 44-46.
- Parry, R. J. and Z. Kurylo-Borowska (1980) Biosynthesis of amino acids: Investigation of the mechanism of  $\beta$ -tyrosine formation, *J. Am. Chem. Soc.*, **102**: 836-837
- Poston, J. M. and B. A. Hemmings (1979) Cobalamins and cobalamin-dependent enzymes in *Candida utilis*, *J. Bacteriol.*, **140**: 1013-1016.
- Rétey, J. (1996) Enzymatic catalysis by Friedel-Crafts-type reactions, *Naturwissenschaften*, **83**: 439-447.
- Rodinov, V. M., A. A. Dudinskaia, V. G. Avramenko and N. N. Suvorov (1958) Synthesis of  $\beta$ -amino acids from aromatic hydroxy and alkoxy aldehydes, *J. Gen. Chem. USSR*, **28**: 2279-2282.
- Roncari, G., Z. Kurylo-Borowska and L. C. Craig (1966) On the chemical nature of the antibiotic edeine, *Biochemistry*, **5**: 2153-2159.
- Tsuboi, A., R. Uchihi, T. Adachi, T. Sasaki, S. Hayakawa, H. Yamagata, N. Tsukagoshi and S. Udaka (1988) Characterization of the genes for the hexagonally arranged surface layer proteins in protein-producing *Bacillus brevis* 47: Complete nucleotide sequence of the middle wall protein, *J. Bacteriol.*, **170**: 935-945.
- Walsh, C. (1979) *Enzymatic reaction mechanisms*, W. H. Freeman, San Francisco.
- Woodcock, J., D. Moazed, M. Cannon, J. Davies and H. F. Noller (1991) Interaction of antibiotics with A- and P- site bases in 16S ribosomal RNA, *EMBO J.*, **10**: 3099-3103.
- Yamada, H., N. Tsukagoshi and S. Udaka (1981) Morphological alterations of cell wall concomitant with protein release in a protein-producing bacterium, *Bacillus brevis* 47, *J. Bacteriol.*, **148**: 322-332.

## **CHAPTER 6**

### **Discussion and Conclusions**

## 6.1 Discussion and Conclusions

Currently, amphotericin B and the azoles are the drugs of choice for serious life-threatening fungal infections caused by organisms such as *Candida*, *Aspergillus* and *Cryptococcus*. Therapeutic use of these compounds are hampered either by severe side effects or by fungal resistance. As a result, the development of effective antifungal drugs attacking new fungal targets is essential for the survival of millions of immunocompromised patients worldwide. The antifungal compound (*S*)-2-amino-4-oxo-5-hydroxypentanoic acid (RI-331) was previously shown to target yeast homoserine dehydrogenase, an enzyme involved in the biosynthesis of Thr, Met and Ile. This amino acid biosynthetic pathway is an ideal fungal target since it is absent in mammals. Consequently, the major focus of the work presented in this thesis was the investigation of HSD from *S. cerevisiae* as a potential target for new potent antifungal agents. The large amounts of yeast HSD required for the studies described in Chapters 2, 3 and 4 were easily produced by overexpression in *E. coli*.

The manuscripts presented in Chapters 2 and 3 furnish much of the groundwork required for fungal HSD inhibitor design. The state of knowledge on fungal HSD was limited and focused on the regulation of the enzyme from *S. cerevisiae*. Although much more was known about the *E. coli* bifunctional enzyme AKHSD I, relatively little was known of the kinetic properties or mechanism of yeast HSD. The results presented in Chapter 3 shows that yeast HSD is indeed very similar to *E. coli* AKHSD I.



Both enzymes operate through an ordered mechanism, whereby NAD(P)H binds HSD before the amino acid and NAD(P)<sup>+</sup> is released after the amino acid. Viscosity and kinetic isotope experiments demonstrated that, like the *E. coli* enzyme and many other dehydrogenases, yeast HSD has a fast catalytic step and NAD(P)<sup>+</sup> release appears to be rate-limiting. Furthermore, kinetic isotope effect experiments revealed that the *pro-S* hydrogen is transferred from C-4 of the nicotinamide cofactor, demonstrating the same stereochemistry as *E. coli* AKHSD I. The phylogenetic tree produced from amino acid sequence alignments illustrates that yeast HSD is closely related to the bifunctional AKHSD of many species including *E. coli*. These results suggest that HSD from other fungal species will likely possess similar properties to yeast HSD and *E. coli* AKHSD I.

In Chapter 2, chemical modification and site-directed mutagenesis studies were performed in an effort to identify active site residues of yeast HSD. Although the functional amino acid residues involved in the aspartate kinase activity of *E. coli* AKHSD I were previously examined, the active site residues involved in the HSD activity are unknown. The reason being that the interpretation of the chemical modification studies on HSD activity was complicated by the allosteric effects of the *E. coli* bifunctional enzyme. Consequently, identification of active site residues should prove more successful by studying yeast HSD. Protein modification by diethyl pyrocarbonate (DEPC) and site-directed mutagenesis of yeast HSD implicated His 309 as an important residue for HSD catalysis. However, the crystal structure of yeast HSD revealed that His 309 may only be involved in dimerization of HSD as it is located near the dimer interface. pH studies described in Chapter 3, on the other hand, suggested that basic

residues are important in substrate binding. This result is in agreement with the identification of Lys117 and Lys223 as key residues in the active site of the yeast HSD X-ray structure. The knowledge gained from the chemical mechanism and structure of yeast HSD will increase our understanding of the active site, thereby facilitating modeling of potential inhibitors.

In addition to contributing to the development of effective HSD inhibitors, the results presented in Chapters 2 and 3 will add insight into *S. cerevisiae* amino acid biosynthesis. These studies demonstrated that, unlike *E. coli* AKHSD, yeast HSD is not regulated by feedback inhibition by the amino acids Met and Thr, since their inhibition constants are too high to be significant. Yeast HSD also appeared to perform equally well with NADPH or NADH as cofactor. As opposed to the usual convention, Michealis constants ( $K_m$ ) suggest that yeast HSD has a higher affinity for NADH than NADPH. Furthermore, viscosity experiments demonstrated that NAD<sup>+</sup> was somewhat “sticky” and, thus, the product also appears to have a high affinity for yeast HSD. As a consequence, the mechanism is ordered and NAD(P)<sup>+</sup> dissociation is rate-limiting. Lastly, cations, such as K<sup>+</sup> and Na<sup>+</sup>, demonstrate significant effects on HSD activity by reducing substrate and cofactor affinities. Although regulation of HSD activity in prokaryotes is different than in yeast, the basic properties of the enzyme and its mechanism will likely be similar in both bacterial and fungal species.

The results in Chapter 4 describe the mechanism of RI-331 inactivation of yeast HSD. This compound demonstrated several properties of a mechanism-based inactivator such as inactivation kinetics, substrate protection, irreversibility, stoichiometry and a

requirement for catalysis. Mechanism-based inactivators usually inactivate their target enzyme by covalent modification. However, in this case, RI-331 appears to covalently modify the cofactor NAD(P)<sup>+</sup>. The resulting product is a NAD(P)-RI-331 adduct which resembles the transition state and, therefore, is expected to be a tight-binding inhibitor of yeast HSD. This discovery will provide an important lead in the design of effective inhibitors of HSD. Furthermore, this type of inactivation of nicotinamide-dependent enzymes has been reported earlier and may represent a different class of mechanism-based inactivators. These novel inactivators will prove useful not only in the design of HSD inhibitors but also in the design of inhibitors targeting other dehydrogenase/reductase enzymes.

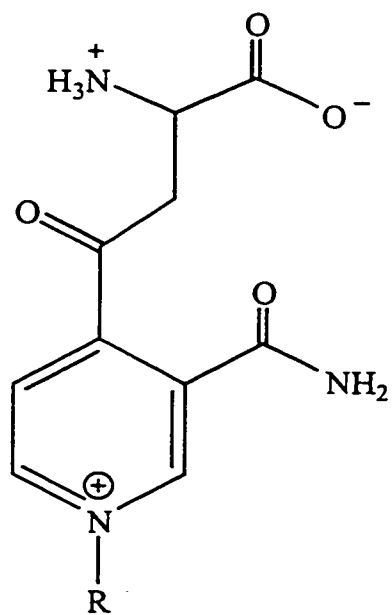
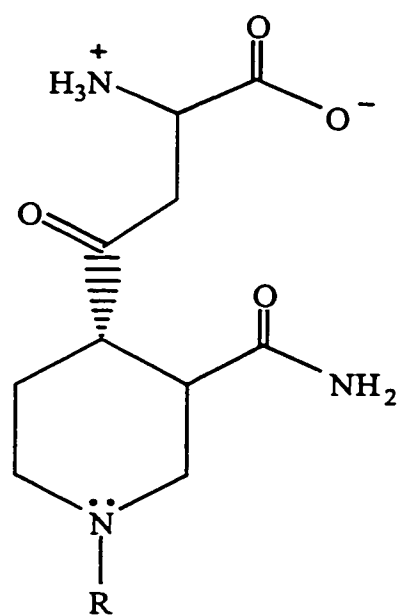
All together the work described in Chapters 2, 3 and 4 of this thesis provides a basis for the development of new potent antifungal agents. Yeast HSD revealed a high substrate specificity with respect to its amino acid substrates, since no conversion was detected with similar compounds such as acetaldehyde, butyraldehyde, serine, isoserine and hydroxynorvaline. In addition, yeast HSD demonstrated high affinity for its nicotinamide cofactor, as the Michealis constants ( $K_m$ ) were in the micromolar range compared to millimolar for the amino acid substrates. Consequently, HSD inhibitors will have to incorporate chemical properties of ASA, Hse and NAD(P)(H). The discovery of the HSD inhibitor H-(1,2,4-triazol-3-yl)-*D,L*-alanine and the characterization of the inactivation mechanism of RI-331 suggest that transition-state analogs are likely the most effective inhibitors of HSD. The NAD(P)-RI-331 adduct appears to have a very slow dissociation rate ( $k_{off}$ ), as illustrated by its irreversibility, and, therefore, a low inhibition

constant ( $K_i$ ). On the other hand, H-(1,2,4-triazol-3-yl)-*D,L*-alanine has larger  $K_i$ s (1.6-3.8 mM) implying that the adenine dinucleotide portion of NAD(P) is important for HSD binding. Likewise, *L*-aspartate  $\beta$ -hydroxamate, an analog of RI-331 which does not demonstrate time-dependent inactivation, also has similar inhibition constants ( $K_i = 0.8$ -3.5 mM).

Therefore, transition-state analogs similar to the compounds in Figure 1, may be effective inhibitors of fungal HSD. It is unclear whether functional groups, such as the keto group or the amide, are necessary to obtain high affinity binding to HSD. An extra methylene ( $\text{CH}_2$ ) group between the keto group and the ring, as is the case for the NAD(P)-RI331 adduct, may also be beneficial by adding more flexibility. On the other hand, it is important that the stereochemistry at the C-4 of the saturated ring reflect that of HSD catalysis (*pro-S*).

In conclusion, the characterization of yeast HSD described in this thesis will provide a strong foundation necessary for the development of potent antifungal drugs targeting fungal HSD. The mechanistic knowledge gained from these studies, coupled with the structural information derived from the recently solved crystal structure of yeast HSD, will greatly facilitate rational-based design of inhibitors. Moreover, the conserved nature of the enzyme suggests that knowledge of yeast HSD can be extended to HSDs of other fungal species. As a result, the identification of effective inhibitors of yeast HSD will provide a powerful platform upon which to build an arsenal of drugs designed to combat the increasing threat of fungal disease in immunocompromised patients.

**Figure 1. Structures of potential HSD inhibitors**

**A. Unsaturated inhibitor****B. Saturated inhibitor**

## 6.2 Future directions

After examining the results described in this thesis, a number of important questions remain. First, the chemical structure of the NAD(P)-RI-331 adduct is speculative and still needs to be determined. To this end, [ $^{14}\text{C}$ ]-labeled RI-331 could be used to inactivate yeast HSD and the radiolabeled adduct purified. In the event of adduct degradation, the structure of the altered [ $^{14}\text{C}$ ]-RI-331 could be determined by nuclear magnetic resonance and mass spectrometry. This information would furnish insight into the structure of the NAD(P)-RI-331 adduct. An easier alternative may be to solve the structure of RI-331 inactivated HSD by molecular replacement. This route would not only provide the molecular structure of the NAD(P)-RI-331 adduct, but would also determine interactions of this adduct with active site residues of yeast HSD.

Synthetic NAD(P) adducts, such as those described in the discussion, should be tested for HSD inhibition and for antifungal activity. It is possible that these compounds will not possess antifungal activity as a result of low cell permeability. Therefore, adducts with varying portions of the adenine dinucleotide could be tested for both antifungal activity and HSD inhibition. Improved HSD inhibitors may also be produced by modelling these compounds into the active site of the new 3D structure of yeast HSD. Moreover, these inhibitors may demonstrate activity against aspartate semialdehyde dehydrogenase, thereby increasing the usefulness of such drugs.

Lastly, in order to ensure that the characteristics of yeast HSD can be translated to other fungal HSDs, this enzyme should be characterized from medically important

fungi, such as *Candida*, *Aspergillus* and *Cryptococcus* species. Potent inhibitors of yeast HSD should also be tested on these enzymes to determine their effectiveness.



## **CHAPTER 7**

### **References**

- Alexander, B. D., and J. R. Perfect (1997) Antifungal resistance trends towards the year 2000: Implications for therapy and new approaches, *Drugs*, **54**: 657-678.
- Angeles, T. S., P. A. Smanik, C. L. Borders, Jr., and R. E. Viola (1989) Aspartokinase-homoserine dehydrogenase I from *Escherichia coli*: pH and chemical modification studies of the kinase activity, *Biochemistry*, **28**: 8771-8777.
- Angeles, T. S., and R. E. Viola (1990) The kinetic mechanism of the bifunctional enzyme aspartokinase-homoserine dehydrogenase I from *Escherichia coli*, *Arch. Biochem. Biophys.*, **283**: 96-101.
- Armstrong, D. (1993) Treatment of opportunistic fungal infections, *Clin. Infect. Dis.*, **16**: 1-9.
- Bennett, J. E. (1990) Antifungal agents, in: *The Pharmacological Basis of Therapeutics* Goodman Gilman, T. W. Rall, A. S. Nies and P. Taylor, eds.) Pergamon Press, New York, pp. 1165-1181.
- Black, S., and N. G. Wright (1955a)  $\beta$ -Aspartokinase and  $\beta$ -aspartyl phosphate, *J. Biol. Chem.*, **213**: 27-38.
- Black, S., and N. G. Wright (1955b) Aspartic  $\beta$ -semialdehyde dehydrogenase and aspartic  $\beta$ -semialdehyde, *J. Biol. Chem.*, **213**: 39-50.
- Black, S., and N. G. Wright (1955c) Homoserine dehydrogenase, *J. Biol. Chem.*, **213**: 51-60
- Cherest, H., Y. Surdin-Kerjan and H. de Robichon-Szulmajster (1971) Methionine-mediated repression in *Saccharomyces cerevisiae*: a pleiotropic regulatory system involving methionyl transfer ribonucleic acid and the product of gene *eth2*, *J. Bacteriol.*, **106**: 758-772.
- Chirpich, T. P., V. Zappia, R. N. Costilow and H. A. Barker (1970) Lysine 2,3-aminomutase: Purification and properties of a pyridoxal phosphate and S-adenosylmethionine activated enzyme, *J. Biol. Chem.*, **245**: 1778-1789.
- Czerwinski, A., H. Wojciechowska, R. Andruszkiewicz, J. Grzybowska, J. Gumieniak and E. Borowski (1983) Total synthesis of edeine D, *J. Antibiotics*, **36**: 1001-1006.

- Datta, P. (1967) Regulation of homoserine biosynthesis by *L*-cysteine, a terminal metabolite of a linked pathway, *Proc. Natl. Acad. Sci. USA*, **58**: 635-641.
- Deepe, G. S., Jr. (1997) *Histoplasma capsulatum*: Darling of the river valleys, *ASM News*, **63**: 599-604.
- Dixon, D. M., M. M. McNeil, M. L. Cohen, B. G. Gellin and J. R. La Montagne (1996) Fungal infections: A growing threat, *Public Health Reports*, **111**: 226-235.
- Endo, M., K. Takesako, I. Kato and H. Yamaguchi (1997) Fungicidal action of aureobasidin A, a cyclic depsipeptide antifungal antibiotic, against *Saccharomyces cerevisiae*, *Antimicrob. Agents Chemother.*, **41**: 672-676.
- Fostel, J., D. Montgomery and P. Lartey (1996) Comparison of responses of DNA topoisomerase I from *Candida albicans* and human cells to four new agents which stimulate topoisomerase-dependent DNA nicking, *FEMS Microbiol. Lett.*, **138**:105-111.
- Fry, W. E., and S. B. Goodwin (1997) Re-emergence of potato and tomato late blight in the United States, *Plant Disease*, **81**:1349-1357.
- Funkhauser, J. D., and W. G. Smith (1974) Monovalent cation effects on lysine-sensitive aspartokinase catalytic activity and allosteric regulation, *J. Biol. Chem.*, **249**: 7580-7583.
- Gale, C. A., C. M. Bendel, M. McClellan, M. Hauser, J. M. Becker, J. Berman and M. K. Hostetter (1998) Linkage of adhesion, filamentous growth, and virulence in *Candida albicans* to a single gene, *INT1*, *Science*, **279**: 1355-1357.
- Georgopapadakou, N. H., and T. J. Walsh (1996) Antifungal agents: Chemotherapeutic targets and immunologic strategies, *Antimicrob. Agents Chemother.*, **40**: 279-291.
- Gozalbo, D., M. V. Elorza, R. Sanjuan, A. Marcilla, E. Valentin and R. Sentandreu (1993) Critical steps in fungal cell wall synthesis: Strategies for their inhibition, *Pharmac. Ther.*, **60**: 337-345.
- Graybill, J. R. (1996) The future of antifungal therapy, *Clin. Infect. Dis.*, **22**: S166-S178.
- Groll, A. H., A. J. De Lucca and T. J. Walsh (1998) Emerging targets for the development of novel antifungal therapeutics, *Trends in Microbiology*, **6**: 117-124.

- Hama, H., Y. Sumita, Y. Kakutani, M. Tsuda and T. Tsuchiya (1990) Target of serine inhibition in *Escherichia coli*, *Biochem. Biophys. Res. Commun.*, **168**: 1211-1216.
- Hanson, K. R., and E. A. Havir (1970) *L*-phenylalanine ammonia-lyase. IV. Evidence that the prosthetic group contains a dehydroalanyl residue and mechanism of action, *Arch. Biochem. Biophys.*, **141**: 1-17.
- Hartsel, S., and J. Bolard (1996) Amphotericin B: New life for an old drug, *Trends Pharm. Sci.*, **17**: 445-449.
- Hay, R. J. (1994) Antifungal drugs on the horizon, *J. Am. Acad. Dermatol.*, **31**: S82-S86.
- Hazen, K. C. (1995) New and emerging yeast pathogens, *Clin. Microbiol. Rev.*, **8**: 462-478.
- Hettinger, T. P. and L. C. Craig (1968) Edeine II: The composition of the antibiotic peptide edeine A, *Biochemistry*, **7**: 4147-4153.
- Hettinger, T. P. and L. C. Craig (1970) Edeine IV: Structures of the antibiotic peptides edeines A<sub>1</sub> and B<sub>1</sub>, *Biochemistry*, **9**: 1224-1232.
- Hettinger, T. P., Z. Kurylo-Borowska and L. C. Craig (1968) Edeine III: The composition of the antibiotic peptide edeine B, *Biochemistry*, **7**: 4153-4160.
- Hill, S. R., R. Bonjouklian, G. Powis, R. T. Abraham, C. L. Ashendel and L. H. Zalkow (1994) A multisample assay for inhibitors of phosphatidylinositol phospholipase C: Identification of naturally occurring peptide inhibitors with antiproliferative activity, *Anti-Cancer Drug Design*, **9**: 353-361.
- Hirth, C. G., M. Veron, C. Villar-Palasi, N. Hurion and G. N. Cohen (1975) The threonine-sensitive homoserine dehydrogenase and aspartokinase activities of *Escherichia coli* K12: Specific inactivation of the homoserine dehydrogenase activity by the affinity label, 2-amino-4-oxo-5-chloropentanoic acid, *Eur. J. Biochem.*, **50**: 425-430.
- Hitchcock, C. A. (1993) Resistance of *Candida albicans* to azole antifungal agents, *Biochem. Soc. Trans.*, **21**: 1039-1047.
- Hollomon, D. W. (1993) Resistance to azole fungicides in the field, *Biochem. Soc. Trans.*, **21**: 1047-1051.
- Joseph-Horne, T., and D. W. Hollomon (1997) Molecular mechanisms of azole resistance in fungi, *FEMS Microbiol. Lett.*, **149**: 141-149.

- Joseph-Horne, T., D. Hollomon, R. S. T. Loeffler and S. L. Kelly (1995) Altered P450 activity associated with direct selection for fungal azole resistance, *FEBS Lett.*, **374**: 174-178.
- Karsten, W. E., and R. E. Viola (1992) Identification of an essential cysteine in the reaction catalyzed by aspartate- $\beta$ -semialdehyde dehydrogenase from *Escherichia coli*, *Biochim. Biophys. Acta*, **1121**: 234-238.
- Kauffman, C. A., and P. L. Carver (1997a) Antifungal agents in the 1990s: Current status and future developments, *Drugs*, **53**: 539-549.
- Kauffman, C. A., and P. L. Carver (1997b) Use of azoles for systemic antifungal therapy, *Adv. Pharmacol.*, **39**: 143-189
- Kendrick, B. (1985) *The fifth kingdom*, Mycologues publications, Waterloo, ON, Canada, p.175
- Kleinkauf, H., and H. von Döhren (1990) Nonribosomal biosynthesis of peptide antibiotics, *Eur. J. Biochem.*, **192**: 1-15.
- Klepser, M. E., E. J. Ernst and M. A. Pfaller (1997) Update on antifungal resistance, *Trends Microbiol.*, **5**: 372-375.
- Kurtz, M. B. (1998) New antifungal drug targets: A vision for the future, *ASM News*, **64**: 31-39.
- Kurylo-Borowska, Z. (1962) On the mode of action of edeine, *Biochim. Biophys. Acta*, **61**: 897-902.
- Kurylo-Borowska, Z. (1964) On the mode of action of edeine: Effect of edeine on the bacterial DNA, *Biochim. Biophys. Acta*, **87**: 305-313.
- Kurylo-Borowska, Z. and T. Abramsky (1972) Biosynthesis of  $\beta$ -tyrosine, *Biochim. Biophys. Acta*, **264**: 1-10.
- Kurylo-Borowska, Z., and J. Heany-Kieras (1979) The uptake and subcellular localization of the peptide antibiotic edeine A in HeLa cells in suspension culture, *Exp. Cell Res.*, **124**: 371-379.
- Kurylo-Borowska, Z., and J. Heany-Kieras (1982) Edeine synthetase: Evidence for bidirectional synthesis of edeines, in: *Peptide Antibiotics*, Walter de Gruyter and Co., New York, pp. 315-324.

- Kurylo-Borowska, Z. and J. Sedkowska (1974) Biosynthesis of edeine: Fractionation and characterization of enzymes responsible for biosynthesis of edeine A and B, *Biochim. Biophys. Acta*, **351**: 42-56.
- Kurylo-Borowska, Z., and W. Szer (1972) Inhibition of bacterial DNA synthesis by edeine: Effect on *Escherichia coli* mutants lacking DNA polymerase I, *Biochim. Biophys. Acta*, **287**: 236-245.
- Kurylo-Borowska, Z., and E. L. Tatum (1966) Biosynthesis of edeine by *Bacillus brevis* Vm4 *in vivo* and *in vitro*, *Biochim. Biophys. Acta*, **114**: 206-209.
- Lacal, J. C., D. Vazquez, J. M. Fernandez-Sousa and L. Carrasco (1980) Antibiotics that specifically block translation in virus-infected cells, *J. Antibiotics*, **33**: 441-446.
- Martin-Rendon, E., M. J. Farfan, C. Ramos and I. L. Calderon (1993) Isolation of a mutant allele that deregulates the threonine biosynthesis in *Saccharomyces cerevisiae*, *Curr. Genet.*, **24**: 465-471.
- Martinez-Force, E., and T Benitez (1993) Regulation of aspartate-derived amino acid biosynthesis in the yeast *Saccharomyces cerevisiae*, *Curr. Microbiol.*, **26**: 313-322.
- Masner, P., P. Muster and J. Schmid (1994) Possible methionine biosynthesis inhibition by pyrimidinamine fungicides, *Pestic. Sci.*, **42**: 163-166.
- Myskowski, P. L., M. H. White and R. Ahkami (1997) Fungal disease in the immunocompromised host, *Dermatol. Clin.*, **15**: 295-.
- Parry, R. J. and Z. Kurylo-Borowska (1980) Biosynthesis of amino acids: Investigation of the mechanism of  $\beta$ -tyrosine formation, *J. Am. Chem. Soc.*, **102**: 836-837
- Patte, J.-C., G. LeBras, T. Loviny and G. N. Cohen (1963) *Biochim. Biophys. Acta*, **67**: 16-30.
- Patte, J.-C., G. LeBras and G. N. Cohen (1967) Regulation by methionine of the synthesis of a third aspartokinase and of a second homoserine dehydrogenase in *Escherichia coli* K12, *Biochim. Biophys. Acta*, **136**: 245-257.
- Poston, J. M. and B. A. Hemmings (1979) Cobalamins and cobalamin-dependent enzymes in *Candida utilis*, *J. Bacteriol.*, **140**: 1013-1016.
- Rafalski, J. A., and S. C. Falco (1988) Structure of the yeast *HOM3* gene which encodes aspartokinase, *J. Biol. Chem.*, **263**: 2146-2151.

- Ramos, C., M. A. Delgado and I. L. Calderon (1991) Inhibition by different amino acids of the aspartate kinase and the homoserine kinase of the yeast *Saccharomyces cerevisiae*, *FEBS Lett.*, **278**: 123-126.
- Ribaud, P. (1997) Fungal infections and the cancer patient, *Eur. J. Cancer*, **33**: S50-S54.
- Seto-Young, D., B. Monk, A. B. Mason and D. S. Perlin (1997) Exploring an antifungal target in the plasma membrane H<sup>+</sup>-ATPase of fungi, *Biochim. Biophys. Acta*, **1326**: 249-256.
- Shaw, J., and W. G. Smith (1977) Studies on the kinetic mechanism of lysine-sensitive aspartate kinase, *J. Biol. Chem.*, **252**: 5304-5309.
- Shen, L. L., and J. M. Fostel (1994) DNA topoisomerase inhibitors as antifungal agents, *Adv. Pharmacology*, **29B**: 227-244.
- Speed, B. (1996) A review of antifungal agents, *Aust. Fam. Physician*, **25**: 717-721.
- Stadtman, E. R., G. N. Cohen, G. LeBras and H. de Robichon-Szulmajster (1961) Feed-back inhibition and repression of aspartokinase activity in *Escherichia coli* and *Saccharomyces cerevisiae*, *J. Biol. Chem.*, **236**: 2033-2038.
- Stencel, C. (1999) Experts probe complexity of *Candida*, *ASM News*, **65**: 542-546.
- Sternberg, S. (1994) The emerging fungal threat, *Science*, **266**: 1632-1634.
- Szer, W., and Z. Kurylo-Borowska (1972) Interactions of edeine with bacterial ribosomal subunits: Selective inhibition of aminoacyl-t-RNA binding sites, *Biochim. Biophys. Acta*, **259**: 357-368.
- Thomas, D., R. Barbey and Y. Surdin-Kerjan (1993) Evolutionary relationships between yeast and bacterial homoserine dehydrogenases, *FEBS Lett.*, **323**: 289-293.
- Timberlake, W. E., and M. A. Marshall (1989) Genetic engineering of filamentous fungi, *Science*, **244**: 1313-1317.
- Veron, M., J. C. Saari, C. Villar-Palasi and G. N. Cohen (1973) The Thr-sensitive homoserine dehydrogenase and aspartate kinase activities of *E. coli* K12. Intra and intersubunit interactions between the catalytic regions of the bifunctional enzyme, *Eur. J. Biochem.*, **38**: 128-138.
- Viscoli, C., E. Castagnola and M. Machetti (1997) Antifungal treatment in patients with cancer, *J. Intern. Med.*, **242**: 89-94.

- Wedler, F. C., B. W. Ley, S. L. Shames, S. J. Rembish and D. L. Kushmaul (1992) Preferred order random kinetic mechanism for homoserine dehydrogenase of *Escherichia coli* (Thr-sensitive) aspartokinase/homoserine dehydrogenase-I: Equilibrium isotope exchange kinetics, *Biochim. Biophys. Acta*, **1119**: 247-249.
- Wedler, F. C., and B. W. Ley (1993a) Homoserine dehydrogenase-I (*Escherichia coli*): Action of monovalent ions on catalysis and substrate association-dissociation, *Arch. Biochem. Biophys.*, **301**: 416-423.
- Wedler, F. C., and B. W. Ley (1993b) Kinetic and regulatory mechanisms for (*Escherichia coli*) homoserine dehydrogenase-I: Equilibrium isotope exchange kinetics, *J. Biol. Chem.*, **268**: 4880-4888.
- White, T. C. (1997) Antifungal drug resistance in *Candida albicans*, *ASM News*, **63**: 427-433.
- Wojciechowska, H., W. Zgoda, E. Borowski, K. Dziegielewski and S. Ulikowski (1983) The antibiotic edeine XII: Isolation and structure of edeine F, *J. Antibiotics*, **36**: 793-798.
- Woodcock, J., D. Moazed, M. Cannon, J. Davies and H. F. Noller (1991) Interaction of antibiotics with A- and P- site bases in 16S ribosomal RNA, *EMBO J.*, **10**: 3099-3103.
- Yamaguchi, H., K. Uchida, T. Hiratani, T. Nagate, N. Watanabe and S. Omura (1988) RI-331, a new antifungal antibiotic, *Ann. N. Y. Acad. Sci.*, **544**: 188-191.
- Yamaki, H., M. Yamaguchi, H. Imamura, H. Suzuki, T. Nishimura, H. Saito and H. Yamaguchi (1990) The mechanism of antifungal action of (*S*)-2-amino-4-oxo-5-hydroxypentanoic acid, RI-331: The inhibition of homoserine dehydrogenase in *Saccharomyces cerevisiae*, *Biochem. Biophys. Res. Commun.*, **168**: 837-843.
- Yamaki, H., M. Yamaguchi, T. Tsuruo and H. Yamaguchi (1992) Mechanism of action of an antifungal antibiotic, RI-331, (*S*) 2-amino-4-oxo-5-hydroxypentanoic acid: Kinetics of inactivation of homoserine dehydrogenase from *Saccharomyces cerevisiae*, *J. Antibiotics*, **45**: 750-755.
- Yumoto, N., Y. Kawata, S. Noda and M. Tokushige (1991) Rapid purification and characterization of homoserine dehydrogenase from *Saccharomyces cerevisiae*, *Arch. Biochem. Biophys.*, **285**: 270-275.



- Zakin, M. M., N. Duchange, P. Ferrara and G. N. Cohen (1983) Nucleotide sequence of the *metL* gene of *Escherichia coli*, *J. Biol. Chem.*, **258**: 3028-3031.
- Zhoa, X.-J., G. E. McElhaney-Feser, W. H. Bowen, M. F. Cole, S. E. Broedel, Jr. and R. L. Cihlar (1996) Requirement for the *Candida albicans FAS2* gene for infection in a rat model of oropharyngeal candidiasis, *Microbiology*, **142**: 2509-2514.
- Zubay, G. (1988) *Biochemistry*, 2nd edition, MacMillan Publishing Co., New York, pp. 768-775.
- Zweerink, M. M., A. M. Edison, G. B. Wells, W. Pinto and R. L. Lester (1992) Characterization of a novel, potent, and specific inhibitor of serine palmitoyltransferase, *J. Biol. Chem.*, **267**: 25032-25038.